UC San Diego

UC San Diego Electronic Theses and Dissertations

Title

Activating mutations of Lys171 in the kinase domain of IKKbeta unleash a novel mechanism of oncogenic signaling

Permalink

https://escholarship.org/uc/item/60j494r4

Author

Gallo, Leandro

Publication Date

2016

Peer reviewed|Thesis/dissertation

eScholarship.org Powered by the California Digital Library
University of California

UNIVERSITY OF CALIFORNIA, SAN DIEGO

Activating mutations of Lys171 in the kinase domain of IKKbeta unleash a novel mechanism of oncogenic signaling

A dissertation submitted in partial satisfaction of the requirements for the degree of Doctor of Philosophy

in

Chemistry

by

Leandro Henrique Gallo

Committee in charge:

Professor Daniel J. Donoghue, Chair
Professor Timothy Baker
Professor Thomas Hermann
Professor Tadeusz Molinski
Professor Tannishtha Reya

2016

The dissertation of Leandro Henrique Gallo is approved, and it is acceptable in quality and form for publication on microfilm and electronically.

_____

_____

_____

_____

_____

Chair

University of California, San Diego

2016

Dedication

I am grateful and humbled by the privilege of graduating with a doctorate in Chemistry from the University of California, San Diego. I did not arrive at this position in my life on my own; I had the great fortune to have kind and supportive family, friends, colleagues and mentors to aid me in my journey.

I dedicate this dissertation to my parents, Neusa and Gerson Gallo, and my brother, Bruno Gallo of Vinhedo, S.P., Brazil; to my life-long companion and best friend, Daniel Bohan of New York City; to Catherine Lee, Esq. of Miami; to Thomas J. Moran of Ft. Lauderdale; to Joseph Kaus of New York City: to Dr. Adrienne Alaie and Dr. David Mootoo of Hunter College of the City University of New York; to the members of my committee, Professors Reya, Baker, Hermann, and Molinski of the University of California, San Diego; to April Meyer and Juyeon Ko of the Donoghue lab at UCSD. And to my adviser, mentor and great friend, Dr. Daniel J. Donoghue.

My parents instilled within me strong values, including honesty and love, diligence and dignity, and respect and self worth. My father also taught me the value of hard work, developing a successful career as a master electrician at the Unilever corporation - without a high school diploma or any higher education. While working as a full-time electrician, my father learned the craft of ironwork from my grandfather, who taught him how to make furniture and a range of items from cast iron. He attracted considerable attention from the community, applying his natural intellect, engineering gifts and artistry, and going on to run his own

very successful small business. My father worked tirelessly, fifteen hours a day in those two jobs, to make certain that my brother, Bruno and I would have a comfortable life and greater opportunities.

While my father was working hard to provide for his family, my mother was the foundation of our home, taking great care of my father, my brother and me, seeing to every need, and keeping us in very close touch with our large extended family, which provided us with a powerful sense of identity, and the love of so many. My mother offered the kind of love and support to my father that enabled him to work long hours and achieve success; together they built a home, providing a sanctuary for Bruno and me. And they cared for us with great wisdom, too; having the foresight, for example, to enroll me in private English classes beginning at age nine, a decision that has profoundly affected the course of my life, enabling me to achieve things undreamed of by a boy in a small Brazilian town.

Yet, even with all the support my parents provided to me, my childhood in Brazil proved to be emotionally and physically challenging, given my natural proclivities and the unspoken rules governing gender, especially the social mores related to masculinity. Throughout elementary and high school, I was ostracized and often suffered severe abuse for simply being who I was, by far the tallest and the least masculine boy in class. Outside of school, some members of the community decided that being different was somehow a threat. The time and energy required to do battle, and to make every effort to fit in, including denying my own sexuality and joining a deeply conservative church,

disrupted my focus and affected my goals. After graduating from high school at 17 - and following a tentative foray into the gay underground community - threats started arriving via anonymous telephone calls. My parents decided to keep me home around the clock. So, while some of my peers were going to college and many were setting goals for the future, I was confined at home, depressed, afraid and at war with myself. Then, an opportunity to go to America changed the course of my life.

I arrived in the U.S. in January, 2005 at the age of nineteen with virtually nothing in my pockets, a visa, my violin and some clothes. In Deerfield Beach, FL, I worked day and night at a Dunkin Donuts shop selling donuts, coffee and bagels. Sometimes I would sit by the window and look up to the skies wondering how I would ever achieve more for myself. Yet, even though I missed my family terribly and I was so frightened to be alone in a foreign land, I was profoundly grateful to be safe and in America, a place famous in Brazil for its tolerance and progressive ideals.

One day in the Fall that same year, a gentleman walked into the shop, ordered some coffee and engaged me in conversation. After speaking to him in greater detail following my work shift, I told him my story and the reason I left my family and native country.

Suddenly, the stars aligned.

As it turned out, the gentleman was a paralegal, and he put me in touch with Catherine Lee, an immigration attorney in Miami, who went on to file an application for political asylum on my behalf. With enormous dedication and great compassion, Cathi gathered the necessary documentation and set about preparing me for a critical interview with the Dept. of Homeland Security.

Weeks after that interview, I found myself sitting across from the the immigration official in charge of my case, the woman who had the power to send me back to Brazil, back to the community from which I had sought escape. I was more nervous than I have ever been in my life. As she spoke, I caught my breath. “Leandro”, she said, “your request for asylum has been approved.” As I broke down, she came around the desk, embraced me and welcomed me as a new resident of the United States of America. This will forever be the greatest moment of my life.

A week later I turned 20. There was much to celebrate; My new friends, my new life as a permanent resident - and my birthday. I went out with some friends to a local restaurant in Fort Lauderdale, where I met the best person one would ever wish for. Daniel Bohan was visiting his cousin, Tom Moran in Boca Raton, down from the Big Apple. After staying in close touch with Dan for three months, I made the brave decision to move to New York. After my arrival, Dan insisted that I apply for college, and he took me to visit Hunter College on Park Ave. at 68th Street. After my acceptance, I started taking my general core requirement courses, but without yet knowing my true vocation. As you’ll recall, back in Brazil, I never had the chance to explore my talent for the sciences or

anything else. There were few opportunities to develop interests and goals in the face of so much instability. Hunter College felt so much safer, and my new and dear friends, Khabiba and Jodi-Ann, showed me respect and loved me for the individual I am, without judgements. This was something quite new to me in an academic environment.

Daniel's cousin, Tom, visited from Boca Raton the following year, and he suggested that I take Principle of Biology I. Intimidated and nervous, I signed up for the course. It turned out to be a natural fit. Dr. Adrienne Alaie, who taught this extraordinary introduction to the sciences, soon became my major undergraduate advisor. While she was unpopular with some given the rigor of her class, Dr. Alaie helped me discover and develop my natural affinity for the sciences and scientific research. She accomplished this through her extraordinary teaching methods and her great talent, bringing science to life in ways that teachers before her never could. Her passion for the subject was infectious; her love for her field was completely exhilarating. Before Dr. Alaie, my major was to be English literature; after Dr. Alaie, science became my poetry. Later, Dr. Alaie brought me on board as a teaching assistant, my first exposure to teaching - and I excelled in this new role, working with students on their skills, but also working to attract them to the field.

My major in Biological Sciences required that I complete a course in Chemistry, which led to an instant attraction to the field, and a particular passion for the space where biology and chemistry intersect. Appreciating my strong interest and my talents, Dr. David Mootoo gave me the opportunity to work as

an undergraduate research assistant in his lab on a project related to the synthesis of pentaerythritol- and Galactosylceramide-based glycopolymers as potential inhibitors of HIV-1 entry into cells. I excelled in Dr. Mootoo's lab with the support of the Minority Biomedical Research Support program, which opened many opportunities for me as a young scientist, including the ability to participate in scientific conferences for the first time. I came to UCSD in the summer of my junior year, to conduct research in the Department of Surgery through the Amgen Scholars Program.

As graduation from Hunter approached, I found myself applying for graduate programs across the country. I chose UCSD because of the diverse student body and faculty, and for its thriving scientific community and world-class reputation. After going through several lab rotations, my choice of the Donoghue lab was an easy decision. My valued and brilliant mentor, Dr. Dan Donoghue has been a wonderful and caring advisor all through my doctoral program. All the progress in my graduate studies, including the achievement of first-author publications, would not have been possible without Dan's mentorship and guidance. He has consistently supported me, providing me with valuable research tools and with enormous intellectual support. Dan has passed his love of research and his intellectual principles on to me; I intend to carry them forward into the future. I also would like to thank Dan's wife, Nancy, who has shown support through friendship by always offering wise words of encouragement in this process.

April Meyer is truly an extraordinary asset in the Donoghue group; a patient teacher and deeply impressive researcher, she has trained me in flawless technique and critical areas of research, all of which will serve me well as I begin my post-doctoral career. Also critical my success in the Donoghue Lab is my outstanding colleague, Juyeon Ko, who has aided me in successful completion of a broad range of experiments that are part of this dissertation.

During my time as a graduate student at UCSD, I had the great pleasure to become friends with Joseph W. Kaus and Jennifer Daluz, whose friendship and support have propelled me to excel in ways large and small toward the completion of my graduate program.

The members of my committee, Professors Reya, Hermann, Molinski and Baker have been valued assets throughout my time in this program. As my program comes to its conclusion, I am especially fortunate to have secured an appointment in the Reya Lab at UCSD. I look forward to applying the knowledge I've gained from the Donoghue group in The Reya Lab, and look forward with great anticipation to learning everything that Professor Reya has to teach me in the coming years.

America has granted me the extraordinary opportunity to live my life in a land where individuals are rewarded for their achievements. As now a citizen of this great country, I will continue to work hard to repay - in every way conceivable - the gifts and opportunities this country has provided to me - and continues to provide to me.

Epigraph

Nothing is impossible,
The word itself says “I’m possible!”

Audrey Hepburn

Education is the most powerful weapon which you can use to change

the world

Nelson Mandela

It is the mark of an educated mind

To be able to entertain a thought without accepting it

Aristotle

The true sign of intelligence is not knowledge but imagination

Albert Einstein

Table of Contents

List of Figures

List of Tables

Acknowledgments

I am very grateful for having great people whom have helped me in the process of studying towards a doctorate degree. This was not an easy task; I encountered various challenges and obstacles that I had to overcome. My colleagues have helped me to grow intellectually and professionally through their mentorship, patience, kindness and passion for teaching. To my advisor, Professor Daniel J. Donoghue, thank you very much for your encouragement and support throughout all the stages of my graduate program. I deeply appreciate your excitement for allowing me to develop the projects herein cited under your mentorship. In addition, I want to thank the members of my doctoral committee Professors Thomas Hermann, Tannishtha Reya, Tadeusz Molinski and Timothy Baker for their valuable guidance and discussions during my progress as a doctorate graduate student at UCSD.

To all the co-authors whom have collaborated in the research projects herein published, thank you for all the work you have done. None of these projects would have come to fruition without your valuable work. I want to thank the members of the Donoghue lab, Juyeon Ko, April Meyer, and Katelyn Nelson for the valuable experimental assistance and discussions. In addition, I would like to acknowledge Khatereh Motamedchaboki and Martin Haas for their collaborations in some of the projects that I have developed.

Chapter 1, in full, is a reprint of the article as it appears in *Cell Cycle*. Gallo L.H., Meyer A. N., Motamedchaboki K., Nelson K.N., Haas M., Donoghue

D. J. “Novel Lys63-Linked Ubiquitination of IKKβ Induces STAT3 Signaling” *Cell Cycle* 2014 Dec; 13(24):3964-76. The first author of the work is the author of this dissertation.

Chapter 2, in full, is the work currently being prepared for submission for publication. Gallo L.H. and Ko J., Meyer A.N., Nelson K.N., Motamedchaboki K., Donoghue D.J. “Mutation of Lys171 in IKKBeta Unleashes a Novel Oncogenic Mechanism Signaling”. The first co-author of the work is the author of this dissertation.

Chapter 3, in full, is the work currently being prepared for submission for publication. Gallo L.H., Ko J., Donoghue D.J. “The Importance of Regulatory Ubiquitination in Cancer and Metastasis”. The first author of the work is the author of this dissertation.

Chapter 4, in full, is a reprint of the article as it appears in *Cytokine Growth Factor Reviews*. Gallo L.H., Nelson K.N., Meyer A., Donoghue D.J. “Functions of FGFR’s in Cancer Defined by Novel Translocations and Mutations” *Cytokine Growth Factor Review*s 2015 Aug; 26(4):425-49. The first author of the work is the author of this dissertation.

This work was supported, in part, by the Graduate Need in Areas of National Assistance (GAANN) fellowship, the NIH/NCI Biochemistry of Growth Regulation and Oncogenesis, and the San Diego and Cota Robles Fellowship.

Vita

Hunter College

2010 Bachelors of Arts, Biological Sciences

University of California, San Diego

2013 Master of Science, Chemistry

2016 Doctor of Philosophy, Chemistry

Publications

Gallo L.H. and Ko J., Meyer A.N., Nelson K.N., Donoghue D.J. “Mutation of Lys171 in IKKBeta Unleashes a Novel Oncogenic Signaling Mechanism”. (Manuscript in preparation).

Gallo L.H., Ko J., Donoghue D.J. “The Importance of Regulatory Ubiquitination in Cancer and Metastasis”. (Manuscript in preparation).

Gallo L.H., Nelson K.N., Meyer A., Donoghue D.J. “Functions of FGFR’s in Cancer Defined by Novel Translocations and Mutations” *Cytokine Growth Factor Review*s 2015 Aug; 26(4):425-49.

Gallo L.H., Meyer A. N., Motamedchaboki K., Nelson K.N., Haas M., Donoghue D. J. “Novel Lys63-Linked Ubiquitination of IKKβ Induces STAT3 Signaling” *Cell Cycle* 2014 Dec; 13(24):3964-76.

Meyer A.N., Drafahl K.A., McAndrew C.W., Gilda J.E., **Gallo L.H.**, Haas M., Brill L.M., Donoghue D.J. “Tyrosine phosphorylation allows integration of multiple signaling inputs by IKKβ” *PLOS One* 2013 Dec 27;8(12)

ABSTRACT OF THE DISSERTATION

Activating mutations of Lys171 in the kinase domain of IKKbeta unleash a novel mechanism of oncogenic signaling

by

Leandro Henrique Gallo

Doctor of Philosophy in Chemistry

University of California, San Diego, 2016

Professor Daniel J. Donoghue, Chair

Inhibitor of kappaB kinase beta (IKKβ) is the master regulatory kinase that modulates canonical nuclear factor kappaB (NFkappaB) inflammatory activation. Under inflammatory conditions, IKKβ is phosphorylated at Ser177/Ser181 sites in the kinase domain, which activates the kinase function of the protein. IKKβ, in turn, phosphorylates its downstream substrate IkappaBalpha, which is subsequently degraded. This event releases NFkappaB, which is normally sequestered in the cytoplasm, to translocate into the nucleus to activate transcription of inflammation-related genes.

In the first chapter of this dissertation, mutations of Lys171 located in the kinase domain of IKKβ are shown to lead to increase the phosphorylation of Ser177/Ser181 sites and result in the upregulation of the kinase activity of IKKβ.

These mutations had been initially identified in tumor samples of Multiple Myeloma, Spleen Marginal Zone Lymphoma and Mantle Cell Lymphoma. Via site-directed mutagenesis, we constructed the K171E mutation in IKKβ. This study further demonstrated that IKKβ is conjugated to Lys63-linked ubiquitin chains, in which the activating K171E mutation upregulated this modification at Lys147. The main discovery of this project is that the K171E mutation in IKKβ induces the activation of STAT3 in the absence of exogenous Interleukin-6 in HEK293T cells. Via LC-MS/MS, we identified various lysine ubiquitination sites in full length activated IKKβ, in which some of these negatively regulate the phosphorylation of Ser177/Ser181. Ubiquitination of Lys147 in activated IKKβ, located in proximity to the activation loop in the kinase domain, is critical to induce STAT3 activation.

The second chapter of this dissertation demonstrates that IKKβ K171E relies on JAK, gp130, and TAK1 to signal to STAT3. In addition, we utilized a method termed Bio-ID proximity dependent biotinylation to identify proteins interacting with activated IKKBeta, in which UBC13 and LRPPRC were identified as interacting partners. Via siRNA, we showed that UBC13 and LRPPRC possibly negatively regulated STAT3 activation induced by IKKβ K171E. Interestingly, IKKβ K171E depends upon UBE2V2 cofactor of UBC13, previously demonstrated to be involved in modulation of DNA damage repair activation, to activate STAT3. Lastly, the oncogenic potential of K171E mutation

is demonstrated by the transformation of murine myeloid 32D cells into Interleukin-3-independent phenotype. In conjunction, these results illustrate a novel mechanism by which the loss of Lys171 in IKKβ induces the activation of STAT3 in the absence of cytokines and growth factors.

The third chapter of this dissertation entails a review article describing that the misregulated expression of members of the ubiquitination cascade contributes to cancer progression and metastasis. Ubiquitination largely serves as a degradation mechanism of proteins. Ubiquitin signaling is further involved in additional cellular processes such as the activation of NFκB inflammatory response and DNA damage repair. In this review, we highlight the E2 ubiquitin conjugating enzymes, E3 ubiquitin ligases and Deubiquitinases that support the proliferation, migration, stemness and metastasis of a plethora of cancers, including their contribution to poor clinical prognosis and modulation of pluripotent cancer stem cells attributed to metastasis. We further describe mutations in E3 ubiquitin ligases that support the proliferation and adaptation to hypoxia of some cancers. Thus, this review illustrates how tumors exploit the members of the vast ubiquitin signaling pathways to support oncogenic signaling for the purposes of survival and metastasis.

The fourth chapter of this dissertation entails a review article related to mutations in Fibroblast Growth Factor Receptors (FGFRs) in cancer and developmental disorders. This comprehensive review describes approximately 200 different mutations in FGFRs in diverse cancers, in which some of these mutations have been found to contribute to developmental syndromes. In

addition, this review shows the occurrence of chromosomal translocations that result in fusion proteins involving FGFR's in cancers, and it illustrates the aberrant signaling mechanisms activated by these oncogenes.

Chapter 1: Novel Lys63-Linked Ubiquitination of IKKβ Induces STAT3 Signaling

1.1 Abstract

NFκB signaling plays a significant role in human disease, including breast and ovarian carcinoma, insulin resistance, embryonic lethality and liver degeneration, rheumatoid arthritis, ageing and Multiple Myeloma (MM). Inhibitor of κB (IκB) kinase β (IKKβ) regulates canonical Nuclear Factor κB (NFκB) signaling in response to inflammation and cellular stresses. NFκB activation requires Lys63-linked (K63-linked) ubiquitination of upstream proteins such as NEMO or TAK1, forming molecular complexes with membrane-bound receptors. We demonstrate that IKKβ itself undergoes K63-linked ubiquitination. Mutations in IKKβ at Lys171, identified in Multiple Myeloma and other cancers, lead to a dramatic increase in kinase activation and K63-linked ubiquitination. These mutations also result in persistent activation of STAT3 signaling. Liquid chromatography (LC)-high mass accuracy tandem mass spectrometry (MS/MS) analysis identified Lys147, Lys418, Lys555 and Lys703 as predominant ubiquitination sites in IKKβ. Specific inhibition of the UBC13-UEV1A complex responsible for K63-linked ubiquitination establishes Lys147 as the predominant site of K63-ubiquitin conjugation and responsible for STAT3 activation. Thus,

IKKβ activation leads to ubiquitination within the kinase domain and assemblage of a K63-ubiquitin conjugated signaling platform. These results are discussed with respect to the importance of upregulated NFκB signaling known to occur frequently in MM and other cancers.

1.2 Introduction

NFκB signaling has been implicated in breast and ovarian carcinoma [1, 2], insulin resistance [3, 4], embryonic lethality and liver degeneration [5], rheumatoid arthritis [6, 7], ageing [8], and Multiple Myeloma [9, 10]. The initiation of the inflammatory response is dependent upon the ubiquitination cascade of proteins upstream of the Inhibitor of κB (IκB) kinase β (IKKβ), which plays a direct role in phosphorylating and targeting IκB proteins for degradation, releasing NFκB for nuclear translocation. Upon stimulation of cells with TNFα and LPS, K63-linked polyubiquitin modifications occur in proteins such as TRAFs (tumor necrosis factor receptor-associated factors), RIP1 (receptor interacting protein-1), IRAKs (IL-1 receptor-associated kinases), and TAK1 (TGFβ-activated kinase 1) [11-14]. Moreover, the NFκB Essential Modulator (NEMO, or IKKγ) is ubiquitinated recruiting TAB1/2 and TAK1 proteins assembled on this platform, which leads to activation of the IKK complex, composed of IKKα, IKKβ, and NEMO [15, 16]

Ubiquitin, a highly conserved 76-amino acid protein, is post-translationally conjugated to a wide variety of substrates. Ubiquitination is essential in myriad biological functions, including DNA damage repair, cell growth, apoptosis and immune responses [17-19]. Ubiquitin has seven lysine residues that can be conjugated to the C-terminal Gly of a subsequent ubiquitin to form polyubiquitin chains with specific linkages and topologies. One of the most studied polyubiquitination chains are Lys48-linked (K48-linked), which serves as a signal for proteasome-mediated degradation of substrates, and K63-linked, which serves as a stabilizing signal for protein function and molecular scaffolding interactions [11, 18]. K63-linked ubiquitination is a proteasomal-independent modification that plays an extensive role in NFκB activation by contributing to the stability and scaffolding functions of proteins such as IRAK-1, RIP1, NEMO, and TAK1[13, 20-24]. Polyubiquitination of NEMO recruits TAK1 for activation of the IKK complex whereas the recruitment of the A20 zinc finger protein onto the ubiquitin platform limits IKK activation [16].

Mutations in the IKBKB gene resulting in Lys171Glu (K171E) and Lys171Arg (K171R) have been identified in Multiple Myeloma (MM), Spleen Marginal Zone Lymphoma (SMZL) and Mantle Cell Lymphoma (MCL) [25-27]. We used these mutations as a starting point to investigate the mechanism of IKKβ activation and downstream effects on cellular signaling. This work reveals that IKKβ is conjugated to both K48- and K63-linked ubiquitin that regulate the wild-type (WT) protein. However, mutation of Lys171 to either Glu or Arg leads to constitutive phosphorylation activity and also increased polyubiquitination of

IKKβ, oth K48- and K63-linked. Surprisingly, mutations at Lys171 also resulted in STAT3 activation. Thus, mutations at Lys171 of IKKβ differ from typical activation mediated by the S177/S181 phosphoryation sites, resulting in hyperactivation of kinase activity as well as increased ubiquitination and, specifically, K63-linked ubiquitin scaffolding that induces STAT3 signaling.

1.3 Results

Mutations at Lys171 activate IKKβ

Lys171 is located within a highly conserved region in the activation loop of the kinase domain of IKKβ, close to the major activating phosphorylation sites Ser177 and Ser181 (Fig 1A) [28]. Lys171 also lies near Tyr169, recently shown to undergo tyrosine phosphorylation in the presence of FGFR2, resulting in IKKβ activation [29]. In addition, Lys171 contributes to the stability of the activated protein via ionic interactions with phosphorylated Ser181 [30]. Hence, this residue plays a critical regulatory role in the activated structure.

Using site-directed mutagenesis, we constructed the mutant K171E observed in the human cancers MM and SMZL [25, 26]. We also constructed all other mutants at this position resulting from single base changes, thus creating the mutants K171R, M, N, Q and T, recognizing that some of these mutations might be identified in future patient cancers. Indeed, while this work was in progress, the mutation K171R was identified in a case of Mantle Cell Lymphoma

[27]. IKKβ constructs were expressed in HEK293 cells: WT, K171-mutated, the positive control S177E/S181E (constitutively activated "EE"), and the negative control S177A/S181A (non-activatable "AA"). IKK complexes were recovered using antisera against NEMO and assayed by *in vitro* kinase assay using [^{32}P]-ATP. The results show that all the mutations at Lys171 exhibited increased phosphorylation of IKKβ relative to the activated "EE" mutant, with the K171E exhibiting approximately 5-fold greater activity (Fig 1B).

The increase in phosphorylation was confirmed to be occurring on the activation loop residues S177/S181 by phospho-specific immunoblotting (Fig 1C). Whereas the activated "EE" mutant is unrecognizable by the antiserum, each of the mutants at Lys171 showed strong activation in the order: R > T > Q > M > E > N. We also examined the stability of S177/S181 phosphorylation in the K171E mutant versus WT in a cycloheximide (CHX) time course over 24 h, with K171E exhibiting higher initial phosphorylation and slower decay ($t_{1/2}$ ~ 20 h for K171E, $t_{1/2}$ ~ 7 h for WT) (Fig 1D). Together, the data presented in Fig 1 suggest that the important feature for mutational activation at Lys171 is not the introduction of a phosphomimic (K171E), nor retention of a basic charge (K171R), but rather the specific loss of the Lys residue.

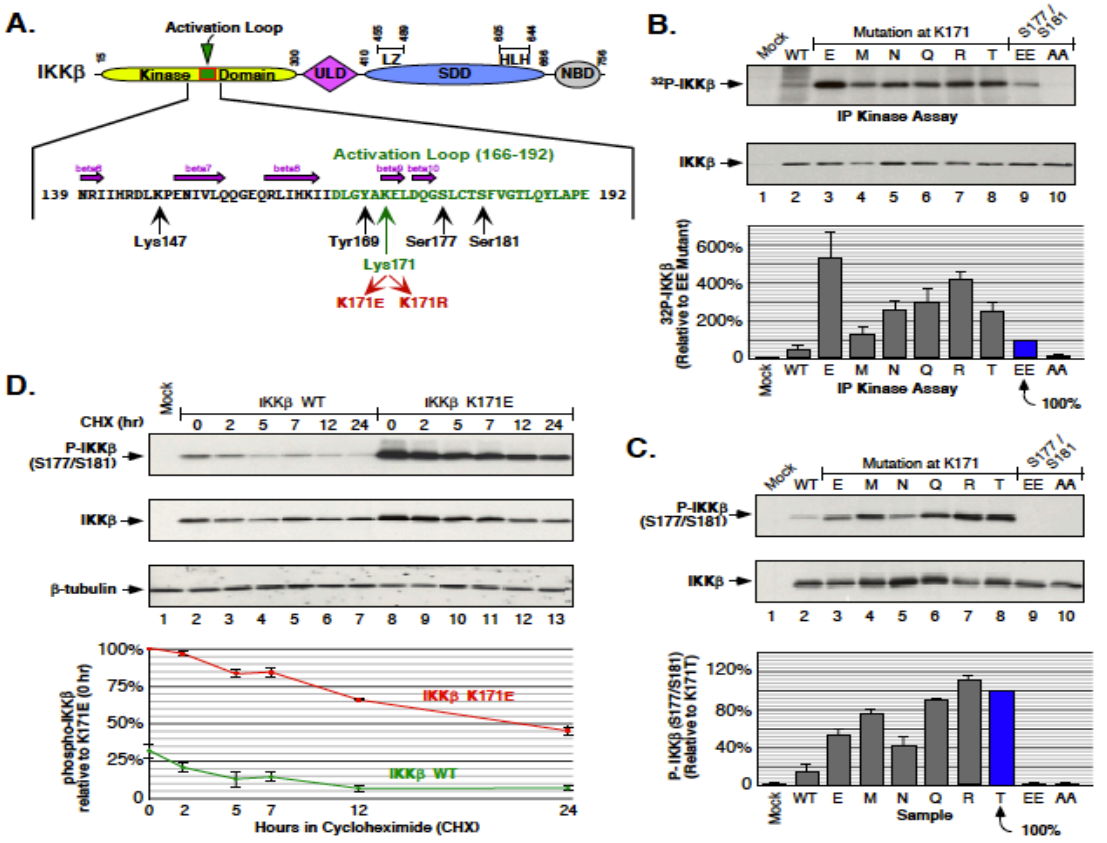

Figure 1.1. Phosphorylation of IKKß Induced by Mutations at Lys171. (A) Schematic of IKKß with the activation loop within the N-terminal kinase domain expanded to show amino acids critical for phosphorylation and signaling. The ubiqutin-like domain (ULD), the scaffold/dimerization domain (SDD) which contains the leucine zipper (LZ) and helix-looop-helix (HLH) regions, and NEMO binding domain (NBD) are indicated. **(B)** IKKß mutant proteins were expressed in HEK293 cells and the IKK complex was immunoprecipitated with IKKγ antisera and assayed for *in vitro* phosphorylation. Samples were separated by SDS-PAGE and detected by autoradiography. IKKß expression is shown by immunoblotting for IKKß (middle panel). Assays were quantitated relative to ^{32}P incorporation of the IKKß S177E/S181E mutant, +/- sem. (bottom) **(C)** HEK293T cells expressing IKKß mutants were analyzed for activation loop serine phosphorylation using Phospho-IKKα/ß antisera (top). The membrane was reprobed for IKKß (middle panel). Serine 177/181 phosphorylation was quantitated relative to the K171T mutant, +/- sem. (bottom panel). **(D)** HEK293T cells expressing IKKß WT or K171E were treated with 50 µg/ml cycloheximide (CHX) for 2, 5, 7, 12 and 24 h. Lysates were examined for IKKß serine phosphorylation and total IKKß as in (C) (top two panels). The membrane was reprobed for ß-tubulin (third panel). Serine 177/181 phosphorylation was quantitated relative to K171E at time zero, +/- sem. (bottom).

IKKβ is conjugated to K63-linked ubiquitin polymers

To examine IKKβ for potential K63-linked ubiquitination, IKKβ immune complexes were collected from cells expressing IKKβ (WT, K171-mutated, EE, AA), HA-Ub and HA-NEMO. Immunoprecipitation and immunoblotting revealed the presence of K63-linked ubiquitin conjugates which were significantly increased by each of the mutations examined at Lys171 (Fig 2A). As the K171E mutation was initially identified in human lymphomas [25, 26], we examined a time course of TNFα stimulation from 0-24 h (Fig 2B). The time course reveals that although WT never exhibited a significant increase, the activated control "EE" mutant displayed a significant K63-linked signal visible out to 12 h, but absent in the 24 h sample. In contrast, the mutant K171E exhibits a very robust K63-linked signal at intermediate time points (2, 5, 8, 12 h) and, significantly, this signal persists even at the 24 h time point. A similar pattern holds true for the total ubiquitination signal, demonstrating the persistence of the signal in the K171E mutant even at 24 h (Fig 2B, 3rd Panel). A similar time course from 0-24 h carried out in the presence of CHX also revealed that under these conditions the K171E mutation leads to a significant increase in the strength and persistence of the K63-linked signal in comparison with the WT protein (Fig 2C). Clearly, the K171E mutation potentiates and stabilizes the total as well as the

specific K63-linked ubiquitination of IKKβ during prolonged stimulation of cells with TNFα.

IKKβ was previously shown to be degraded by the 26S proteasome pathway via KEAP1-mediated ubiquitination [31]. Therefore, we looked into the effects of simultaneous treatment of cells with TNFα to activate inflammatory signaling plus MG132 to inhibit proteasomal degradation (Fig 2D). For the WT protein, for both K48-linked and K63-linked ubiquitination, treatment with MG132 significantly increased ubiquitination (Lanes 5 vs 8). In contrast, the K48-linked and K63-linked ubiquitination of the “EE” and K171E proteins was largely unaffected by TNFα treatment alone or in the presence of MG132 (Lanes 6, 7, 9, 10). Perhaps the most striking observation from Fig 2D is the strength of the K171E signal which, under all conditions, exceeds the maximal signal from either the WT or “EE” protein. These results show that the K171E mutant, and to a lesser extent the activated “EE” control, exhibit constitutive K48-linked and K63-linked ubiquitination of IKKβ.

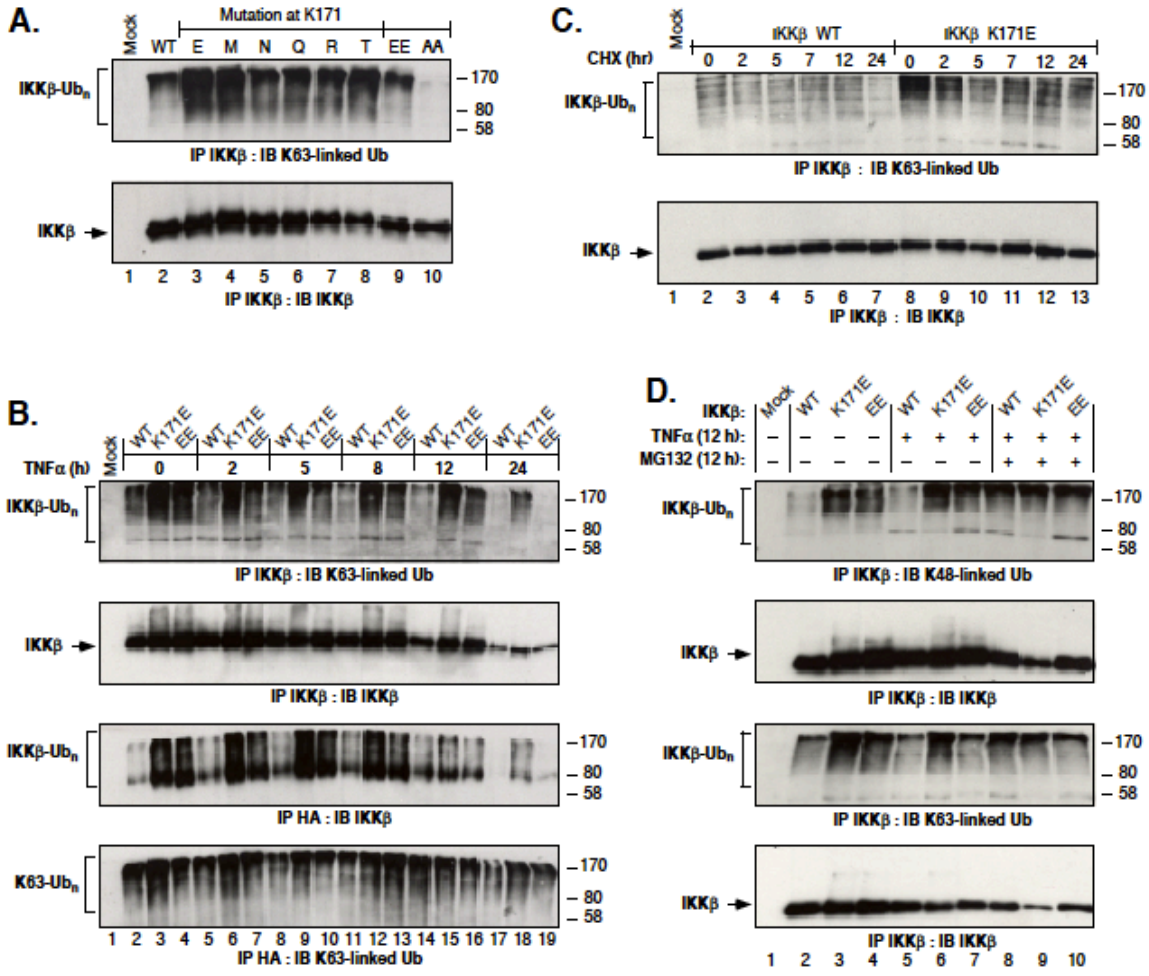

Figure 1.2. IKKß Ubiquitination Regulated by Lys171. (A) HEK293T cells expressing IKKß WT or Lys171 mutants, HA-Ub and HA-NEMO, were lysed and immunoprecipitated with IKKß antisera. Samples were immoblotted for K63-linkage specific polyubiquitin (top panel). The membrane was reprobed for IKKß (bottom panel). (B) Cells as in Panel A were treated with 10 ng/ml of TNF for 2, 5, 8, 12 and 24 h. Samples were immunoprecipitated and blotted as decribed in (A) (top two panels). Duplicate samples were immunoprecipitaed with HA-probe antisera and immunoblotted for IKKß (third panel). The membrane was reprobed for K63-linkage specific polyubiquitin (bottom). (C) Cells as in Panel A were treated with 50 µg/ml CHX for 2, 5, 7, 12 and 24 h. IKKß immunoprecipitates were blotted as in (A). (D) Cells as in Panel A were treated with +/- 10ng/ml TNF and +/- 10 µM MG132 for 12 h. IKKß immunoprecipitates were blotted for K63-linkage specific polyubiquitin (top panel) or K48-linkage specific polyubiquitin (third panel). Membranes were reprobed for IKKß (2nd and 4th panels).

IKKβ K171E constitutively activates STAT3 signaling independently of NFκB

Interleukin-6 (IL-6) is deregulated in various carcinomas resulting in abnormal cellular proliferation, drug-resistance, cell cycle progression and migration [32]. IL-6 signaling activates STAT proteins which have been implicated in cellular transformation and oncogenesis in MM, endometrial, lung, colorectal and breast carcinomas, and other human diseases [33, 34]. In addition, STAT3 activation has been linked to inflammation-induced tumorigenesis initiated by malignant cells [35-38], including persistent activation of NFκB signaling, establishing a positive tumorigenic feedback loop [39-41].

We investigated the effects of IL-6 stimulation on K171E-expressing cells (Fig 3A). When HEK293T cells expressing WT, K171E, "EE" and "AA" IKKß proteins were stimulated with IL-6, activation of endogenous STAT3 was observed by immunoblotting for phospho-Y705 (Lanes 11-15). In contrast, TNFα treatment showed little or no observable STAT3 activation in all samples except for K171E (Lanes 6-10). Surprisingly, IKKß K171E expression leads to activation of STAT3 in the absence of IL-6 (Lanes 3, 8).

We further examined the effects of TNFα stimulation over a 1 h time course, comparing cells expressing WT, K171E and "EE" mutants (Fig 3B). The K171E mutant induced robust constitutive STAT3 activation that increased following TNFα and peaked at 150% at 15 min. Although the WT and "EE"

mutant proteins exhibited TNFα-responsiveness, the magnitude of STAT3 phosphorylation was always significantly less than for K171E. The phosphorylation of S32/S36 of IκBα provides another downstream effect of NFκB signaling stimulated by TNFα. In contrast to the P-STAT3 signal, the appearance of IκBα P-S32/S36 was rapid, peaking at 5 min and then decaying, similar to WT, K171E or "EE" mutants (Fig 3B, 3rd Panel, Lanes 5-7).

When treating cells with TNFα and the proteasome inhibitor MG132 for a period of 12 h, the K171E mutant activation of P-STAT3 was largely TNFα-independent, although it did increase modestly in response to MG132 (Fig 3C, Lanes 3, 6, 9). TNFα-stimulation resulted in detectable phosphorylation of IκBα S32/S36 for both the WT and "EE" mutant proteins, which increased massively when combined with MG132 treatment, demonstrating that these proteins are typically subject to proteasomal degradation (Fig 3C, 3rd Panel, Lanes 8, 10). In addition, the various mutations at Lys171 induced significant activation of STAT3 (Fig 3D). Thus, although K171E significantly activated P-STAT3, the other substitutions (M, N, Q, R, T) at this position were more robust.

The observations presented in Fig 3 demonstrate that mutational activation of IKKß at Lys171 is significantly different than the phospho-mimic S177E/S181E "EE" mutant. Mutations at Lys171 lead to constitutive activation of STAT3 that is independent of TNFα or IL-6 stimulation, and only marginally regulated by proteasomal degradation.

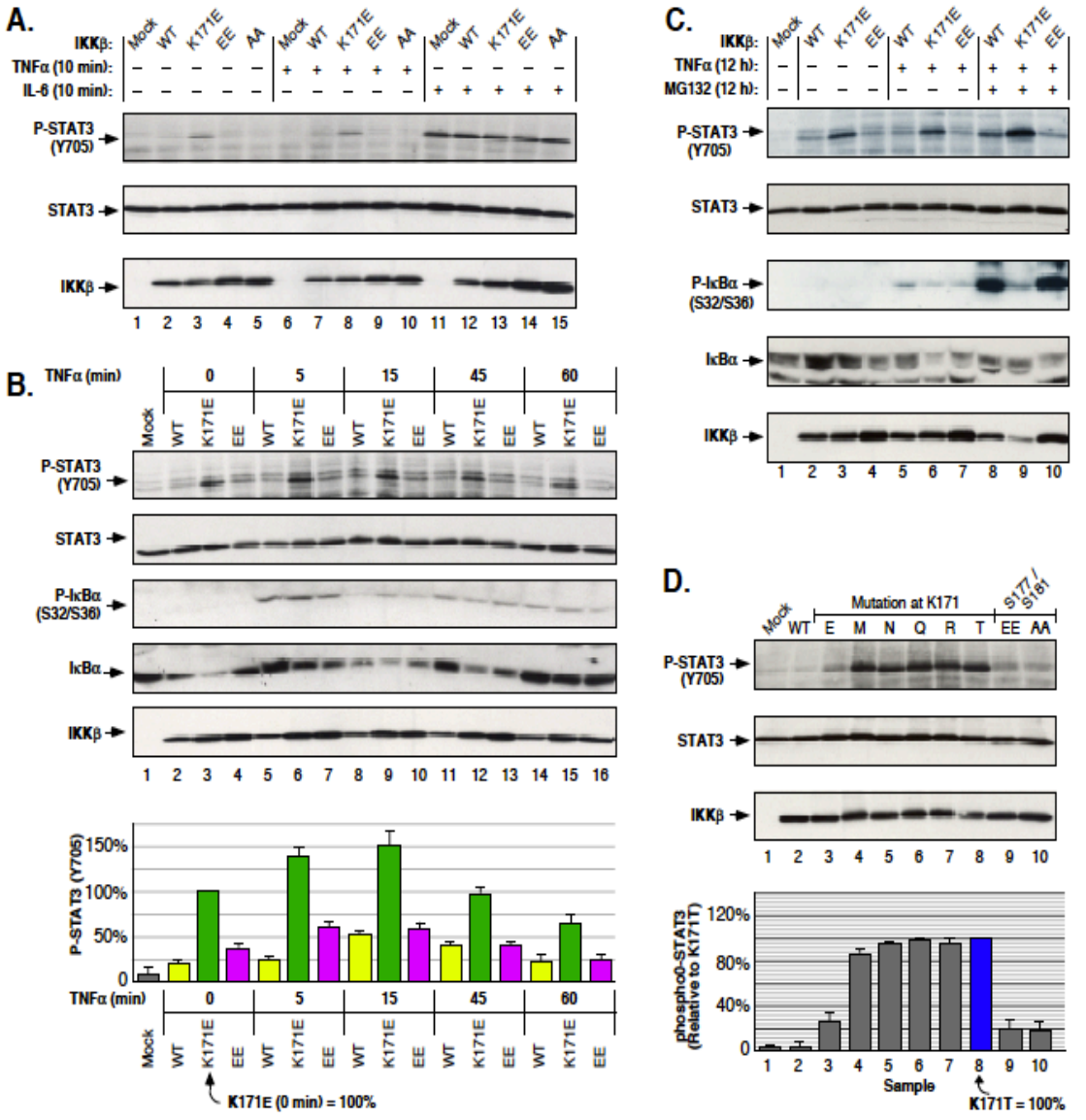

Figure 1.3. IKKß Lys171 Activation of STAT3. (A) HEK293T cells expressing IKKß derivatives were treated with 10 ng/ml TNFα or 10 ng/ml IL-6 for 10 min. Lysates were immunoblotted for Phospho-STAT3 (Tyr705) (top), STAT3 (middle panel) and IKKß (bottom). **(B)** HEK293T cells expressing IKKß mutants were treated with 10 ng/ml of TNFα for 5, 15, 45 and 60 min. Lysates were immunoblotted for Phospho-STAT3 (Tyr705) (top), STAT3 (2nd panel), Phospho-IκBα (Ser32/36) (3rd panel), IκBα (4th panel), and IKKß (bottom). Phosphorylation of STAT3 was quantitated relative to the K171E mutant at time zero, +/- sem. (bottom panel). **(C)** HEK293T cells expressing IKKß WT, K171E and S177E/S181E were treated with +/- 10 ng/ml TNFα and +/- 10 μM MG132 for 12 h. Lysates were immublotted as in (B). **(D)** Lysates from HEK293T cells expressing IKKß derivatives were immunoblotted as in (A). STAT3 phosphorylation was quantitated relative to the Lys171Thr mutant, +/- sem. (bottom)

LC-MS/MS analysis identifies ubiquitination sites in IKKβ

Samples from HEK293T cells expressing either IKKß WT or K171E proteins were analyzed by LC-MS/MS to identify significant posttranslational modifications. Proteins to be analyzed were recovered in immune complexes with antisera against IKKß or the HA-tag of HA-Ub and HA-NEMO. Lys147, Lys418, Lys555 and Lys703 were identified as predominant ubiquitination sites on tryptic peptides based on the additional mass of 114 Da arising from the C-terminal di-Gly residues of Ub bonded by an isopeptide linkage to the modified Lys residue in IKKß (Table 1). Lys301 was also identified as a minor site. A representative spectrum is presented identifying each of the diGly-tagged residues Lys147, Lys418, Lys555 and Lys703 (Fig 4A). The frequency which different sites are detected with, termed spectral counting, is a widely accepted method of label-free quantification [29, 42, 43]. While spectral counts of different peptides are not strictly comparable, large differences correlate with relative abundance for the same peptide despite limitations arising from differing ionization efficiencies comparing different peptides. For each of the predominant sites of ubiquitination, Lys147, Lys418, Lys555 and Lys703, spectral counts in Table 1 suggest that ubiquitination at each of these sites was increased modestly in cells expressing K171E versus WT IKKß, except for Lys147 which exhibited a ~5-fold increase in K171E samples.

Table 1.1. Ubiquitination IKKß Peptides Identified by LC-MS/MS. In addition to the peptide sequences identified, also shown here are TPP adjusted minimum probabilities, charge states, Xcorr values, initial and combined spectral count of each identified ubiquitinated peptides.

Residue	IKKβ	Prep #	Precursor Ion Charge	Peptide Sequence	Adjusted Probability	Instances	Xcorr	Partial Spectral Count	Total Spectral Count
K147	WT	#6628	3	DLK[242]PENIVLQQGEQR	0.9998	2	3.55-3.71	2	13
	K171E	#6629	2	DLK[242]PENIVLQQGEQR	0.9998	5	3.28-4.50	11	
		#6629	3	DLK[242]PENIVLQQGEQR	0.9998	4	2.29-4.54		
		#6645	3	DLK[242]PENIVLQQGEQR	0.9984	1	2.92		
		#6629	2	LK[242]PENIVLQQGEQR	0.8414	1	2.84		
K301	K171E	#6629	3	GTDPTYGPNGCFK[242]ALDDILNLK	0.2656	2	3.30-3.75	2	2
K418	WT	#6628	3	PQPESVSCILQEPK[242]R	0.237	3	3.37-4.15	15	32
		#6644	3	PQPESVSCILQEPK[242]R	0.2112	12	3.34-3.88		
	K171E	#6629	2	PQPESVSCILQEPK[242]R	0.3313	4	3.75-4.33	17	
		#6629	3	PQPESVSCILQEPK[242]R	0.3117	7	3.50-4.53		
		#6645	3	PQPESVSCILQEPK[242]R	0.304	6	3.28-4.38		
K555	WT	#6628	3	K[242]QGGTLDDLEEQAR	0.9998	7	3.53-4.46	9	22
		#6644	3	K[242]QGGTLDDLEEQAR	0.9997	2	2.83-3.94		
	K171E	#6629	2	K[242]QGGTLDDLEEQAR	0.9998	7	3.63-4.64	13	
		#6629	3	K[242]QGGTLDDLEEQAR	0.9998	5	3.63-4.49		
		#6645	3	K[242]QGGTLDDLEEQAR	0.9835	1	3.58		
K703	WT	#6628	3	LSQPGQLMSQPSTASNSLPEPAK[242]K	0.9815	4	2.68-3.42	4	10
	K171E	#6629	3	LSQPGQLMSQPSTASNSLPEPAK[242]K	0.9613	6	2.84-3.63	6	

To assess the importance of individual IKKß ubiquitination sites, each was mutated to Arg, either alone or in combination with the activating mutation K171E. When assayed for K63-linked ubiquitination, each single mutant resembled the WT protein except for K147R, which exhibited little or no detectable K63-linked ubiquitin (Fig 4B, Lane 3). When combined with the activating K171E mutation, all but one double mutant protein exhibited K63-linked ubiquitination similar to the K171E mutant alone (Lanes 8, 10-13). The notable exception was the double mutant K171E/K147R (Lane 9), which exhibited little or no detectable K63-linked ubiquitination. These results are consistent with a preliminary identification of Lys147 as the principal site of K63-linked ubiquitination in IKKß.

Next, we examined phosphorylation of the single and double mutants of IKKß (Fig 4C). Each of the single mutations resulted in significantly increased phosphorylation (Lanes 4-7), with the exception of K147R (Lane 3). The single ubiquitination site mutations in combination with K171E did not result in any further increase in phosphorylation (Lanes 10-13). The unique exception was again provided by the double mutant K171E/K147R which exhibited only slight phosphorylation, as best seen in the long exposure (2nd Panel, Lane 9). Thus, each Lys identified in our MS/MS analysis contributes to the regulatory function of IKKß, including those distant from the kinase domain.

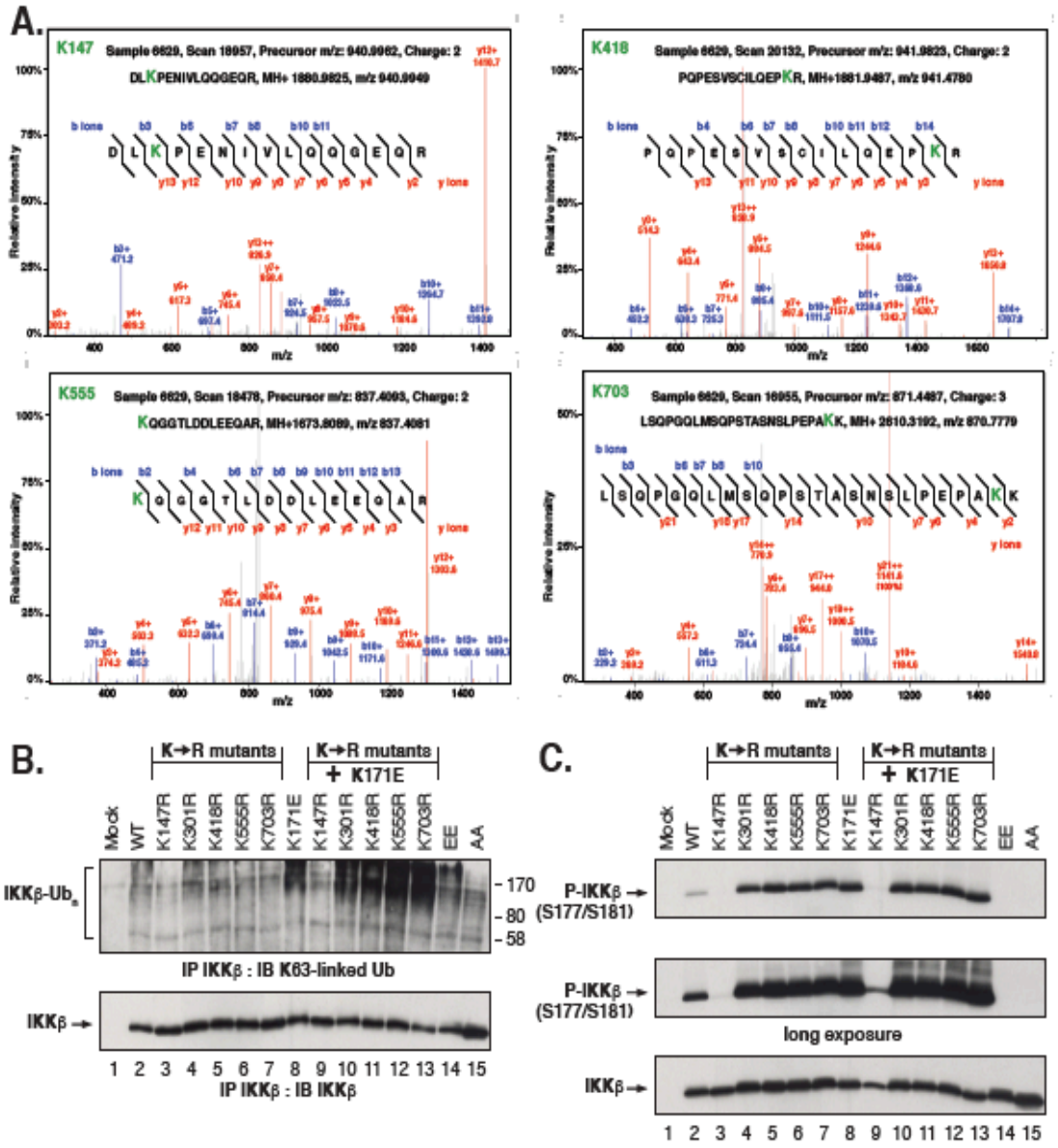

Figure 1.4. Identification and Biological Function of IKKß Ubiquitination Sites. (A) Representative spectrum of peptides showing the relative intensity of selected b and y ions for the major sites of IKKß ubiqitination. Note that not all identified ions are labeled due to space constraints. **(B)** HEK293T cells expressing IKKß Lys to Arg mutants were immunoprecipitated and immunoblotted as in Fig 2(A). **(C)** Lysates from HEK293T cells expressing IKKß Lys to Arg mutants were immunoblotted as in Fig 1(C).

K63-linked ubiquitination is required for STAT3 activation

The identification of residues Lys147, Lys418, Lys555 and Lys703 as predominant ubiquitination sites does not reveal whether each site is K48-linked versus K63-linked nor its role in STAT3 activation. Because K63-linked ubiquitination is preferentially involved in cellular signaling rather than proteasomal degradation, we hypothesized that STAT3 activation by IKKß K171E may be dependent upon its increased K63-linked ubiquitination. Therefore, we used the small molecule inhibitor NSC697923 to inhibit the E2 ubiquitin-conjugating enzyme UBC13-UEV1A complex, selectively inhibiting K63-linked ubiquitination [44].

HEK293T cells expressing WT or K171E were treated with the inhibitor NSC697923 and examined for IKKß S177/S181 phosphorylation. Although some increased phosphorylation was observed for WT IKKß, the activation of IKKß kinase in the K171E mutant protein was largely independent of K63-linked ubiquitination (Fig 5A). We also examined the effect of the K63-linked inhibitor NSC697923 on STAT3 activation in IKKß WT- and K171E-expressing cells (Fig 5B). The activation of STAT3 by the IKKß mutant K171E (Lane 5) was blocked by treatment with NSC697923 (Lanes 6, 7).

Following IL-6 treatment, both mock and K171E-expressing cells exhibited STAT3 activation (Fig 5C Lanes 5, 6). When cells were pretreated with the inhibitor NSC697923, the P-STAT3 signal was largely ablated (Lanes 7, 8).

These results show that STAT3 activation, whether in response to IL-6 stimulation or IKKß K171E expression, is dependent upon K63-linked ubiquitination. Lastly, among the IKKß ubiqutination sites identified, the activation of STAT3 was dependent upon Lys147 as shown by the ability of K147R to block the K171E-induced STAT3 phosphorylation (Fig 5D, Lane 9).

Taken together, the results presented in Fig 5 demonstrate that STAT3 activation in response to the IKKß K171E mutation is dependent on the presence of the ubiquitination site Lys147, and that ubiquitination at this site is K63-linked as shown by its sensitivity to the selective inhibitor NSC697923.

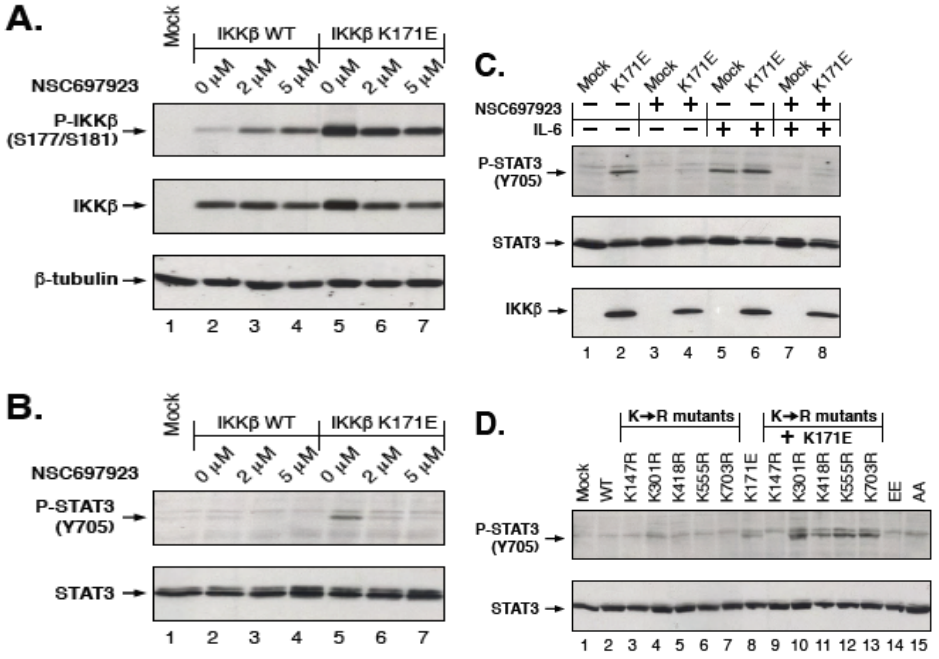

Figure 1.5. Inhibition of K63-linked Ubiquitiation Blocks IKKß Lys171 Signaling. (A) Lysates from HEK293T cells expressing IKKß WT and K171E were treated with 2 μM and 5 μM NSC697923 for 2 h and immunoblotted for Phospho-IKKα/ß (top), IKKß (middle panel) and ß-tubulin (bottom). **(B)** Duplicate samples from (A) were immunoblotted for Phospho-STAT3 (Tyr705) (top) and STAT3 (bottom). **(C)** Lysates from HEK293T cells expressing IKKß K171E treated with +/- 5 μM NSC697923 for 2 h and +/- 10 ng/ml IL-6 for 10 min were immunoblotted as in (B). **(D)** Lysates from HEK293T cells expressing IKKß Lys to Arg mutants were immunoblotted as in (B).

1.4 Discussion

This is the first report to show that IKKß is modified by the addition of K63-linked ubiquitination. We demonstrate that the mutation K171E leads to constitutive activation of the intrinsic kinase activity of IKKß, suggesting a role of the normal Lys171 side chain in stabilizing an inactive kinase in addition to its documented importance in the activated structure [30]. Other mutations at this position also result in constitutive activation of IKKß, demonstrated by *in vitro* kinase assay and phosphorylation of the activation loop residues S177/S181. Such mutations also result in significant activation of STAT3 signaling, which is independent of TNFα or IL-6 stimulation.

Other members of the NFκB pathway also undergo K63-linked regulatory ubiquitination. The K63-linked ubiquitination of NEMO has been reported as critical for the activation of T-cell receptor signaling; specifically, overexpression of Bcl10 recruits MALT-1 which induces K63-linked ubiquitination of Lys399 in NEMO that activates NFκB in lymphocytes [45]. In addition, misregulation of K63-ubiquitination at Lys285 in NEMO occurs in Crohn's Disease via Nod2 [46]. In breast cancer cells, IKKε was shown to undergo K63-linked ubiquitination at Lys30 and Lys401. K63-linked ubiquitination is essential for the oncogenic activity of IKKε that contributes to the hyperactivation of NFκB [47].

Previous reports, examining IKKß ubiquitination, showed by site-directed mutagenesis and immunoblotting that IKKß is mono-ubiquitinated at Lys163 in

Tax-transfected HEK293T cells [48]. The mono-ubiquitination of IKKß was attributed to the E3 ligase RING-finger Ro52, which then leads to autophagy-mediated degradation of the protein and subsequent downregulation of NFκB signaling [31, 49]. Furthermore, the K171R mutation was shown to cause constitutive phosphorylation IKKβ during a screen of kinase domain Lys residues [48]. Another report illustrated that IKKβ is polyubiquitinated at Lys555 by the E3 ligase KEAP1 in TNFα-stimulated HEK293T cells, resulting in a downregulation of NFκB signaling due to 26S-proteasomal degradation of the protein [50].

Using LC-MS/MS, we identified four predominant ubiquitination sites in IKKß, Lys147, Lys418, Lys555 and Lys703. Spectral counts suggest the extent of ubiquitination at each of these sites was increased modestly in cells expressing K171E versus WT IKKß. Lys147 was the only major site to show a significant increase in K171E samples, exhibiting a 5-fold increase. This is significant because Lys147 was also the only ubiquitination site required for STAT3 activation and the primary site of K63-linked ubiquitination. Ubiquitination at a different Lys residue, Lys163, suggested by site-directed mutagenesis and immunoblotting in an earlier study, was not observed in our work, possibly reflecting the inclusion of Tax expression in this prior work [48]. Although the ubiquitination sites identified here were all initially identified in a study of the human cellular ubiquitinome [51], we have determined here that each site contributes to the regulation of IKKß kinase function.

Lys147 in IKKß lies within the highly conserved sequence DLKPEN between the beta6 and beta7 regions of the kinase [30]. A comparison of other species shows this region to be highly conserved among IKKß orthologs (Table 2A). Even more surprising is the very strict conservation of this region, including the Lys corresponding to Lys147 of IKKß, in a very large number of human kinase paralogs (Table 2B). This raises the possibility that many kinases exhibiting a Lys at the corresponding position may undergo K63-linked ubiquitination as a regulatory modification. This has already been demonstrated for the corresponding Lys158 of TAK1, required for the subsequent phosphorylation of MKK6 which activates the JNK-p38 kinase pathway [52]. Lys158 residue in TAK1 has also been suggested as a site of K63-linked ubiquitination involved in the activation of TAK1 in *Helicobacter pilori* infections [53], and in genotoxic stress-induced NFκB activation [54]. Notably, the kinase activity of TAK1 is abrogated when Lys158 is mutated to Arg, as is the case for the K147R mutation in IKKß. Another clinically important example is provided by the K63-linked ubiquitination at the corresponding Lys578 residue of BRAF, required for BRAF-mediated signaling [55]. The unequivocal mass spectrometry evidence presented here that Lys147 of IKKß undergoes ubiquitination, together with the biochemical evidence that this is the major site of K63-linked ubiquitination in IKKß, will likely be relevant to TAK1 and other related protein kinases.

Table 1.2. Conservation of IKKß Lys171 in Orthologous and Paralogous Proteins. Amino acids shown are the residue corresponding to Lys171 (Red), identities (Green), and non-identical residues (Blue).

Species	Common Name	Identity with IKKβ Kinase	Sequence aligning with AA #139-192 of IKKβ	Residues	Identifier
Homo sapiens	Human	100%	NRIIHRDLKPENIVLQQGEQ-RLIHKIIDLGYAK-ELDQGSLCTSFVGTLQYLAPE	139-192	O14920
Pan troglodytes	Chimp	98%	NRIIHRDLKPENIVLQQGEQ-RLIHKIIDLGYAK-ELDQGSLCTSFVGTLQYLAPE	139-192	XP_001142461.2
Felis catus	Cat	98%	NRIIHRDLKPENIVLQQGEQ-RLIHKIIDLGYAK-ELDQGSLCTSFVGTLQYLAPE	139-192	ENSFCAP00000012705
Loxodonta africana	African elephant	96%	NRIIHRDLKPENIVLQQGEQ-RLIHKIIDLGYAK-ELDQGSLCTSFVGTLQYLAPE	139-192	ENSLAFG00000004558
Canis lupus	Dog	95%	NRIIHRDLKPENIVLQQGEQ-RLIHKIIDLGYAK-ELDQGSLCTSFVGTLQYLAPE	139-192	XP_539954.2
Anas platyrhynchos	Duck	94%	NRIIHRDLKPENIVLQQGEQ-RLIHKIIDLGYAK-ELDQGSLCTSFVGTLQYLAPE	73-126	ENSAPLG00000006379
Mus musculus	Mouse	93%	NRIIHRDLKPENIVLQQGEK-RLIHKIIDLGYAK-ELDQGSLCTSFVGTLQYLAPE	139-192	NP_001153246.1
Ficedula albicollis	Flycatcher	93%	NRIIHRDLKPENIVLQQGEQ-RLIHKIIDLGYAK-ELDQGSLCTSFVGTLQYLAPE	75-128	ENSFALP00000006679
Columba livia	Dove	91%	NRIIHRDLKPENIVLQQGEQ-RLIHKIIDLGYAK-ELDQGSLCTSFVGTLQYLAPE	125-178	XP_005510959.1
Tursiops truncatus	Dolphin	90%	NRIIHRDLKPENIVLQQGEQ-RLIHKIIDLGYAK-ELDQGSLCTSFVGTLQYLAPE	139-192	ENSTTRP00000002143
Monodelphis domestica	Opossum	89%	NRIIHRDLKPENIVLQQGEK-RLIHKIIDLGYAK-ELDQGSLCTSFVGTLQYLAPE	139-192	ENSMODP00000012792
Ornithorhynchus anatinus	Platypus	89%	NRIIHRDLKPENIVLQQGQQ-RLIHKIIDLGYAK-ELDQGSLCTSFVGTLQYLAPE	139-192	F6ZE58
Sarcophilus harrisii	Tasmanian devil	88%	NRIIHRDLKPENIVLQQGEK-RLIHKIIDLGYAK-ELDQGSLCTSFVGTLQYLAPE	139-192	ENSSHAP00000020986
Astyanax mexicanus	Cave fish	80%	KRIIHRDLKPENIVLQQGEK-RLIHKIIDLGYAK-ELDQGSLCTSFVGTLQYLAPE	44-97	ENSAMXG00000013072
Xenopus tropicalis	Western clawed frog	73%	NRIIHRDLKPENIVLQFGEQ-RLIHKIIDLGYAK-ELDQGSLCTSFVGTLQYLAPE	150-203	F7A2B9_XENTR
Danio rerio	Zebrafish	62%	NRIIHRDLKPENIVLQQGEK-RLVHKIIDLGYAK-ELDQGSLCTSFVGTLQYLAPE	139-192	NP_001116737.1
Tetraodon nigroviridis	Pufferfish	61%	KRIIHRDLKPENIVLQQGEK-RLIHKIIDLGYAK-QLDHGSLCVSFVGTLQYLAPE	142-195	ENSTNIP00000019003
Drosophila melanogaster	Fruit fly	34%	CGICHRDLKPQNIVLQRGVDGKKIVKLIDFGLARGTPDQ-IMVQSVVGTRHYMAPE	178-232	Q9VEZ5

Table 2B: IKKβ Paralogs

Name	Alternate Name	E-Value	Sequence aligning with AA #139-192 of IKKβ	Residues	Identifier
IKBKB	IKK2	0	NRIIHRDLKPENIVLQQGEQR------LIHKIIDLGYAKELDQGSLCTSFVGTLQYLAPE	139-192	O14920
CHUK	IKBKA; IKK1	3.0E-129	NKIIHRDLKPENIVLQQVGGK------IIHKIIDLGYAKDVDQGSLCTSFVGTLQYLAPE	138-191	O15111
ULK2	UNC51.2	3.0E-35	KGIIHRDLKPQNILLSYANRRKSSVSGIRIKIADFGFARYLQSNMMAATLCGSPMYMAPE	125-184	Q8IYT8
IKBKE	IKKE; KIAA0151	3.0E-34	NGIVHRDLKPGNIMRLVGEEG-----QSIYKLTDFGAARELDDGEKFVSVYGTEEYLHPD	129-183	Q14164
ULK1	UNC51.1	3.0E-32	KGIIHRDLKPQNILLSNPAGRRANPNSIRVKIADFGFARYLQSNMMAATLCGSPMYMAPE	132-191	O75385
PNCK	CAMK1B; KCC1B	6.0E-32	LGIVHRDLKPENLLYATPFED------SKIMVSDFGLSK-IQAGNMLSTACGTPGYVAPE	130-182	Q6P2M8
TBK1	NAK; T2K	9.0E-31	NGIVHRDIKPGNIMRVIGEDG-----QSVYKLTDFGAARELKDDSQFVSLYGTEEYLHPD	129-183	Q9UHD2
CAMK1D	KCC1D	2.0E-30	MGIVHRDLKPENLLYYSQDEE------SKIMISDFGLSKMEGKGDVMSTACGTPGYVAPE	138-191	Q8IU85
CAMK1A	KCC1A	3.0E-29	LGIVHRDLKPENLLYYSLDED------SKIMISDFGLSKMEDPGSVLSTACGTPGYVAPE	135-188	Q14012
ULK3	UNC51.3	3.0E-28	RNISHLDLKPQNILLSSLEKP-------HLKLADFGFAQHMSPWDKHVLRGSPLYMAPE	131-183	Q6PHR2
MARK3	STK10; CTAK1	2.0E-27	KRIVHRDLKAENLLL---DADMNIKIADFGFSNEFTVGGKLDTFCGSPPYAAPE	172-222	P27448
CHEK2	CHK2; RAD53	3.0E-27	NGIIHRDLKPENVLLSSQEED------CLIKITDFGHSKILGETSLMRTLCGTPTYLAPE	341-394	O96017
MARK1	PAR1; KIAA1477	3.0E-27	KYIVHRDLKAENLLL-DGDMNI--------KIADFGFSNEFTVGNKLDTFCGSPPYAAPE	176-226	Q9P0L2
DAPK2	DRP1	3.0E-27	KKIAHFDLKPENIMLLDKNIPIP-----NIKLIDFGLAHEIEDGVEFKNIFGTPEFVAPE	143-197	Q9UIK4
STK36	FUSED; KIAA1278	4.0E-27	KRILHRDMKPQNILLARGGGI---------KLCDFGFARAMSTNTMVLTSIKGTPLYMSPE	119-270	Q9NRP7
DAPK3	DLK; ZIPK	1.0E-26	KRIAHFDLKPENIMLLDKNVPNP-----NIKLIDFGIAHKIEAGNEFKNIFGTPEFVAPE	133-187	O43293
MARK4	PAR1D; KIAA1860	3.0E-26	KNIVHRDLKAENLLL-DAEANI--------KIADFGFSNEFTLGSKLDTFCGSPPYAAPE	175-225	Q96L34
NIM1	NIM1K	3.0E-26	NQIIHRDLKAENVFYTSN----------TCVKVGDFGLSTVSKEGEMLNTFCGSPPYAAPE	190-240	Q8IY84
PRKACG	KAPCG	5.0E-26	LDLIHRDLKPENLLI---DQQ-------GYLQVTDFGFAKRV-KGRTWT-LCGTPEYLAPE	161-209	P22612
CAMK1G	CKLIK3; KCC1G	6.0E-26	NGIVHRDLKPENLLYLTPEEN------SKIMITDFGLSK-MEQNGIMSTACGTPGYVAPE	137-189	Q96NX5
RPS6KA2	KS6A2; RSK3	7.0E-26	LGIIYRDLKPENILLDE-EGHI-------KITDFGLSKEAIDHDKRAYSFCGTIEYMAPE	178-229	Q15349
NUAK2	SNARK; OMPHK2	7.0E-26	NRVVHRDLKLENILLDANCNI---------KIADFGLSNLYHQGKFLQTFCGSPLYASPE	169-219	Q9H093

As previously mentioned, the K171E mutation was initially identified via genetic sequencing of MM and SMZL [25, 26]. As this work was in progress, the K171R mutation was identified in MCL [27] and shown in the data above to be even more strongly activating than K171E. A survey of mutations in IKKß that occur in human cancer is presented in Table 3, some of which may be without effect whereas others, such as the Lys171 mutations we have characterized, have significant biochemical ramifications. Previously, in a receptor tyrosine kinase of importance both in development and in human cancer, we demonstrated profound FGFR3 kinase activation due to the K650E mutation as responsible for the lethal developmental disorder Thanatophoric Dysplasia type II (TDII) [56]. A comparison of other amino acid substitutions at Lys650 of FGFR3 also identified K650M as strongly activating, which was identified several years later in individuals with the rare developmental syndrome Severe Achondroplasia with Delayed Development and Acanthosis Nigricans (SADDAN) [57]. In the case of IKKß, as genetic sequencing of additional cancers becomes widely available, our results predict that other substitutions at this position which are accessible by single nucleotide changes in addition to K and R will be observed, such as M, N, Q and T.

Table 1.3. Genetic Changes Identified in IKKß in Human Cancer.

Mutation	Cancer	Effect Reported	Biological Effect	Ref
E81Q	Breast Cancer	Disease causing	(–)	61
K171E K171E K171R	Multiple Myeloma Spleen Marginal Zone Lymphoma Mantle Cell Lymphoma	Activating Damaging (–)	IKKβ activation; STAT3 activation; Lys63-Ub	25 26 27
A360S	Breast Cancer	Disease causing	(–)	61-64
Amplification	Ovarian Cancer	(–)	(–)	65
R144Q R446W S598S E707*	Colorectal Cancer	Benign Probably damaging Probably damaging (–)	(–)	66
G667C	Lung Adenocarcinoma	(–)	(–)	67
D484Y	Esophageal Adenocarcinoma	(–)	(–)	68
R53W	Spinal Cord Ependynoma	(–)	(–)	69
R47R Q175* I314M	Transitional Cell Carcinoma (Bladder Cancer)	(–)	(–)	70
L679_fs	Clear-Cell Renal Carcinoma	(–)	(–)	71
R288S	Chondrosarcoma	(–)	(–)	72
A212T A357S S474Y M454I	Colorectal Cancer	(–)	(–)	73
K603R	Small-Cell Lung Carcinoma	(–)	(–)	74
N667D	Gastric Cancer	Benign	(–)	75

Future work is necessary to identify the interacting proteins that associate with a K63-ubiquitination scaffold assembled by IKKß, which we show is responsible for IL-6-dependent STAT3 activation and for the unusual STAT3 signaling demonstrated by the K171E mutation. The activation of additional signaling pathways such as STAT3 may be expected to confer significant proliferative or antiapoptotic properties to human cancer cells expressing IKKß mutant proteins. In addition, the identification of K63-linked ubiquitination potentially provides a novel selective chemotherapeutic target.

1.5 Methods

Cell Culture. HEK293 and HEK293T cells were grown in DMEM with 10% FBS and 1% Pen/Strep and maintained in 10% CO_2 at 37˚C. Cells were transfected with plasmid DNA using calcium phosphate precipitation at 3% CO_2, as previously described [29].

Plasmid constructs. IKKß wild-type (WT) has been described previously [58], which was not epitope-tagged. Mutations in IKKß were created by Quikchange site-directed mutagenesis and confirmed by DNA sequencing. The haemagglutinin (HA)-tagged ubiquitin (HA-Ub_3) expression plasmid was a gift from Dr. Tony Hunter and Dr. Andrea Carrano (Salk Institute, La Jolla CA) [59]. The expression plasmid containing murine NEMO (HA-NEMO) was a gift from Dr. Mark Hannink (University of Missouri, Columbia MO).

Antibodies, immunoprecipitation and immunoblot. Antibodies were obtained from the following sources: IKKγ (FL-419), IKKß (H-4), IKKß (G-8), ß-tubulin (H-235), HA-probe (F-7), STAT3 (C-20), IκBα (C-21) from Santa Cruz Biotechnology; Phospho-IKKα/ß (Ser176/180) (16A6), K63-linkage Specific Polyubiquitin (D7A11), K48-linkage Specific Polyubiquitin (D9D5), Phospho-STAT3 (Tyr705) (D3A7), Phospho-IκBα (Ser32/36) (5A5) from Cell Signaling Technology; horseradish peroxidase (HRP) anti-mouse, HPR anti-rabbit from GE Healthcare. Enhanced chemiluminence (ECL) reagents were from GE Healthcare. TNFα and MG132 were obtained from Bio-techne; recombinant

human Interleukin-6 (IL-6) from Life Technologies; and NSC697923 from Santa Cruz Biotechnology.

HEK293 and HEK293T cells were transfected, starved and collected in RIPA Buffer [29]. Immunopreciptation and immunoblotting experiments were performed as described [29, 60]. 5 mM N-Ethylmaleimide (NEM) was added to RIPA buffer when lysates were examined for ubiquitination by immunoblotting.

Mass spectrometry analysis. HEK293T cells were plated one day prior to transfection at 3.0 x 10^6 cells per 15cm tissue culture plate. 10 plates per sample were transfected with IKKß WT or IKKß K171E, HA-Ub_3 and HA-NEMO. Cells were treated with 10μM MG132 for approximately 5 h prior to lysis. Lysates were collected and immunoprecipitated as described [29]. Analysis of tryptic peptides by the Sanford-Burnham Medical Research Institute Proteomics Facility was carried out by high-resolution, high-accuracy 1D LC-MS/MS, consisting of a Michrom HPLC, a 15-cm Michrom Magic C18 column, a low-flow ADVANCED Michrom MS source, and LTQ-Orbitrap XL and Velos Pro with ETD (Thermo Fisher Scientific). MS/MS spectra were submitted to Sorcerer Enterprise v.3.5 release (Sage-N Research Inc.) with SEQUEST algorithm as the search program for peptide/protein identification. Search results were further analyzed using Peptide/Protein prophet v.4.5.2 (ISB). Spectra annotated with fragment ions were captured using the Javascript MS/MS spectrum viewer Lorikeet, and annotated using Adobe Illustrator to show selected b and y ions.

Presented in Table 1, Samples #6628 and #6629, from IKKß WT and K171E expressing cells, respectively, were collected as IKKß immune

complexes. Samples #6644 and #6645, from IKKß WT and K171E expressing cells, respectively, were collected as HA (hemagglutinin) immune complexes. Tryptic peptide coverage of IKKß in the 4 samples was: #6628, 69%; #6629, 70%; #6644, 56%; #6645, 55%. Total IKKß spectra analyzed in the 4 samples was: #6628, 2473 spectra; #6629, 2249 spectra; #6644, 2521 spectra; #6645, 1990 spectra.

In vitro kinase assays. HEK293 cells were transfected and starved overnight prior to lysing in Cytoplasmic Extract Buffer as described [29]. Lysates were immunoprecipitated with IKKγ anitsera, collected on Protein A-Sepharose, washed with Cytoplasmic Extract Buffer and Wash Buffer and subjected to *in vitro* phosphorylation kinase assay. Kinase reactions containing 10 µCi of [γ-^{32}P]- with 20 µM ATP were incubated at 30 ˚C for 30 min, and separated by 12.5% SDS-PAGE. Gels were stained, destained, dried and exposed to film.

1.6 Acknowledgments

We thank Dr. Alexandre Rosa Campos of The Sanford-Burnham Medical Research Institute for technical assistance and Dr. Andrea C. Carrano of UC San Diego for valuable technical suggestions. LHG received support from the Graduate Assistance in Areas of National Need (GAANN) Fellowship Program (L.H.G), and KM received support from grant P20 CA132386 from the National Institutes of Health which funds The Sanford-Burnham Medical Research Institute Proteomics Facility (K.M.). We also thank Laura Castrejon for

assistance with manuscript preparation and submission. We also thank April Meyer for constructing the IKKBeta clones using in this work, including the execution of *in vitro* kinase assays.

Chapter 1, in full, is a reprint of the article as it appears in *Cell Cycle*. Gallo L.H., Meyer A. N., Motamedchaboki K., Nelson K.N., Haas M., Donoghue D. J. “Novel Lys63-Linked Ubiquitination of IKKβ Induces STAT3 Signaling” *Cell Cycle* 2014 Dec; 13(24):3964-76. The first author of the work is the author of this dissertation.

1.7 References

1.Hernandez L, Hsu SC, Davidson B, Birrer MJ, Kohn EC, Annunziata CM. Activation of NF-kappaB signaling by inhibitor of NF-kappaB kinase beta increases aggressiveness of ovarian cancer. Cancer Res 2010; 70:4005-14.

2. Hu MC, Lee DF, Xia W, Golfman LS, Ou-Yang F, Yang JY, Zou Y, Bao S, Hanada N, Saso H, Kobayashi R, Hung MC. IkappaB kinase promotes tumorigenesis through inhibition of forkhead FOXO3a. Cell 2004; 117:225-37.

3. Arkan MC, Hevener AL, Greten FR, Maeda S, Li ZW, Long JM, Wynshaw-Boris A, Poli G, Olefsky J, Karin M. IKK-beta links inflammation to obesity-induced insulin resistance. Nat Med 2005; 11:191-8.

4. Cai D, Yuan M, Frantz DF, Melendez PA, Hansen L, Lee J, Shoelson SE. Local and systemic insulin resistance resulting from hepatic activation of IKK-beta and NF-kappaB. Nat Med 2005; 11:183-90.

5. Tanaka M, Fuentes ME, Yamaguchi K, Durnin MH, Dalrymple SA, Hardy KL, Goeddel DV. Embryonic lethality, liver degeneration, and impaired NF-kappa B activation in IKK-beta-deficient mice. Immunity 1999; 10:421-9.

6. Andreakos E, Smith C, Kiriakidis S, Monaco C, de Martin R, Brennan FM, Paleolog E, Feldmann M, Foxwell BM. Heterogeneous requirement of IkappaB kinase 2 for inflammatory cytokine and matrix metalloproteinase production in rheumatoid arthritis: implications for therapy. Arthritis and rheumatism 2003; 48:1901-12.

7. Aupperle K, Bennett B, Han Z, Boyle D, Manning A, Firestein G. NF-kappa B regulation by I kappa B kinase-2 in rheumatoid arthritis synoviocytes. J Immunol 2001; 166:2705-11.

8. Zhang G, Li J, Purkayastha S, Tang Y, Zhang H, Yin Y, Li B, Liu G, Cai D. Hypothalamic programming of systemic ageing involving IKK-beta, NF-kappaB and GnRH. Nature 2013; 497:211-6.

9. Annunziata CM, Davis RE, Demchenko Y, Bellamy W, Gabrea A, Zhan F, Lenz G, Hanamura I, Wright G, Xiao W, Dave S, Hurt EM, Tan B, Zhao H, Stephens O, Santra M, Williams DR, Dang L, Barlogie B, Shaughnessy JD, Jr., Kuehl WM, Staudt LM. Frequent engagement of the classical and alternative

NF-kappaB pathways by diverse genetic abnormalities in multiple myeloma. Cancer Cell 2007; 12:115-30.

10. Gilmore TD. Multiple myeloma: lusting for NF-kappaB. Cancer Cell 2007; 12:95-7.

11. Wertz IE, Dixit VM. Signaling to NF-kappaB: regulation by ubiquitination. Cold Spring Harbor perspectives in biology 2010; 2:a003350.

12. Chen ZJ. Ubiquitination in signaling to and activation of IKK. Immunol Rev 2012; 246:95-106.

13. Ea CK, Deng L, Xia ZP, Pineda G, Chen ZJ. Activation of IKK by TNFalpha requires site-specific ubiquitination of RIP1 and polyubiquitin binding by NEMO. Mol Cell 2006; 22:245-57.

14. Yamazaki K, Gohda J, Kanayama A, Miyamoto Y, Sakurai H, Yamamoto M, Akira S, Hayashi H, Su B, Inoue J. Two mechanistically and temporally distinct NF-kappaB activation pathways in IL-1 signaling. Science signaling 2009; 2:ra66.

15. Rahighi S, Ikeda F, Kawasaki M, Akutsu M, Suzuki N, Kato R, Kensche T, Uejima T, Bloor S, Komander D, Randow F, Wakatsuki S, Dikic I. Specific recognition of linear ubiquitin chains by NEMO is important for NF-kappaB activation. Cell 2009; 136:1098-109.

16. Skaug B, Chen J, Du F, He J, Ma A, Chen ZJ. Direct, noncatalytic mechanism of IKK inhibition by A20. Mol Cell 2011; 44:559-71.

17. Bhoj VG, Chen ZJ. Ubiquitylation in innate and adaptive immunity. Nature 2009; 458:430-7.

18. Chen ZJ, Sun LJ. Nonproteolytic functions of ubiquitin in cell signaling. Mol Cell 2009; 33:275-86.

19. Yang WL, Zhang X, Lin HK. Emerging role of Lys-63 ubiquitination in protein kinase and phosphatase activation and cancer development. Oncogene 2010; 29:4493-503.

20. Xia ZP, Sun L, Chen X, Pineda G, Jiang X, Adhikari A, Zeng W, Chen ZJ. Direct activation of protein kinases by unanchored polyubiquitin chains. Nature 2009; 461:114-9.

21. Lamothe B, Besse A, Campos AD, Webster WK, Wu H, Darnay BG. Site-specific Lys-63-linked tumor necrosis factor receptor-associated factor 6 auto-ubiquitination is a critical determinant of I kappa B kinase activation. J Biol Chem 2007; 282:4102-12.

22. Windheim M, Stafford M, Peggie M, Cohen P. Interleukin-1 (IL-1) induces the Lys63-linked polyubiquitination of IL-1 receptor-associated kinase 1 to facilitate NEMO binding and the activation of IkappaBalpha kinase. Mol Cell Biol 2008; 28:1783-91.

23. Conze DB, Wu CJ, Thomas JA, Landstrom A, Ashwell JD. Lys63-linked polyubiquitination of IRAK-1 is required for interleukin-1 receptor- and toll-like receptor-mediated NF-kappaB activation. Mol Cell Biol 2008; 28:3538-47.

24. Wu CJ, Conze DB, Li T, Srinivasula SM, Ashwell JD. Sensing of Lys 63-linked polyubiquitination by NEMO is a key event in NF-kappaB activation [corrected]. Nat Cell Biol 2006; 8:398-406.

25. Chapman MA, Lawrence MS, Keats JJ, Cibulskis K, Sougnez C, Schinzel AC, Harview CL, Brunet JP, Ahmann GJ, Adli M, Anderson KC, Ardlie KG, Auclair D, Baker A, Bergsagel PL, Bernstein BE, Drier Y, Fonseca R, Gabriel SB, Hofmeister CC, Jagannath S, Jakubowiak AJ, Krishnan A, Levy J, Liefeld T, Lonial S, Mahan S, Mfuko B, Monti S, Perkins LM, Onofrio R, Pugh TJ, Rajkumar SV, Ramos AH, Siegel DS, Sivachenko A, Stewart AK, Trudel S, Vij R, Voet D, Winckler W, Zimmerman T, Carpten J, Trent J, Hahn WC, Garraway LA, Meyerson M, Lander ES, Getz G, Golub TR. Initial genome sequencing and analysis of multiple myeloma. Nature 2011; 471:467-72.

26. Rossi D, Deaglio S, Dominguez-Sola D, Rasi S, Vaisitti T, Agostinelli C, Spina V, Bruscaggin A, Monti S, Cerri M, Cresta S, Fangazio M, Arcaini L, Lucioni M, Marasca R, Thieblemont C, Capello D, Facchetti F, Kwee I, Pileri SA, Foa R, Bertoni F, Dalla-Favera R, Pasqualucci L, Gaidano G. Alteration of BIRC3 and multiple other NF-kappaB pathway genes in splenic marginal zone lymphoma. Blood 2011; 118:4930-4.

27. Bea S, Valdes-Mas R, Navarro A, Salaverria I, Martin-Garcia D, Jares P, Gine E, Pinyol M, Royo C, Nadeu F, Conde L, Juan M, Clot G, Vizan P, Di Croce L, Puente DA, Lopez-Guerra M, Moros A, Roue G, Aymerich M, Villamor N, Colomo L, Martinez A, Valera A, Martin-Subero JI, Amador V, Hernandez L, Rozman M, Enjuanes A, Forcada P, Muntanola A, Hartmann EM, Calasanz MJ, Rosenwald A, Ott G, Hernandez-Rivas JM, Klapper W, Siebert R, Wiestner A, Wilson WH, Colomer D, Lopez-Guillermo A, Lopez-Otin C, Puente XS, Campo

E. Landscape of somatic mutations and clonal evolution in mantle cell lymphoma. Proc Natl Acad Sci U S A 2013; 110:18250-5.

28. Delhase M, Hayakawa M, Chen Y, Karin M. Positive and negative regulation of IkappaB kinase activity through IKKbeta subunit phosphorylation. Science 1999; 284:309-13.

29. Meyer AN, Drafahl KA, McAndrew CW, Gilda JE, Gallo LH, Haas M, Brill LM, Donoghue DJ. Tyrosine Phosphorylation Allows Integration of Multiple Signaling Inputs by IKKbeta. PLoS One 2013; 8:e84497.

30. Liu S, Misquitta YR, Olland A, Johnson MA, Kelleher KS, Kriz R, Lin LL, Stahl M, Mosyak L. Crystal Structure of A Human IkappaB Kinase beta Asymmetric Dimer. J Biol Chem 2013.

31. Wada K, Niida M, Tanaka M, Kamitani T. Ro52-mediated monoubiquitination of IKK{beta} down-regulates NF-kappaB signalling. J Biochem 2009; 146:821-32.

32. Hideshima T, Anderson KC. Molecular mechanisms of novel therapeutic approaches for multiple myeloma. Nat Rev Cancer 2002; 2:927-37.

33. Bromberg JF, Wrzeszczynska MH, Devgan G, Zhao Y, Pestell RG, Albanese C, Darnell JE, Jr. Stat3 as an oncogene. Cell 1999; 98:295-303.

34. Hodge DR, Hurt EM, Farrar WL. The role of IL-6 and STAT3 in inflammation and cancer. Eur J Cancer 2005; 41:2502-12.

35. Liang J, Nagahashi M, Kim EY, Harikumar KB, Yamada A, Huang WC, Hait NC, Allegood JC, Price MM, Avni D, Takabe K, Kordula T, Milstien S, Spiegel S. Sphingosine-1-phosphate links persistent STAT3 activation, chronic intestinal inflammation, and development of colitis-associated cancer. Cancer Cell 2013; 23:107-20.

36. Catlett-Falcone R, Landowski TH, Oshiro MM, Turkson J, Levitzki A, Savino R, Ciliberto G, Moscinski L, Fernandez-Luna JL, Nunez G, Dalton WS, Jove R. Constitutive activation of Stat3 signaling confers resistance to apoptosis in human U266 myeloma cells. Immunity 1999; 10:105-15.

37. Yu H, Pardoll D, Jove R. STATs in cancer inflammation and immunity: a leading role for STAT3. Nat Rev Cancer 2009; 9:798-809.

38. Yu H, Kortylewski M, Pardoll D. Crosstalk between cancer and immune cells: role of STAT3 in the tumour microenvironment. Nat Rev Immunol 2007; 7:41-51.

39. Chauhan D, Uchiyama H, Akbarali Y, Urashima M, Yamamoto K, Libermann TA, Anderson KC. Multiple myeloma cell adhesion-induced interleukin-6 expression in bone marrow stromal cells involves activation of NF-kappa B. Blood 1996; 87:1104-12.

40. Bharti AC, Shishodia S, Reuben JM, Weber D, Alexanian R, Raj-Vadhan S, Estrov Z, Talpaz M, Aggarwal BB. Nuclear factor-kappaB and STAT3 are constitutively active in CD138+ cells derived from multiple myeloma patients, and suppression of these transcription factors leads to apoptosis. Blood 2004; 103:3175-84.

41. Ben-Neriah Y, Karin M. Inflammation meets cancer, with NF-kappaB as the matchmaker. Nat Immunol 2011; 12:715-23.

42. Liu H, Sadygov RG, Yates JR, 3rd. A model for random sampling and estimation of relative protein abundance in shotgun proteomics. Anal Chem 2004; 76:4193-201.

43. Huttlin EL, Jedrychowski MP, Elias JE, Goswami T, Rad R, Beausoleil SA, Villen J, Haas W, Sowa ME, Gygi SP. A tissue-specific atlas of mouse protein phosphorylation and expression. Cell 2010; 143:1174-89.

44. Pulvino M, Liang Y, Oleksyn D, DeRan M, Van Pelt E, Shapiro J, Sanz I, Chen L, Zhao J. Inhibition of proliferation and survival of diffuse large B-cell lymphoma cells by a small-molecule inhibitor of the ubiquitin-conjugating enzyme Ubc13-Uev1A. Blood 2012; 120:1668-77.

45. Zhou H, Wertz I, O'Rourke K, Ultsch M, Seshagiri S, Eby M, Xiao W, Dixit VM. Bcl10 activates the NF-kappaB pathway through ubiquitination of NEMO. Nature 2004; 427:167-71.

46. Abbott DW, Wilkins A, Asara JM, Cantley LC. The Crohn's disease protein, NOD2, requires RIP2 in order to induce ubiquitinylation of a novel site on NEMO. Curr Biol 2004; 14:2217-27.

47. Zhou AY, Shen RR, Kim E, Lock YJ, Xu M, Chen ZJ, Hahn WC. IKKepsilon-mediated tumorigenesis requires K63-linked polyubiquitination by a cIAP1/cIAP2/TRAF2 E3 ubiquitin ligase complex. Cell reports 2013; 3:724-33.

48. Carter RS, Pennington KN, Arrate P, Oltz EM, Ballard DW. Site-specific monoubiquitination of IkappaB kinase IKKbeta regulates its phosphorylation and persistent activation. J Biol Chem 2005; 280:43272-9.

49. Niida M, Tanaka M, Kamitani T. Downregulation of active IKK beta by Ro52-mediated autophagy. Mol Immunol 2010; 47:2378-87.

50. Lee DF, Kuo HP, Liu M, Chou CK, Xia W, Du Y, Shen J, Chen CT, Huo L, Hsu MC, Li CW, Ding Q, Liao TL, Lai CC, Lin AC, Chang YH, Tsai SF, Li LY, Hung MC. KEAP1 E3 ligase-mediated downregulation of NF-kappaB signaling by targeting IKKbeta. Mol Cell 2009; 36:131-40.

51. Udeshi ND, Svinkina T, Mertins P, Kuhn E, Mani DR, Qiao JW, Carr SA. Refined preparation and use of anti-diglycine remnant (K-epsilon-GG) antibody enables routine quantification of 10,000s of ubiquitination sites in single proteomics experiments. Mol Cell Proteomics 2013; 12:825-31.

52. Wang C, Deng L, Hong M, Akkaraju GR, Inoue J, Chen ZJ. TAK1 is a ubiquitin-dependent kinase of MKK and IKK. Nature 2001; 412:346-51.

53. Lamb A, Chen J, Blanke SR, Chen LF. Helicobacter pylori activates NF-kappaB by inducing Ubc13-mediated ubiquitination of lysine 158 of TAK1. J Cell Biochem 2013; 114:2284-92.

54. Liang L, Fan Y, Cheng J, Cheng D, Zhao Y, Cao B, Ma L, An L, Jia W, Su X, Yang J, Zhang H. TAK1 ubiquitination regulates doxorubicin-induced NF-kappaB activation. Cell Signal 2013; 25:247-54.

55. An L, Jia W, Yu Y, Zou N, Liang L, Zhao Y, Fan Y, Cheng J, Shi Z, Xu G, Li G, Yang J, Zhang H. Lys63-linked polyubiquitination of BRAF at lysine 578 is required for BRAF-mediated signaling. Scientific reports 2013; 3:2344.

56. Webster MK, D'Avis PY, Robertson SC, Donoghue DJ. Profound ligand-independent kinase activation of fibroblast growth factor receptor 3 by the activation loop mutation responsible for a lethal skeletal dysplasia, thanatophoric dysplasia type II. Mol Cell Biol 1996; 16:4081-7.

57. Tavormina PL, Bellus GA, Webster MK, Bamshad MJ, Fraley AE, McIntosh I, Szabo J, Jiang W, Jabs EW, Wilcox WR, Wasmuth JJ, Donoghue DJ, Thompson LM, Francomano CA. A novel skeletal dysplasia with developmental delay and acanthosis nigricans is caused by a Lys650Met mutation in the fibroblast growth factor receptor 3 gene. Am J Hum Genet 1999; 64:722-31.

58. Drafahl KA, McAndrew CW, Meyer AN, Haas M, Donoghue DJ. The receptor tyrosine kinase FGFR4 negatively regulates NFkappaB signaling. PLoS One 2010; 5:e14412.

59. Carrano AC, Dillin A, Hunter T. A Kruppel-like factor downstream of the E3 ligase WWP-1 mediates dietary-restriction-induced longevity in Caenorhabditis elegans. Nature communications 2014; 5:3772.

60. Meyer AN, McAndrew CW, Donoghue DJ. Nordihydroguaiaretic acid inhibits an activated fibroblast growth factor receptor 3 mutant and blocks downstream signaling in multiple myeloma cells. Cancer Res 2008; 68:7362-70.

61. Jiao X, Wood LD, Lindman M, Jones S, Buckhaults P, Polyak K, Sukumar S, Carter H, Kim D, Karchin R, Sjoblom T. Somatic mutations in the Notch, NF-KB, PIK3CA, and Hedgehog pathways in human breast cancers. Genes Chromosomes Cancer 2012; 51:480-9.

62. Stephens P, Edkins S, Davies H, Greenman C, Cox C, Hunter C, Bignell G, Teague J, Smith R, Stevens C, O'Meara S, Parker A, Tarpey P, Avis T, Barthorpe A, Brackenbury L, Buck G, Butler A, Clements J, Cole J, Dicks E, Edwards K, Forbes S, Gorton M, Gray K, Halliday K, Harrison R, Hills K, Hinton J, Jones D, Kosmidou V, Laman R, Lugg R, Menzies A, Perry J, Petty R, Raine K, Shepherd R, Small A, Solomon H, Stephens Y, Tofts C, Varian J, Webb A, West S, Widaa S, Yates A, Brasseur F, Cooper CS, Flanagan AM, Green A, Knowles M, Leung SY, Looijenga LH, Malkowicz B, Pierotti MA, Teh B, Yuen ST, Nicholson AG, Lakhani S, Easton DF, Weber BL, Stratton MR, Futreal PA, Wooster R. A screen of the complete protein kinase gene family identifies diverse patterns of somatic mutations in human breast cancer. Nat Genet 2005; 37:590-2.

63. Sjoblom T, Jones S, Wood LD, Parsons DW, Lin J, Barber TD, Mandelker D, Leary RJ, Ptak J, Silliman N, Szabo S, Buckhaults P, Farrell C, Meeh P, Markowitz SD, Willis J, Dawson D, Willson JK, Gazdar AF, Hartigan J, Wu L, Liu C, Parmigiani G, Park BH, Bachman KE, Papadopoulos N, Vogelstein B, Kinzler KW, Velculescu VE. The consensus coding sequences of human breast and colorectal cancers. Science 2006; 314:268-74.

64. Wood LD, Parsons DW, Jones S, Lin J, Sjoblom T, Leary RJ, Shen D, Boca SM, Barber T, Ptak J, Silliman N, Szabo S, Dezso Z, Ustyanksky V, Nikolskaya T, Nikolsky Y, Karchin R, Wilson PA, Kaminker JS, Zhang Z, Croshaw R, Willis J, Dawson D, Shipitsin M, Willson JK, Sukumar S, Polyak K, Park BH, Pethiyagoda CL, Pant PV, Ballinger DG, Sparks AB, Hartigan J, Smith DR, Suh E, Papadopoulos N, Buckhaults P, Markowitz SD, Parmigiani G, Kinzler KW,

Velculescu VE, Vogelstein B. The genomic landscapes of human breast and colorectal cancers. Science 2007; 318:1108-13.

65. Integrated genomic analyses of ovarian carcinoma. Nature 2011; 474:609-15.

66. Seshagiri S, Stawiski EW, Durinck S, Modrusan Z, Storm EE, Conboy CB, Chaudhuri S, Guan Y, Janakiraman V, Jaiswal BS, Guillory J, Ha C, Dijkgraaf GJ, Stinson J, Gnad F, Huntley MA, Degenhardt JD, Haverty PM, Bourgon R, Wang W, Koeppen H, Gentleman R, Starr TK, Zhang Z, Largaespada DA, Wu TD, de Sauvage FJ. Recurrent R-spondin fusions in colon cancer. Nature 2012; 488:660-4.

67. Kan Z, Jaiswal BS, Stinson J, Janakiraman V, Bhatt D, Stern HM, Yue P, Haverty PM, Bourgon R, Zheng J, Moorhead M, Chaudhuri S, Tomsho LP, Peters BA, Pujara K, Cordes S, Davis DP, Carlton VE, Yuan W, Li L, Wang W, Eigenbrot C, Kaminker JS, Eberhard DA, Waring P, Schuster SC, Modrusan Z, Zhang Z, Stokoe D, de Sauvage FJ, Faham M, Seshagiri S. Diverse somatic mutation patterns and pathway alterations in human cancers. Nature 2010; 466:869-73.

68. Dulak AM, Stojanov P, Peng S, Lawrence MS, Fox C, Stewart C, Bandla S, Imamura Y, Schumacher SE, Shefler E, McKenna A, Carter SL, Cibulskis K, Sivachenko A, Saksena G, Voet D, Ramos AH, Auclair D, Thompson K, Sougnez C, Onofrio RC, Guiducci C, Beroukhim R, Zhou Z, Lin L, Lin J, Reddy R, Chang A, Landrenau R, Pennathur A, Ogino S, Luketich JD, Golub TR, Gabriel SB, Lander ES, Beer DG, Godfrey TE, Getz G, Bass AJ. Exome and whole-genome sequencing of esophageal adenocarcinoma identifies recurrent driver events and mutational complexity. Nat Genet 2013; 45:478-86.

69. Bettegowda C, Agrawal N, Jiao Y, Wang Y, Wood LD, Rodriguez FJ, Hruban RH, Gallia GL, Binder ZA, Riggins CJ, Salmasi V, Riggins GJ, Reitman ZJ, Rasheed A, Keir S, Shinjo S, Marie S, McLendon R, Jallo G, Vogelstein B, Bigner D, Yan H, Kinzler KW, Papadopoulos N. Exomic sequencing of four rare central nervous system tumor types. Oncotarget 2013; 4:572-83.

70. Guo G, Sun X, Chen C, Wu S, Huang P, Li Z, Dean M, Huang Y, Jia W, Zhou Q, Tang A, Yang Z, Li X, Song P, Zhao X, Ye R, Zhang S, Lin Z, Qi M, Wan S, Xie L, Fan F, Nickerson ML, Zou X, Hu X, Xing L, Lv Z, Mei H, Gao S, Liang C, Gao Z, Lu J, Yu Y, Liu C, Li L, Fang X, Jiang Z, Yang J, Li C, Zhao X, Chen J, Zhang F, Lai Y, Lin Z, Zhou F, Chen H, Chan HC, Tsang S, Theodorescu D, Li Y, Zhang X, Wang J, Yang H, Gui Y, Wang J, Cai Z. Whole-genome and whole-exome sequencing of bladder cancer identifies frequent

alterations in genes involved in sister chromatid cohesion and segregation. Nat Genet 2013; 45:1459-63.

71. Sato Y, Yoshizato T, Shiraishi Y, Maekawa S, Okuno Y, Kamura T, Shimamura T, Sato-Otsubo A, Nagae G, Suzuki H, Nagata Y, Yoshida K, Kon A, Suzuki Y, Chiba K, Tanaka H, Niida A, Fujimoto A, Tsunoda T, Morikawa T, Maeda D, Kume H, Sugano S, Fukayama M, Aburatani H, Sanada M, Miyano S, Homma Y, Ogawa S. Integrated molecular analysis of clear-cell renal cell carcinoma. Nat Genet 2013; 45:860-7.

72. Tarpey PS, Behjati S, Cooke SL, Van Loo P, Wedge DC, Pillay N, Marshall J, O'Meara S, Davies H, Nik-Zainal S, Beare D, Butler A, Gamble J, Hardy C, Hinton J, Jia MM, Jayakumar A, Jones D, Latimer C, Maddison M, Martin S, McLaren S, Menzies A, Mudie L, Raine K, Teague JW, Tubio JM, Halai D, Tirabosco R, Amary F, Campbell PJ, Stratton MR, Flanagan AM, Futreal PA. Frequent mutation of the major cartilage collagen gene COL2A1 in chondrosarcoma. Nat Genet 2013; 45:923-6.

73. Comprehensive molecular characterization of human colon and rectal cancer. Nature 2012; 487:330-7.

74. Rudin CM, Durinck S, Stawiski EW, Poirier JT, Modrusan Z, Shames DS, Bergbower EA, Guan Y, Shin J, Guillory J, Rivers CS, Foo CK, Bhatt D, Stinson J, Gnad F, Haverty PM, Gentleman R, Chaudhuri S, Janakiraman V, Jaiswal BS, Parikh C, Yuan W, Zhang Z, Koeppen H, Wu TD, Stern HM, Yauch RL, Huffman KE, Paskulin DD, Illei PB, Varella-Garcia M, Gazdar AF, de Sauvage FJ, Bourgon R, Minna JD, Brock MV, Seshagiri S. Comprehensive genomic analysis identifies SOX2 as a frequently amplified gene in small-cell lung cancer. Nat Genet 2012; 44:1111-6.

75. Zang ZJ, Ong CK, Cutcutache I, Yu W, Zhang SL, Huang D, Ler LD, Dykema K, Gan A, Tao J, Lim S, Liu Y, Futreal PA, Grabsch H, Furge KA, Goh LK, Rozen S, Teh BT, Tan P. Genetic and structural variation in the gastric cancer kinome revealed through targeted deep sequencing. Cancer Res 2011; 71:29-39.

Chapter 2: Mutation of Lys171 in IKKβ unleashes a novel mechanism of oncogenic signaling

2.1 Abstract

We reveal that the mutation K171E in IKKβ relies on JAK, gp130 of IL-6 Receptor and TAK1 to induce STAT3 activation without exogenous IL-6. Through BioID-proximity-dependent biotinylation, we identified proteins interacting with activated IKKβ, and via siRNA, we demonstrate that LRPPRC modulates the canonical IL-6- and IKKβ K171E-mediated STAT3 activation. IKKβ K171E further selects for UBE2V2, the human homologue of MMS2 in *Saccharomyces cerevisiae*, to activate STAT3 independently of HUWE1 E3 ubiquitin ligase. We also show that UBC13/UEV1A mediates the ubiquitination of IKKβ K171E. Via LC-MS/MS, we identified 10 major ubiquitination sites in activated IKKβ, in which some Lysines control the phosphorylation of Ser177/Ser181. The oncogenic potential of the K171E mutation is demonstrated by the transformation of IGF-1-stimulated murine myeloid 32D cells into IL3-independent phenotype. This report unravels a mechanism by which the loss of a Lys licenses a Ser/Thr kinase to activate a Tyr phosphorylated transcription factor.

2.2 Statement of Significance

IKKβ modulates the inflammatory NFκB pathway extensively implicated in numerous human diseases, such as cancer. This work elucidates a novel signaling pathway induced by the K171E mutation in IKKβ, initially identified in human hematological malignancies, and proposes a model for the effect of this mutation in cancer.

2.3 Introduction

Inhibitor of κB kinase beta (IKKβ) is the master regulatory kinase that activates the canonical nuclear factor κB (NFκB) inflammatory pathway via Ser/Thr phosphorylation of inhibitor of κB (IκB), which releases NFκB to translocate to the nucleus. IKKβ contributes to survival, stemness, migration and proliferation of prostate cancer (1), including inflammation-induced colitis-associated carcinogenesis (2) and viability of diffuse large B-cell lymphoma (3). IKKβ is part of the IKK complex further composed of IKK and IKK , also known as NFκB essential modulator (NEMO). In response to inflammatory stimuli, IKKβ is activated by MAP3K7, also referred to as Transforming Growth Factor-Beta-Activated Kinase 1 (TAK1), complexed with TAB1/2 that in turn phosphorylates Ser177 priming the autophosphorylation of Ser181 in IKKβ resulting in the activation of the IKK complex (4). The activation of IKK complex, and hence the canonical NFκB signaling, depends on the Lys63-linked ubiquitination of TAK1 and the linear ubiquitination of NEMO (5,6).

The binding of Interleukin-6 (IL-6) to the IL-6 Receptor (IL-6R) leads to the formation of an activated hexameric complex composed of two IL-6/IL-6R heterodimers with gp130 homodimer. Upon dimerization of gp130 subunits, the constitutively bound Janus Kinases (JAKs) become activated and phosphorylate Tyr705 of cytosolic Signal Transducer and Activator of Transcription 3 (STAT3), which translocates into the nucleus (7). Aberrant STAT3 activation contributes to doxorubicin and cisplatin resistance in osteosarcoma (8) and correlates highly with brain metastasis of breast cancer cells (9). Drug-mediated ablation of STAT3 signaling causes inhibition of multiple myeloma (10), liver and colon cancer (11) and lung cancer (12).

Positive feedback regulatory mechanisms upon inflammatory and growth factor stimuli causes STAT3 and NFkB transcription factors to regulate an overlapping set of anti-apoptotic, proliferative and protumorigenic genes (13). The NFκB-STAT3 signaling axis is critical in metastatic breast cancer (14) and chemotherapy responsiveness in patients with chronic lymphocytic leukemia (15). Disruption of these pathways ablates breast cancer stem cell formation implicated in chemotherapy resistance (16), pancreatic tumorigenesis (17) and hepatocellular carcinoma (18).

We previously reported that mutations of Lys at position 171 in the kinase domain of IKKβ, initially identified in hematological malignancies, induce the activation of STAT3 independently of exogenous IL-6 (19). In this work, we reveal that IKKβ K171E relies upon JAK, TAK1 and gp130 subunit of IL-6R to signal to STAT3. In addition, the TAK1 activity is indispensable for STAT3

activation induced by IKKβ K171E. We also observed that the K171E mutation activates p44/42 MAPK (Erk1/2) signaling in the absence of exogenous stimuli, and this mechanism is dependent upon TAK1. Through BioID-proximity dependent biotinylation (20), we identified several interacting partners of IKKβ K171E. Via siRNA, we show that LRPPRC negatively regulates STAT3 signaling mediated by IKKβ K171E and IL-6, while IGF2BP1 and ILK2 have no effect in this pathway. In addition, we show that UBC13 E2 ubiquitin conjugating enzyme further modulates STAT3 signaling induced by IKKβ K171E, while knocking down HECT-domain HUWE1 E3 ubiquitin ligase does not affect the activation of this pathway. In addition, this activated kinase selects for UBE2V2, a cofactor of UBC13 previously shown to be required for DNA damage repair (21), to signal to STAT3.

Inflammation-induced activation of IKKβ has been attributed to the phosphorylation of Ser177/Ser181 in the kinase domain (22). Mutations at Lys171 upregulate the phosphorylation of these sites (19), and this work shows that the constitutive autophosphorylation of activated IKKβ is independent of canonical TAK1. Via LC-MS/MS, we identified a total of 24 ubiquitinated Lysines in full-length IKKβ K171E, in which 10 of these are majorly ubiquitinated. We illustrate that some of these ubiquitinated Lysines regulate the autophosphorylation of Ser177/Ser181. Ubiquitinated Lys147, when mutated, impairs IKKβ kinase activity.

In addition, mutations at Lys171 upregulate the Lys63-linked ubiquitination of Lys147 in IKKβ (19). Lys63-linked ubiquitination stabilizes

signaling functions of proteins in a non-proteasome manner and is an indispensable modification for innate and acquired immune response and DNA damage repair pathway (23). Lys63-linked ubiquitination of homologous sites to Lys147 is further observed at Lys158 in TAK1 required for MKK6 and JNK activation (24) and NFkB signaling during inflammatory stimuli (25-27), and at Lys578 in BRAF V600E (28), in which the latter mutation is an oncogenic driver in melanoma (29). Silencing these ubiquitinated Lys residues, however, abrogates the kinase function of these proteins, attenuates their effector downstream signaling and ablates the Lys63-linked ubiquitination (19,25,28). We solved this challenge by performing various substitutions at Lys147 of IKKβ K171E, creating constructs with partial kinase activity but completely ablated ubiquitination, revealing that Lys147 is solely responsible for STAT3 activation. This suggests that the ubiquitinated Lys147 modulates IKKβ function and activation of signaling pathways.

Lastly, the oncogenic potential of K171E mutation in IKKβ is demonstrated by the transformation of murine myeloid 32D cells into IL-3 independent phenotype.

2.4 Results

Ubiquitinated Lysines modulate the autophosphorylation of IKKβ

We previously reported that ubiquitinated Lys147 is critical for the kinase function of IKKβ (19). In this work, we identified via LC-MS/MS a total of 24 ubiquitinated lysines in full-length IKKβ K171E, in which 10 of these are major sites of ubiquitination (Table 1). Via site-directed mutagenesis, we created various IKKβ constructs in which these ubiquitination sites are mutated (Figure 1). For instance, the previously identified ubiquitination sites Lys301, Lys418, Lys555 and Lys703 (19) are silenced in WT kinase (IKKβ 4KR construct) or in the background of activating mutation (IKKβ K171E 4KR construct). Silencing these four sites in addition to newly identified Lys310, Lys428, Lys509, Lys614, Lys641 creates IKKβ constructs either in the absence (IKKβ 9KR) or presence of the activating mutation (IKKβ K171E 9KR). Lys147 is the main ubiqutination site responsible for the biological activity induced by K171E mutation (19). Therefore, the IKKβ 5KR and IKKβ K171E 10KR constructs contains the K147R mutation.

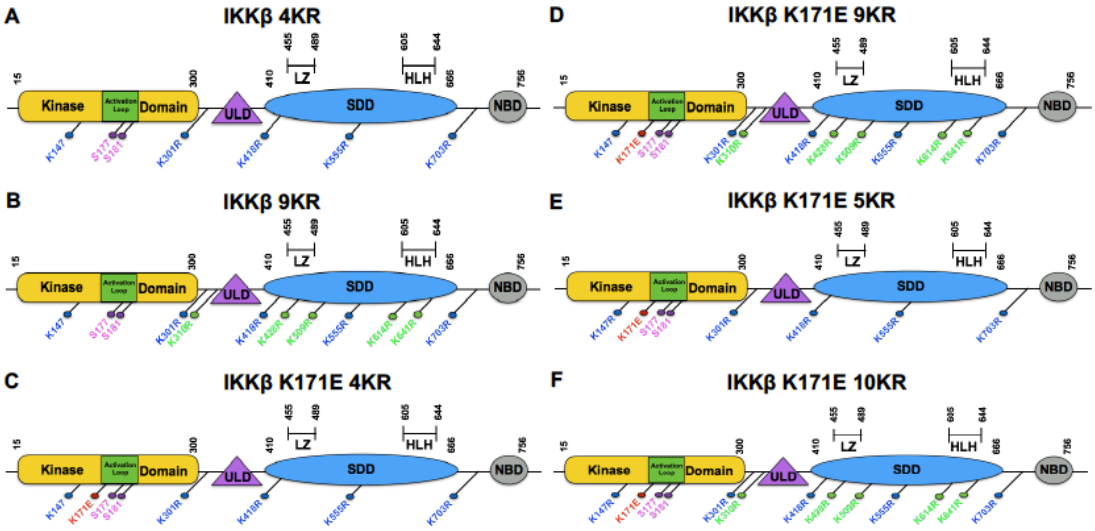

Figure 2.1. Schematic of IKKβ constructs showing mutations of ubiquitination sites identified via LC/MS-MS. Immunoprecipitation of IKKβ from HEK293T cells, followed by LC/MS-MS, revealed ten major sites of ubiquitination in full length protein. Via site-directed mutagenesis, we constructed various mutants of IKKβ harboring mutated Lysine residues (**A-F**). Briefly, IKKβ constructs without the activating K171E mutation, but including K147 ubiquitination site, are IKKβ 4KR (**A**) and IKKβ 9KR (**B**). Constructs with the activating mutation, including K147, are IKKβ K171E 4KR (**C**) and IKKβ K171E 9KR (**D**), and constructs with the activating mutation but mutated K147 are IKKβ K171E 5KR (**E**) and K171E 10KR (**F**).

HEK293T cells were transfected with these IKKβ constructs to analyze whether these ubiquitination sites modulate the autophosphorylation of Ser177/Ser181. It is evident that mutations of Lys301, Lys418, Lys555 and Lys703 sites upregulate the autophosphorylation of Ser177/Ser181 in IKKβ 4KR (Figure 2.A, lane 3), whereas this construct does not exhibit upregulated ubiquitination since it lacks the activating K171E mutation (Figure 2.B, lane 3). Interestingly, the IKKβ 9KR construct exhibits abrogated autophosphorylation and ubiquitination (Figures 2.A and 2.B, lane 4). A signature of the K171E is demonstrated by a phosphorylation laddering that is absent in the IKKβ 4KR construct, for instance (Figure 2.A, lanes 5-8 vs lane 3). The K171E mutation

depends upon ubiquitinated Lys147 to upregulate the autophosphorylation and ubiquitination of IKKβ, a shown by the K171E K147R, K171E 5KR and K171E 10KR constructs which exhibit abrogated modifications (Figures 2.A and 2.B, lanes 9-11 vs. lanes 5-8). Lys147 also controls the phosphorylation of WT IKKβ (19). These results indicate that Lys301, Lys418, Lys555 and Lys703 upregulate the autophosphorylation of IKKβ and Lys147 is the main site that abrogates the kinase function when mutated.

In order to examine the importance of K63-linked ubiquitin linkage, various IKKβ constructs were expressed in HEK293T cells followed by treatment with UBC13 E2 conjugating enzyme inhibitor NSC697923. This molecule covalently binds to Cys87 in the active site of UBC13 E2 conjugating enzyme (30), and it showed to inhibit the total polyubiquitination of TRAF6 *in vitro* (31). Inflammation-induced activation of NFκB has been shown to induce UBC13/UEV1A to build Lys63-linked ubiquitin polymers that contribute to the activation of IKK complex (32). We observed that NSC697923 leads to the phosphorylation of a high-molecular weight species of IKKβ above 190 kDa, and such modification is dependent upon both the K171E mutation and Lys147 (Figure 2.C, lanes 6, 12, 14 versus lanes 8, 10, 16). Immunoprecipitation of total HA-tagged ubiquitinated proteins in lysates, followed by IKKβ immunoblotting, showed a decrease in the ubiquitination signal of K171E 9KR construct in cells treated with NSC697923 (Figure 2.D, lane 14 vs. 13), suggesting that K147 is conjugated to Lys63-linked ubiquitin chains. The high-molecular weight species of ubiquitinated IKKβ is also observed in these samples, which is dependent

upon K171E mutation and Lys147 (Figure 2.D, lanes 6, 12, 14 versus lanes 8, 10,16).

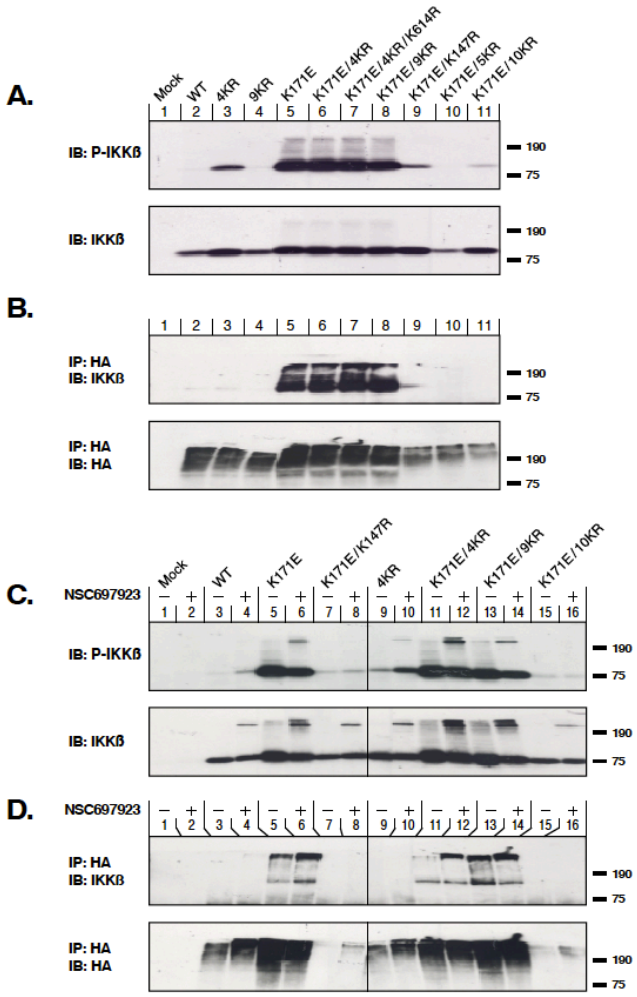

Figure 2.2. Lysines modulate the phosphorylation and ubiquitination of IKKβ. **A**. Transient co-expression of various IKKβ mutants and HA-Ub_3 in HEK293T cells, followed by protein separation via electrophoresis and immunoblotting of membrane with antisera against phosphorylated Ser177/Ser181 epitopes. **B**. Immunoprecipitation of HA-tagged ubiquitinated proteins from lysates derived from experiment as in (A), followed by immunoblotting of membrane with antisera against IKKβ and HA. **C**. Treatment of of HEK293T cells co-expressing IKKβ mutants and HA-Ub_3 with 2uM NSC697923 for 2 hrs, followed by protein separation via electrophoresis mobility shift and immunoblotting of membrane with antisera against phosphorylated Ser177/Ser181 epitopes of IKKβ. **D**. Immunoprecipitation of HA-tagged ubiquitinated proteins from lysates derived from experiment as in (C), followed by immunoblotting of membrane with antisera against IKKβ and HA.

A Lys at position 147 is necessary but not required for autophosphorylation of IKKβ

Mutating Lys147 to Arg, although a conservative substitution, decreases the phosphorylation of IKKβ K171E.

The crystal structure of human activated IKKβ (PDB code 4KIK) reveals that the side chain of Lys147 participates in intermolecular interactions with the side chains of Asp145 and Thr185, which are approximately 4A in proximity to Lys147. Lys171 and Arg144 further stabilize the structure of activated IKKβ via ionic interactions with oxygen atoms of phosphorylated Ser181 in the activation loop (Figure 3.A) (33). Therefore, we aimed to further investigate whether the autophosphorylation of IKKβ K171E can be rescued by introducing residues at position 147 with intrinsic ability to hydrogen bond.

The presence of the Lys at position 147 contributes to the maximal level of autophosphorylation of Ser177/Ser181 induced by K171E, whereas an Arg at K147 decreases this modification in the activation loop (Figure 3.B, lanes 3 vs 12). However, the introduction of Cys, His, Asn and Thr residues partially rescues the autophosphorylation of the Serines (Figure 3.B, lanes 4, 7, 9, 14). The introduction of phosphomimic Asp and Glu, or a Pro, abrogates the kinase function (Figure 3.B, lanes 5, 6, 10). These results illustrate that a Lys at position 147 is necessary but not required for the kinase function of IKKβ K171E.

In addition, the ubiquitination of Lys147 in IKKβ K171E is responsible for the STAT3 signaling, since the removal of Lys147 completely abrogates STAT3 activation (Figure 3.C, lane 3 vs lanes 4-16).

It has been previously reported that loss-of-function mutations that abrogate the phosphorylation of Ser177/Ser181 of IKKβ further decrease the ubiquitination of the kinase (34). Lys147 is a site of ubiquitination in IKKβ WT (19). By introducing various residues at position 147, we uncoupled the phosphorylation from the ubiquitination of this activated kinase. The results show that only the IKKβ K171E construct, which contains Lys147, exhibits the ubiquitin modification (Figure 3.D, lane 3). Although the introduction of additional residues at this site partially rescues the phosphorylation of the kinase (Figure 3.B), as expected none of these constructs show detectable ubiquitination signals (Figure 3.D, lanes 4-16).

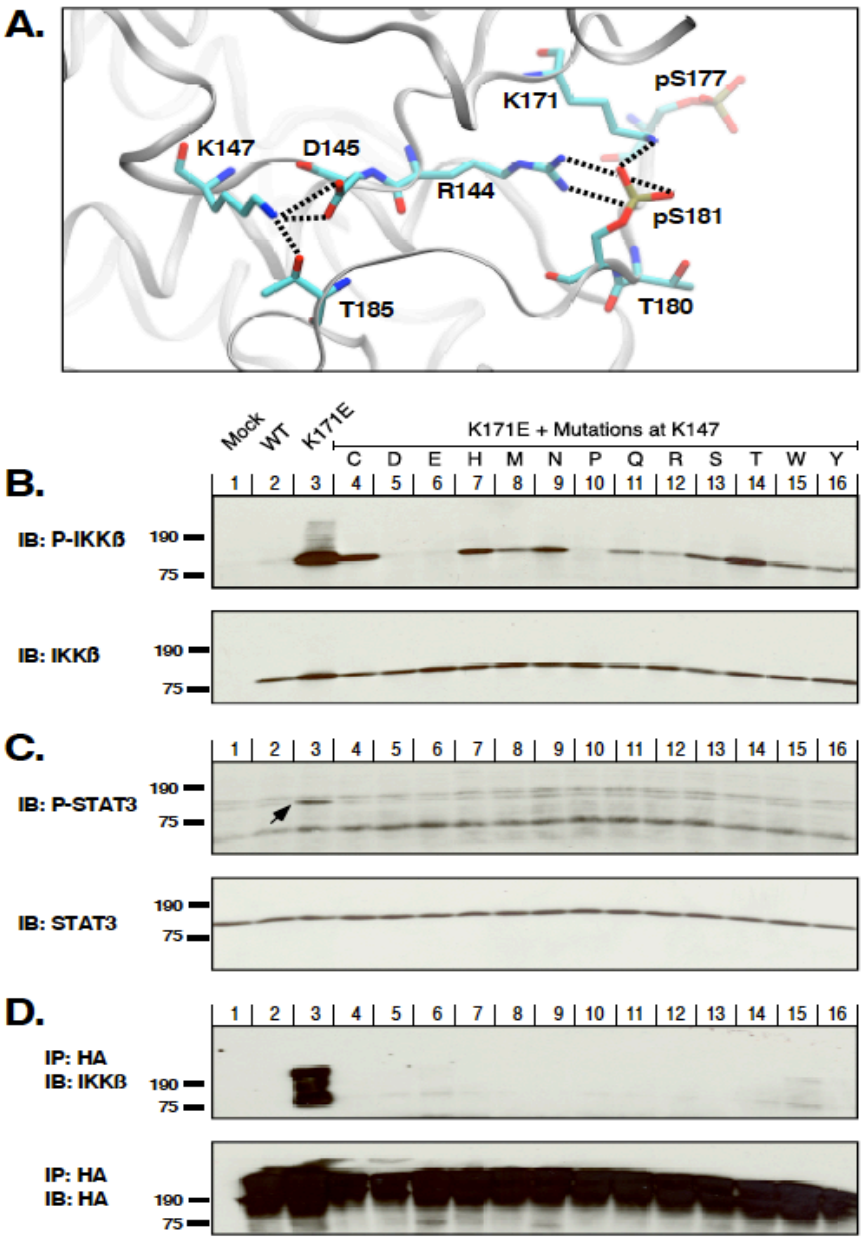

Figure 2.3. **Introduction of residues at position 147 with intrinsic ability to hydrogen bond rescues the kinase function of activated IKKβ**. **A**. Crystal structure representation of the active site of human phosphorylated IKKβ (PDB code 4KIK) by Visual Molecular Dynamics. **B**. Overexpression of IKKβ K171E K147X (X = C, D, E, H, M, N, P, Q, R, T, W, Y) mutants and HA-Ub_3 in HEK293T cells, followed by electrophoresis and immunoblotting with antisera against phosphorylated Ser177/Ser181 epitopes. **C**. Electrophoresis of lysates derived from experiment as in (A), followed by immunoblotting with antisera against phosphorylated Tyr705 epitope of STAT3. **D**. Immunoprecipitation of HA-tagged ubiquitinated proteins from lysates derived from experiment as in (B), followed by immunoblotting of membrane with antisera against IKKβ and HA.

Activated IKKβ signals to STAT3 via JAK, UBC13, gp130 and TAK1

We sought to investigate the mechanism by which the loss of Lys171 in IKKβ induces the Tyr phosphorylation of STAT3. HEK293T cells stimulated with exogenous IL-6 exhibit canonical activated STAT3, whereas control cells pre-treated with JAK inhibitor I, previously shown to inhibit JAK2/STAT3 activation in basal-like breast cancer cells (35), followed by IL-6 stimuli show ablated Tyr-705 phosphorylation of STAT3. (Figure 4.A, lanes 2, 3). Interestingly, HEK293T cells pre-treated with NSC697923 followed by IL-6 stimuli exhibit ablated STAT3 activation (Figure 4.A, lane 4). HEK293T cells overexpressing either IKKβ K171E or IKKβ K171E 4KR show constitutive STAT3 activation in the absence of exogenous cytokines, whereas IKKβ 4KR-overexpressing cells treated with either JAK inhibitor I or NSC697923 exhibit abrogated STAT3 activation (Figure 4.A, lanes 8 and 9). Furthermore, IL-6 does not rescue STAT3 signaling in cells overexpressing IKKβ K171E 4KR pre-treated with JAK inhibitor (Figure 4.A, lane 10), whereas there is a rescue of STAT3 signaling in IKKβ K171E-expressing cells pre-treated with NSC697923 followed by IL-6 stimuli (Figure 4.A, lane 11). These results indicate that K171E mutation in IKKβ, similarly to the canonical IL-6/JAK pathway, relies on UBC13 E2 enzyme and JAK to activate STAT3.

The IL-6-induced activation of STAT3 depends on the cell surface expression and glycosylation of gp130. SC144 hydrochloride, a quinoxalinhydrazide derivative (36), downregulates the glycosylation and

induces the internalization of gp130, leading to impaired STAT3 activation (37). Control HEK293T cells pre-treated with SC144, followed by IL-6 stimuli, exhibit inhibited phosphorylation of STAT3 compared with cells stimulated with IL-6 only (Figure 4.B, lanes 2 and 4). IKKβ K171E mutation, interestingly, relies on gp130 membrane signaling to induce the Tyr phosphorylation of STAT3 as shown by the inhibition of STAT3 phosphorylation in cells treated with SC144 (Figure 4.B, lane 6 vs. lane 5). In addition, IL-6 does not rescue STAT3 phosphorylation in cells IKKβ K171E-expressing pre-treated with SC144 (Figure 4.B, lane 7). These results suggest that, although IKKβ K171E does not require exogenous IL-6 to activate STAT3, it may rely on endogenous IL-6 signaling.

We also aimed to investigate whether TAK1, the upstream kinase of IKKβ, is involved in the activation of STAT3. A selective and irreversible TAK1 inhibitor, (5Z)-7-Oxoeaenol, covalently binds to TAK1 and inhibits its intrinsic ATPase activity and abolishes downstream TAK1-induced p38 MAPK signaling (38). Treatment of HEK293T cells with (5Z)-7-Oxoeaenol completely ablated TAK1 phosphorylation co-transfected with IKKβ constructs (Figure 4.C, panel E, lanes 4, 5 vs 9, 10). Cells overexpressing TAK1/TAB and IKKβ WT showed phosphorylated STAT3 similarly to the overexpression of IKKβ K171E only and TAK1/TAB/ IKKβ K171E (Figure 4.C, lanes 3, 4, 5). Treatment of HEK293T cells overexpressing such constructs with (5Z)-7-Oxoeaenol impaired STAT3 activation in all samples (Figure 4.C, lanes 8-10). In addition, the phosphorylation of Ser177/Ser181 in IKKβ WT is inhibited by (5Z)-7-Oxoeaenol in cells overexpressing TAK1/TAB (Figure 4.C, lane 4 vs 9), whereas the

phosphorylation of IKKβ K171E is not (Figure 4.C, lane 5 vs 10). Therefore, the autophosphorylation of the constitutively activated IKKβ is independent of the canonical TAK1.

We further observed that overexpression of IKKβ K171E induces the phosphorylation of Erk1/2 (p44/p42 MAPK) signaling, which is enhanced by the co-overexpression of IKKβ constructs with TAK1/TAB (Figure 4.C, lane 3, 4, 5). The inhibition of TAK1 activity with (5Z)-7-Oxoeaenol impairs Erk1/2 signaling in cells expressing IKKβ K171E alone and IKKβ constructs co-expressed with TAK1/TAB (Figure 4.C, lanes 8, 9, 10).

IKKβ K171E depends upon TAK1 activity to signal to STAT3 and Erk1/2 in the absence of exogenous IL-6 stimulus.

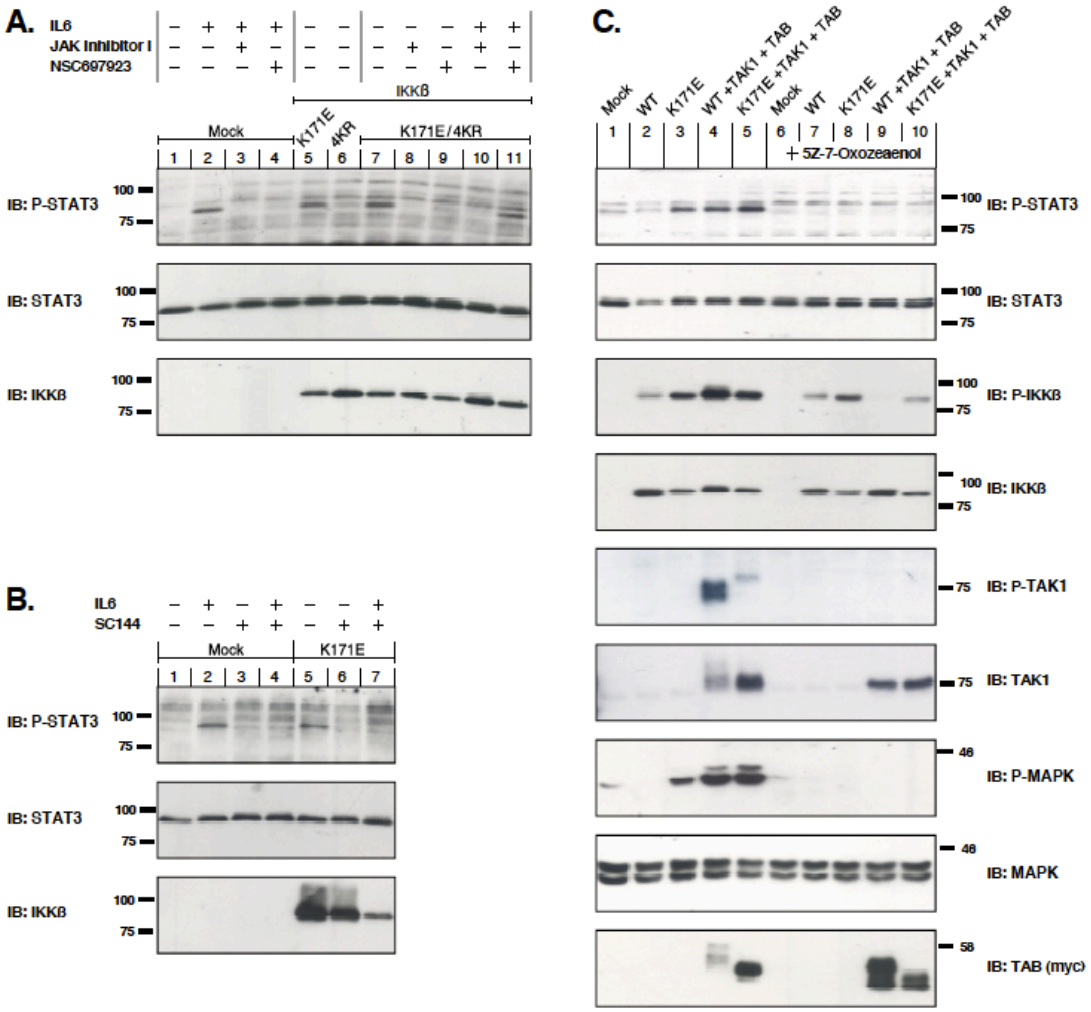

Figure 2.4. Elucidation of a mechanism by which the activating K171E mutation induces STAT3 activation. **A**. HEK293T cells expressing IKKβ constructs were treated with 2uM JAK inhibitor I and 2uM NSC697923 for 2 hrs, followed by electrophoresis and immunoblotting with antisera against phosphorylated Tyr705_STAT3. Membrane was stripped ad immunoblotted for total STAT3, followed by stripping and immunoblotting for IKKβ. **B**. HEK293T cells expressing IKKβ constructs were treated with 50uM SC144 for 8 hrs, and immunoblotting was performed as in (A). **C**. HEK293T cells expressing various combinations of IKKβ, TAK1 and TAB1 constructs were treated with 10uM (5Z)-7-Oxoeaenol for 2 hrs. Lysates were collected and proteins were separated via electrophoresis, followed by immunoblotting of membrane with antibodies against phospho-Tyr705_STAT3, phospho-Ser177/Ser181_IKKβ, phospho-Tyr202/204_MAPK, phospho-T184/187_TAK1, myc to detect myc-tagged TAB, followed by immunoblotting for total STAT3, MAPK, TAK1, and IKKβ. Membrane was stripped in between blots.

Bio-ID identifies proteins interacting with IKKβ K171E 4KR that modulate STAT3 signaling

We aimed to identify proteins interacting with IKKβ K171E 4KR, which may mediate STAT3 activation.

We used the proximity-based biotinylation (BioID) method, which utilizes a constitutively active biotin ligase (BirA R118G, BirA*) fused to a protein of interest (39), in this case IKKβ K171E 4KR (Figure 5.A). We created two independent HEK293T cell lines that stably express Myc-BirA*-IKKβ K171E 4KR (myc-tagged BirA* fused to N-terminus of IKKβ K171E 4KR) and IKKβ K171E 4KR-BirA*-HA (HA-tagged BirA* fused to C-terminus of IKKβ K171E 4KR) (Figure 5.B). By expressing these constructs in HEK293T cells, BirA* biotinylates endogenous proteins interacting with either the N-terminus or C-terminus regions of IKKβ, which are then selectively isolated and purified through biotin-affinity streptavidin columns followed by the identification of the interacting partners via mass spectrometry. The advantage of utilizing this method is the ability to identify weak and transient interacting partners or insoluble proteins such as substrates of E3 ligases, components of nuclear pore complex, and kinase-phosphatase interactions of the Hippo pathway (40-42).

Controls included HEK293T cells not expressing the BirA*- IKKβ constructs but treated with biotin, in which lysates were subjected to similar purification techniques to verify whether nonspecific biotinylated proteins can bind to the streptavidin columns (Figure 5B, lane 1). Immunoblotting for biotin

in lysates derived from both N-terminus BirA* and C-terminus BirA* cell lines showed a significant difference between the samples. Lysates derived from BirA* fused to the N-terminus of IKKβ K171E 4KR exhibited a robust biotinylation profile compared to the lysates derived from BirA* fused to C-terminus region of activated IKKβ (Figure 5B, lanes 2 and 3). This may suggest that the N-terminus region of IKKβ K171E 4KR interacts with more promiscuous and diverse signaling partners compared with the C-terminus region of the protein.

We chose to identify proteins interacting with the N-terminus region of IKKβ K171E 4KR, since they would be in proximity to the kinase domain. Immunoprecipitation of the biotinylated proteins from the N-terminus BioID cell line, followed by MS analysis, led to the identification of 2,469 potential interacting proteins with IKKβ K171E 4KR (data not shown). The proteins were sorted by their abundance represented by the normalized spectral count. Via small interfering RNA (siRNA) analysis, we set out to study the impact of some candidate proteins on the activation of STAT3 induced by both the IL-6 ligand and IKKβ K171E 4KR.

Leucine rich pentatricopeptide repeat containing (LRPPRC) is a mitochondrion-associated protein that stabilizes Bcl-2 to suppress autophagy and enhance cellular survival (43). SiRNA-mediated *LRPPRC* knockdown in IL6-stimulated- and IKKβ K171E 4KR-expressing HEK293T cells resulted in the upregulation of STAT3 phosphorylation (Figure 5.C), suggesting that LRPPRC may play an inhibitory role in the activation of STAT3.

We further investigated the role of Insulin like growth factor 2 mRNA binding protein 2 (IGF2BP1) and Integrin-linked kinase 2 (ILK2) in the activation of STAT3. Briefly, downregulation of IGF2BP1 has been shown to decrease *STAT3* transcript in t(12;21)(p13;q22)-positive acute lymphoblastic leukemia cells (44). In addition, selective inhibition of ILK in promyelocytic leukemic ND4 cells ablates JAK/STAT3 signaling (45). SiRNA-mediated inhibition of *IGF2BP1* had no apparent effect on the level of STAT3 induced by IL-6 and the activated IKKβ (Figure 5.D). In addition, ILK2 further did not impact this pathway (data not shown).

The HECT domain HUWE1 E3 ubiquitin ligase is the most abundant E3 ligase interacting with IKKβ K171E 4KR. HUWE1 has shown to regulate the stability of Shoc-2, which further binds to K63-linked ubiquitin (46). Since we have shown that the ubiquitinated Lys147 in IKKβ K171E is responsible for STAT3 activation, we proposed that HECT domain HUWE1 could be the E3 ubiquitin ligase mediating this signaling mechanism. SiRNA-mediated knockdown of HUWE1 did not impact STAT3 activation in HEK293T cells either stimulated by IL-6 or expressing IKKβ K171E 4KR (Figure 5.E). We further analyzed whether other interacting E3 ligases such as CHIP, UBR4, HERC2, UHRF1, RNF40 and SHPRH mediate STAT3 activation, and none of these candidates impact the activation of STAT3 induced by IL-6 and activated IKKβ (data not shown). Interestingly, we observed that knockdown of UBR4 leads to upregulated phosphorylation of STAT3 in HEK293T cells (data not shown).

Since knocking down various E3 ligases did not impact STAT3 activation, we then hypothesized that the activated IKKβ depends upon the UBC13/UEV1A E2 ubiquitin conjugating enzyme complex. Our mass spectroscopy analysis confirmed that UBC13 and UBE2V1, or UEV1A, interact with the N-terminus region of IKKβ K171E 4KR (data not shown). To our surprise, knockdown of *UBE2N* (UBC13) alone or combined with knockdown of either *UBE2V1* or *UBE2V2* cofactors leads to the upregulation of STAT3 activation in cells expressing IKKβ K171E 4KR (Figure 5.F, lane 3 vs lane 2). Knocking down *UBE2V1*, the cofactor for UBC13, decreases the phosphorylation of STAT3 (Figure 5.F, lane 4 vs lane 3). Interestingly, knockdown of *UBE2V2* alone abolishes the activation of STAT3 in cells expressing IKKβ K171E 4KR (Figure 5.F, lane 5 vs lane 2). A double knockdown of *UBE2N* and *UBE2V2* exhibits lower activation of STAT3 compared with *UBE2N* and *UBE2V1* double knockdown (Figure 5.F, lane 7 vs lane 6). In contrast, knocking down each *UBE2N*, *UBE2V1* and *UBE2V2*, or in various combinations, does not impact STAT3 signaling activated by exogenous recombinant IL-6 ligand, whereas knocking down *UBE2V2* abrogates STAT3 activation induced by IKKβ K171E 4KR (Figure 5.G, lanes 1-8 vs lanes 9-10). These results reveal that IKKβ K171E specifically selects for UVE2V2, the human homologue of MMS2 in *Saccharomyces cerevisiae*, to induce STAT3 activation. The activation of this signaling mechanism, unlike the canonical IL-6-induced STAT3 pathway, is a signature of the K171E mutation of IKKβ.

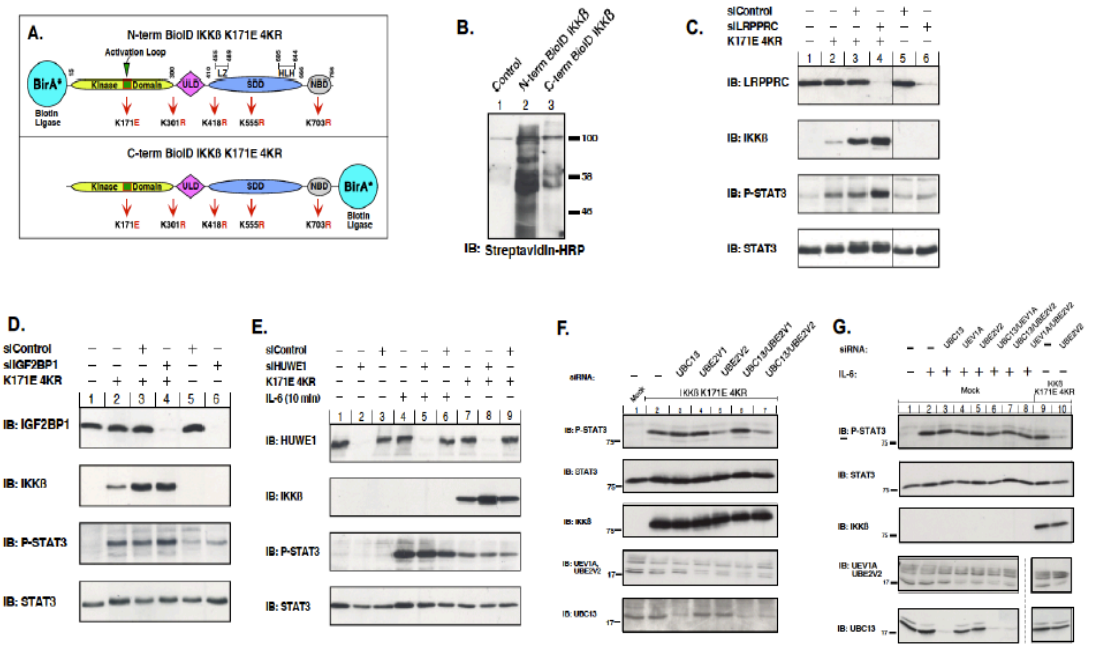

Figure 2.5. siRNA-mediated validation of additional proteins modulating STAT3 activation induced by K171E IKKβ. **A**. Representation of BirA*- IKKβ K171E 4KR stably expressed in HEK293 cells for Bio-ID analysis. **B**. IKKβ HEK293 cell lines were transfected with BirA*- IKKβ K171E 4KR constructs followed by G418 selection to create stable cell lines. Cells were then treated with biotin, followed by immunosera detection in total lysates. **C-G**. HEK293T cells were transfected with siRNA against each target gene for 24 hrs followed by transient transfection with IKKβ constructs for additional 24hrs. Cells were then starved overnight and collected. For experiments involving recombinant human IL-6 stimuli, cells were stimulated with 10ng/mL rhIL-6 for 10 min before collection. Lysates were separated by electrophoresis and transferred to membrane, followed by immunoblotting for phospho-Tyr705_STAT3, total STAT3 and IKKβ. Membrane was stripped in between blots.

Oncogenic potential of IKKβ K171E via transformation of 32D cells

The K171E mutation in IKKβ was initially identified in patients with Multiple Myeloma and Spleen Marginal Zone Lymphoma, and the K171R mutation in Mantle Cell Lymphoma (19).

In order to investigate the biological significance of this activating mutation, we chose to perform assays encompassing the murine myeloid 32D

cells that depend on IL-3 in the culture media for viability. This cell line has been extensively used to determine the oncogenic potential of aberrantly activated proteins, such as FGFR3-TACC3 that occurs in glioblastoma and bladder cancer (47) and FLT3 that is commonly mutated in acute myeloid leukemia (48).

We programmed 32D cells through G418 (Geneticin) selection to stably express the IKKβ constructs, WT, K171E, and K171E 4KR, and confirmed the expression of these constructs (Figure 6.A). We assessed the oncogenic potential of the K171E activating mutation by culturing Insulin Growth Factor-1 (IGF-1)-stimulated IKKβ-expressing 32D cells in the absence of IL-3, and determined the viability of cells by MTT assay.

The viability of control 32D cells remained low in the absence of IL-3 (Figure 6.B, days 2-11). The K171E mutation, in contrast, transformed the cells into IL-3 independent phenotype and contributed to a 4-fold increase in viability compared to the control 32D cells at day 11 (Figure 6.B). Interestingly, the IKKβ K171E 4KR, which harbors the mutations K301R, K418R, K555R and K703R led to the highest increase in cellular viability with a 3-fold increase in viability compared to K171E mutant at day 5 (Figure 6.B). These results indicate that those ubiquitination sites negatively regulate the oncogenic biological property of the K171E mutation. Interestingly, the IKKβ WT also led to the transformation of 32D cells in the presence of IGF-1 (Figure 6.B).

IKKβ activates proliferative and survival cellular pathways, which are enhanced by the oncogenic K171E mutation.

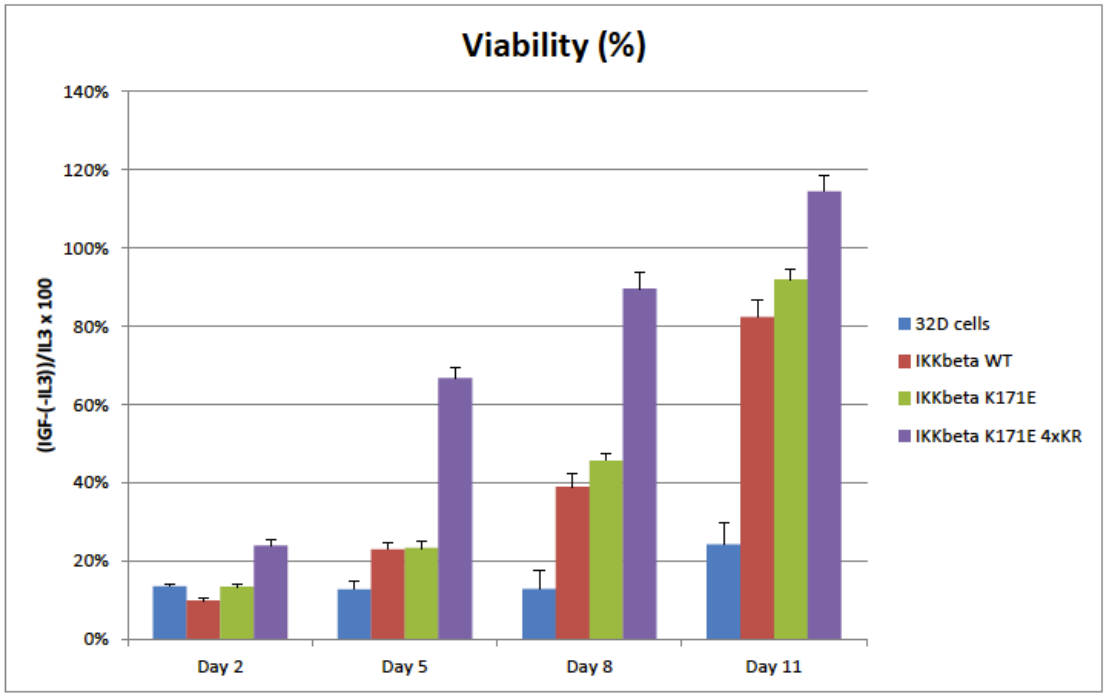

Figure 2.6. Assessing the oncogenic potential of K171E mutation in IKKβ in 32D cells. Murine myeloid 32C cells were electroporated with IKKβ constructs followed by G418 selection creating stable cell lines. Cells were cultured in the presence of murine IGF-1 but in the absence of IL-3 for various time points. During each time point, metabolic and viability readout were assessed by using the MTT assay.

2.5 Discussion

Mutations of the Lysine at position 171 in IKKβ induces the activation of STAT3, which is usually activated via cytokine and growth factor stimuli. This signaling event occurs in the absence of exogenous cytokines and growth factors under our experimental conditions. It is not clear, however, whether this signaling mechanism is dependent upon a specific cellular phenotype.

As with the canonical JAK-STAT3 pathway activated by IL-6 ligand, the activated IKKβ relies upon gp130 membrane signaling of IL-6R and JAK to activate STAT3. We used the SC144 agent to inhibit gp130 membrane signaling and JAK inhibitor I to inhibit JAK activation. SC144 has shown promising combinatorial chemotherapeutic action in colorectal cancer and mouse xenograft breast cancer model (49), and it inhibits cytokine-induced activation of STAT3 in ovarian cancer resulting in impaired ovarian tumor growth *in vivo* (37). JAK inhibitor I has been shown to inhibit JAK2/STAT3 signaling that supports breast cancer proliferation (35).

In addition, we showed that STAT3 phosphorylation activated by either IL-6 or IKKβ K171E is inhibited by treatment of cells with NSC697923, a known inhibitor of UBC13, which has been shown to impair the proliferation and survival of diffuse large B-cell lymphoma cancer cells (31). In contrast, knocking down *UBE2N*, the gene that encodes for UBC13, did not affect IL-6-induced STAT3 activation. This suggests an inhibitory role of NSC697923 beyond UBC13 signaling.

Initially we had hypothesized that some E3 ubiquitin ligase may potentially regulate STAT3 activation induced by IKKβ 171E. We knocked down various E3 ubiquitin ligases, specifically HECT domain HUWE1, identified via LC-MS/MS as a potential interacting partner of IKKβ K171E. The results showed that knocking down E3 ubiquitin ligases did not impact STAT3 activation induced by either exogenous IL-6 or activated IKKβ. This observation may suggest that IKKβ K171E activates STAT3 independently of E3 ubiquitin ligases, or this mutation induces STAT3 activation via some other mechanism to compensate for the loss of E3 ubiquitin ligases.

We then speculated that IKKβ K171E activates STAT3 through UBC13 E2 conjugating enzyme signaling. UBC13, when bound to UBE2V2, catalyzes nuclear Lys63-linked ubiquitination essential for the modulation of DNA damage repair. When bound to UBE2V1, UBC13 catalyzes this non-proteasomal ubiquitin linkage that is indispensable for inflammation-induced NFkB activation (21,32,50). Surprisingly, we were able to impair STAT3 activation induced by K171E IKKβ via the knockdown of UBE2V2 alone, while it did not affect exogenous IL-6-mediated STAT3 activation. Knocking down *UBE2N*, alone or in combination with either *UBE2V1* or *UBE2V2*, upregulated STAT3 signaling. UBE2V1, or UEV1A, and UBE2V2 share >90% sequence similarity and they are structurally similar to UBC13 except that these cofactors lack the catalytic cysteine in the active site (21). This finding may suggest that IKKβ K171E may induce STAT3 activation for nuclear functions that will require further investigation.

It is worth mentioning that we have identified the mitochondrion-associated LRPPRC as an interacting partner of IKKβ. Knocking down *LRPPRC* revealed an increase in the activation of STAT3 in cells stimulated with either IL-6 or expressing activated IKKβ. LRPPRC regulates mitochondrial potential and stabilizes the pro-survival Bcl-2 protein, inhibiting mitochondria degradation through autophagy (43,51). Therefore, it is possible that this activated mutant of IKKβ may rely on the metabolic pathway for signaling.

The TAK1 upstream kinase modulates the phosphorylation of IKKβ and activation of IKK complex (4). Unlike the WT kinase, the activation of IKKβ K171E does not depend upon the canonical TAK1. However, STAT3 signaling induced by this constitutively activated IKKβ does depend upon TAK1. In addition, the K171E mutation induces the phosphorylation of Erk1/2 independently of exogenous cytokines and this event is enhanced by the co-overexpression with TAK1/TAB.

The activity of IKKβ K171E is further dependent upon ubiquitination of Lys147. This site is located in the kinase domain adjacent to the activation loop that harbors the Ser177/Ser181 sites. Other kinases also contain homologous ubiquitinated Lys residues reported to be conjugated to Lys63-linked ubiquitination polymers, such as Lys578 in BRAF V600E (28) and Lys158 in TAK1 (25). Mutating Lys147 to Arg in IKKβ K171E abrogates the ubiquitination at this site, but it also impairs kinase function. In addition, STAT3 signaling is impaired. The same observations have been reported for other sites, such as Lys578Arg mutation in BRAF V600E (28) that impairs MAPK signaling and

Lys158Arg in TAK1 that ablates impair MKK6, JNK, p38 and NFκB signaling (25,27).

Lastly, we have identified 24 total sites of ubiquitination in activated IKKβ, in which 10 of them are major sites of ubiquitination. We have previously reported that Lys301, Lys418, Lys555 and Lys703 are ubiquitinated in IKKβ WT and K171E, but the activating mutation upregulates this modification at these sites (19). In this work, we have shown that these sites when mutated upregulate the phosphorylation of IKKβ, suggesting that these ubiquitinated lysine residues modulate the kinase function. In addition, mutating Lys301, Lys418, Lys555 and Lys703 unleashes the oncogenic potential of K171E mutation in IKKβ, leading to the transformation of 32D cells phenotype.

Ours is the first work to unravel a signaling mechanism unleashed as a result of the K171E mutation in IKKβ. A vast number of reports have focused their efforts on understanding how mutations in receptor and cytoplasmic tyrosine kinases contribute to aberrant cellular signaling and cancer aggressiveness. We have previously described mutations in IKKβ in diverse cancers (19). It is not clear whether such mutations are active or passenger drivers of tumorigenesis. Additional work will be required to further investigate whether mutations in IKKβ, if any beyond the one described herein, can activate pathways beyong NFkB and perform oncogenic functions.

2.6 Methods

Cell culture and transfections: HEK293T cells were cultured and transfected with various IKKβ constructs, HA-Ub and HA-NEMO as previously described (19).

Plasmid constructs: IKKβ WT 4KR (K301R, K418R, K555R and K703R) and IKKβ K171E 4KR plasmids were generated by Quikchange site-directed mutagenesis and confirmed by DNA sequencing as previously described (19). The IKKβ K171E 4KR construct was sub-cloned into mycBioID pcDNA3.1 using EcoRV and AflII sites and also into BioID-HA tag pcDNA3.1 using AfeI and BsiWI sites.

IKKbeta WT was subcloned into pLXSN by three-part ligation using EcoRI, KpnI and NotI. Subsequent IKKbeta derivatives were generated by ligation into IKKbeta WT pLXSN using BspEI and SalI sites. hTAK1 in pCMV6-XL5 was a gift from Dr. Leslie Thompson (UC Irvine) and myc-TAB1 in pcDNA3 was a gift from Dr. Carol Prives (Columbia University).

Cell culture for immunoblot and siRNA analysis: HEK293T cells were grown in DMEM with 10% FBS and maintained in 10% CO_2 at 37°C. Cells were transfected with plasmid DNA using calcium phosphate precipitation at 3% CO_2.

BioID Cell Lines and Transfection: HEK 293 cells were maintained at 10% CO_2 at 37˚C in DMEM supplemented with 10% FBS. The cells were transfected via calcium phosphate method and the transfected cells were subjected to G418 sulfate (Geneticin from Gibco, 0.5 mg/mL) selection for about 3 weeks while passing.

Ubiquitination assay: HEK293T cells were co-transfected with constructs to express IKKβ and HA-Ub_3 clones as previously described (19). Briefly, cells were starved and collected in RIPA lysis buffer with protease and phosphatase inhibitors, including 5mM NEM. For immunoprecipitation of HA-tagged ubiquitinated proteins, lysates were incubated overnight with HA antisera (F-7, Santa Cruz Biotechnology), followed by the addition of 50% Protein A Sepharose. Samples were then washed extensively in ELB buffer (50mM HEPES-KOH pH 7.41, 250mM NaCl, 0.1%NP40, 5mM EDTA, 2M urea) followed by RIPA buffer, as previously described (19). Proteins were separated by electrophoresis (10% SDS-PAGE), followed by transfer to membrane. Ubiquitinated IKKβ was analyzed by immunoblotting with antisera (G-8, Santa Crus Biotechnology).

Electrophoresis, Immunoblotting and additional reagents: Lysates were collected in RIPA lysis buffer and loaded in 10-12.5% SDS-PAGE, followed by transfer to Immobilon membrane. Immunoprecipitation and immunoblotting experiments have been performed as previously described (19). Immunoblotting reagents are obtained from the following sources: Antibodies of IKKβ (H-4), IKKβ (G-8), HA-probe (F-7), STAT3 (C-20), IGF2BP1 (D-9), Myc (9E10), LRPPRC (H-300), TAK1 (M-579) from Santa Cruz Biotechnology; Phospho-IKKα/β (Ser176/180) (16A6), Phospho-STAT3 (Tyr705) (D3A7), Phospho-TAK1 (T184/187) (4531S) from Cell Signaling Technology; HUWE1 (A300-486A) from Bethyl Laboratories; Streptavidin Horseradish Peroxidase (HRP) Conjugate (Cat. 434323) from Invitrogen; horseradish peroxidase (HRP)

anti-mouse, HRP anti-rabbit from GE Healthcare. Enhanced chemiluminence (ECL) reagents were from GE Healthcare; NSC697923 was obtained from Santa Cruz Biotechnology; MG132 and (5Z)-7-Oxoeaenol from Tocris Bioscience; recombinant human IL-6 and recombinant human IGF-1 from Life Technologies; JAK inhibitor I from EMD Millipore; SC144 hydrochloride from Sigma-Aldrich; recombinant mouse IL-3 from R&D Systems.

32D cells and viability assay: 32D clone 3 (ATCC CRL-11346) cells were maintained in RPMI1640 medium with 10% FBS, 1% penicillin/streptomycin, and 5 ng/mL mouse IL3 in 5% CO_2 at 37°C. A total of 1 × 10^6 exponentially growing 32D cells were electroporated (1,500 V, 10 ms, 3 pulse) by the Neon Transfection System (Invitrogen) using 25 µg of IKKbeta derivatives in pLXSN plus 5 ug of pZap. Twenty-four hours after transfection, cells were refed and maintained for 1 week prior to beginning selection with 1.5 mg/mL Geneticin (G418) sulfate to generate stable cell lines.

For metabolic assays, MTT assays were performed. Cell lines were seeded at 4 × 10^5 cell/ml in 50 ml flasks containing RPMI with 10% FBS, 5 ng/mL IL3 (+IL3) or RPMI with 10% FBS, 50 ng/ml hIFG-1 (+IGF) or RPMI with 10% FBS (-IL3) in triplicate. On days, 2,5,8 and 11, flasks were scraped and 500 ul of cultures were transferred to 24 well plates in triplicate. 50 ul of a stock solution of 5 mg/mL in PBS of thiazolyl blue tetrazolium bromide (MTT) (Sigma) was added. After incubation at 37°C, 5% CO_2 for approximately 4 hours, 500 ul of 0.04 mol/L HCl in isopropanol was added and incubated again for at least 30

minutes. Samples were transferred to cuvettes and absorbance was measured at 570 nm.

siRNA experiments: 7×10^4 ~1.3×10^5 of HEK293T cells were plated into 6-well plates and incubated at 10% CO_2 at 37˚C in DMEM supplemented with 10% FBS for 24 h. All siRNA reagents used were siGENOME SMARTpool purchased from GE Dharmacon. Cells were transfected with targeting or Non-targeting (Negative) siRNA (GE Dharmacon) using DharmaFECT reagent (GE Dharmacon) according to the manufacturer's instructions (Final concentration varied from 25nM to 100nM). The DMEM media was replaced 24h after the transfection to reduce cytotoxicity. 48h after the siRNA transfection, IKKβ K171E 4KR plasmid was transfected using calcium phosphate method and incubated at 3% CO_2 overnight. Cells were starved for 18h before harvest and lysis using RIPA buffer (50mM Tris pH 7.5, 150mM NaCl, 1% Triton X-100, 1% DOC, 0.1% SDS, 50mM NaF, 0.1mM PMSF, 10µg/ml Aprotinin, 1mM Na_3VO_4).

Bio-ID proximity-dependent biotinylation: HEK293 cells were maintained at 10% CO_2 at 37˚C in DMEM supplemented with 10% FBS. The cells were transfected with Myc-BirA*-IKKβ K171E 4KR and IKKβ K171E 4KR-BirA*-HA via calcium phosphate method and the transfected cells were subjected to G418 sulfate (Geneticin from Gibco, 0.5 mg/mL) selection for about 3 weeks while passing stable cell lines. Cells were then incubated for 24h in DMEM with 0.5mg/mL G418 sulfate and 50µM Biotin. Cells were treated with 10µM of MG132 ~4h prior to lysis. Cells were lysed at 25˚C in 1ml BioID lysis buffer. Triton X-100 was added to 2% final concentration. Cells were sonicated

following the protocol (20). Supernatants were incubated with 600 µL of streptavidin conjugated Dynabeads (Dynabeads® MyOne™ Streptavidin C1 from Invitrogen) overnight at 4˚C. Beads were collected and washed as previously indicated (20). 10% of samples were reserved for Western Blot analysis. 90% of the samples were analyzed by mass spectrometry.

Mass spectroscopy: HEK293T cells were co-transfected with IKKβ, HA-Ub_3 and HA-NEMO clones, starved before collection, and lysates were collected in RIPA as previously described (19). Briefly, after collection lysates were sonicated and KKβ was immunoprecipitated with antiserum (H-4, Santa Cruz Biotechnology). Samples were analyzes as previously described (19).

2.7 Acknowledgments

We would like to thank Joseph W. Kaus and Ignacio Lópes-Peña for their assistance in the preparation of the Figure 3, panel A, related to the crystal structure of human activated IKKβ. We also want to thank Khatereh Motamedchaboki for her assistance in experiments related to LC/MS-MS analysis.

Chapter 2, in full, is the work currently being prepared for submission for publication. Gallo L.H. and Ko J., Meyer A.N., Nelson K.N., Motamedchaboki K., Donoghue D.J. “Mutation of Lys171 in IKKBeta Unleashes a Novel Oncogenic Mechanism Signaling”. The first co-author of the work is the author of this dissertation.

2.8 References

1. Zhang Y, Lapidus RG, Liu P, Choi EY, Adediran S, Hussain A, Wang X, Liu X, Dan HC. Targeting IkappaB Kinase beta/NF-kappaB Signaling in Human Prostate Cancer by a Novel IkappaB Kinase beta Inhibitor CmpdA. Mol Cancer Ther **2016**;15(7):1504-14 doi 10.1158/1535-7163.MCT-15-0999.

2. Koliaraki V, Pasparakis M, Kollias G. IKKbeta in intestinal mesenchymal cells promotes initiation of colitis-associated cancer. J Exp Med **2015**;212(13):2235-51 doi 10.1084/jem.20150542.

3. Agarwal NK, Kim CH, Kunkalla K, Konno H, Tjendra Y, Kwon D, Blonska M, Kozloski GA, Moy VT, Verdun RE, Barber GN, Lossos IS, Vega F. Active IKKbeta promotes the stability of GLI1 oncogene in diffuse large B-cell lymphoma. Blood **2016**;127(5):605-15 doi 10.1182/blood-2015-07-658781.

4. Zhang J, Clark K, Lawrence T, Peggie MW, Cohen P. An unexpected twist to the activation of IKKbeta: TAK1 primes IKKbeta for activation by autophosphorylation. Biochem J **2014**;461(3):531-7 doi 10.1042/BJ20140444.

5. Chen J, Chen ZJ. Regulation of NF-kappaB by ubiquitination. Curr Opin Immunol **2013**;25(1):4-12 doi 10.1016/j.coi.2012.12.005.

6. Iwai K, Fujita H, Sasaki Y. Linear ubiquitin chains: NF-kappaB signalling, cell death and beyond. Nat Rev Mol Cell Biol **2014**;15(8):503-8 doi 10.1038/nrm3836.

7. Yu H, Lee H, Herrmann A, Buettner R, Jove R. Revisiting STAT3 signalling in cancer: new and unexpected biological functions. Nat Rev Cancer **2014**;14(11):736-46 doi 10.1038/nrc3818.

8. Tu B, Zhu J, Liu S, Wang L, Fan Q, Hao Y, Fan C, Tang TT. Mesenchymal stem cells promote osteosarcoma cell survival and drug resistance through activation of STAT3. Oncotarget **2016**;7(30):48296-308 doi 10.18632/oncotarget.10219.

9. Lee HT, Xue J, Chou PC, Zhou A, Yang P, Conrad CA, Aldape KD, Priebe W, Patterson C, Sawaya R, Xie K, Huang S. Stat3 orchestrates

interaction between endothelial and tumor cells and inhibition of Stat3 suppresses brain metastasis of breast cancer cells. Oncotarget **2015**;6(12):10016-29 doi 10.18632/oncotarget.3540.

10. Sagawa M, Tabayashi T, Kimura Y, Tomikawa T, Nemoto-Anan T, Watanabe R, Tokuhira M, Ri M, Hashimoto Y, Iida D, Kizaki M. TM-233, a novel analog of 1'-acetoxychavicol acetate, induces cell death in myeloma cells by inhibiting both JAK/STAT and proteasome activities. Cancer Sci **2015**;106(4):438-46 doi 10.1111/cas.12616.

11. Zhao C, Wang W, Yu W, Jou D, Wang Y, Ma H, Xiao H, Qin H, Zhang C, Lu J, Li S, Li C, Lin J, Lin L. A novel small molecule STAT3 inhibitor, LY5, inhibits cell viability, colony formation, and migration of colon and liver cancer cells. Oncotarget **2016**;7(11):12917-26 doi 10.18632/oncotarget.7338.

12. Guo S, Luo W, Liu L, Pang X, Zhu H, Liu A, Lu J, Ma DL, Leung CH, Wang Y, Chen X. Isocryptotanshinone, a STAT3 inhibitor, induces apoptosis and pro-death autophagy in A549 lung cancer cells. J Drug Target **2016**:1-28 doi 10.3109/1061186X.2016.1157882.

13. Grivennikov SI, Karin M. Dangerous liaisons: STAT3 and NF-kappaB collaboration and crosstalk in cancer. Cytokine Growth Factor Rev **2010**;21(1):11-9 doi 10.1016/j.cytogfr.2009.11.005.

14. Snyder M, Huang J, Huang XY, Zhang JJ. A signal transducer and activator of transcription 3.Nuclear Factor kappaB (Stat3.NFkappaB) complex is necessary for the expression of fascin in metastatic breast cancer cells in response to interleukin (IL)-6 and tumor necrosis factor (TNF)-alpha. J Biol Chem **2014**;289(43):30082-9 doi 10.1074/jbc.M114.591719.

15. Liu FT, Jia L, Wang P, Wang H, Farren TW, Agrawal SG. STAT3 and NF-kappaB cooperatively control in vitro spontaneous apoptosis and poor chemo-responsiveness in patients with chronic lymphocytic leukemia. Oncotarget **2016**;7(22):32031-45 doi 10.18632/oncotarget.8672.

16. Saha S, Mukherjee S, Khan P, Kajal K, Mazumdar M, Manna A, Mukherjee S, De S, Jana D, Sarkar D, Das T. Aspirin Suppresses the Acquisition of Chemoresistance in Breast Cancer by Disrupting an NFkappaB-IL6 Signaling Axis Responsible for the Generation of Cancer

Stem Cells. Cancer Res **2016**;76(7):2000-12 doi 10.1158/0008-5472.CAN-15-1360.

17. Tan XL, Bhattacharyya KK, Dutta SK, Bamlet WR, Rabe KG, Wang E, Smyrk TC, Oberg AL, petersen GM, Mukhopadhyay D. Metformin suppresses pancreatic tumor growth with inhibition of NFkappaB/STAT3 inflammatory signaling. Pancreas **2015**;44(4):636-47 doi 10.1097/MPA.0000000000000308.

18. Lin WL, Lai DY, Lee YJ, Chen NF, Tseng TH. Antitumor progression potential of morusin suppressing STAT3 and NFkappaB in human hepatoma SK-Hep1 cells. Toxicol Lett **2015**;232(2):490-8 doi 10.1016/j.toxlet.2014.11.031.

19. Gallo LH, Meyer AN, Motamedchaboki K, Nelson KN, Haas M, Donoghue DJ. Novel Lys63-linked ubiquitination of IKKbeta induces STAT3 signaling. Cell Cycle **2014**;13(24):3964-76 doi 10.4161/15384101.2014.988026.

20. Roux KJ, Kim DI, Burke B. BioID: a screen for protein-protein interactions. Current protocols in protein science / editorial board, John E Coligan [**2013**;74:Unit 19 23].

21. Andersen PL, Zhou H, Pastushok L, Moraes T, McKenna S, Ziola B, Ellison MJ, Dixit VM, Xiao W. Distinct regulation of Ubc13 functions by the two ubiquitin-conjugating enzyme variants Mms2 and Uev1A. J Cell Biol **2005**;170(5):745-55 doi 10.1083/jcb.200502113.

22. Carter RS, Geyer BC, Xie M, Acevedo-Suarez CA, Ballard DW. Persistent activation of NF-kappa B by the tax transforming protein involves chronic phosphorylation of IkappaB kinase subunits IKKbeta and IKKgamma. J Biol Chem **2001**;276(27):24445-8.

23. Wu X, Karin M. Emerging roles of Lys63-linked polyubiquitylation in immune responses. Immunol Rev **2015**;266(1):161-74 doi 10.1111/imr.12310.

24. Wang C, Deng L, Hong M, Akkaraju GR, Inoue J, Chen ZJ. TAK1 is a ubiquitin-dependent kinase of MKK and IKK. Nature **2001**;412(6844):346-51.

25. Fan Y, Yu Y, Shi Y, Sun W, Xie M, Ge N, Mao R, Chang A, Xu G, Schneider MD, Zhang H, Fu S, Qin J, Yang J. Lysine 63-linked polyubiquitination of TAK1 at lysine 158 is required for tumor necrosis factor alpha- and interleukin-1beta-induced IKK/NF-kappaB and JNK/AP-1 activation. J Biol Chem **2010**;285(8):5347-60.

26. Liang L, Fan Y, Cheng J, Cheng D, Zhao Y, Cao B, Ma L, An L, Jia W, Su X, Yang J, Zhang H. TAK1 ubiquitination regulates doxorubicin-induced NF-kappaB activation. Cell Signal **2013**;25(1):247-54.

27. Fan Y, Yu Y, Mao R, Zhang H, Yang J. TAK1 Lys-158 but not Lys-209 is required for IL-1beta-induced Lys63-linked TAK1 polyubiquitination and IKK/NF-kappaB activation. Cell Signal **2011**;23(4):660-5.

28. An L, Jia W, Yu Y, Zou N, Liang L, Zhao Y, Fan Y, Cheng J, Shi Z, Xu G, Li G, Yang J, Zhang H. Lys63-linked polyubiquitination of BRAF at lysine 578 is required for BRAF-mediated signaling. Scientific reports **2013**;3:2344.

29. Holderfield M, Deuker MM, McCormick F, McMahon M. Targeting RAF kinases for cancer therapy: BRAF-mutated melanoma and beyond. Nat Rev Cancer **2014**;14(7):455-67 doi 10.1038/nrc3760.

30. Hodge CD, Edwards RA, Markin CJ, McDonald D, Pulvino M, Huen MS, Zhao J, Spyracopoulos L, Hendzel MJ, Glover JNM. Covalent Inhibition of Ubc13 Affects Ubiquitin Signaling and Reveals Active Site Elements Important for Targeting. ACS Chem Biol **2015**;10(7):1718-28 doi 10.1021/acschembio.5b00222.

31. Pulvino M, Liang Y, Oleksyn D, DeRan M, Van Pelt E, Shapiro J, Sanz I, Chen L, Zhao J. Inhibition of proliferation and survival of diffuse large B-cell lymphoma cells by a small-molecule inhibitor of the ubiquitin-conjugating enzyme Ubc13-Uev1A. Blood **2012**;120(8):1668-77.

32. Hodge CD, Spyracopoulos L, Glover JN. Ubc13: the Lys63 ubiquitin chain building machine. Oncotarget **2016** doi 10.18632/oncotarget.10948.

33. Liu S, Misquitta YR, Olland A, Johnson MA, Kelleher KS, Kriz R, Lin LL, Stahl M, Mosyak L. Crystal Structure of A Human IkappaB Kinase beta Asymmetric Dimer. J Biol Chem **2013**.

34. Carter RS, Pennington KN, Ungurait BJ, Arrate P, Ballard DW. Signal-induced ubiquitination of I kappaB Kinase-beta. J Biol Chem **2003**;278(49):48903-6.

35. Marotta LL, Almendro V, Marusyk A, Shipitsin M, Schemme J, Walker SR, Bloushtain-Qimron N, Kim JJ, Choudhury SA, Maruyama R, Wu Z Gonen M, Mulvey LA, Bessarabova MO, Huh SJ, Silver SJ, Kim SY, Park SY, Lee SY, Lee HE, Anderson KS, Richardson AL, Nikolskaya T, Nikolsky Y, Liu XS, Root DE, Hahn WC, Franck DA, Polyak K. The JAK2/STAT3 signaling pathway is required for growth of CD44(+)CD24(-) stem cell-like breast cancer cells in human tumors. J Clin Invest **2011**;121(7):2723-35.

36. Grande F, Aiello F, Grazia OD, Brizzi A, Garofalo A, Neamati N. Synthesis and antitumor activities of a series of novel quinoxalinhydrazides. Bioorg Med Chem **2007**;15(1):288-94 doi 10.1016/j.bmc.2006.09.073.

37. Xu S, Grande F, Garofalo A, Neamati N. Discovery of a novel orally active small-molecule gp130 inhibitor for the treatment of ovarian cancer. Mol Cancer Ther **2013**;12(6):937-49 doi 10.1158/1535-7163.MCT-12-1082.

38. Wu J, Powell F, Larsen NA, Lai Z, Byth KF, Read J, Gu RF, Roth M, Toader D, Saeh JC, Chen H. Mechanism and in vitro pharmacology of TAK1 inhibition by (5Z)-7-Oxozeaenol. ACS Chem Biol **2013**;8(3):643-50 doi 10.1021/cb3005897.

39. Roux KJ, Kim DI, Raida M, Burke B. A promiscuous biotin ligase fusion protein identifies proximal and interacting proteins in mammalian cells. J Cell Biol **2012**;196(6):801-10.

40. Coyaud E, Mis M, Laurent EM, Dunham WH, Couzens AL, Robitaille M, Gingras AC, Angers S, Raught B. BioID-based Identification of Skp Cullin F-box (SCF)beta-TrCP1/2 E3 Ligase Substrates. Mol Cell Proteomics **2015**;14(7):1781-95 doi 10.1074/mcp.M114.045658.

41. Kim DI, Birendra KC, Zhu W, Motamedchaboki K, Doye V, Roux KJ. Probing nuclear pore complex architecture with proximity-dependent biotinylation. Proc Natl Acad Sci U S A **2014**;111(24):E2453-61.

42. Couzens AL, Knight JD, Kean MJ, Teo G, Weiss A, Dunham WH, Lin ZY, Bagshaw RD, Sicheri F, Pawson T, Wrana JL, Choi H, Gingras AC. Protein interaction network of the mammalian Hippo pathway reveals

mechanisms of kinase-phosphatase interactions. Science signaling **2013**;6(302):rs15.

43. Zou J, Yue F, Jiang X, Li W, Yi J, Liu L. Mitochondrion-associated protein LRPPRC suppresses the initiation of basal levels of autophagy via enhancing Bcl-2 stability. Biochem J **2013**;454(3):447-57 doi 10.1042/BJ20130306.

44. Stoskus M, Eidukaite A, Griskevicius L. Defining the significance of IGF2BP1 overexpression in t(12;21)(p13;q22)-positive leukemia REH cells. Leuk Res **2016**;47:16-21 doi 10.1016/j.leukres.2016.05.009.

45. Tabe Y, Jin L, Tsutsumi-Ishii Y, Xu Y, McQueen T, Priebe W, Mills GB, Ohsaka A, Nagaoka I, Andreeff M, Konopleva M. Activation of integrin-linked kinase is a critical prosurvival pathway induced in leukemic cells by bone marrow-derived stromal cells. Cancer Res **2007**;67(2):684-94 doi 10.1158/0008-5472.CAN-06-3166.

46. Jang ER, Shi P, Bryant J, Chen J, Dukhande V, Gentry MS, Jang H, Jeoung M, Galperin E. HUWE1 is a molecular link controlling RAF-1 activity supported by the Shoc2 scaffold. Mol Cell Biol **2014**;34(19):3579-93 doi 10.1128/MCB.00811-14.

47. Nelson KN, Meyer AN, Siari A, Campos AR, Motamedchaboki K, Donoghue DJ. Oncogenic Gene Fusion FGFR3-TACC3 Is Regulated by Tyrosine Phosphorylation. Mol Cancer Res **2016**;14(5):458-69 doi 10.1158/1541-7786.MCR-15-0497.

48. Mizuki M, Fenski R, Halfter H, Matsumura I, Schmidt R, Muller C, Gruning W, Krats-Albers K, Serve S, Steur C, Buchner T, Kienast J, Kanakura Y, berdel WE, Serve H. Flt3 mutations from patients with acute myeloid leukemia induce transformation of 32D cells mediated by the Ras and STAT5 pathways. Blood **2000**;96(12):3907-14.

49. Oshima T, Cao X, Grande F, Yamada R, Garofalo A, Louie S, Neamati N. Combination effects of SC144 and cytotoxic anticancer agents. Anticancer Drugs **2009**;20(5):312-20 doi 10.1097/CAD.0b013e328323a7ca.

50. Ho YK, Zhi H, Bowlin T, Dorjbal B, Philip S, Zahoor MA, Shih HM, Semmes OJ, Schaefer B, Glover JNM, Giam CZ. HTLV-1 Tax Stimulates Ubiquitin E3 Ligase, Ring Finger Protein 8, to Assemble Lysine 63-

Linked Polyubiquitin Chains for TAK1 and IKK Activation. PLoS Pathog **2015**;11(8):e1005102 doi 10.1371/journal.ppat.1005102.

51. Zou J, Yue F, Li W, Song K, Jiang X, Yi J, Liu L. Autophagy inhibitor LRPPRC suppresses mitophagy through interaction with mitophagy initiator Parkin. PLoS One **2014**;9(4):e94903 doi 10.1371/journal.pone.0094903.

Chapter 3: The importance of regulatory ubiquitination in cancer and metastasis

3.1 Abstract

Ubiquitination serves as a degradation mechanism of proteins, but is involved in additional cellular processes such as activation of NFκB inflammatory response and DNA damage repair. We highlight the E2 ubiquitin conjugating enzymes, E3 ubiquitin ligases and Deubiquitinases that support the metastasis of a plethora of cancers. E3 ubiquitin ligases also modulate pluripotent cancer stem cells attributed to chemotherapy resistance. We further describe mutations in E3 ubiquitin ligases that support tumor proliferation and adaptation to hypoxia. Thus, this review describes how tumors exploit members of the vast ubiquitin signaling pathways to support aberrant oncogenic signaling for survival and metastasis.

3.2. Ubiquitination signaling overview

Ubiquitin (Ub), a highly conserved 76-amino acid protein expressed in all cell types, has seven lysine residues (K6, K11, K27, K29, K33, K48, K63) that can be polymerized into various linkages. The resulting linkage of Ub chains creates a certain topology that can be sampled by interacting proteins and

dictates the fate of the substrate. For instance, K48- and K11-linked Ub chains adopt a “closed” or compact conformation and lead to 26S-mediated proteasomal degradation of substrates. In contrast, unanchored K63- or a mix of K63/M1-linked ubiquitination chains adopt an “open” conformation, and are involved in non-proteasomal functions such as TAK1 and IKK complex activation culminating in NFκB inflammatory signaling (Chen & Chen, 2013, Emmerich, Ordureau et al., 2013), activation of DNA damage repair signaling (Messick & Greenberg, 2009) and B cell activation via MAPK by TAB2/TAB3 (Ori, Kato et al., 2013).

Ubiquitination is a conserved multistep process that begins with the activation of ubiquitin with ATP by the E1 ubiquitin activating enzyme, followed by the formation of a thioester linkage between the ubiquitin transferred from the E1 to the cysteine in the active site of an E2 ubiquitin conjugating enzyme. The E3 ubiquitin ligase participates in the ubiquitination of a target substrate through the formation of an isopeptide bond between the carboxyl group of Gly76 of ubiquitin and the ε-amine of Lys in the substrate. Deubiquitinating enzymes (DUBs) remove the ubiquitin from the target substrates and recycles ubiquitin into the cytosolic pool.

Ubiquitination regulates the function and signaling of a profusion of proteins in various cellular pathways. This review describes how various cancers take advantage of the misregulated expression of the members of the ubiquitination cascade for proliferation, survival and metastasis (Figure 1).

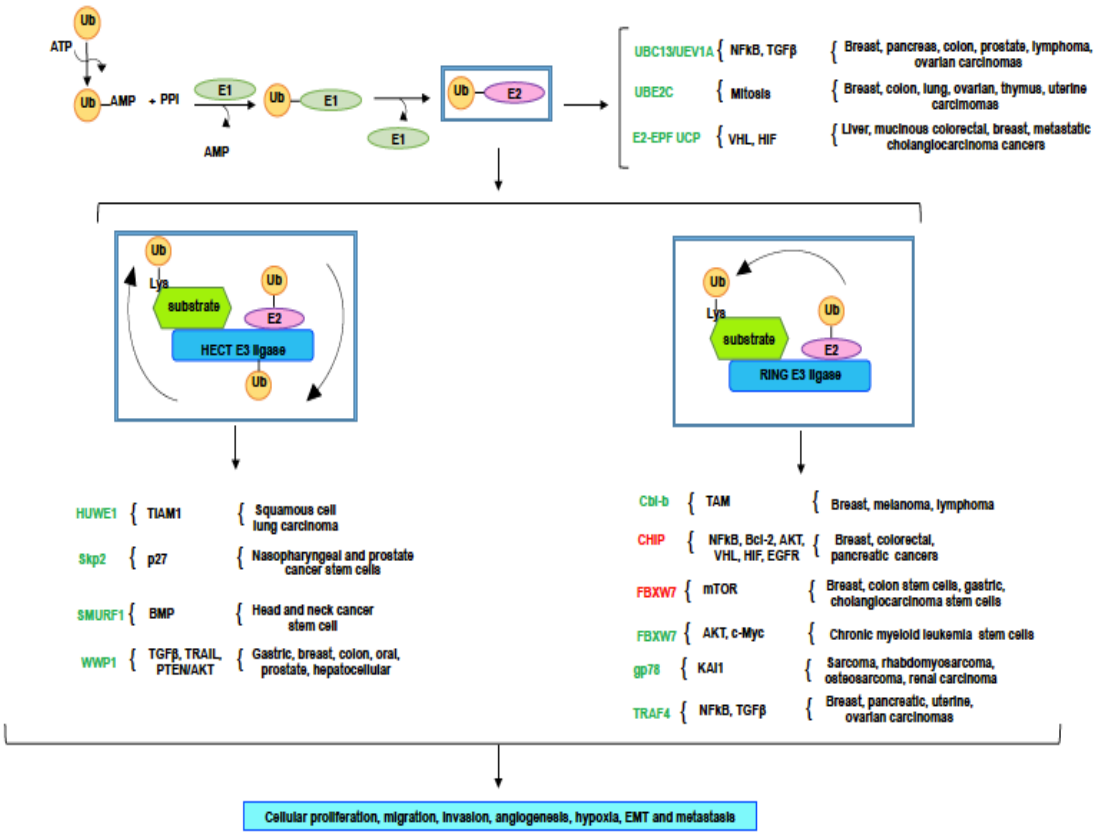

Figure 3.1: The misregulated expression of E2 ubiquitin conjugating enzymes and E3 ubiquitin ligases in various human cancers. The ubiquitination reaction initiates with the activation of ubiquitin by ATP, in which ubiquitin is then transferred to the active site of E1 ubiquitin conjugating enzyme. The E1 transfers the ubiquitin to a Cys in the catalytic active site of the E2 ubiquitin conjugating enzyme. The HECT domain E3 ligases ubiquitinate the target substrates by two mechanisms: first, the ubiquitin is transferred from the active site of the E2 to the Cys in the active site of the E3, which then ubiquitinates the Lys residue in the target substrate. RING- and RING-related domain E3 ligases, in contrast, serve as scaffolds to ubiquitinate target substrates in one step: the E2 transfers the ubiquitin directly to the Lys residue in the target substrate. Various tumors take advantage of the misregulated expression of E2's and E3's for the aberrant activation of oncogenic pathways. E2's and E3's colored in **green** indicate the importance of their expression or overexpression in cancer, while those in **red** indicate their downregulated expression in cancer. These genomic events result in cancer cell proliferation, migration, invasion, angiogenesis, hypoxia, EMT and metastasis.

3.3. The challenging route to metastasis

Cancer progression eventually may lead to metastasis, which is the final stage responsible for more than 90% of all terminal cancer deaths. Various

genomic abnormalities must be present to allow cells of a primary tumor to ignore apoptotic signals, proliferate and survive. Before metastasis occurs, tumor cells undergo phenotypic changes through epithelial-mesenchymal transition (EMT) similar to signaling events during embryonic development. EMT is marked by a loss of cell-cell adhesion through decreased expression of E-cadherin, increased motility by actin reorganization and upregulated expression of N-cadherin, Vimentin, Snail and Twist (Cheung & Ewald, 2016). Cells are then able to move through the stroma, resist the attack of immune cells, survive and travel through the bloodstream. Finally, metastasized cells arrive at the secondary site, resisting rejection and apoptosis to form malignant microtumors. Eventually, these progress to clinically observable macro metastasized tumors. Only a small percentage of metastasized cells survive this migratory journey and successfully colonize the secondary tissue, classifying metastasis as a rare event.

Since most proteins undergo ubiquitination as a post-translational modification in most cell types, it is not surprising that cancer cells exploit the members of the ubiquitination pathway to stabilize aberrant oncogenic signaling. This review describes that the misregulated expression of E2's, E3 ligases and DUBs contributes to the signaling of various oncogenes, leading to cancer progression and metastasis.

3.4 The overexpression of E2s supports aberrant oncogenic signaling in tumor metastasis

E2s play an active role in the regulation of cell cycle progression, inflammation and the mechanisms by which they modulate cancer metastasis. There are approximately 40 E2 family members encoded by the human genome (Clague, Heride et al., 2015). E2s share a highly conserved 150-amino acid catalytic core, the ubiquitin conjugating (UBC) domain, responsible for ubiquitination.

UBC13/UEV1A modulates breast cancer metastasis

Ubiquitin-Conjugating Enzyme E2N (UBC13), together with the UEV1A co-factor, specifically builds Lys63-linked ubiquitin chains that are indispensable for NFκB inflammatory activation (Chen & Chen, 2013). UBC13 is overexpressed in myriad tumors such as breast, pancreas, colon, prostate, lymphoma and ovarian carcinomas. UBC13 is required for breast cancer metastasis to the lung *in vivo* through TGFβ-mediated activation of TAK1 and p38, culminating in the expression of metastasis-associated genes *CNN2, PLTP, IGFBP3, IL13RA2, CD44, VCAM-1 and ICAM-1* (Figure 2). ShRNA-mediated inhibition of *UBC13* or treatment of breast cancer cells with SB203580, small molecule inhibitor of p38 MAPK, interestingly result in the suppression of breast cancer metastasis to the lung (Wu, Zhang et al., 2014).

In addition, the cofactor for UBC13, Ubiquitin-Conjugating Enzyme E2 Variant 1 (UEV1A) is upregulated in breast cancer and increases the

invasiveness and migration of breast cancer cells, including tumor growth and upregulated metastasis to lymph nodes and lung. ShRNA-mediated inhibition of *UEV1A* ablates breast tumor growth and metastasis *in vivo*. These tumors exhibit increased expression of Matrix Metalloproteinase-1 (MMP1) through activation of NFκB signaling (Wu, Shen et al., 2014) (Figure 2), in which MMPs are involved in extracellular matrix degradation for tumor cell migration and invasion (Deryugina & Quigley, 2006). UEV1A, in marked contrast to UBC13, lacks the catalytic Cys and therefore catalytically inactive to perform the polyubiquitination of substrates.

It is not clear, however, whether these tumors exhibit the upregulated expression of both UBC13 and UEV1A, or whether the upregulated expression of one member only is sufficient to aberrantly induce NFκB and TGFβ signaling to drive metastasis. The UBC13/UEV1A complex, critical for NFκB signaling, is overexpressed in some breast cancer samples; this may contribute to the hyperactivation of an inflammatory response in the tumor microenvironment.

UBE2C regulates chromosomal alignment in mitosis

Overexpression of UBE2C (Ubiquitin-Conjugating Enzyme E2C, termed UBE2C or UBCH10) is detected in breast, colon, lung, ovary, thymus and uterine cervix tumors, lung adenocarcinoma and squamous cell carcinomas (Fujita, Ikeda et al., 2009) (van Ree, Jeganathan et al., 2010). UBE2C functions with the Anaphase-promoting complex/cyclosome (APC/C) to ensure proper

chromosome alignment and segregation in mitosis. UBE2C expression fluctuates during the cell cycle, peaking at prometaphase to regulate chromosomal segregation and decreasing in anaphase. Overexpression of UBE2C causes the missegregation of chromosomes (aneuploidy), chromosome misalignment and lagging, mitotic slippage and increased number of centrioles, in addition to a decrease in cyclin B1 levels. Mice engineered to overexpress UBE2C exhibit elevated lung tumor burden, including the emergence of lymphomas, lipomas, liver and skin tumors (van Ree et al., 2010) (Figure 1).

Since the misregulated expression of UBE2C contributes to the emergence of tumors in tissues and cells from various lineages, it is possible that this E2 modulates chromosomal segregation during mitosis of different cancers, classifying it as a tempting target to treat a broad range of tumors.

E2-EPF UCP regulates E3 ligase VHL in hypoxia

Ubiquitin-Conjugating Enzyme E2S, or E2-EPF ubiquitin carrier protein (UCP), catalyzes the ubiquitination of von Hippel-Lindau (VHL) protein, targeting it for proteasomal degradation (Jung, Hwang et al., 2006). VHL mediates the stability of HIF transcription factors that induce expression of protumorigenic and mitogenic growth factor genes such as *VEGF*, *MMPs*, *SNAIL*, *TWIST* and *PDGF* involved in hypoxia, EMT, angiogenesis, migration, proliferation and metastasis (Figure 2) (Rankin & Giaccia, 2016).

The overexpression of UCP and HIF1α, with low VHL expression, is detected in various tumors such as primary liver, mucinous colorectal and breast cancer, and in metastatic cholangiocarcinoma in soft tissue and metastatic colorectal cancer in lymph VHL controls the stability of hypoxia-inducible factors HIF-1 and HIF-2 that mediate the adaptation of cells to varying levels of oxygen. Overexpression of UCP in CAKI cells (clear cell carcinoma derived from metastatic skin site) and C8161 (highly invasive and metastatic human melanoma cells) contributes to increased degradation of VHL, while it increases HIF1α expression and *VEGF* transcription, contributing to the increased proliferation and metastasis to the lung (Jung et al., 2006).

In summary, this section illustrates that overexpression of E2 ubiquitin conjugating enzymes supports aberrant oncogenic signaling of inflammatory NFκB and TGFβ, receptor tyrosine kinases, mitogenic growth factors and HIF transcription factors. These E2's drive aneuploidy, proliferation, migration and metastasis of a variety of tumors.

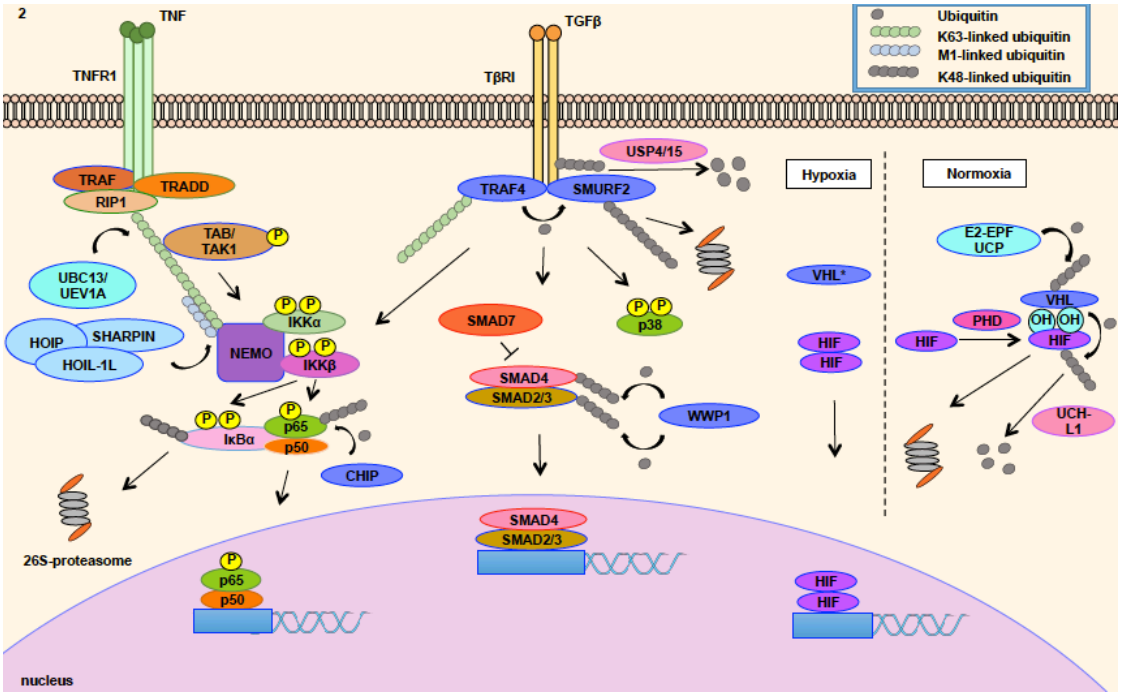

Figure 3.2. Misregulated expression of members of the ubiquitin cascade contributes to the aberrant signaling of various pathways in cancer. **(LEFT)** The UBC13/UEV1A E2 ubiquitin conjugating enzyme complex catalyzes the Lys63-linked ubiquitination of NEMO that recruits the TAK1/TAB1/2 complex to activate the IKK complex, which is composed of IKKβ, IKKα and NEMO. IKKβ phosphorylates IκBα, which is Lys48-linked ubiquitinated and subsequently degraded by the 26S-proteasome (Chen & Chen, 2013). This event releases NFκB to translocate into the nucleus to mediate the transcription of a signature of genes involved in inflammatory response. CHIP E3 ligase negatively regulates NFκB signaling by catalyzing the degradation-inducing Lys48-linked ubiquitination of p65 subunit of NFκB (Wang et al., 2014c). **(CENTER)** In addition, cancer cells take advantage of overexpressed TRAF4 to modulate TGFβ signaling. TGFβ activation culminates in the nuclear translocation of SMAD2/3/4 complex to modulate gene transcription. SMAD7 is a negative regulator of TGFβ signaling by recruiting SMURF2 E3 ubiquitin ligase to ubiquitinate TβRI, leading to the proteasomal degradation of the receptor and mitigation of signaling (Zhang et al., 2012) TGFβ signaling is regulated by TRAF4 E3 ligase mediated Lys48-linked ubiquitination of SMURF2 E3 ligase. The latter E3 ligase catalyzes the degradation signal of TGFβ receptor I (TβRI), in which these events mitigate the activation of the signaling pathway. TRAF4, on the other hand, is conjugated to Lys63-linked ubiquitin polymers to activate TAK1/TAB1/2 complex that induces the signaling of p38 MAPK and NFκB. TRAF4 further interacts with deubiquitinating enzyme USP15 and USP4, which remove the degradation signal from TGFβ receptor I. These events contribute to the stabilization of TGFβ signaling (Zhang et al., 2013). **(RIGHT)** Tumor adaptation to hypoxia is highly attributed to HIF signaling. Under normal oxygen level condition (normoxia), VHL E3 ligase binds to hydroxylated Proline residue in HIF catalyzed by PHD proteins. VHL then catalyzes the Lys48-linked ubiquitination of HIF, leading to proteasome degradation. E2-EPF UCP E2 enzyme controls VHL protein stability. Under low oxygen conditions (hypoxia), inactivating of VHL (either by mutations or decreased expression) contributes to HIF isoform stabilization, which mediates the transcription of genes involved in tumor adaptation to hypoxia, including angiogenesis (Jung et al., 2006, Rechsteiner et al., 2011). These signaling events governed by members of the ubiquitin cascade all contribute to EMT, cellular proliferation, migration, invasion, chemotherapy resistance and metastasis.

3.5. The misregulated expression of E3 ubiquitin ligases in cancer

There are approximately 600 E3 ubiquitin ligases encoded by the human genome and the mechanism of ubiquitination of target substrates depends upon the conserved catalytic domains: RING (Really Interesting New Gene), HECT (Homology to E6AP C Terminus) and RING-related (PHD, LIM, F-box, B-box and U-box). RING and RING-related E3 ligases catalyze a one-step reaction of ubiquitin transfer from the E2 to the lysine residue in the substrate. In contrast, HECT E3 ligases catalyze a two-step reaction: first the ubiquitin is transferred from the E2 to the cysteine in the active site of the E3 ligase, which then ubiquitinates the lysine residue in the target substrate (Berndsen & Wolberger, 2014, Deshaies & Joazeiro, 2009) (Figure 1).

As with the E2 ubiquitin conjugating enzymes, misregulated expression of E3 ubiquitin ligases contributes to aberrant oncogenic signaling, metastasis and resistance to chemotherapy, including the modulation of pluripotency of cancer stem cells in tumor niches.

The downregulated expression of E3's in cancer

CHIP – more than just an E3 ligase

Cancer cells take advantage of downregulated expression of Carboxy terminus of Hsc70-Interacting Protein (CHIP), also known as STUB1, a U-box ligase that functions as a chaperone for protein quality control and promotes the

ubiquitination of various cell cycle regulators, such as c-Myc and SRC-3. *CHIP* transcript is lower in malignant stage II and node-positive breast cancer than in stage I and node-negative patients. The downregulated expression of CHIP upregulates NFκB signaling and anti-apoptotic proteins Bcl-2 and AKT, supporting inflammation, survival, invasiveness and metastatic potential of breast cancer cells (Jang, Lee et al., 2011, Kajiro, Hirota et al., 2009). In colorectal cancer, CHIP is the E3 ubiquitin ligase that regulates the stability of p65 subunit of NFκB (Figure 2). Downregulated CHIP in colorectal cancer decreases the degradation of p65 subunit and increases the expression of NFκB-controlled *VEGF*, *Cyclin D1*, *c-Myc*, *IL-8* and *MMP-2* genes involved in angiogenesis and metastasis (Wang, Ren et al., 2014c).

In pancreatic cancer, CHIP is a tumor suppressor and it modulates the stability of EGFR via proteasomal-mediated degradation of this receptor tyrosine kinase (RTK). CHIP regulates the phosphorylation of Tyr845 and Tyr1068 of EGFR, activating downstream PI3K/AKT and Src/FAK/paxillin signaling pathways. Downregulated CHIP expression increases oncogenic EGFR signaling and sensitizes pancreatic cancer cells to RTK inhibitor, erlotinib, which leads to apoptosis and decreased tumor volume *in vivo* (Wang, Yang et al., 2014b).

CHIP modulates the proteasomal-mediated degradation of NFκB and EGFR oncogenes in various tumors (Figure 1). Tumors harboring downregulated CHIP expression exhibit aberrant NFκB signaling and some tumors may rely on RTK's for proliferative advantages. The role of CHIP may

extend beyond these pathways to include additional oncogenes in other classes of tumors.

FBXW7 – a key component of the SCF complex

F-Box And WD Repeat Domain Containing 7 (FBXW7) E3 ligase is a component of the SCF (SKP1, CUL-1, F-box protein) E3 ubiquitin ligase complex that regulates the stability of cell-cycle regulators such as c-Myc, cyclin E and Notch (Welcker & Clurman, 2008).

FBXW7 is downregulated in breast, colorectal, gastric and cholangiocarcinoma (CCA) tumors correlated with poor prognosis and survival, elevated tumor invasion and occurrence of metastasis (Ibusuki, Yamamoto et al., 2011, Iwatsuki, Mimori et al., 2010, Yang, Lu et al., 2015) (Figure 1). FBXW7 regulates the stability and turnover of mTOR. Downregulated FBXW7 expression increases mTOR levels that support the metastastic potential of CCA tumors to the liver and lung. These tumors are sensitive to mTOR inhibitorrapamycin, which impairs tumor growth (Yang et al., 2015).

In summary, this section illustrates that the downregulated expression of the E3 ubiquitin ligases stabilizes aberrant oncogenic signaling. Some of these reports, additionally, show that a rescue in the expression of these E3 ligases leads to increased degradation of key oncogenic signaling proteins, potentially resulting in the inhibition of tumor proliferation and metastasis.

The importance of the expression, or overexpression, of E3's in tumors

The contribution of Cbl-b to melanoma and breast cancer metastasis

The recruitment of immune system cells to the tumor microenvironment has been suggested to play an important role in tumor metastasis (Quail & Joyce, 2013). The E3 ligase activity of Casitas B-lineage lymphoma-b, Cbl-b or RNF56, is a negative regulator of anti-tumor function of natural killer (NK) cells. Genetic deletion of Cbl-b, or targeted inhibition of its E3 ubiquitin ligase activity, awakens the antitumor response of NK cells and educates these lymphoid cells to recognize and kill melanoma tumors, inhibiting lung metastasis. The TAM family of receptor tyrosine kinases, Tyro3, Axl and Mer, has been identified as substrates of Cbl-b for ubiquitination. Treatment of NK cells with selective TAM inhibitor, LDC1267, ablates melanoma and breast cancer metastasis (Paolino, Choidas et al., 2014). This indicates that some E3 ligases, exemplified by Cbl-b, can modulate the immune system's ability to recognize and kill tumor cells.

HUWE1 controls cell-to-cell adhesion

In order for cancer cells to leave the primary tissue and metastasize to secondary sites, cell-to-cell adhesion must be disrupted for their movement through the stroma. The HECT, UBA, and WWE domain-containing protein 1

(HUWE1) E3 ubiquitin ligase has been implicated in the modulation of cell-to-cell adhesion. The expression of TIAM1, a guanine nucleotide exchange factor, at cell-to-cell junctions is critical to maintain cells in contact with one another. HUWE1-mediated degradation of TIAM1 leads to scattering, dissemination and invasion of epithelial cells, including the dissemination and local invasion of metastatic lung cells. Knockdown of HUWE1 decreases the dissemination of cells, leading to the stabilization of TIAM1 at cell-to-cell junctions. Stage I and stage II squamous cell lung carcinoma tissue samples show an inverse correlation between HUWE1 and TIAM1 expression (Vaughan, Tan et al., 2015) (Figure 1), suggesting that metastasis of lung cells may be modulated by the misregulated expression of HUWE1.

GP78 in sarcoma metastasis

The metastasis of sarcoma tumors is dependent upon the E3 ligase activity of GP78, also known as autocrine motility factor receptor (AMFR). GP78 is a RING-finger E3 ubiquitin ligase that localizes to the endoplasmic reticulum (ER) and it participates in ER-associated degradation (ERAD), a pathway that leads to the degradation of misfolded or denatured proteins. Inhibition of GP78 expression in highly metastatic human sarcoma cells inhibits lung metastasis, but it does not affect primary tumor growth. Stable *gp78* knockdown decreases the survival of metastasized HT1080 sarcoma, RH30 rhabdomyosarcoma, HOS-MNNG osteosarcoma, including 786-O renal carcinoma (Figure 1). The

metastasis-suppressor KAI1 has been identified as a substrate of gp78-mediated degradation, in which an inverse correlation of KAI1 and GP78 expression is found in sarcoma samples. Downregulated gp78 leads to the accumulation of KAI1 that results in apoptosis and reduces the metastatic potential of sarcoma cells (Tsai, Mendoza et al., 2007). This event illustrates the importance of gp78 expression in sarcomas.

TRAF4 modulates inflammatory signaling of multiple tumors

Tumor necrosis factor receptor-associated factor 4 is a RING domain E3 ligase with well-documented signaling functions associated with the activation of TNFRs and IL-1R/TLRs, playing critical roles in immune system responses (Zhang, Zhou et al., 2013).

TRAF4 has been implicated in the regulation of both SMAD-dependent and SMAD-independent TGFβ receptor (TβRI)-induced signaling. TRAF4 ubiquitinates SMURF2 leading to the degradation of the latter E3 ligase and enhancement of TGFβ signaling. On the other hand, SMURF2 can ubiquitinate both TβRI and TRAF4 to terminate TGFβ signaling. TRAF4 also interacts with deubiquitinating enzyme USP15, which deubiquitinates TβRI upon SMURF2-mediated ubiquitination of TβRI, stabilizing this signaling pathway. In addition, TGFβ induces the Lys63-linked ubiquitination of TRAF4 to promote TAK1 activation, leading to p38 and NFκB signaling (Zhang et al., 2013) (Figure 2).

TRAF4 is amplified in invasive breast carcinoma, pancreatic adenocarcinoma, uterine carcinoma and ovarian carcinoma (Figure 1). TRAF4 overexpression contributes to poor overall survival in ovarian cancer and, in breast cancer, it is correlated with *ERBB2* amplification and bone metastasis. TRAF4 further supports the expression of EMT makers such as N-cadherin, Vimentin, Fibronectin and TGFβ-associated expression of IL-11, PTHrP, CXCR4 and SNAIL. Knockdown of *TRAF4* results in ablation of TGFβ-induced phosphorylation of SMAD2 and p38 MAPK, showing the importance of TRAF4 in the regulation of SMAD-dependent and -independent signaling (Zhang et al., 2013).

WWP1 – a phosphotyrosine binding E3

WW Domain Containing E3 Ubiquitin Protein Ligase 1 (WWP1) is a HECT domain E3 ubiquitin ligase that binds to phosphotyrosine (PPXY)domains in substrates.

WWP1 overexpression supports the proliferation and survival of oral, and hepatocellular carcinoma (HCC) (Cheng, Cao et al., 2014, Lin, Hsieh et al., 2013) (Figure 1). Additionally, WWP1 positively regulates PTEN/AKT signaling to support the proliferation and cell cycle progression of gastric tumors, contributing to poor survival and lymph node metastasis (Zhang, Wu et al., 2015). In breast cancer, WWP1 is overexpressed in 51% of transformed cell lines and supports the expression of estrogen receptor and Insulin-like growth

factor receptor-1, resulting in aberrant proliferation. Inhibition of *WWP1* expression sensitizes TRAIL-resistant breast cancer cells to TRAIL-induced activation of the extrinsic apoptotic pathway. In addition, efficient inhibition of breast cancer proliferation has been achieved by combining knockdown of *WWP1* with anti-estrogen tamoxifen drug therapy (Chen, Zhou et al., 2007, Chen, Zhou et al., 2009, Zhou, Liu et al., 2012).

Overall, this section illustrates that the overexpression of E3 ubiquitin ligases supports aberrant oncogenic signaling in various types of cancers. These reports show that inhibition of expression of each of these E3 ubiquitin ligase is sufficient to ablate tumor progression and metastasis.

3.6 E3 ubiquitin ligases in pluripotent cancer stem cells

Conventional chemotherapies often fail to target metastasized tumors, which may be due to the emergence of a subpopulation of cells, the cancer initiating cells or cancer stem cells (CSCs). CSCs are not only capable of self-renewal and differentiation like normal stem cells, but they are also capable of tumor initiation, relapse, chemotherapeutic resistance and metastasis.

CSCs are characterized by up-regulated expression of embryonic stem cells markers, SOX2 (SRY-Box 2), OCT4 (Octamer-Binding Protein 4) and NANOG (Nanog Homeobox). These transcription factors are the key regulators of pluripotency, activating self-renewal-associated genes and inhibiting differentiation by suppressing lineage-specific transcription factors. Expression

of these regulators confers stem cell-like characteristics, and silencing them results in decreased tumorigenicity. CSC's express surface markers CD133 and CD44, including increased expression of aldehyde dehydrogenase (ALDH) and increased ATP binding cassette (ABC) transporter drug efflux, which all contribute to chemotherapy resistance (Morrison, Morris et al., 2013) (Figure 3A).

E3 ligases are strongly associated with either promoting or suppressing the CSC population in various cancers (Figure 3B). Investigating the mechanisms by which E3 ligases confer stem-cell like characteristics to a subpopulation of tumorigenic cells is of great interest to develop novel compounds to selectively target CSC's, possibly overcoming metastasis.

SMURF1 in head and neck cancer stem cells

SMURF1 (SMAD specific E3 ubiquitin protein ligase 1) suppresses bone marrow morphogenic (BMP) signaling contributing to the maintenance of the CSC subpopulation ($ALDH^{high}/CD44^{high}$) in head and neck squamous cell carcinoma (HNSCC). BMP proteins are growth factor members of the TGFβ superfamily that restrict hematopoietic stem cell proliferation and induce cellular differentiation. The overexpression of SMURF1 in CSCs derived from HNSCC leads to decreased levels of SMADs 1/5/8 and attenuates BMP signaling, keeping cells in an undifferentiated stem-cell like phenotype (Khammanivong, Gopalakrishnan et al., 2014).

Skp2 in nasopharyngeal and prostate cancer stem cells

Skp2 (S-Phase kinase-associated protein 2 also known as FBXL1) is an F-box protein; one of its main targets for degradation is the G1/S cyclin-dependent kinase inhibitor p27, a tumor suppressor.

Overexpression of Skp2 correlates with poor prognosis of nasopharyngeal carcinoma (NPC), one of the most common head and neck carcinomas (Wang, Huang et al., 2014a), and of prostate cancer (Chan, Morrow et al., 2013) (Figure 1). NPC patients with high expression of Skp2 have a correlation with tumor recurrence and metastasis. Knockdown of *Skp2* decreases sphere colony formation of NPC cell lines, and it impairs the proliferation of $ALDH1^+$ subpopulation of cells, indicating reduced CSC phenotypes (Wang et al., 2014a). In prostate cancer, a small molecule inhibitor of Skp2 reduces prostate CSC population through p53-independent cellular senescence and inhibition of aerobic glycolysis. Moreover, the Skp2 inhibitor sensitizes prostate CSC's to doxorubicin and cyclophosphamide drug treatments (Chan et al., 2013).

Taken together, Skp2 promotes CSC properties and decreases drug treatment efficacy, showing the importance of targeting Skp2 to ablate CSC in tumor niches.

ITCH in lung cancer stem cells

ITCH is a HECT E3 ligase that performs essential regulatory functions in immune cells such as ubiquitination of Bcl10, PKC and PLC-γ, leading to nuclear translocation of NFκB and NFAT (nuclear factor of activated T-cells) during T-cell signaling activation. ITCH further regulates the stability of p63 and Notch (Aki, Zhang et al., 2015).

Desmethylclomipramine (DCMI), identified via high-throughput screening as a specific inhibitor of E3 ligase activity of ITCH (Rossi, Rotblat et al., 2014), has shown promising chemotherapeutic action against non-small cell lung CSCs in patient samples whom acquired resistance to chemotherapeutic drugs Cisplatin, Gemcitabine and Paclitaxel. DCMI leads to reduced sphere forming ability and inhibition of proliferation of this subpopulation of lung cancer stem cells. In addition, shRNA-mediated silencing of *ITCH* decreases ALDH-positive lung CSCs and sensitizes cells to Gemcitabine-induced apoptosis (Bongiorno-Borbone, Giacobbe et al., 2015).

FBXW7 in colonic and leukemia cancer stem cell maintenance

FBXW7 is known to target oncoproteins such as mTOR, cyclin-E, Jun, Myc and Notch1 for degradation, which are usually involved in the signaling of various cancers. The role of FBXW7 in the maintenance of normal stem cells has been previously shown (Takeishi & Nakayama, 2014). However, the role of

FBXW7 in the maintenance of CSCs can vary, depending on the type of tumor (Figure 3.B).

In colon cancer, downregulated FBXW7 expression promotes EMT as shown by the increased epxression of mesenchymal stem cell markers, SOX2, OCT4 and NANOG, leading to invasive phenotype, greater tumor initiating potential and non-adherent growth ability. As previously mentioned, mTOR is a downstream target of FBXW7. Treatment of colon cancer cells with the mTOR inhibitor rapamycin suppresses their migration and tumor-sphere formation (Wang, Liu et al., 2013). Loss of *FBXW7* is also associated with stem-like competence in cholangiocarcinoma (CCA), and rapamycin treatment of CCA cells suppresses invasion, metastatic potential and tumor sphere formation (Yang et al., 2015).

In contrast, expression of FBXW7 is critical in the maintenance of leukemia-initiating cells (LICs) in chronic myeloid leukemia (CML), a disease associated with the BCR-ABL fusion protein. FBXW7 supports stem cell properties in LICs and maintains these cells in a quiescent state. Inhibition of *FBXW7* expression decreases colony formation potential, eliminates leukemic cell infiltration in peripheral blood, spleen, liver and lungs, and leads to induction of apoptosis in a p53-dependent manner. In addition, knockdown of *FBXW7* causes LIC's to differentiate and enter the cell cycle becoming sensitized to imatinib and cytosine arabinoside drug treatments (Takeishi, Matsumoto et al., 2013).

In summary, the levels in the expression of E3 ubiquitin ligases maintain a subpopulation of cancer stem cells in an undifferentiated state (Figure 3.A and 3.B). Most of these reports show that inhibition of E3 ligase expression, with the exception of FBXW7 in LIC's, sensitizes CSC's to chemotherapeutic agents suggesting a clinical approach to eradicate this subpopulation of cells attributed to chemotherapy resistance and metastasis.

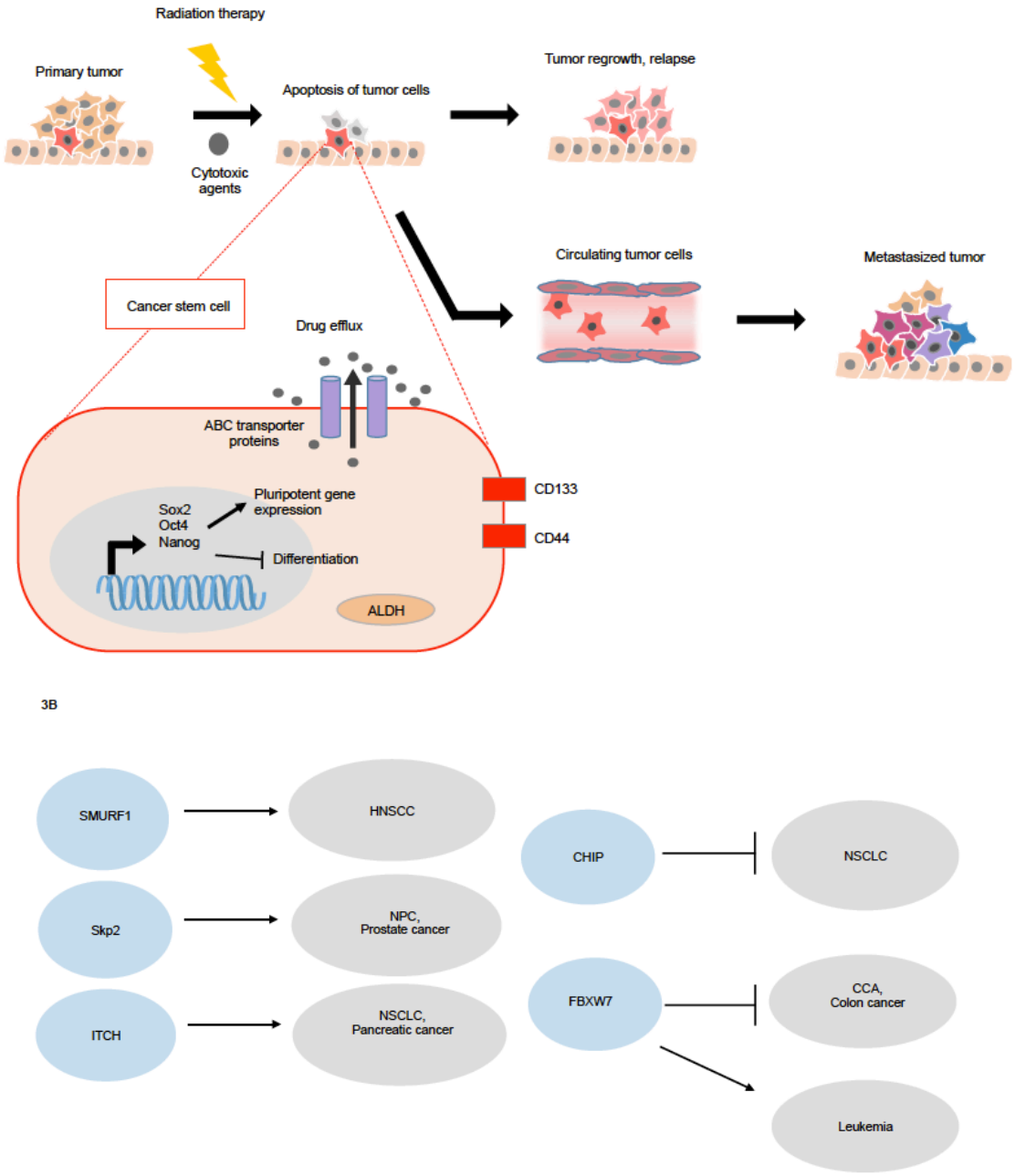

Figure 3.3. E3 ubiquitin ligases in pluripotent stem cells. (A). Cancer stem cells are characterized by the up-regulation of Sox2, Oct4, and Nanog, which activates self-renewal associated genes and inhibits cellular differentiation. Cell surface markers, CD133 and CD44 are associated with CSC properties. Conventional chemotherapeutic agents target differentiated cells, thus quiescent CSCs are innately chemo-resistant. Moreover, CSCs show increased ABC multi-drug transporters, which pump the cytotoxic drugs out of the cells. CSCs also show high aldehyde dehydrogenase activity (ALDH), which detoxifies the aldehydes generated by the chemotherapeutic agents. As a result, the surviving CSCs can re-populate or metastasize, and these cancer cells that possess self-renewal advantages are very challenging to eradicate by using conventional chemotherapeutic agents. (Morrison et al., 2013) **(B).** E3 ligases can either promote or suppress CSCs in different cancers.

3.7 Mutated E3 ligases proliferate different tumors

A list of mutations in E3 ubiquitin ligases, and their potential biological effects in various tumors, is described in Table 1. We herein bring attention to the fact that mutated E3 ligases contribute to tumor hypoxia and vascularization, and upregulated inflammatory NFκB and growth factor mitogenic signaling pathways.

VHL adapts renal cell carcinoma to hypoxia

VHL is part of the VCB E3 ubiquitin ligase complex further composed of elongin B, elongin C and cullin-2. Under normoxia, VHL induces the ubiquitination of HIF1α for degradation. On the other hand, inactivation of VHL results in the stabilization of HIF isoforms that support vascularization and adaptation of tumors to hypoxia (Rankin & Giaccia, 2016). (Figure 2).

Germ line mutations in tumor suppressor *VHL* cause von Hippel-Lindau syndrome characterized by the emergence of highly vascularized tumors, such as clear cell renal cell carcinoma (ccRCC), central nervous system hemagioblastoma, pheochromocytoma and pancreatic cysts (Maher, Neumann et al., 2011, Rankin & Giaccia, 2016). Inactivated *VHL* is observed in approximately 80-90% of ccRCC, which includes >90% of allelic deletion or loss of heterozygosity, >50% mutations and approximately 10% of promoter hypermethylation (Feng, Sun et al., 2015). Over 800 distinct mutations in *VHL*

have been detected in sporadic and hereditary ccRCC, in which the majority of these genetic instabilities results in loss of VHL function (Rechsteiner, von Teichman et al., 2011).

Mutated VHL causes tumors to become sensitive to PI3K p110β inhibitor, TGX221, which decreases the proliferation, migration and invasion of cells (Feng et al., 2015). *In silico* analysis revealed that the majority of missense mutations affecting the surface of VHL impact the interaction of VHL with HIF isoforms, elongin B, elongin C and other binding partners such as p53 and PKC. For instance, the L101P mutation, and other VHL disease-causing mutations such as N78S, S80N and Y98H/N cause a dramatic loss-of-function in VHL and stabilize HIF1 isoforms. In addition, frameshift mutations in exons 1, 2 and 3, with the exception of Glu204fsX44 at the very end of exon 3, inactivate VHL and lead to increased stability of HIF isoforms (Table 1). Such alterations in VHL possibly affect the hydroxylation of HIF isoforms by prolyl 4-hydroxylases (Figure 2) (Rechsteiner et al., 2011). Hence, the stabilization of HIF isoforms via the inactivation of the E3 ligase activity of VHL possibly contributes to hypoxia and the highly vascularized characteristics observed in these cancers

c-*Cbl* drives myeloproliferative neoplasms

Casitas B-Lineage Lymphoma, c-Cbl or RNF55, is member of the Cbl family of E3 ubiquitin ligases previously mentioned. Mutations in *c-Cbl* in myeloproliferative neoplasms usually occur due to acquired 11q uniparental

disomy, an event similar to loss of heterozygosity in which a part of the DNA is lost from one chromosome but the remaining homologue is duplicated resulting in two copies at the locus per cell. Myeloproliferative neoplasms include chronic myelomonocytic leukemia (CMML), atypical chronic myeloid leukemia (aCML; BCR-ABL negative), myelofribrosis (MF), secondary acute myelogenous leukemia (sAML), acute myeloid leukemia and juvenile myelomonocytic leukemia (JMML) (Grand, Hidalgo-Curtis et al., 2009, Loh, Sakai et al., 2009, Makishima, Cazzolli et al., 2009, Muramatsu, Makishima et al., 2010). Homozygous mutations in *c-Cbl* in myeloproliferative neoplasms contribute to poor survival rates of patients. Mutations in c-Cbl contribute to earlier presentation of JMML disease (age of 12 months at diagnosis) compared with patients without these alterations (29 months) (Loh et al., 2009, Muramatsu et al., 2010).

c-Cbl mutations themselves are able to lead to neoplasms, as they have been identified in JMML tumors that do not harbor any other mutated *RAS, PTN11* or *NF1* genes known to be involved in JMML (Muramatsu et al., 2010). The mutations S376F (aCML), H398Y (CMML), P417A (aCML) and R420Q (AML, aCML, MF, sAML) in c-Cbl when co-transfected with FLT3 confer IL3-independence in 32D cells reflecting their oncogenic transforming activities (Table 1). These mutations also impair c-Cbl-mediated ubiquitination of FLT3 and internalization of EGFR and PDGFR (Grand et al., 2009, Makishima et al., 2009, Sargin, Choudhary et al., 2007), while they induce activated phospho-STAT5 signaling (Sargin et al., 2007). Mutation at the “hot spot” Y371 site of c-

Cbl is rarely found in other myeloid neoplasms. The Y371C/D/H mutations located in the linker domain adjacent to the RING domain have been identified in JMML patients (Table 1). A similar phosphomimic mutation to Asp, Y371E, constitutively activates the autoubiquitination E3 ligase activity of c-Cbl and it interacts with EGFR (Kassenbrock & Anderson, 2004), showing that c-Cbl modulates RTK signaling.

Activating mutations in c-Cbl lead to constitutive RTK signaling by impairing receptor internalization and degradation, driving myeloproliferative disorders.

Mutations in HOIP in ABC DLBCL

The Linear Polyubiquitin Chain Assembly Complex (LUBAC) is composed of HOIP (RNF31), HOIL-1 (RBCK1) and SHARPIN. LUBAC catalyzes the linear ubiquitination of NEMO, a scaffold member of the IKK complex that activates the canonical NFκB signaling pathway (Figure 2).

Activated B cell-like (ABC) subtype of diffuse large B-cell lymphoma (DLBCL) malignant progression is dependent upon constitutive B-cell receptor (BCR) activation that upregulates NFκB signaling. Inhibition of HOIP or SHARPIN decreases LUBAC-mediated linear polyubiquitination of NEMO and impaires IKK and NFκB activation, leading to a decrease in viability of ABC DLBCL (Yang, Schmitz et al., 2014). In addition, inhibition of HOIP sensitizes ABC DLBCL tumors to Bruton agammaglobulinemia tyrosine kinase (BTK)

inhibitor, Ibrutinib, and IRF4 transcription factor inhibitor, Lenalidomine, leading to decreased viability of this subclass of B-cell lymphoma.

Two rare germline SNP polymorphisms in *HOIP* are enriched 8-fold in ABC DLBCL biopsies (Table 1). These mutations, Q584H and Q622L, are found in the ubiquitin-associated domain of HOIP known to interact with the ubiquitin-like domain of RBCK1, leading to upregulation of LUBAC-mediated linear polyubiquitination of NEMO, increased IKK and NFκB activation in ABC DLBCL tumors (Yang et al., 2014).

Inactivating driver mutations in FBXW7

Mutations in FBXW7 have been identified in various tumors (Table 1). The F-box domain of FBXW7 is important for the interaction with the SCF complex, while the WD40 domain recognizes phosphorylation sites in a conserved Cdc4 phospho-degron motif in the target substrate (Welcker & Clurman, 2008). Inactivating mutations in the WD40 domain of FBXW7 often impair substrate binding and subsequently diminish protein turnover, contributing to aberrant oncogenic signaling of targets mentioned below.

T cell acute lymphoblastic leukemia (T-ALL) is a malignant neoplasm characterized by mutations mostly in *NOTCH1* and *FBXW7* (Yuan, Lu et al., 2015). Mutations in *FBXW7,* studied in a population of pediatric Chinese T-ALL patients, contribute to poor overall survival and higher incidence of tumor relapse. These FBXW7 mutations affect codons R465, R479, R505 and R689

in the WD40 domain, critical for the interaction with the PEST domain of NOTCH1. These mutations may further impact signaling pathways beyond NOTCH1, since FBXW7 mediates the stability of oncogenic proteins such as mTOR, Cyclin E and MYC.

In addition, mutations in FBXW7 are found in 8% of melanomas and interestingly, some have been reported in the absence of the classic BRAF V600E and NRAS G12D, G13R and Q61K/L/S mutations. This may indicate that mutations in FBXW7 are drivers of melanoma progression (Aydin, Melamed et al., 2014). FBXW7 R505C and W486* mutants in melanocytes, which harbor the NRAS G12D mutation, lead to aberrant tumor volume. As a proof-of-concept for the inactivating mutations in FBXW7, knockdown of *FBXW7* in melanoma cell lines leads to the accumulation of NOTCH1, HEY1 and downstream effectors Cyclin E, Aurora A and MYC, resulting in increased tumor volume. In addition, this event leads to the upregulation of angiogenesis-promoting genes such as *IL-6*, *CXCL2*, *SERPINE1* and *PGF1*, and increased phosphorylation of STAT3. Mice grafted with melanoma cells with knockdown *FBXW7,* treated with NOTCH1 inhibitors dibenzazepine (DBZ) and compound E, showed substantial melanoma tumor shrinkage (Aydin et al., 2014).

Other inactivating mutations in *FBXW7* were identified in various advanced cancers such as colorectal, squamous head and neck, bladder, cervix, endometrial, liver, ovarian, mesothelioma, pancreatic and teratoma. In these tumors, most of these mutations concomitantly occur with mutations in *TP53*, followed by *KRAS*, *PI3KCA* and *APC* (Jardim, Wheler et al., 2014). As

mTOR is a downstream target of FBXW7, tumors harboring inactivating mutations in FBXW7 are sensitive to mTOR inhibitors. For instance, treatment of patients, whose tumors exhibit mutated *FBXW7*, with mTOR inhibitors (Sirolimus, Everolimus, and Temsirolimus) resulted in tumor shrinkage (Jardim et al., 2014). In addition, Temsirolimus showed promising results in a patient with metastatic lung adenocarcinoma with mutated FBXW7 R465H, leading to shrinkage of mediastinal lymphadenopathy (Table 1) (Villaruz & Socinski, 2014).

Table 3.1. Mutations in E3 ligases identified in cancers

E3 Ligase	Mutation	Tumor	Biological Effect	Therapy	Reference
c-Cbl	Y371C/D/H	aCML, JMML			(Grand et al., 2009, Loh et al., 2009, Muramatsu et al., 2010)
	S376F	aCML	transformation of 32D cells; decreased FLT3 ubiquitination		(Grand et al., 2009)
	L380P	aCML, MF, JMML			(Grand et al., 2009, Loh et al., 2009)
	C381R/Y	CMML, JMML			(Grand et al., 2009, Loh et al., 2009)
	C384R/Y	CMML, JMML, MDS-MPDu			(Grand et al., 2009, Loh et al., 2009)
	C396G/R	CMML, JMML			(Grand et al., 2009, Loh et al., 2009)
	H398Y	CMML	transformation of 32D cells; decreased FLT3 ubiquitination		(Grand et al., 2009)
	C401S	JMML			(Muramatsu et al., 2010)
	C404R	JMML			(Loh et al., 2009)

Table 3.1. Mutations in E3 ligases identified in cancers, continued

E3 Ligase	Mutation	Tumor	Biological Effect	Therapy	Reference
	W408C/R	aCML, JMML			(Grand et al., 2009, Loh et al., 2009)
	G415V	JMML			(Loh et al., 2009)
	P417A	aCML	transformation of 32D cells; decreased FLT3 ubiquitination		(Grand et al., 2009)
	P417L	CMML			(Grand et al., 2009)
	F418L	aCML			(Grand et al., 2009)
	R420Q (proliferation of 32Dcells)	AML, aCML, MF, sAML	transformation of 32D cells; decreased FLT3 ubiquitination; inhibition of PDGFR and EGFR internalization		(Grand et al., 2009, Makishima et al., 2009, Sargin et al., 2007)
	R420L	aCML			(Grand et al., 2009)
	N454D	CMML			(Grand et al., 2009)
	R462X	aCML			(Grand et al., 2009)
	1106 del (66 bp)	JMML			(Muramatsu et al., 2010
	1228-2 A>G splice site	JMML			(Muramatsu et al., 2010)
	c.1227-1227 + 4 del ggtac	CMML			(Grand et al., 2009)
	1190 del 99bp	JMML			(Loh et al., 2009)
	1227 + 4C>T splice site	JMML			(Loh et al., 2009)
	1228 - 2A>G splice site	JMML			(Loh et al., 2009)
	int + 5 G>A	aCML			(Grand et al., 2009)
	int + 4 C>T	CMML			(Grand et al., 2009)
	int - 1 G>C	CMML			(Grand et al., 2009)
Fbxw7	E113D	pancreatic			(Jardim et al., 2014)
	E192A	liver		Sirolimus, Vorinostat: stable disease	(Jardim et al., 2014)

Table 3.1. Mutations in E3 ligases identified in cancers, continued

E3 Ligase	Mutation	Tumor	Biological Effect	Therapy	Reference
	R222*	colorectal		Temsirolimus, Bevacizumab, Cetuximab: stable disease	(Jardim et al., 2014)
	W244*	bladder, cervix		Sirolimus, Hydroxichloroquine: stable disease (bladder)	(Jardim et al., 2014)
	R278*	colorectal			(Jardim et al., 2014)
	S282*	head and neck		Temsirolimus, Bevacizumab,	(Jardim et al., 2014)
	K299fs	melanoma			(Aydin et al., 2014)
	W368*	melanoma			(Aydin et al., 2014)
	W406*	melanoma			(Aydin et al., 2014)
	G423R	melanoma	lower tumor volume *in vivo* compared with FBXW7 WT		(Aydin et al., 2014)
	G437*	T-ALL			(Yuan et al., 2015)
	R441Q	T-ALL			(Yuan et al., 2015)
	R465C/H	T-ALL, colorectal, endometrial, ovarian, extrahepatic, metastatic lung adenocarcinoma	R465H: metastatic lung adenocarcinoma	Temsirolimus: stable disease (R465H in metastatic lung adenocarcinoma); Everolimus, Anastrozole: progressive disease (R465H in ovarian cancer)	(Jardim et al., 2014, Villaruz & Socinski, 2014, Yuan et al., 2015)
	R479G/P/Q	colorectal, head and neck, T-ALL			(Jardim et al., 2014, Yuan et al., 2015)
	W486*	melanoma	increased melanoma tumor volume *in vivo* compared with FBXW7 WT		(Aydin et al., 2014)
	G499Vfs*25	colorectal		Sirolimus, Hydroxichloroquine: stable disease	(Jardim et al., 2014)

Table 3.1. Mutations in E3 ligases identified in cancers, continued

E3 Ligase	Mutation	Tumor	Biological Effect	Therapy	Reference
	R505C/G	colorectal, melanoma, intrahepatic, T-ALL	R505C: increased melanoma tumor volume *in vivo* compared with FBXW7 WT	Everolimus, Pazopanib: stable disease (R505C in colorectal cancer); Everolimus, Anakinra: progressive disease (R505C in colorectal cancer)	(Aydin et al., 2014, Jardim et al., 2014, Yuan et al., 2015)
	H540Y	T-ALL			(Yuan et al., 2015)
	S562L	melanoma	similar tumor volume *in vivo* compared with FBXW7 WT		(Aydin et al., 2014)
	R658*	melanoma, pleura		Sirolimus, Lapatinib: progressive disease (pleura)	(Aydin et al., 2014, Jardim et al., 2014)
	R689W	T-ALL			(Yuan et al., 2015)
	726+1 G>A splice	teratoma		Temsirolimus, Bevacizumab, Carboplatin: stable disease	(Jardim et al., 2014)
HOIP	Q584H	ABC DLBCL	upregulation of LUBAC linear polyubiquitination of NEMO; increased NFκB signaling		(Yang et al., 2014)
	Q622L	ABC DLBCL	upregulation of LUBAC linear polyubiquitination of NEMO; increased NFκB signaling		(Yang et al., 2014)
VHL	S72P	ccRCC	stabilization of HIF1		(Rechsteiner et al., 2011)
	N78K/S/Y	ccRCC	stabilization of HIF1		(Rechsteiner et al., 2011)
	V84E	ccRCC	stabilization of HIF1		(Rechsteiner et al., 2011)
	P86H	ccRCC	stabilization of HIF1		(Rechsteiner et al., 2011)
	W88C	ccRCC	stabilization of HIF1		(Rechsteiner et al., 2011)
	G93E	ccRCC	stabilization of HIF1		(Rechsteiner et al., 2011)
	Y98H/N	ccRCC	stabilization of HIF1		(Rechsteiner et al., 2011)

Table 3.1. Mutations in E3 ligases identified in cancers, continued

E3 Ligase	Mutation	Tumor	Biological Effect	Therapy	Reference
	L101P	ccRCC	stabilization of HIF1		(Rechsteiner et al., 2011)
	Y112D/H/N	ccRCC	stabilization of HIF1		(Rechsteiner et al., 2011)
	G114R	ccRCC	stabilization of HIF1		(Rechsteiner et al., 2011)
	W117L/R	ccRCC	stabilization of HIF1		(Rechsteiner et al., 2011)
	P119L	ccRCC	stabilization of HIF1		(Rechsteiner et al., 2011)
	D121G/Y	ccRCC	stabilization of HIF1		(Rechsteiner et al., 2011)
	V130D/P	ccRCC	stabilization of HIF1		(Rechsteiner et al., 2011)
	L153P	ccRCC	stabilization of HIF1		(Rechsteiner et al., 2011)
	K159N	ccRCC	stabilization of HIF1		(Rechsteiner et al., 2011)
	R161P/Q	ccRCC	stabilization of HIF1		(Rechsteiner et al., 2011)
	L169P	ccRCC	stabilization of HIF1		(Rechsteiner et al., 2011)
	V170E	ccRCC	stabilization of HIF1		(Rechsteiner et al., 2011)
	I180V	ccRCC	stabilization of HIF1		(Rechsteiner et al., 2011)
	L63fsX67	ccRCC	stabilization of HIF1		(Rechsteiner et al., 2011)
	H115SfsX17	ccRCC	stabilization of HIF1		(Rechsteiner et al., 2011)
	L153TfsX21	ccRCC	stabilization of HIF1		(Rechsteiner et al., 2011)
	R117fsX25	ccRCC	stabilization of HIF1		(Rechsteiner et al., 2011)

Table 3.2. Aberrant expression of DUBs associated with cancers

DUB	Upregulated in Tumor	EMT and/or Metastasis	Signaling Effect	Reference
USP9X	Follicular lymphoma, Diffuse Large B-cell Lymphoma, breast adenocarcinoma, colon adenocarcinoma, small cell lung carcinoma	Lymph node	Mcl-1 (stabilization)	(Schwickart et al., 2010)

Table 3.2. Aberrant expression of DUBs associated with cancers, continued

DUB	Upregulated in Tumor	EMT and/or Metastasis	Signaling Effect	Reference
UCHL-1	Gastric (in liver metastasis), NSCLC, breast (can also be downregulated), prostate (downregulated)	Liver, lung	Akt, Erk1/2, p38 MAPK, JNK	(Goto et al., 2015, Gu et al., 2015, Kim et al., 2009, Ummanni et al., 2011)
OTUB1	Colorectal, breast, prostate	Liver, pelvic, ovary, lymph node	TGFβ , MAPK, FOXM1	(Iglesias-Gato et al., 2015, Karunarathna et al., 2016, Zhou et al., 2014)

3.8 The misregulated expression of DUBs in metastatic cancers

Deubiquitinating enzymes (DUBs) play the reverse role of E3 ligases by cleaving the isopeptide bond between the ubiquitin and the substrate. DUBs have been described to play important roles in cellular processes, such as gene transcription, DNA repair and cell cycle progression. There are about 80 functional DUBs and they can be divided into 6 classes: ubiquitin-specific proteases (USPs), ubiquitin carboxy-terminal hydrolases (UCHs), ovarian-tumor proteases (OTUs), Machado-Joseph disease protein domain proteases (MJD), JAMM/MPN domain-associated metallopeptidases (JAMMs) and monocyte chemotactic protein-induced protein (MCPIP) (D'Arcy, Wang et al., 2015).

In cancer, DUBs can stabilize proteins by removing the degradation-inducing ubiquitin signal, contributing to aberrant signaling (Figure 4). Many studies have shown that deregulation of DUBs is involved in cancer progression, recurrence and metastasis (Table 2).

USP7 promotes APL, aggressive prostate cancer, and NSCLC metastasis

USP7 (also known as HAUSP, Herpesvirus-associated ubiquitin protease) plays a crucial role in regulating tumor suppressors p53 and PTEN. A small molecule inhibitor of USP7 (HBX 41,108) inhibits USP7-mediated deubiquitination of p53 and induces apoptosis in colon carcinoma, suggesting the therapeutic potential in targeting USP7 (Colland, Formstecher et al., 2009). USP7 is frequently overexpressed in non-small cell lung carcinoma (NSCLC) and also correlates with lymph node metastasis. Inhibition of *USP7* upregulates E-cadherin and downregulates Vimentin and N-cadherin, indicating USP7 promotes EMT in NSCLC (Zhao, Lin et al., 2015).

Moreover, USP7 may contribute to cancer by modulating the nuclear localization of PTEN. Acute promyelocytic leukaemia (APL) harboring the t(15; 17) chromosomal translocation, which encodes the PML–RARα fusion protein that inhibits differentiation, exhibits aberrant nuclear exclusion of PTEN. As USP7 co-localizes to nuclear bodies, studies using prostate and colon tumor models have shown USP7 to interact with and deubiquitinate PTEN, leading to the nuclear exclusion and impairment of tumor suppressor function of PTEN. In addition, USP7 is overexpressed in prostate cancer tissue, in which the USP7/PTEN signaling axis is misregulated (Song, Salmena et al., 2008).

USP4 and USP9X support oncogenic signaling in various tumors

Ubiquitin-specific peptidase 4 (USP4) is overexpressed in multiple cancers, such as breast and lung cancers (Table 2). Some cancers rely on aberrant TGFβ signaling for the purposes of EMT, proliferation, invasion and metastasis. As previously mentioned, TGFβ-induced activation of TβRI eventually results in the ubiquitination of TβRI and subsequent membrane internalization and degradation of the receptor, terminating downstream signaling. USP4 overexpression is detected in invasive breast carcinoma and it enhances aberrant TGFβ signaling. A mechanism by which this oncogenic signaling occurs has been proposed. AKT-mediated phosphorylation of USP4 at a consensus motif stabilizes this DUB, which in turn deubiquitinates the TGFβ-induced activated TβRI and leads to the stabilization of downstream activation of phosphorylated SMAD2 and SMAD2/SMAD4 complex formation (Figure 2). USP4-mediated stabilization of TGFβ signaling leads to the expression of metastasis-inducing genes such as *IL-11, CXCR4* and *MMPs* in breast cancer cells (Zhang, Zhou et al., 2012).

In addition, the overexpression of another DUB - USP9X - has been detected in follicular lymphoma, breast and colon adenocarcinomas, and small cell lung carcinoma (Schwickart, Huang et al., 2010) (Table 2). Various lymphomas, such as B- and mantle-cell lymphomas and multiple myeloma usually rely on the overexpressed MCL1, a member of the pro-survival BCL family of proteins. In multiple myeloma, overexpression of USP9X is correlated with poor survival. A mechanism by which MCL1 is stabilized has been

proposed. The overexpression of USP9X results in the deubiquitination of MCL1 by this DUB, stabilizing pro-survival oncogenic signaling in cancers. Although knocking down USP9X does not affect cell proliferation *in vitro*, it does sensitize tumors to ABT-737 small molecule antagonist of BCL proteins resulting in apoptosis (Schwickart et al., 2010). More recently, in non-small cell lung carcinoma, inhibition of USP9X by either siRNA knockdown or via a small molecule inhibitor WP1130 decreased MCL1 expression and sensitized cells to radiation therapy (Kushwaha, O'Leary et al., 2015).

UCH-L1 plays a contradicting role in different tumors

Overexpression of UCH-L1 (Ubiquitin carboxy-terminal hydrolase L1) in gastric cancer promotes colony formation, migration and liver metastasis of gastric cancer cells *in vitro* due to significant upregulation of AKT and Erk1/2 signaling (Gu, Yang et al., 2015). Moreover, UCH-L1 is overexpressed in highly invasive NSCLC and melanoma. In lung cells, UCH-L1 supports the EGF-induced activation of Akt, JNK, and p38 MAPK signaling (Kim, Kim et al., 2009).

In addition, high expression of UCH-L1 positively correlates with that of HIF1α and hence activation of hypoxia conditions in some breast and lung cancer, and it contributes to poor overall survival and distant metastasis-free survival in breast, lung and melanoma cancer. UCH-L1 is shown to deubiquitinate and stabilize HIF1α, inducing hypoxia (Figure 2). UCHL1 expression supports breast and melanoma metastasis to lungs; inhibition of

metastasis is achieved by a UCH-L1 inhibitor, LDN57444.(Goto, Zeng et al., 2015).

However, the role of UCH-L1 is not as straightforward as suggested by these studies. Another study reported that *UCHL1* can be downregulated in other breast cancer tissue samples and cell lines due to frequent gene methylation. Overexpression of UCHL1 in MB231 breast cells significantly decreases proliferation due to G0/G1 cell cycle arrest and apoptosis (Xiang, Li et al., 2012). Similarly, this DUB is downregulated in some prostate cancer samples and in LNCaP cell line, and overexpression of UCHL-1 suppresses the proliferation and anchorage-independent growth of LNCaP cells (Ummanni, Jost et al., 2011). Further research will be required to unravel the contradicting role of UCH-L1 in different cancers.

OTUB1 contributes to drug resistance and promotes metastasis

OTU domain-containing ubiquitin aldehyde-binding protein 1 (OTUB1) plays diverse roles such as stabilizing p53, inhibiting K63-linked polyubiquitination for DNA double strand break repair by targeting UBC13 for degradation, the E2 enzyme that catalyzes this ubiquitin linkage in proteins members of the NFκB pathway. High expression of OTUB1 is detected in approximately 50% of colorectal cancer and correlates with lymph node status, liver, pelvic and ovary distant metastasis, in addition to low overall and progression-free survival rates. OTUB1 is also found to be important in prostate

cancer by regulating androgen signaling. (Iglesias-Gato, Chuan et al., 2015, Zhou, Wu et al., 2014). In breast cancer, OTUB1 decreases the Lys48-linked ubiquitination of FOXM1 stabilizing the expression of the protein. FOXM1 is a transcription factor that is important for DNA damage responses and its overexpression is associated with genotoxic drug resistance in tumors. Hence, the overexpression of OTUB1 contributes to the aberrant proliferation and epirubicin resistance of MCF7 cells and correlates with poor survival and chemotherapy resistance of breast cancer cohort (Karunarathna, Kongsema et al., 2016). In summary, it is evident that some DUBS are either upregulated or downregulated in some tumors, promoting oncogenic signaling.

3.9 Concluding Remarks

The information presented herein reveals a common pattern: the misregulated expression of various E2 ubiquitin conjugating enzymes, E3 ubiquitin ligases and DUBs supports aberrant oncogenic signaling in a plethora of tumors. Since the misregulated expression of these proteins overlaps among many different types of cancers, there may exist subpopulations of cells within tumors exhibiting the misregulated expression of a specific member of the ubiquitination pathway. Alternatively, cells may take advantage of a combinatorial misregulated expression of these proteins to support oncogenic signaling. Lastly, it is not clear whether E2's and E3's catalyze non-proteasomal ubiquitin linkages that stabilize the function of oncogenes, and/or DUB's remove

the ubiquitin linkages that would otherwise result in the degradation of oncogenes. Several models are presented by which members of the ubiquitination pathway support oncogenic signaling in cancers (Figure 4). Nevertheless, it is clear that the inhibition of a specific E2, E3 or DUB seems to halt tumor progression and metastasis.

The development of chemotherapeutic agents against E2's, E3's and DUBs, is an attractive strategy that may lead to the inhibition of multiple oncogenic pathways in tumors. So far, the FDA has approved very few drugs targeting members of the ubiquitination cascade. Proteasome inhibitors, Bortezomib and Carfilzomib, are limited to multiple myeloma and mantle cell lymphoma treatments. Various strategies to develop inhibitors to target E1's, E2's, E3's have been recently described (Huang & Dixit, 2016). For instance, targeting the MDM2 E3 ligase - a p53 negative regulator - with RG7112 (cis-imidazoline analogues) has been tested in clinical trials for the treatment of advanced solid and hematological malignancies, including liposarcoma (Burgess, Chia et al., 2016).

An interesting concept to enhance the ubiquitination and degradation of "undruggable" oncogenic proteins is the development of protein-targeting chimeric molecules (PROTACs). These molecules are bifunctional in which they include an E3 ligase-recruiting moiety linked by a short linker to a ligand that targets the substrate of interest, placing them in proximity for ubiquitination leading to subsequent degradation (Huang & Dixit, 2016). Therefore, targeting

the E3 ligases and their co-expressed substrates with PROTAC may be a promising therapeutic intervention in various tumors herein described.

Major advances have been made to target oncogenic protein kinases in clinical settings through the development of TKIs. Here, we present evidence from multiple papers demonstrating that mechanistic studies of the ubiquitination pathway will open new therapeutic approaches, potentially allowing the development of novel inhibitors to suppress cancer progression and metastasis.

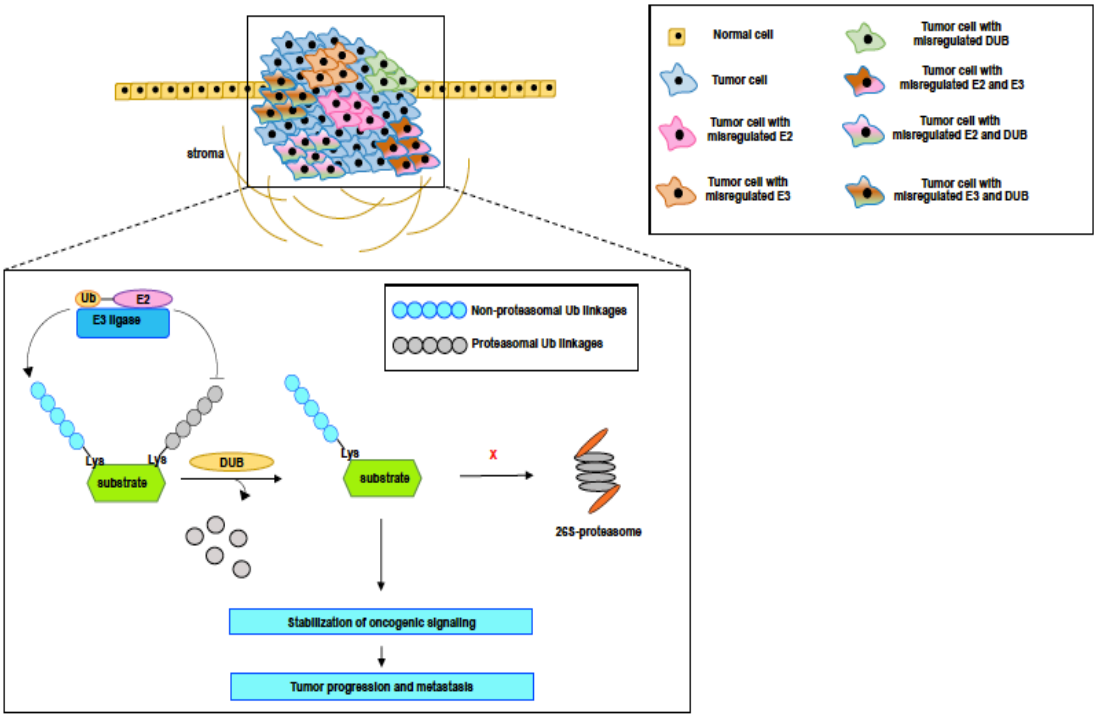

Figure 3.4. **Proposed model of the mechanism by which the misregulated expression of E2's, E3's and DUB's may contribute to tumorigenesis and metastasis**. The information from the reports described in this review reveals that inhibition of E2's, E3's and DUB's with either small interfering RNA or small molecule inhibitors is sufficient to inhibit the progression and metastasis of tumors. However, some of these reports show that the misregulated expression of the members of the ubiquitination pathway occurs in multiple tumors. It is not clear whether a subpopulation of cells within a tumor, for instance, may rely on the misregulated expression of one member only or on a combination of the misregulated expression of these proteins to support aberrant oncogenic signaling. In addition, it is not clearly demonstrated whether the misregulated expression of E2's and E3's stabilizes oncogenic signaling via the catalysis of non-proteasomal ubiquitin linkages, while DUB's remove ubiquitin linkages that would otherwise lead to proteasomal degradation. Nevertheless, we describe a common conclusion from multiple reports that members of the ubiquitination pathway drive tumor aggressiveness and culminate in metastasis.

3.10 Acknowledgments

We thank all lab members for advice and encouragement. We also acknowledge generous support from the UC San Diego Foundation.

Chapter 3, in full, is the work currently being prepared for submission for publication. Gallo L.H., Ko J., Donoghue D.J. “The Importance of Regulatory Ubiquitination in Cancer and Metastasis”. The first author of the work is the author of this dissertation.

3.11 References

1. Aki D, Zhang W, Liu YC (2015) The E3 ligase Itch in immune regulation and beyond. Immunol Rev 266: 6-26

2. Aydin IT, Melamed RD, Adams SJ, Castillo-Martin M, Demir A, Bryk D, Brunner G, Cordon-Cardo C, Osman I, Rabadan R, Celebi JT (2014) FBXW7 mutations in melanoma and a new therapeutic paradigm. J Natl Cancer Inst 106: dju107

3. Berndsen CE, Wolberger C (2014) New insights into ubiquitin E3 ligase mechanism. Nat Struct Mol Biol 21: 301-7

4. Bongiorno-Borbone L, Giacobbe A, Compagnone M, Eramo A, De Maria R, Peschiaroli A, Melino G (2015) Anti-tumoral effect of desmethylclomipramine in lung cancer stem cells. Oncotarget 6: 16926-38

5. Burgess A, Chia KM, Haupt S, Thomas D, Haupt Y, Lim E (2016) Clinical Overview of MDM2/X-Targeted Therapies. Front Oncol 6: 7

6. Chan CH, Morrow JK, Li CF, Gao Y, Jin G, Moten A, Stagg LJ, Ladbury JE, Cai Z, Xu D, Logothetis CJ, Hung MC, Zhang S, Lin HK (2013) Pharmacological inactivation of Skp2 SCF ubiquitin ligase restricts cancer stem cell traits and cancer progression. Cell 154: 556-68

7. Chen C, Zhou Z, Ross JS, Zhou W, Dong JT (2007) The amplified WWP1 gene is a potential molecular target in breast cancer. Int J Cancer 121: 80-87

8. Chen C, Zhou Z, Sheehan CE, Slodkowska E, Sheehan CB, Boguniewicz A, Ross JS (2009) Overexpression of WWP1 is associated

with the estrogen receptor and insulin-like growth factor receptor 1 in breast carcinoma. Int J Cancer 124: 2829-36

9. Chen J, Chen ZJ (2013) Regulation of NF-kappaB by ubiquitination. Curr Opin Immunol 25: 4-12

10. Cheng Q, Cao X, Yuan F, Li G, Tong T (2014) Knockdown of WWP1 inhibits growth and induces apoptosis in hepatoma carcinoma cells through the activation of caspase3 and p53. Biochem Biophys Res Commun 448: 248-54

11. Cheung KJ, Ewald AJ (2016) A collective route to metastasis: Seeding by tumor cell clusters. Science 352: 167-9

12. Clague MJ, Heride C, Urbe S (2015) The demographics of the ubiquitin system. Trends Cell Biol 25: 417-26

13. Colland F, Formstecher E, Jacq X, Reverdy C, Planquette C, Conrath S, Trouplin V, Bianchi J, Aushev VN, Camonis J, Calabrese A, Borg-Capra C, Sippl W, Collura V, Boissy G, Rain JC, Guedat P, Delansorne R, Daviet L (2009) Small-molecule inhibitor of USP7/HAUSP ubiquitin protease stabilizes and activates p53 in cells. Mol Cancer Ther 8: 2286-95

14. D'Arcy P, Wang X, Linder S (2015) Deubiquitinase inhibition as a cancer therapeutic strategy. Pharmacol Ther 147: 32-54

15. Deryugina EI, Quigley JP (2006) Matrix metalloproteinases and tumor metastasis. Cancer Metastasis Rev 25: 9-34

16. Deshaies RJ, Joazeiro CA (2009) RING domain E3 ubiquitin ligases. Annu Rev Biochem 78: 399-434

17. Emmerich CH, Ordureau A, Strickson S, Arthur JS, Pedrioli PG, Komander D, Cohen P (2013) Activation of the canonical IKK complex by K63/M1-linked hybrid ubiquitin chains. Proc Natl Acad Sci U S A 110: 15247-52

18. Feng C, Sun Y, Ding G, Wu Z, Jiang H, Wang L, Ding Q, Wen H (2015) PI3Kbeta inhibitor TGX221 selectively inhibits renal cell carcinoma cells with both VHL and SETD2 mutations and links multiple pathways. Scientific reports 5: 9465

19. Fujita T, Ikeda H, Kawasaki K, Taira N, Ogasawara Y, Nakagawara A, Doihara H (2009) Clinicopathological relevance of UbcH10 in breast cancer. Cancer Sci 100: 238-48

20. Goto Y, Zeng L, Yeom CJ, Zhu Y, Morinibu A, Shinomiya K, Kobayashi M, Hirota K, Itasaka S, Yoshimura M, Tanimoto K, Torii M, Sowa T, Menju T, Sonobe M, Kakeya H, Toi M, Date H, Hammond EM, Hiraoka M, Harada H. (2015) UCHL1 provides diagnostic and antimetastatic strategies due to its deubiquitinating effect on HIF-1alpha. Nature communications 6: 6153

21. Grand FH, Hidalgo-Curtis CE, Ernst T, Zoi K, Zoi C, McGuire C, Kreil S, Jones A, Score J, Metzgeroth G, Oscier D, Hall A, Brandts C, Serve H, Reiter A, Chase AJ, Cross NC (2009) Frequent CBL mutations associated with 11q acquired uniparental disomy in myeloproliferative neoplasms. Blood 113: 6182-92

22. Gu YY, Yang M, Zhao M, Luo Q, Yang L, Peng H, Wang J, Huang SK, Zheng ZX, Yuan XH, Liu P, Huang CZ (2015) The de-ubiquitinase UCHL1 promotes gastric cancer metastasis via the Akt and Erk1/2 pathways. Tumour Biol 36: 8379-87

23. Huang X, Dixit VM (2016) Drugging the undruggables: exploring the ubiquitin system for drug development. Cell Res 26: 484-98

24. Ibusuki M, Yamamoto Y, Shinriki S, Ando Y, Iwase H (2011) Reduced expression of ubiquitin ligase FBXW7 mRNA is associated with poor prognosis in breast cancer patients. Cancer Sci 102: 439-45

25. Iglesias-Gato D, Chuan YC, Jiang N, Svensson C, Bao J, Paul I, Egevad L, Kessler BM, Wikstrom P, Niu Y, Flores-Morales A (2015) OTUB1 de-ubiquitinating enzyme promotes prostate cancer cell invasion in vitro and tumorigenesis in vivo. Molecular cancer 14: 8

26. Iwatsuki M, Mimori K, Ishii H, Yokobori T, Takatsuno Y, Sato T, Toh H, Onoyama I, Nakayama KI, Baba H, Mori M (2010) Loss of FBXW7, a cell cycle regulating gene, in colorectal cancer: clinical significance. Int J Cancer 126: 1828-37

27. Jang KW, Lee KH, Kim SH, Jin T, Choi EY, Jeon HJ, Kim E, Han YS, Chung JH (2011) Ubiquitin ligase CHIP induces TRAF2 proteasomal degradation and NF-kappaB inactivation to regulate breast cancer cell invasion. J Cell Biochem 112: 3612-20

28. Jardim DL, Wheler JJ, Hess K, Tsimberidou AM, Zinner R, Janku F, Subbiah V, Naing A, Piha-Paul SA, Westin SN, Roy-Chowdhuri S, Meric-Bernstam F, Hong DS (2014) FBXW7 mutations in patients with advanced cancers: clinical and molecular characteristics and outcomes with mTOR inhibitors. PLoS One 9: e89388

29. Jung CR, Hwang KS, Yoo J, Cho WK, Kim JM, Kim WH, Im DS (2006) E2-EPF UCP targets pVHL for degradation and associates with tumor growth and metastasis. Nat Med 12: 809-16

30. Kajiro M, Hirota R, Nakajima Y, Kawanowa K, So-ma K, Ito I, Yamaguchi Y, Ohie SH, Kobayashi Y, Seino Y, Kawano M, Kawabe Y, Takei H, Hayashi S, Kurosumi M, Murayama A, Kimura K, Yanagisawa J (2009) The ubiquitin ligase CHIP acts as an upstream regulator of oncogenic pathways. Nat Cell Biol 11: 312-9

31. Karunarathna U, Kongsema M, Zona S, Gong C, Cabrera E, Gomes AR, Man EP, Khongkow P, Tsang JW, Khoo US, Medema RH, Freire R, Lam EW (2016) OTUB1 inhibits the ubiquitination and degradation of FOXM1 in breast cancer and epirubicin resistance. Oncogene 35: 1433-44

32. Kassenbrock CK, Anderson SM (2004) Regulation of ubiquitin protein ligase activity in c-Cbl by phosphorylation-induced conformational change and constitutive activation by tyrosine to glutamate point mutations. J Biol Chem 279: 28017-27

33. Khammanivong A, Gopalakrishnan R, Dickerson EB (2014) SMURF1 silencing diminishes a CD44-high cancer stem cell-like population in head and neck squamous cell carcinoma. Molecular cancer 13: 260

34. Kim HJ, Kim YM, Lim S, Nam YK, Jeong J, Kim HJ, Lee KJ (2009) Ubiquitin C-terminal hydrolase-L1 is a key regulator of tumor cell invasion and metastasis. Oncogene 28: 117-27

35. Kushwaha D, O'Leary C, Cron KR, Deraska P, Zhu K, D'Andrea AD, Kozono D (2015) USP9X inhibition promotes radiation-induced apoptosis in non-small cell lung cancer cells expressing mid-to-high MCL1. Cancer Biol Ther 16: 392-401

36. Lin JH, Hsieh SC, Chen JN, Tsai MH, Chang CC (2013) WWP1 gene is a potential molecular target of human oral cancer. Oral Surg Oral Med Oral Pathol Oral Radiol 116: 221-31

37. Loh ML, Sakai DS, Flotho C, Kang M, Fliegauf M, Archambeault S, Mullighan CG, Chen L, Bergstraesser E, Bueso-Ramos CE, Emanuel PD, Hasle H, Issa JP, van den Heuvel-Eibrink MM, Locatelli F, Stary J, Trebo M, Wlodarski M, Zecca M, Shannon KM, Niemeyer CM. (2009) Mutations in CBL occur frequently in juvenile myelomonocytic leukemia. Blood 114: 1859-63

38. Maher ER, Neumann HP, Richard S (2011) von Hippel-Lindau disease: a clinical and scientific review. Eur J Hum Genet 19: 617-23

39. Makishima H, Cazzolli H, Szpurka H, Dunbar A, Tiu R, Huh J, Muramatsu H, O'Keefe C, Hsi E, Paquette RL, Kojima S, List AF, Sekeres MA, McDevitt MA, Maciejewski JP (2009) Mutations of e3 ubiquitin ligase cbl family members constitute a novel common pathogenic lesion in myeloid malignancies. J Clin Oncol 27: 6109-16

40. Messick TE, Greenberg RA (2009) The ubiquitin landscape at DNA double-strand breaks. J Cell Biol 187: 319-26

41. Morrison BJ, Morris JC, Steel JC (2013) Lung cancer-initiating cells: a novel target for cancer therapy. Target Oncol 8: 159-72

42. Muramatsu H, Makishima H, Jankowska AM, Cazzolli H, O'Keefe C, Yoshida N, Xu Y, Nishio N, Hama A, Yagasaki H, Takahashi Y, Kato K, Manabe A, Kojima S, Maciejewski JP (2010) Mutations of an E3 ubiquitin ligase c-Cbl but not TET2 mutations are pathogenic in juvenile myelomonocytic leukemia. Blood 115: 1969-75

43. Ori D, Kato H, Sanjo H, Tartey S, Mino T, Akira S, Takeuchi O (2013) Essential roles of K63-linked polyubiquitin-binding proteins TAB2 and TAB3 in B cell activation via MAPKs. J Immunol 190: 4037-45

44. Paolino M, Choidas A, Wallner S, Pranjic B, Uribesalgo I, Loeser S, Jamieson AM, Langdon WY, Ikeda F, Fededa JP, Cronin SJ, Nitsch R, Schultz-Fademrecht C, Eickhoff J, Menninger S, Unger A, Torka R,

Gruber T, Hinterleitner R, Baier G, Wolf D, Ullrich A, Klebl BM, Penninger JM. (2014) The E3 ligase Cbl-b and TAM receptors regulate cancer metastasis via natural killer cells. Nature 507: 508-12

45. Quail DF, Joyce JA (2013) Microenvironmental regulation of tumor progression and metastasis. Nat Med 19: 1423-37

46. Rankin EB, Giaccia AJ (2016) Hypoxic control of metastasis. Science 352: 175-80

47. Rechsteiner MP, von Teichman A, Nowicka A, Sulser T, Schraml P, Moch H (2011) VHL gene mutations and their effects on hypoxia inducible factor HIFalpha: identification of potential driver and passenger mutations. Cancer Res 71: 5500-11

48. Rossi M, Rotblat B, Ansell K, Amelio I, Caraglia M, Misso G, Bernassola F, Cavasotto CN, Knight RA, Ciechanover A, Melino G (2014) High throughput screening for inhibitors of the HECT ubiquitin E3 ligase ITCH identifies antidepressant drugs as regulators of autophagy. Cell death & disease 5: e1203

49. Sargin B, Choudhary C, Crosetto N, Schmidt MH, Grundler R, Rensinghoff M, Thiessen C, Tickenbrock L, Schwable J, Brandts C, August B, Koschmieder S, Bandi SR, Duyster J, Berdel WE, Muller-Tidow C, Dikic I, Serve H (2007) Flt3-dependent transformation by inactivating c-Cbl mutations in AML. Blood 110: 1004-12

50. Schwickart M, Huang X, Lill JR, Liu J, Ferrando R, French DM, Maecker H, O'Rourke K, Bazan F, Eastham-Anderson J, Yue P, Dornan D, Huang DC, Dixit VM (2010) Deubiquitinase USP9X stabilizes MCL1 and promotes tumour cell survival. Nature 463: 103-7

51. Song MS, Salmena L, Carracedo A, Egia A, Lo-Coco F, Teruya-Feldstein J, Pandolfi PP (2008) The deubiquitinylation and localization of PTEN are regulated by a HAUSP-PML network. Nature 455: 813-7

52. Takeishi S, Matsumoto A, Onoyama I, Naka K, Hirao A, Nakayama KI (2013) Ablation of Fbxw7 eliminates leukemia-initiating cells by preventing quiescence. Cancer Cell 23: 347-61

53. Takeishi S, Nakayama KI (2014) Role of Fbxw7 in the maintenance of normal stem cells and cancer-initiating cells. Br J Cancer 111: 1054-9

54. Tsai YC, Mendoza A, Mariano JM, Zhou M, Kostova Z, Chen B, Veenstra T, Hewitt SM, Helman LJ, Khanna C, Weissman AM (2007) The ubiquitin ligase gp78 promotes sarcoma metastasis by targeting KAI1 for degradation. Nat Med 13: 1504-9

55. Ummanni R, Jost E, Braig M, Lohmann F, Mundt F, Barett C, Schlomm T, Sauter G, Senff T, Bokemeyer C, Sultmann H, Meyer-Schwesinger C, Brummendorf TH, Balabanov S (2011) Ubiquitin carboxyl-terminal hydrolase 1 (UCHL1) is a potential tumour suppressor in prostate cancer and is frequently silenced by promoter methylation. Molecular cancer 10: 129

56. van Ree JH, Jeganathan KB, Malureanu L, van Deursen JM (2010) Overexpression of the E2 ubiquitin-conjugating enzyme UbcH10 causes chromosome missegregation and tumor formation. J Cell Biol 188: 83-100

57. Vaughan L, Tan CT, Chapman A, Nonaka D, Mack NA, Smith D, Booton R, Hurlstone AF, Malliri A (2015) HUWE1 ubiquitylates and degrades the RAC activator TIAM1 promoting cell-cell adhesion disassembly, migration, and invasion. Cell reports 10: 88-102

58. Villaruz LC, Socinski MA (2014) Temsirolimus therapy in a patient with lung adenocarcinoma harboring an FBXW7 mutation. Lung cancer (Amsterdam, Netherlands) 83: 300-1

59. Wang J, Huang Y, Guan Z, Zhang JL, Su HK, Zhang W, Yue CF, Yan M, Guan S, Liu QQ (2014a) E3-ligase Skp2 predicts poor prognosis and maintains cancer stem cell pool in nasopharyngeal carcinoma. Oncotarget 5: 5591-601

60. Wang T, Yang J, Xu J, Li J, Cao Z, Zhou L, You L, Shu H, Lu Z, Li H, Li M, Zhang T, Zhao Y (2014b) CHIP is a novel tumor suppressor in pancreatic cancer through targeting EGFR. Oncotarget 5: 1969-86

61. Wang Y, Liu Y, Lu J, Zhang P, Wang Y, Xu Y, Wang Z, Mao JH, Wei G (2013) Rapamycin inhibits FBXW7 loss-induced epithelial-mesenchymal transition and cancer stem cell-like characteristics in colorectal cancer cells. Biochem Biophys Res Commun 434: 352-6

62. Wang Y, Ren F, Wang Y, Feng Y, Wang D, Jia B, Qiu Y, Wang S, Yu J, Sung JJ, Xu J, Zeps N, Chang Z (2014c) CHIP/Stub1 functions as a tumor suppressor and represses NF-kappaB-mediated signaling in colorectal cancer. Carcinogenesis 35: 983-91

63. Welcker M, Clurman BE (2008) FBW7 ubiquitin ligase: a tumour suppressor at the crossroads of cell division, growth and differentiation. Nat Rev Cancer 8: 83-93

64. Wu X, Zhang W, Font-Burgada J, Palmer T, Hamil AS, Biswas SK, Poidinger M, Borcherding N, Xie Q, Ellies LG, Lytle NK, Wu LW, Fox RG, Yang J, Dowdy SF, Reya T, Karin M (2014) Ubiquitin-conjugating enzyme Ubc13 controls breast cancer metastasis through a TAK1-p38 MAP kinase cascade. Proc Natl Acad Sci U S A 111: 13870-5

65. Wu Z, Shen S, Zhang Z, Zhang W, Xiao W (2014) Ubiquitin-conjugating enzyme complex Uev1A-Ubc13 promotes breast cancer metastasis through nuclear factor-small ka, CyrillicB mediated matrix metalloproteinase-1 gene regulation. Breast Cancer Res 16: R75

66. Xiang T, Li L, Yin X, Yuan C, Tan C, Su X, Xiong L, Putti TC, Oberst M, Kelly K, Ren G, Tao Q (2012) The ubiquitin peptidase UCHL1 induces G0/G1 cell cycle arrest and apoptosis through stabilizing p53 and is frequently silenced in breast cancer. PLoS One 7: e29783

67. Yang H, Lu X, Liu Z, Chen L, Xu Y, Wang Y, Wei G, Chen Y (2015) FBXW7 suppresses epithelial-mesenchymal transition, stemness and metastatic potential of cholangiocarcinoma cells. Oncotarget 6: 6310-25

68. Yang Y, Schmitz R, Mitala J, Whiting A, Xiao W, Ceribelli M, Wright GW, Zhao H, Yang Y, Xu W, Rosenwald A, Ott G, Gascoyne RD, Connors JM, Rimsza LM, Campo E, Jaffe ES, Delabie J, Smeland EB, Braziel RM Tubbs RR, Cook JR, Weinsenburger DD, Chan WC, Wiestner A, Kruhlak MJ, Iwai K, Bernal F, Staudt LM. (2014) Essential role of the linear ubiquitin chain assembly complex in lymphoma revealed by rare germline polymorphisms. Cancer discovery 4: 480-93

69. Yuan L, Lu L, Yang Y, Sun H, Chen X, Huang Y, Wang X, Zou L, Bao L (2015) Genetic mutational profiling analysis of T cell acute lymphoblastic leukemia reveal mutant FBXW7 as a prognostic indicator for inferior survival. Ann Hematol 94: 1817-28

70. Zhang L, Wu Z, Ma Z, Liu H, Wu Y, Zhang Q (2015) WWP1 as a potential tumor oncogene regulates PTEN-Akt signaling pathway in human gastric carcinoma. Tumour Biol 36: 787-98

71. Zhang L, Zhou F, Drabsch Y, Gao R, Snaar-Jagalska BE, Mickanin C, Huang H, Sheppard KA, Porter JA, Lu CX, ten Dijke P (2012) USP4 is regulated by AKT phosphorylation and directly deubiquitylates TGF-beta type I receptor. Nat Cell Biol 14: 717-26

72. Zhang L, Zhou F, Garcia de Vinuesa A, de Kruijf EM, Mesker WE, Hui L, Drabsch Y, Li Y, Bauer A, Rousseau A, Sheppard KA, Mickanin C, Kuppen PJ, Lu CX, Ten Dijke P (2013) TRAF4 promotes TGF-beta receptor signaling and drives breast cancer metastasis. Mol Cell 51: 559-72

73. Zhao GY, Lin ZW, Lu CL, Gu J, Yuan YF, Xu FK, Liu RH, Ge D, Ding JY (2015) USP7 overexpression predicts a poor prognosis in lung squamous cell carcinoma and large cell carcinoma. Tumour Biol 36: 1721-9

74. Zhou Y, Wu J, Fu X, Du W, Zhou L, Meng X, Yu H, Lin J, Ye W, Liu J, Peng H, Liu RY, Pan C, Huang W (2014) OTUB1 promotes metastasis and serves as a marker of poor prognosis in colorectal cancer. Molecular cancer 13: 258

75. Zhou Z, Liu R, Chen C (2012) The WWP1 ubiquitin E3 ligase increases TRAIL resistance in breast cancer. Int J Cancer 130: 1504-10

Chapter 4: Functions of Fibroblast Growth Factor Receptors in Cancer Defined by Novel Translocations and Mutations

4.1 Abstract

The four receptor tyrosine kinases (RTKs) within the family of Fibroblast Growth Factor Receptors (FGFRs) are critical for normal development but also play an enormous role in oncogenesis. Mutations and/or abnormal expression often lead to constitutive dimerization and kinase activation of FGFRs, and represent the primary mechanism for aberrant signaling. Sequencing of human tumors has revealed a plethora of somatic mutations in FGFRs that are frequently identical to germline mutations in developmental syndromes, and has also identified novel FGFR fusion proteins arising from chromosomal rearrangements that contribute to malignancy. This review details approximately 200 specific point mutations in FGFRs and 40 different fusion proteins created by translocations involving FGFRs that have been identified in human cancer. This review discusses the effects of these genetic alterations on downstream signaling cascades, and the challenge of drug resistance in cancer treatment with antagonists of FGFRs.

4.2 Overview of canonical FGFR signaling

Receptor tyrosine kinases (RTKs) represent important signal transducers in the cell membrane and are comprised of nearly twenty families of homologous proteins in humans, with almost 60 distinct members (1). In the FGFR family, four homologous human receptors have been identified: FGFR1, FGFR2, FGFR3 and FGFR4. All of the FGFRs exhibit three extracellular immunoglobulin (Ig)-like domains, a membrane-spanning segment and a split tyrosine kinase domain. Fibroblast growth factors (FGFs), a large family of related growth factors, act in concert with heparin sulfate proteoglycans (HSPGs) as high-affinity FGFR agonists (2, 3). The splicing of FGFRs results in further distinction of ligand specificity accompanied by altered biological properties, in which the most studied splicing isoforms involve the third immunoglobulin-like domain of the receptors (4). For FGFR2 and FGFR3, the first half of third Ig domain consists of an invariant exon (IIIa), and splicing of the second half of third Ig domain results in either IIIb isoform (exons 7 and 8) or IIIc isoform (exons 7 and 9). Generally, the IIIb isoforms of FGFRs are expressed in tissues of epithelial origin whereas the IIIc isoforms are expressed in mesenchymal tissues (5).

Binding of FGF/HSPG to FGFR induces the dimerization of receptor monomers in the plasma membrane, followed by trans-autophosphorylation of tyrosine residues located in the cytoplasmic kinase domain. This tyrosine phosphorylation triggers the binding of Src homology (SH2) domain of phospholipase C gamma (PLCγ) to the receptor, resulting in the activation of PKC. Activation also induces RAS-MAPK and PI3K-AKT signaling via FRS2

and GRB2 adaptor proteins. Additional pathways activated by FGFRs include Jun N-terminal kinase and JAK/STAT pathways. FGFR signaling results in cellular proliferation and migration, anti-apoptosis, angiogenesis and wound healing (**Fig 1**) (6).

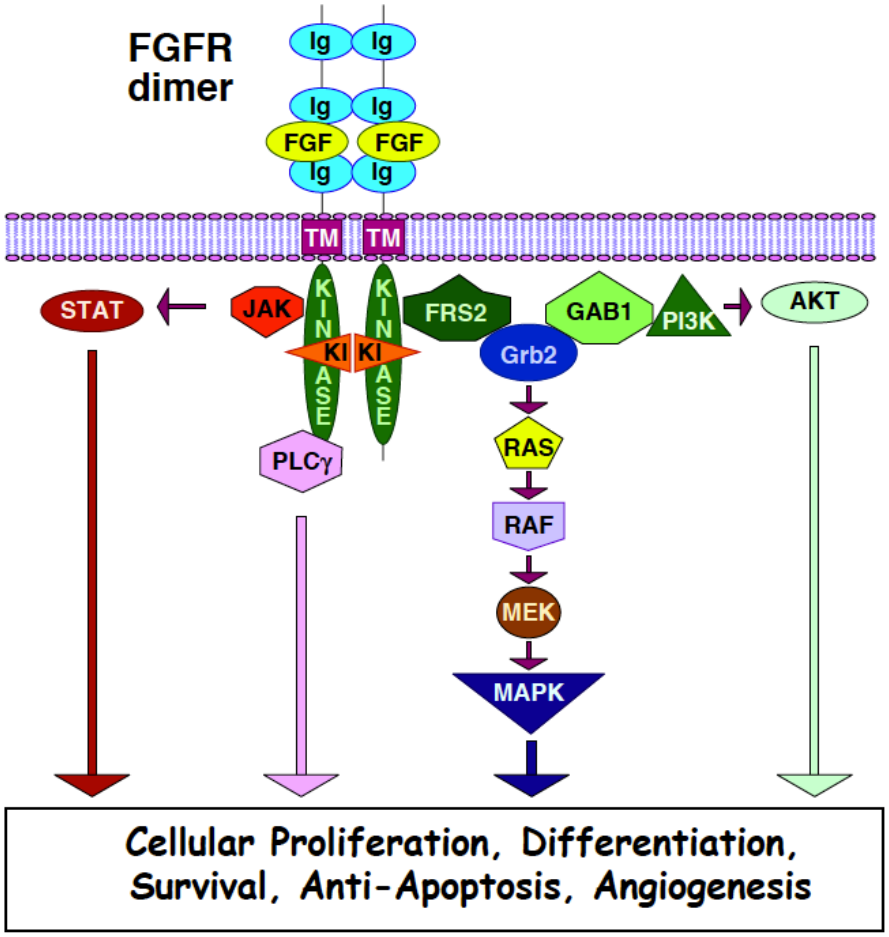

Figure 4.1. FGFR Signaling Pathways. FGF ligand binds to FGFR monomers, leading to the dimerization and subsequent tyrosine autophosphorylation of the receptor. This event leads to activaton of FGFRs and various downstream proteins, resulting in cellular proliferation, differentiation, survival, anti-apoptosis and angiogenesis.

4.3 FGFRs are mutated in human syndromes and cancer

Nomenclature of mutations with respect to isoforms

The alternatively spliced isoforms of FGFR1, FGFR2 and FGFR3 result in considerable confusion in numbering specific mutations, depending upon the convention employed by the original authors. In **Table 1,** we have presented the residue numbers in FGFR1 for both the αA1 and αB1 isoforms, in FGFR2 for the IIIb and IIIc isoforms, in FGFR3 for the IIIb and IIIc isoforms, and FGFR4 for the Uniprot P22455-1 and P22455-2 isoforms. Throughout this manuscript, we will refer to the numbering for the isoforms FGFR1 αA1, FGFR2 IIIb, FGFR3 IIIb, and full-length FGFR4 (Uniprot P22455-1), although a specific mutation may have been described initially in the other isoform. Rarely, a mutation may occur at a residue that is not present in either of the most common isoforms; in these unusual cases, this other isoform is identified in **Table 1.**

Cysteine mutations in the extracellular domain lead to aberrant activation of FGFRs

Many mutations in the extracellular domains of FGFRs induce tyrosine kinase activation by disulfide bond disruption. For instance, each Ig domain of FGFR2 is stabilized by a disulfide bond between pairs of cysteine residues: Cys62 and Cys107 in Ig-I, Cys179 and Cys231 in Ig-II, Cys278 and Cys340 in

Ig-III (7). Mutations in FGFR2 that perturb a disulfide bond in the extracellular domain result in increased receptor activation, such as the C278F mutation in Crouzon and Pfeiffer Syndromes, or the mutation of C340 to S or Y in Crouzon Syndrome. These are examples of craniosynostosis syndromes exhibiting premature closure of cranial sutures, accompanied by defects in chondrocyte signaling and brain development (8). This same theme is recapitulated in somatic mutations involved in human cancer as exemplified by the C278F mutation and the mutations C340F/R/S/W/Y identified in spermatocytic seminoma (9). Conceptually similar mutations that remove a critical Cys residue also occur in FGFR3 and FGFR4 (**Table 1, Fig 2**).

Conversely, the *addition* of a single cysteine mutation creates an unpaired cysteine that can participate in abnormal intermolecular disulfide bond formation leading to receptor activation. One such example is FGFR2 W290C, a mutation causing Pfeiffer Syndrome, which has also been identified in lung squamous cell carcinoma and spermatocytic seminoma (**Table 1**). A conceptually similar mutation is that of FGFR2 S352C in Crouzon Syndrome (10, 11), also identified in spermatocytic seminoma. Other examples of FGFR2 mutations that introduce a new cysteine residue in the extracellular domain include R203C, Y281C, S320C, Y338C, and S373C, which have been identified in various cancers including breast cancer, endometrial carcinoma, lung squamous cell carcinoma and spermatocytic seminoma (**Table 1, Fig 2**). Some of these mutations have been shown to result in increased receptor autophosphorylation and elevated phosphorylation of FRS2, MAPK and STAT3

(12). The FGFR2 W290C and S320C mutants have been shown to contribute to tumor formation in xenograft models, and such tumors were sensitive to a selective FGFR inhibitor BJG398, which caused dramatic tumor shrinkage (12). Overall, these gain-of-function mutations lead to constitutive FGFR activation and drive cellular proliferation and tumor progression. Note that in Fig 2, all mutations such as W290C that have been identified in human cancer and as developmental syndromes are shown in red. Mutations identified only in human cancer are shown in black.

Mutations that introduce a novel cysteine residue also occur in FGFR3, such as R248C and S249C which, as congenital mutations, cause Thanatophoric Dysplasia Type I (TDI), a severe achondroplasia typically causing neonatal lethality. As somatic mutations, they have been identified in bladder cancer, cervical cancer, gallbladder cancer, head and neck squamous cell carcinoma, lung squamous cell carcinoma, multiple myeloma, sebborheic keratosis, and spermatocytic seminoma (**Table 1**). These mutations are able to induce colony formation in NIH3T3 anchorage-independent assays, transform myeloid Ba/F3 cells to IL-3 independence (13) and cause ligand-independent receptor activation (14). Treating IL-3-independent Ba/F3 cells expressing these FGFR mutants with the multikinase inhibitor ponatinib (AP24534) inhibited proliferation (13).

Non-cysteine mutations in the extracellular domain lead to aberrant activation

Non-cysteine mutations in the extracellular domain are also able to activate FGFRs, such as P252R/S/T mutations in FGFR1 in melanoma, lung adenocarcinoma and spermatocytic seminoma (**Table 1**). Autosomal dominant mutations at this codon lead to Pfeiffer Syndrome (15). This residue is located in the IgII-IgIII linker region and contributes to increased receptor activation by decreasing the dissociation rate of the receptor and the FGF ligand (16). Mutations in the analogous FGFR2 residue, P253R/S, are associated with Apert Syndrome (17, 18) and have been frequently identified in cancers, including endometrial carcinoma, lung adenocarcinoma, oral squamous cell carcinoma and spermatocytic seminoma (**Table 1**). Cells expressing FGFR2 P253R exhibit increased FRS2 phosphorylation and increased FGF2- and FGF9-induced activation of MAPK signaling (19). A patient with oral squamous cell carcinoma expressing FGFR2 P253R responded to the multikinase inhibitor pazopanib (GW786034B), which effectively reversed cellular transformation and contributed to tumor shrinkage (13).

Another well-studied non-cysteine substitution is S252W in FGFR2, which occurs in approximately 67% of patients with Apert Syndrome, a developmental syndrome characterized by craniosynostosis and syndactyly (20, 21). The pathophysiological effect of this mutation comes from the higher affinity of FGFR2 for a greater repertoire of FGF ligands due to the formation of a hydrophobic patch that stabilizes the ligand-receptor interaction (16). This mutation leads to aberrant activation of MAPK signaling and interferes with

proper endochondral bone development (22). Mutations at this position, either S252W, S252F, or S252L, have been identified in cervical squamous cell carcinoma, endometrial carcinoma, gallbladder cancer and spermatocytic seminoma (**Table 1**). FGFR2 S252W leads to colony formation and anchorage-independent proliferation of endometrial carcinoma cells, whereas treatment with FGFR inhibitor PD173074 results in decreased FRS2 phosphorylation, colony formation and tumor cell proliferation (23).

Overall, mutations in the extracellular domains of FGFRs, especially numerous for FGFR2 (**Fig 2**), have been overwhelmingly detected in both developmental syndromes and cancers. These mutations lead to aberrant receptor signaling either by abnormal disulfide bond formation and receptor dimerization or by increasing the affinity of the receptor for an expanded repertoire of FGF ligands.

Activating mutations in the transmembrane domain of FGFRs

Biochemical studies suggest that activating mutations adjacent to or within the transmembrane domain of RTKs induce a rotation in the dimer interface of receptor monomers, contributing to increased receptor activation (24). Recently, the juxtamembrane domain has been shown to synergize with the transmembrane domain to stabilize the unliganded FGFR3 dimer (25).

The introduction of an abnormal Cys residue in the transmembrane domain of FGFRs represents one category of activating mutation. For instance,

the Y376C mutation in the transmembrane domain of FGFR2 has been identified in adenoid cystic carcinoma, endometrial carcinoma and spermatocytic seminoma (**Table 1**). Ba/F3 cells, normally IL-3 dependent, exhibit proliferation and survival in the absence of IL-3 when expressing FGFR2 Y376C (26). As a congenital mutation, it causes Beare-Stevenson Cutis Gyrata Syndrome (BSS), a severe craniosynostosis syndrome with a high risk of infant death due to respiratory complications (27). In FGFR3, the introduction of a cysteine residue adjacent to or within the transmembrane domain, such as G372C, S373C, Y375C, G377C, I378C or Y381C, also leads to ligand-independent receptor activation (28). Such mutations have been identified in a variety of cancers, including bladder cancer, gallbladder cancer, multiple myeloma, sebborheic keratosis and spermatocytic seminoma (**Table 1**). Some of these same mutations have been identified congenitally as causing TDI (29).

Other mutations within the transmembrane domain do not involve the creation of a novel cysteine residue, such as the I379V mutation in FGFR2 identified in lung adenocarcinoma (**Table 1**). Another example in FGFR3 is G382R that leads to achondroplasia, the most common rhizomelic dwarfism, originally identified in the IIIc isoform as the famous G380R mutation (30, 31). This mutation leads to abnormal localization of FGFR3 to the plasma membrane, including a slower rate of internalization and degradation. In addition, this mutation leads to increased receptor activation (28), dimerization and MAPK activation (32). A mutation at the paralogous site in FGFR2, C383R, has been identified in endometrial carcinoma, esophageal adenocarcinoma and

lung squamous cell carcinomas. Expression of FGFR2 C383R has been shown to transform NIH3T3 cells (33).

A similar mutation in the transmembrane domain of FGFR4, G388R, is a common single nucleotide polymorphism (SNP) which has been examined in many cancers, including bladder, breast, colon, head and neck, kidney, liver, lung and ovarian cancers, and neuroblastoma (34). It is still unclear whether the G388R mutation is a reliable marker for cancer risk and prognosis. Genomic analysis of breast epithelial cells revealed that roughly half of the patients (53%) exhibited a heterozygous FGFR4 G388R variant (35). Breast cancer cells expressing FGFR4 G388R exhibit increased motility and proliferation (36) and acquire resistance to adjuvant therapy (37). In contrast, another report found that this SNP is not a relevant prognostic marker for both node-positive and node-negative breast cancers (38). In prostate cancer, cells expressing FGFR4 G388R display increased proliferation, motility, invasion and metastasis (39). In pituitary tumors, the G388R mutation changes hormone secretion by enhancing growth hormone (GH) production and leads to S727 phosphorylation of STAT3 that translocates to the mitochondria and modulates changes in cellular metabolism (40). The long term significance of this common polymorphism in human cancer will require further study.

Mutations in the kinase domain of FGFRs

The kinase domain of FGFRs is the site of several mutations with significant impact both in human cancer and developmental syndromes. Of particular importance are mutations within the activation loop containing the signature motif YYKK and the major autophosphorylation site, present in all FGFR family members. First identified in FGFR3, mutations within this motif profoundly increase kinase activation, receptor autophosphorylation and downstream signaling (41-43). These mutations were initially identified in the IIIc isoform as K650E or K650M, with the former causing the neonatal lethal syndrome TDII, and the latter causing SADDAN (Severe Achondroplasia with Delayed Development and Acanthosis Nigricans) (29, 44, 45). The homologous mutations K655I and K656D/E/M/N in FGFR1 have been identified in pilocytic astrocytoma, glioblastoma and rosette forming glioneural tumor (**Table 1**). Similarly, in FGFR2, the mutations K660E/M/N have been identified in breast cancer, cervical squamous cell carcinoma, endometrial carcinoma, lung squamous cell carcinoma, medulloblastoma, pilocytic astrocytoma and spermatocytic seminoma (**Table 1**). In FGFR3, the mutations K652E/M/N/Q/T have been identified in bladder cancer, gallbladder cancer, head and neck squamous cell carcinoma, multiple myeloma, seborrheic keratosis and spermatocytic seminoma (**Table 1**). Curiously, somatic mutations in the YYKK motif of FGFR4 have not yet been identified in human cancer, but this seems only a matter of time.

These activating mutations lead to different processing and trafficking of the receptors through the secretory pathway (46, 47). For instance, the FGFR3

mutations K652E/M lead to intense receptor phosphorylation and also defects in glycosylation and maturation, causing intracellular localization within the endoplasmic reticulum (ER). The high level of tyrosine phosphorylation associated with the receptors in the ER induces activation of STAT1, STAT3 and STAT5 through the direct recruitment of JAK1 to the ER and/or Golgi (46). Nordihydroguaiaretic acid (NDGA), a compound that inhibits protein trafficking from the ER to Golgi, was found to inhibit tyrosine phosphorylation of FGFR3 K650E resulting in impairment of STAT1, STAT3 and MAPK signaling (48).

Although activating mutations in the kinase domain of FGFR3 have been overwhelmingly detected in aggressive cancers, these mutations are often present in low-grade papillary urothelial bladder cancers (49, 50). Generation of a mouse model with the murine equivalent of FGFR3 K652E expressed in the urothelium did not induce the onset of bladder tumors in mice, but when combined with deletion of PTEN (a negative regulator of PI3K-AKT), urothelial tumorigenesis occurred. Combining the activated FGFR3 with mutations in KRAS or Beta-catenin led to tumor formation in skin and lung through upregulation of PI3K-AKT signaling (51). Thus, in these microenvironmental contexts, it appears that activating mutations in FGFR3 may synergize with other mutations that activate PI3K-AKT signaling in these cancers (52, 53).

Another mutation originally identified as a human developmental syndrome deserves special mention. As a congenital mutation, the FGFR3 mutation N542K, originally described in the IIIc isoform as N540K, causes the mild dwarfing syndrome hypochondroplasia (54). Biochemical studies have

shown that this mutation provides constitutive kinase activation, but much less than mutations in the YYKK motif (41, 55). This site is located in the loop between the αC helix and the 4 strand in the kinase hinge region. This residue participates in a network of hydrogen bonds that functions as a molecular brake to inhibit FGFR2. This activating mutation disengages this inhibitory network in the hinge region and constitutively activates the kinase activity of the receptor (56). Somatic mutations at this site commonly occur in human cancer. In FGFR1, the mutation N546K occurs in glioblastoma, pilocytic astrocytoma and rosette forming glioneural tumors. In FGFR2, the mutations N550D/H/K have been identified in breast cancer, endometrial carcinoma, gallbladder cancer, head and neck squamous cell carcinoma and spermatocytic seminoma. In FGFR3, the mutations N542K/S/T/V have been found in bladder cancer and spermatocytic seminoma. Lastly, in FGFR4, the mutations N535D/K have been identified in rhabdomyosarcoma (**Table 1**).

Recently, the importance of the kinase insert (KI) domain in the functionality of RTK families was described (57). In comparison with other RTKs, FGFRs exhibit a short 15-amino acid kinase insert domain. The KI domain of each FGFR contains possible phospho-acceptor sites, such as Y583 and Y585 in FGFR1. Interestingly, a phosphomimic mutation of Y589D has been identified in the kinase insert domain of FGFR2 in cervical carcinoma (58). This residue is analogous to Y585 in FGFR1, in which phosphorylation of Y583 and Y585 has been shown to be critical for mitogenesis, transformation of Ba/F3 cells to IL3-independence and cellular proliferation (59). Mutations in this region

may provide a conformational change that increases kinase activation. In FGFR2, these mutations include P583L in colorectal cancer, G584V/W in lung adenocarcinoma and lung squamous cell carcinoma, M585V in cervical squamous cell carcinoma, S588C in breast cancer and I591M in lung adenocarcinoma. These mutations collectively define a patch from P583-I591 in the KI domain of FGFR2 which must be involved in the regulation of normal receptor activity and, when disturbed by mutation, participates in oncogenesis. In FGFR4, KI domain mutations include G576D in rhabdomyosarcoma and P583Q in colorectal cancer (**Table 1**).

FGFR mutations in cancers of the central nervous system

Pilocytic astrocytoma (PA) is a common central nervous system neoplasm that accounts for approximately 20% of pediatric tumors (60) and usually involves alterations within the MAPK pathway; frequent mutations occur in BRAF such as V600E, or translocations resulting in a KIAA1549-BRAF fusion protein (61, 62). Genetic sequencing of non-cerebellar PA tumors identified mutations in the kinase domain of FGFR1, including N546K and K656E/M/N (63) (**Table 1**). These N546K and K656E mutations have recently been identified in rosette-forming glioneuronal tumors (RFNTs), which are rare cerebellar parenchyma-derived tumors histologically similar to PA (64). These mutations, interestingly, have been found in RFNT occurring in the fourth ventricle, a rare site for PA. These studies indicate that FGFR1 plays a critical

and active role in the tumorigenesis of a subset of extracerebellar tumors in the absence of activated BRAF.

Several mutations in each FGFR have been identified in glioblastoma. In FGFR1, these mutations include N546K, R576W and K656E; in FGFR2, Q212K and G463K; in FGFR3, E468K and R605Q; and in FGFR4, Q144E and R434Q (**Table 1**) (65). Except for the FGFR1 N546K and K656E mutations, analogous to the hypochondroplasia and TDII mutations in FGFR3, the mode of action for most of these mutations is not well understood. Of much greater significance in glioblastoma are translocations involving FGFRs, which will be discussed later.

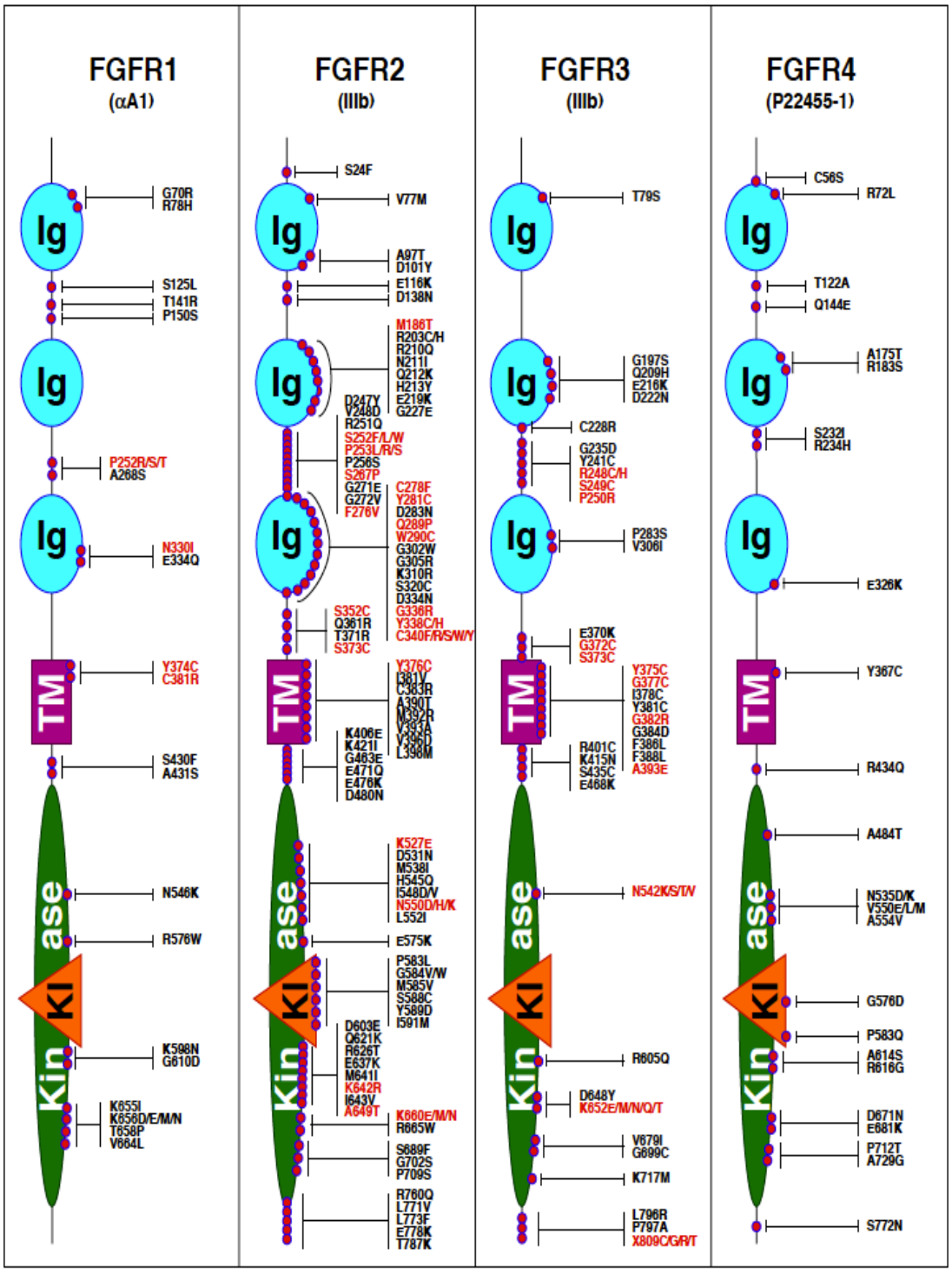

Figure 4.2: FGFR Mutations Identified in Human Cancer. Mutations present in both developmental syndromes and cancers are highlighted in red. Mutations present only in cancer are shown in black. The residue numbers are based on the following isoforms according to Table 1: αA1 for FGFR1, IIIb for FGFR2, IIIb for FGFR3, and full-length form FGFR4 (Uniprot P22455-1).

FGFR4 activation in Rhabdomyosarcoma (RMS)

Activating mutations in FGFR4 have not, so far, been linked to developmental syndromes. However, it is clear that activating mutations in FGFR4 play a direct role in the aggressiveness of some pediatric tumors. Rhabdomyosarcoma (RMS), a soft-tissue sarcoma, is a relatively common type of pediatric tumor histologically divided into two subtypes: embryonal (ERMS) that occurs in the head, neck and trunk, and alveolar (ARMS) often found in the extremities (66, 67).

Activating mutations in the kinase domain of FGFR4 have been identified in approximately 7.5% of primary RMS tumors, including N535D/K, V550E/L, A554V and G576D mutations (**Table 1, Table 2**) (68). FGFR4 N535K and V550E mutants lead to increased STAT3 activation and drive *in vivo* pulmonary metastasis in xenograft models. Dose-dependent inhibition of mutated FGFR4 signaling by the multi-kinase inhibitor ponatinib leads to ablation of STAT3 signaling resulting in decreased RMS tumor growth *in vivo* (69). This small-molecule inhibitor may be a promising candidate to treat other cancers harboring these FGFR4 mutations (70). Additionally, recent genomic sequencing of RMS tumors has revealed the V550L/M mutations in the kinase domain of FGFR4 in ERMS tumors (**Table 1**) (71). The Val residue at codon 550 is a gatekeeper residue that controls the accessibility of ATP in the FGFR catalytic pocket (72).

ARMS is the more severe subtype and 75-80% of ARMS tumors exhibit a t(2;13) or t(1;13) chromosomal translocation that generates PAX3-FKHR or PAX7-FKHR fusion proteins, respectively. FGFR4 is a direct transcriptional target of PAX3-FKHR in which the enhancer PAX motif is downstream of the *FGFR4* gene, and PAX3-FKHR binding leads to increased expression of FGFR4 in ARMS. Inhibition of PAX3-FKHR with shRNA leads to reduced expression in ARMS tumors (73). PAX3-FKHR-mediated increased transcription of FGFR4 supports cell survival via the increased expression of antiapoptotic protein BCL2L1, as shown by shRNA-mediated suppression of FGFR4 that decreases BCL2L1 expression (74) (**Fig 3**).

The existence of activating mutations in FGFR4, more commonly found in ERMS, suggests a similar functional role as fulfilled by the fusion protein PAX-FKHR in ARMS; both pathways result in increased FGFR4 activation.

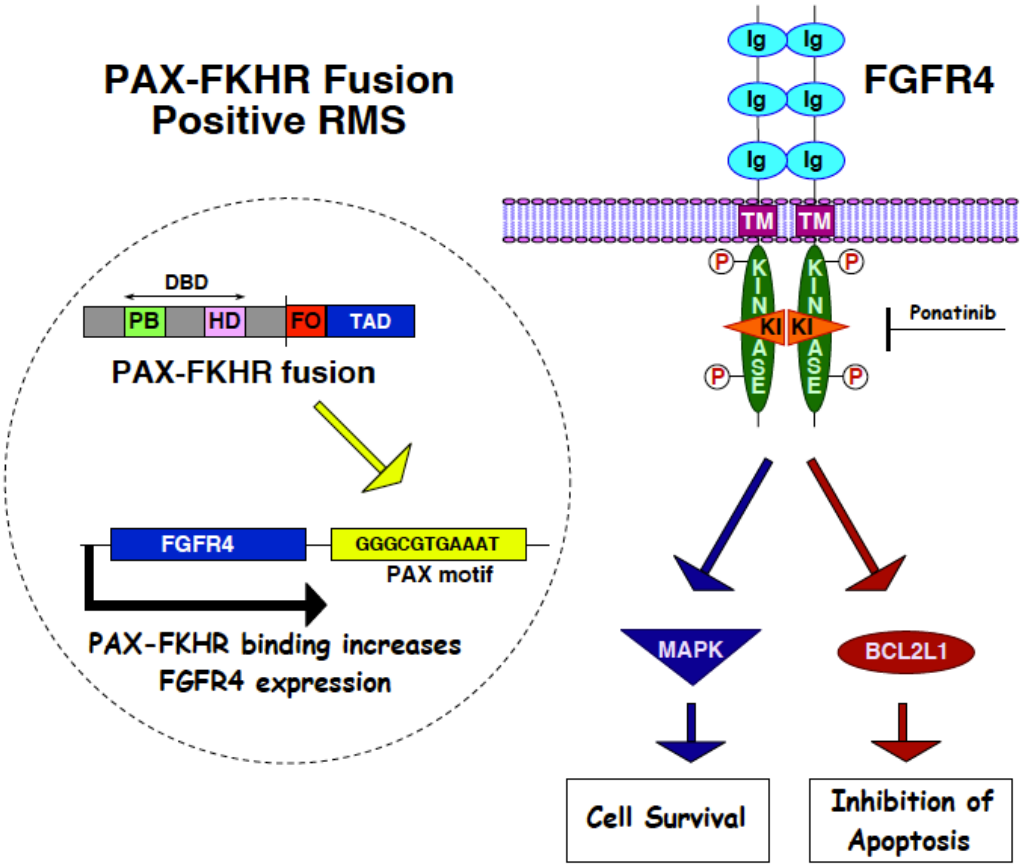

Figure 4.3: FGFR4 signaling contributes to progression of RMS. In ARMS, the PAX-FKHR fusion protein functions as a transcriptional factor to stimulate FGFR4 expression, which upregulates proliferative and anti-apoptotic pathways. Inhibition of FGFR4 with ponatinib suppresses these effects.

Loss-of-function mutations in FGFR2 in Melanoma

Thus far, mutations in FGFRs have been described as resulting in increased kinase activation. In contrast, all FGFR2 mutations in melanoma – including mutations located in the kinase domain – lead to loss-of-function of the receptor (**Table 1**). Of particular interest is A649T in FGFR2 detected in a patient homozygous for this mutation in melanoma (75). This residue is located

in the FGFR2 activation loop. The introduction of the Thr side chain hinders the phosphotransfer reaction that is critical for proper receptor activation, thus resulting in loss-of-function (76). Ba/F3 cells expressing FGFR2 A649T exhibit decreased cellular proliferation compared to wild-type FGFR2, and this mutation blocks FGF2-induced activation of MAPK signaling. This mutation was first detected as an autosomal dominant mutation in lacrimo-auriculo-dento-digital (LADD) Syndrome (77). These patients exhibit congenital anomalies affecting the salivary glands, lacrimal glands, teeth and ears. In contrast with activating mutations in FGFR2 that generally lead to Pfeiffer, Apert, Crouzon and Beare-Stevenson Syndromes marked by severe craniosynostosis, LADD patients do not exhibit such severe phenotypes.

Stop codon read-through mutations in FGFR3

Thanatophoric Dysplasia (TD) is the most common lethal form of chondrodysplasia. The K652E activation loop mutation in the FGFR3 causes TDII, and mutations in the extracellular domains are usually responsible for TDI. However, TDI can also be caused by unusual mutations at the stop codon of FGFR3, allowing additional in-frame translation of an additional 423 nt. These read-through mutations can result in the introduction of a Cys, Gly or Arg (X809C/G/R). The resulting FGFR3 is 114 amino acids longer, and the elongated hydrophobic C-terminal region adopts an α-helix conformation suggested to serve as a second transmembrane domain that activates FGFR3

(78, 79). Recently, additional mutations to Leu, Ser, or Trp at the stop codon have been detected in patients with TDI (80). Remarkably, in spermatocytic seminoma, stop codon mutations X809C/G/R/T in FGFR3 have been observed in 21/29 (72%) of patients (9) (**Table 1**). These mutations clearly support cellular proliferation and clonal expansion of spermatogonia via FGFR3 activation in these tumors.

The challenges of drug resistance in tumors with mutated FGFRs

The overall efficacy of tyrosine kinase inhibitors can be limited due to acquired mechanisms of chemotherapy resistance, which impedes treatments and leads to tumor relapse (81). A well-documented drug resistance mechanism may include the emergence of secondary mutations in gatekeeper residues, such as T790M in EGFR in 50% of erlotinib- and gefitinib-resistant tumors (82, 83) and T315I mutation in BCR-ABL in imatinib-resistant Chronic Myelogenous Leukemia (CML) (84, 85). Similarly, mutation of the gatekeeper residue V561M in FGFR1 has been shown to confer *in vitro* drug resistance to pyrido-[2,3-d]pyrimidine multikinase inhibitor PP58 (86).

Dovitinib (TKI-258) is an ATP-competitive multikinase inhibitor with activity against FGFRs (87). This drug has shown promising pre-clinical anti-tumor activity in cancers driven by FGFR activation such as multiple myeloma and acute myelogenous leukemia (88-90). In response to dovitinib, FGFR2 mutations were observed including N550H/K/S/T, V565I, E566A/G and K642N,

which resulted in increased receptor kinase activity. Residues N550, E566 and K642 are part of a triad that forms a network of autoinhibitory hydrogen bonds termed the molecular brake. Drug-resistant mutations at these sites disrupt this molecular brake in the kinase hinge region of FGFR2 (91). Furthermore, FGFR2 mutations at N550 and K642 have been identified in adenoid cystic carcinoma, breast cancer, endometrial carcinoma, gallbladder cancer, head and neck squamous cell carcinoma and spermatocytic seminoma (**Table 1**) (23, 32, 92, 93).

Furthermore, the use of FGFR inhibitors AZD4547 and AZ8010 for diseases such as multiple myeloma, gastric cancer and urothelial cancer, has been shown to decrease tumor proliferation (94). In order to identify potential mechanisms of resistance to FGFR inhibitor AZ8010 in multiple myeloma, AZ8010-resistant multiple myeloma KMS11 cells (KMS11-R) were generated. KMS11-R cells, which express FGFR3 Y375C, exhibited elevated levels of phosphorylated FGFR and FRS2, and increased STAT3 and MAPK signaling (94). Genomic sequencing of KMS11-R cells revealed a secondary mutation in the gatekeeper residue V557M in FGFR3, which is analogous to the V561M mutation in FGFR1 in PP58-resistant cells. Molecular simulation predicts that the Met side chain is approximately 25% bulkier than the Val at position 561 in FGFR1, and it restricts the binding of FGFR inhibitor PD173074 to the catalytic domain (86).

Effective cancer treatments depend upon the prediction of drug-resistance mechanisms evolved in tumor cells. Without such predictions, the

efficacy of chemotherapy agents is compromised, contributing to a decrease in treatment progression resulting in tumor relapse.

4.4 FGFR translocations and fusion proteins in cancer

FGFR fusion protein discovery across a variety of cancers

Fusion proteins are continually being discovered in a variety of human cancers. Particularly, fusions involving FGFRs are prevalent in hematological cancers and solid tumors. The existence of translocations involving FGFRs has been known since the late 1990s, when a patient with T-cell lymphoblastic lymphoma was found to harbor a ZNF198-FGFR1 fusion, now also referred to as ZMYM2-FGFR1. Lymphoma or leukemia cases from the 1970s and 1980s described disease characteristics similar to the now well-defined disease, 8p11 myeloproliferative syndrome (EMS). This correlation may arise because FGFR1 fusions in leukemia and lymphoma often originate as EMS. According to the World Health Organization, EMS is classified as “myeloid and lymphoid neoplasms with FGFR1 abnormalities,” and has also been called “stem cell leukemia/lymphoma” (95).

In EMS, FGFR1 located at 8p11.22 is often disrupted by chromosomal translocation, resulting in a fused coding region. The fusions in EMS consistently result in FGFR1 fused to an N-terminal dimerization domain (**Fig 4**), an alteration that has also been found in breast cancer, lung squamous cell

carcinoma, phosphaturic mesenchymal tumor, rhabdomyosarcoma and leukemia (**Table 3**) (96-99). With FGFR as the 3' partner, the ligand-binding extracellular domain and transmembrane domain are excluded from the fusion protein, with only the FGFR kinase domain attached to the 5' protein partner. Dimerization of this fusion type would result only from the N-terminal oligomerization domain, not FGF ligand binding. In solid tumors, it is more common to find FGFR as the 5' fusion gene, with the breakpoint consistently found in exons 17, 18, or 19, leaving the extracellular, transmembrane and kinase domains intact. When the extracellular domain is present, dimerization is thought to increase with the addition of FGF ligand. Although the domains present in fusion proteins vary, the intact FGFR kinase domain is always retained, indicating this domain is critical for a functioning fusion protein and cancer progression. It is rare to see an FGFR fusion protein with an additional FGFR activating mutation. The reason may be that either event alone may be sufficient for cancer to progress, although the dual activation of an FGFR both by mutation and translocation could provide additional oncogenic potential. Additionally, while some FGFR fusions occur with high tissue specificity, others occur across many cancer types (100).

Dimerization of FGFR induced by the fusion partner

In FGFR fusion proteins, almost all fusion partners contribute a known dimerization domain which allows the FGFR to dimerize and autophosphorylate

the kinase domain, leading to activation and downstream signaling, increased cell proliferation and cancer progression (**Fig 1**). Recently, an FGFR3 fused to transforming acidic coiled-coil containing 3 (TACC3) has been discovered in glioblastoma, bladder cancer, lung cancer, oral cancer, head and neck squamous cell carcinoma and gallbladder cancer (96, 97, 101-107) (**Table 3**). Additionally, FGFR1-TACC1 has been identified in glioblastoma (106, 108). The coiled-coil domain of TACC3 is assumed to bring the FGFR3 portion of the fusion proteins close together, inducing activation. FGFR3-TACC3, FGFR3-BAIAP2L1, and FGFR2-CCDC6 have been shown to dimerize presumably through their coiled-coil domains (96). The FGFR2-BICC1 gene fusion has been found in cholangiocarcinoma, colorectal cancer and hepatocellular carcinoma (96, 109-111). The self-associating sterile alpha motif domain (SAM) of BICC1, containing a helix-loop-helix domain, fused 3' to FGFR2, is believed to instigate constitutive dimerization of FGFR2 in order to produce an active receptor (100) (**Fig 4**).

Other dimerization domains found in FGFR fusion proteins are believed to have the same function. FGFR fusion partner domains include zinc-finger, leucine zipper, coiled-coil, SAM, LIS1-homologous (LIsH), IRSp53/MIM (IMD), BAG, FN1, AFF3, and stomatin/prohibitin/flotillin/HflK/C (SPFH) domains (also known as the prohibitin PHB domain) (**Table 3**). Other fusions thought to dimerize by self-association domain include FGFR2-CASP7 in breast cancer, which dimerizes through active site loops, and CPSF6-FGFR1, which dimerizes through a RNA recognition motif (95, 96, 112). The most frequent fusion partner

domain is the coiled-coil, occurring in the proteins mentioned above; in addition, the other coiled-coil fusion proteins are BCR-FGFR1 (113), CEP110-FGFR1 (95), CUX1-FGFR1 (114), FGFR1OP2-FGFR1 (115), FGFR2-AHCYL1 (109), FGFR2-CIT (116), FGFR2-FAM76A (117), FGFR2-KIAA1598 (110), FGFR2-KIAA1967 (96), FGFR2-OFD1 (96), FGFR2-PPHLN1 (118), FGFR2-TACC3 (111), LRRFIP1-FGFR1 (95), MYO18A-FGFR1 (95), TRIM24-FGFR1 (95), and TPR-FGFR1 (119).

In order for autophosphorylation to occur, RTKs need to be exactly aligned. It has been shown that dimerization of the intracellular domain alone will not activate the receptor. Ligand binding rotates and aligns the extracellular juxtamembrane domain and intramembrane α-helices, leading to intracellular kinase domain alignment, dimerization and activation (24). To create an active FGFR fusion protein, the dimerization domain must provide the correct alignment. The most common FGFR1 fusion in EMS is ZNF198-FGFR1, which contains either 4 or 10 zinc finger domains and a proline-rich domain from ZNF198, followed by the tyrosine kinase domain of FGFR1 (**Fig 4**) (95). The proline-rich domain is a self association domain and is essential for dimerization and activation of FGFR1 (120).

An exception to the activation-by-oligomerization theme is an internal tandem duplication (ITD) of FGFR1 in a patient with pilocytic astrocytoma (60), resulting in a duplication of the FGFR1 kinase domain. ITD has previously been observed in Acute Myeloid Leukemia with FLT3, another receptor tyrosine kinase. This ITD, which occurs in the juxtamembrane domain of FLT3, leads to

enhanced receptor activation and increased downstream signaling of MAPK and STAT5 (121).

Altered cellular localization of FGFR by the fusion partner

Often, the creation of FGFR fusion proteins not only activates FGFR and its canonical pathways, but results in an incongruous FGFR localization as well. Some partner proteins can lead to localization of FGFR to a cellular compartment other than the plasma membrane. Fusion proteins that have been shown to have irregular localization include FGFR1OP-FGFR1, CEP110-FGFR1, ZNF198-FGFR1, and TEL-FGFR3 in lymphoma and FGFR3-TACC3 in glioblastoma. Wild-type FGFR1OP (FGFR1 oncogenic partner) and CEP110 (centriolin) are centrosomal proteins. Once engaged in a fusion with FGFR1, FGFR1OP localizes the kinase domain to the centrosome through a CAP350 interaction (122). CEP110 is involved in centriole maturation and localizes to the centrosome via an 170-amino acid region in the C-terminus, a region retained in the CEP110-FGFR1 fusion. Instead of the expected localization to the centrosome, cytoplasmic expression of the fusion protein was observed (123). Continuous kinase activity and inappropriate cytoplasmic localization due to CEP110-FGFR1 fusion formation may result in increased cell viability and hematopoietic stem cell growth. The fusion proteins ZNF198-FGFR1 and TEL-FGFR1 have been identified as cytoplasmic proteins (95, 99). The translocation of ZNF198 and FGFR1 genes removes the FGFR1 transmembrane domain and

the C-terminal nuclear localization signal of ZNF198, which most likely leads to cytoplasmic localization.

Expressed FGFR3-TACC3 has been shown to localize to the mitotic spindle poles in dividing mouse astrocytes, most likely due to recruiting effects of TACC3. In addition, the fusion protein increased the percentage of aneuploidy by greater than 2.5-fold (106). As TACC3 is an important component of mitotic spindle assembly and is involved with the attachment of chromosomes to microtubules, it is most likely playing a role in chromosomal segregation errors. During mitosis, wild-type TACC3 is strongly diffused around centrosomes, due to the localizing effects of the C-terminal coiled-coil (124). As this domain is present in the FGFR3 fusion, multiple effects could be implicated by the fusion protein such as localization of FGFR3-TACC3 to the centrosome or a novel biochemical activity. During interphase, wild-type TACC3 has been found to be concentrated in the nucleus (124). The location of the FGFR3-TACC3 fusion in non-dividing cells has not yet been identified.

Although the localization of ERLIN2-FGFR1 has not yet been investigated, wild-type ERLIN2 anchors to the ER membrane via an N-terminal binding motif. This motif is still present when ERLIN2 is fused to FGFR1, and may be affecting fusion protein location (125). The fusion results in the SPFH oligomerization domain of ERLIN2 fused 5’ to exon 4 of FGFR1, and was detected in breast cancer.

Thus, for these and other FGFR fusion proteins discussed: is the salient biological feature the localization of the FGFR kinase domain to a novel cellular

compartment? Or, is it the constitutive dimerization and activation of the FGFR kinase domain, regardless of the localization of the normal fusion partner, that is determinative? Much further experimental research will be required to arrive at a definitive answer.

Downstream signaling impacts of fusion proteins

FGFR fusion proteins have been shown to activate the normal FGFR pathways, specifically the PI3K/AKT, MAPK, and JAK/STAT pathways (**Fig 1**). FGFR3-TACC3, FGFR3-BAIAP2L1, and FGFR2-CCDC6 increase activation of PI3K/AKT and MAPK pathways (100). FGFR2-TACC3 has also been shown to increase MAPK activation, but only a moderate increase of FRS2 phosphorylation of the PI3K pathway has been seen (111). In wild-type FGFR1, FRS2 normally binds to the juxtamembrane domain between amino acids 407 and 433. In many FGFR1 fusions, this domain is either fully or partially disrupted by translocation of the fusion partner, which results in an inability to recruit FRS2. This has been shown to occur in ZNF198-FGFR1, but may occur in other fusion proteins with FGFR as the 3' partner. However, although FRS2 interaction with ZNF198-FGFR1 was undetectable, the PI3K pathway remained active (95).

In addition to the activation of MAPK and PI3K pathways, cells expressing FGFR1OP-FGFR1 exhibit increased phosphorylation of STAT1 and STAT3, but not STAT5 (126). Furthermore, ZNF198-FGFR1 activates STAT5,

FGFR3-TACC3 activates STAT3, and FGFR3-BAIAP2L1 and FGFR2-CCDC6 increase STAT1 activation (100, 122). ERLIN2-FGFR1 and CEP110-FGFR1 have been shown to be biologically active through tyrosine phosphorylation of the respective fusion proteins, but further downstream signaling activation has not been explored (96, 123). Despite an overall increase in cell proliferation pathway activation, a contrasting study reports a failure to over-activate MAPK and AKT by FGFR3-TACC3 (106). Studies exploring FGFR2-AHCYL1 and FGFR2-BICC1 fusions report an absence of AKT and STAT3 phosphorylation, although the MAPK pathway remained active (109). Additionally, TEL-FGFR3 directly interacts with and activates STAT3 and STAT5, presumably through the FGFR3 portion of the protein, an interaction that has not been shown with other fusion proteins (99).

Fusions with FGFR as the 5' partner usually result in a deletion of the last exon of FGFR, which includes the tyrosine residue important for PLCγ binding (127). In bladder cancer, cells transfected with FGFR3-TACC3 or FGFR3-BAIAP2L1 were unable to activate PLCγ, due to a deletion of the last exon of FGFR3 in both fusion proteins (102) (**Fig 4**) Chromosomal rearrangements such as these also result in the loss of the 3' UTR (untranslated region) of FGFR, significant as a region that contains various microRNA (miRNA) regulation sites. MiR-99a is normally present at high levels in the brain and results in a downregulation of FGFR3 translation. The formation of FGFR3-TACC3 fusion in glioblastoma results in a loss of the miR-99a site, which leads to the overexpression of FGFR3-TACC3. This miRNA site is unique to FGFR3,

but overexpression due to a loss of miRNA regulation could occur in any FGFR fusion where the 3' UTR region contains a regulatory miRNA site (105).

Interestingly, nuclear pore complex proteins have been identified in fusion proteins with FGFR1. RANBP2-FGFR1, TPR-FGFR1, and NUP98-FGFR1 have all been identified in EMS (95, 119, 128). Mechanistically, these may be similar to other fusion proteins discussed previously in that two of these possess dimerization domains, with RANBP2 (RAN binding protein 2, also NUP358) containing a leucine zipper domain and TPR (Translocated Promoter Region) containing a coiled-coil domain (**Table 3**). A dimerization motif in NUP98 has not yet been identified, however. Also mechanistically unclear is the fusion partner AFF3 (AF4/FMR2 Family, Member 3, also known as LAF4), a nuclear transcriptional activator, which has been identified as the 3' fusion partner with FGFR2 (**Table 3**). AFF3 has also been found fused to the MLL gene in acute lymphoblastic leukemia (129). It is unclear whether the significant biochemical consequence of these fusion proteins is manifested in the dimerization and activation of the FGFR partner, or whether the abnormal nuclear localization of the FGFR component represents the key event.

All EMS cases with FGFR1 fusions have thus far been negative for the BCR-ABL fusion gene, which occurs in 85-90% of CML. The remaining cases either contain other translocations or are classified as BCR-ABL negative CML, or atypical CML. Some of these atypical CML cases are now linked to the broad spectrum of EMS cases, due to the presence of a translocation involving the 8p11 region (130). Patients with BCR-FGFR1 [t(8;22)(p11;q11)] fusion are often

referred to as CML-like due to their greater resemblance to CML than to EMS. BCR has been shown to interact with Grb2 by phosphorylation of Y177 (95). This interaction is thought to be important for BCR-ABL signaling in CML patients, and may be playing a role in EMS patients with BCR-FGFR1 as well.

Inhibition of FGFR fusion proteins

Through the use of various drug treatments, a reduction of cell proliferation and FGFR fusion protein activity has been accomplished. Studies indicate that an active FGFR kinase domain drives cancer progression, thus the goal of many cancer treatments is to inhibit the FGFR portion of the fusion (106) (109). FGFR inhibitors have been used *in vitro* to reduce phosphorylation of FGFR and subsequent downstream signaling proteins. FGFR kinase inhibitors AZD4547, BGJ398, and PD173074 have inhibited growth of FGFR3-TACC3-expressing Rat1A and glioma stem-like cells (GSC-1123). PD173074 and AZD4547 both resulted in tumor shrinkage during *in vivo* mouse xenograft studies as well (106). For fusions FGFR2-AHCYL1 and FGFR2-BHCC1, both BGJ398 and PD173074 were successful in reducing *in vitro* fusion activity and cell growth (109). In bladder cancer, sensitivity of FGFR3-TACC3 and FGFR3-BAIAP2L1 to the kinase inhibitors PD173074, dovitinib, SU5402, and BGJ398 has been reported (102). BGJ398 and dovitinib are currently involved in numerous clinical trials (clinicaltrials.gov).

FGFR3 translocations were also targeted using the heat shock protein

90 (HSP90) inhibitor, ganetespib (STA-9090). By inhibiting HSP90, hundreds of proteins soon become degraded, which disrupts oncogenic signaling pathways. Ganetespib treatment of bladder cancer cell line RT112, which contains FGFR3-TACC3, resulted in a decrease of fusion protein expression and cell viability. Expression of the apoptosis facilitator protein BIM (BCL2-Like 11, or BLC2L11) was induced, indicative of apoptotic pathway activation. Combination of ganetespib with BGJ398 proved to be the most effective in causing cell death. However, ganetespib had differential effects on protein expression and cell viability in RT4 and SW780 cell lines, which contain FGFR3-TACC3 and FGFR3-BAI1AP2L1, respectively. While HSP90 inhibitors 17-AAG and 17-DMAG reduced cell viability, resistance to ganetespib was exhibited. This discrepancy may be due to differences in drug movement or metabolism (131). Other HSP90 inhibitory compounds were effective in killing cells expressing BCR-ABL *in vitro* (122). These results collectively indicate the potential of HSP90 inhibitors against fusion positive cases.

In cholangiocarcinoma, pazopanib (GW786034B) followed by ponatinib (AP24534) treatment, both RTK inhibitors, induced anti-tumor activity in a patient with FGFR2-TACC3. Ponatinib treatment also led to anti-tumor activity in a patient exhibiting FGFR2-MGEA5 fusion. Ponatinib has been FDA approved for treatment of the drug resistant T315I mutation in BCR-ABL fusion protein in CML (111).

In EMS, the small number of patients who have achieved long term remission have received hematopoietic stem cell transplantation. Many

therapies used for acute lymphoblastic leukemia, acute myeloid leukemia, and myeloproliferative neoplasms have proven unsuccessful or display only short term remission against EMS. FGFR1 kinase inhibitor SU5402 has shown promise, demonstrating inhibitory effects in cells expressing BCR-FGFR1 or ZNF198-FGFR1. Interestingly, PI3K, farnesyltransferase, and p38 inhibitors were also successful in reducing growth of these cells, whereas MEK inhibitor PD98059 was not (130). This is distinct from the MEK inhibitor U0126, which was shown to inhibit growth of cells expressing FGFR3-TACC3 (105). While dovitinib has been successful in inhibiting the proliferation of Ba/F3 cells transfected with ZNF198-FGFR1 or BCR-FGFR1 and cell lines expressing FGFR1OP2-FGFR1, a push for effective FGFR1 inhibitors is needed for EMS cases (132).

Translocations leading to FGFR overexpression without creation of a fusion protein

Some translocations do not create a novel fusion protein; rather, these result in overexpression of FGFR. In the translocations of SLC45A3-FGFR2 in prostate cancer and IgH-MMSET-FGFR3 in Multiple Myeloma (MM), the partner gene promoter now controls FGFR transcription, which alters the expression levels of the receptor. SLC45A3-FGFR2 translocation results in the endogenous promoter and exon 1 noncoding region of SLC45A3 attached 5’ to the FGFR2 gene, which places FGFR2 transcription under the control of an androgen-

regulated promoter. This leads to FGFR2 overexpression and oncogenicity (96).

Multiple Myeloma (MM) is characterized by a growth of malignant cells in the bone marrow. In approximately 20% of MM cases, a t(4;14) (p16.3;q32) translocation places MMSET and FGFR3 under the control of the IgH promoter, leading to overexpression of FGFR3 (133). The overexpressed FGFR3 often contains an additional mutation, resulting in functional changes such as resistance to tyrosine kinase inhibitors (V557M), constitutive dimerization (Y375C), or constitutive kinase activation (K652E) (94). However, one third of cases with this translocation lose FGFR3 expression while IgH is overexpressed. Additionally, although rare, translocations between FGFR3 and an immunoglobulin gene enhancer have been found in chronic lymphocytic leukemia (CLL), including t(4;14) (p16;q32) between FGFR3 and IgH, and t(4;22) (p16;q11.2) involving FGFR3 and IgL (134, 135).

MM cases with the t(4;14) translocation have shown partial responsiveness to the FGFR3 inhibitor PD173074 and RTK inhibitor sunitinib (SU-11248). During *in vitro* studies, both inhibitors halted cell growth and inhibited FGFR3 activity, inducing an apoptotic response. However, during *in vivo* studies, tumor growth in the translocation-positive model was not inhibited by sunitinib, even though sunitinib was active in the translocation-negative tumors. The difference between the *in vitro* and *in vivo* data may be due to a difference in tumor microenvironment (133). These studies also revealed that RTK inhibitors PD173074, sunitinib, and vandetanib (ZD6474) inhibited viability of Ba/F3 cells transformed with ZNF198-FGFR1. Sunitinib, which inhibits many

RTKs, is approved for metastatic renal cell carcinoma treatment (133), and is being examined in clinical trials for relapsed multiple myeloma patients. Additionally, masitinib (AB1010, a TK inhibitor) has entered phase II clinical trials for MM patients with the t(4;14) translocation. [clinicaltrials.gov]

Genomic events that contribute to FGFR fusion proteins

Although the occurrence of FGFR fusion proteins may be rare, there are similarities between fusions. Fusions with FGFR as the 5' partner have only been found in solid tumors so far. In contrast, fusions with FGFR as the 3' partner have consistently been found in EMS, which predisposes patients to either lymphoma, leukemia, or both. A few exceptions have been ERLIN2-FGFR1 found in breast cancer (96), BAG4-FGFR1 in lung squamous cell carcinoma (LUSC) (96), FOXO1-FGFR1 in rhabdomyosarcoma (136), TEL-FGFR3 in lymphoma (99), FN1-FGFR1 in phosphaturic mesenchymal tumor (137), and SQSTM1-FGFR1 in leukemia (138) (**Table 3**).

While the mechanism and cause of gene rearrangements is unknown, both intrachromosomal and interchromosomal rearrangements have been identified. Rearrangements in the form of tandem duplication, inversion, deletion, or translocation have all been identified as FGFR fusion formation events. Translocations occur when two double stranded breaks on different chromosomes rearrange and repair (100). Fusion genes joined by a translocation can result in the formation of a reciprocal gene (i.e. FGFR2-BICC1

and BICC1-FGFR2 genes). This has been reported in some cases, such as BCR-FGFR1, CEP110-FGFR1, FGFR1OP-FGFR1, FGFR2-AHCYL1, FGFR2-BICC1, HERVK-FGFR1, LRRFIP1-FGFR1, RANBP2-FGFR1, SQSTM1-FGFR1, TIF1-FGFR1, and ZNF198-FGFR1 fusions (95, 109-111, 123, 128, 138, 139). However, reciprocal translocations have not been shown to be translated into functional proteins. The majority of these studies do not report the presence of a reciprocal fusion gene, and this may be indicative of another genetic alteration, such as an insertion or complex rearrangement, which would preclude the formation of the reciprocal gene (95).

The formation of these chromosomal rearrangements may occur due to common chromosomal fragile sites (CFSs). An increasing number of studies have identified CFSs as areas commonly affected by deletions, amplifications, and rearrangements in cancer (140). CFSs have become linked to genomic instability, the driving force of cancer. Chromosomal breakpoints identified in cancer match to 67% of fragile sites induced *in vitro* (140). All individuals posses CFSs, and these regions have been identified as evolutionarily conserved. CFSs contain tandem repeat sequences, often flexible AT-rich repeats and the formation of non-B-DNA secondary structures. Additionally, the fragile nature of CFSs has been linked to a lack of replicating origins within the CFS region, which may lead to incomplete replication. CFS expression is also specific to tissue or cell type. An investigation should be made into the correlation between CFS and tumor-specific gene rearrangements, as seen with some FGFR fusion protein expression. Mutagens and carcinogens often target CFS regions.

Regulation of CFS occurs by DNA damage response proteins, including the ataxia telangiectasia mutated (ATM) pathway. This pathway is downregulated in cholangiocarcinoma patients with FGFR2 fusions (118).

CFS FRA10F has been identified at 10q26, a region which contains the FGFR2 gene (111), though some indicate FGFR2 is proximal to FRA10F (140). FGFR2 is also surrounded by ribosomal protein pseudogenes (RPS15AP5 and RPL19P16), which contain repetitive bases, leading to genomic instability (111). Although not thoroughly investigated, these factors could be an indication of the high level of genomic rearrangements seen in the FGFR2 region. In this regard, it may be noteworthy that 10 of 107 cholangiocarcinoma patients simultaneously exhibited two different fusions, FGFR2-BICC1 and FGFR2-PPHLN1 (118). CFS regions have also been identified on the X chromosome, in regions flanking the ODF1 gene, which has been identified in a FGFR2-ODF1 fusion in thyroid cancer (96, 140). As seen (**Table 3**), FGFR1, FGFR2, and FGFR3 rearrangements predominate while, for unknown reasons, FGFR4 fusions are strikingly absent.

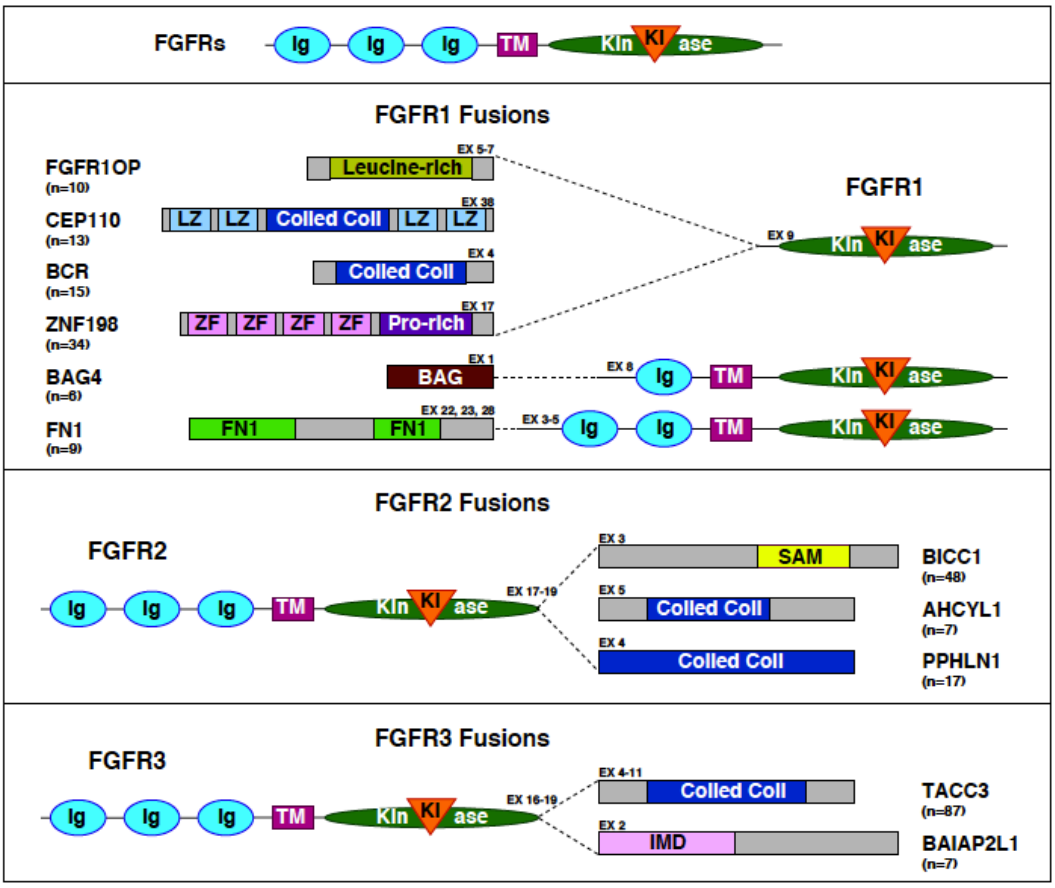

Figure 4.4: Structural Organization of Select FGFR Fusion Proteins. Schematic representations are presented for the more common (n>5) FGFR fusions identified in human cancers and cell lines. The most common breakpoint of each fusion is shown. Occurrence numbers (n) indicate the total number of times the fusion has been identified, including breakpoints not shown in the figure. See Table 3 for full list of FGFR fusions and translocations.

4.5. Concluding Remarks

Aberrant FGFR signaling, either due to activating mutations or the presence of fusion proteins, supports cellular proliferation, tumorigenesis, and cancer progression. Although extensive research has shown that targeting FGFRs with small molecule inhibitors halts receptor activation, downstream signaling and results in tumor shrinkage, secondary mutations that contribute to

drug resistance in tumors are challenges to successful clinical treatment. In addition, FGFRs fused to dimerizing partners brings a new level of complexity in terms of receptor activation and the specificity of small-molecule inhibitors. The development of FGFR therapeutics with personalized specificity will advance treatments of patients whose tumors harbor activated FGFRs via mutation or fusion protein.

4.6 Acknowledgments

We thank all lab members for advice and encouragement. We also thank the GAANN fellowship for financial assistance.

Chapter 4, in full, is a reprint of the article as it appears in *Cytokine Growth Factor Reviews*. Gallo L.H., Nelson K.N., Meyer A., Donoghue D.J. “Functions of FGFR’s in Cancer Defined by Novel Translocations and Mutations” *Cytokine Growth Factor Review*s 2015 Aug; 26(4):425-49. The first author of the work is the author of this dissertation.

Table 4.1: Mutations in FGFRs Identified in Diverse Human Cancer

FGFR1						
Disease	**Mutation/Isoform**			**Location in Receptor**	**Role in Developmental Syndromes**	**Reference**
	Residue in αA1	**Residue in αB1**	**Other Isoform**			
Breast Cancer	S125L	S125L		IgI - IgII		(141)
Colorectal Cancer	P150S	P150S	βA1: P61S	IgI - IgII		(142)
	A268S	A268S		IgII - IgIII		(34)
	S430F	S428F	A	JM		(142)
	A431S	A429S		JM		(143)
	G610D	G608D	A	KD2		(142)
Esophageal Adenocarcinoma	K598N	K596N		KD2		(144)
Gallbladder Cancer	S125L	S125L		IgI – IgII		(107)
Gastric Cancer	A268S	A268S		IgII-IgIII		(34)
Glioblastoma	N546K	N544K		KD1	Analogous to FGFR2 N549K in Crouzon and Pfeiffer Syndromes; Analogous to FGFR3 N540K in Hypochondroplasia	(145)
	R576W	R574W		KD1		(145)
	K656E	K654E		KD2	Analogous to FGFR2 mutation K659E in Syndromic Craniosynostosis; Analogous to FGFR3 mutation K650E in TDII	(65)
Head and Neck Squamous Cell Carcinoma	n/a	n/a	P11362-21 G33R	N-term		(146)
	E334Q	E334Q		IgIII		(70)
Lung Adenocarcinoma	P252T	P252T		IgII - IgIII	Mutation causes Pfeiffer Syndrome; Analogous to FGFR2 mutations at P253 in Pfeiffer and Apert Syndromes; Analogous to FGFR3 mutation at P250 in Syndromic Craniosynostosis	(141, 147)
Lung Large Cell Carcinoma	V664L	V662L		KD2		(141)
Lung Squamous Cell Carcinoma	G70R	G70R		IgI		(148)
	T141R	T141R		IgI - IgII		(148)
Melanoma	P252S	P252S		IgII - IgIII	Mutation causes Pfeiffer Syndrome; Analogous to FGFR2 mutations at P253 in Pfeiffer and Apert Syndromes; Analogous to FGFR3 mutation at P250 in Syndromic Craniosynostosis	(34, 149)
Pilocytic Astrocytoma	N546K	N544K		KD1	Analogous to FGFR2 N549K in Crouzon and Pfeiffer Syndromes; Analogous to FGFR3 N540K in Hypochondroplasia	(60)
	K655I	K653I		KD2		(60)
	K656D/E/M/N	K654D/E/M/N		KD2	Analogous to FGFR2 mutation K659E in Syndromic Craniosynostosis; Analogous to FGFR3 mutations: K650E in TDII, K650M in SADDAN, K650N in Hypochondroplasia	(60)
	T658P	T656P		KD2		(60)
Prostate Cancer	R78H	R78H		IgI		(34)
Rosette Forming Glioneuronal Tumor	N546K	N544K		KD1	Analogous to FGFR2 N549K in Crouzon and Pfeiffer Syndromes; Analogous to FGFR3 N540K in Hypochondroplasia	(64)
	K656E	K654E		KD2	Analogous to FGFR2 mutation K659E in Syndromic Craniosynostosis; Analogous to FGFR3 mutation K650E in TDII	(64)
Spermatocytic Seminoma	P252R/T	P252R/T		IgII - IgIII	Mutation causes Pfeiffer Syndrome; Analogous to FGFR2 mutations at P253 in Pfeiffer and Apert Syndromes; Analogous to FGFR3 mutation at P250 in Syndromic Craniosynostosis	(9)
	N330I	N330I		IgIII	Mutation causes Osteoglophonic Dysplasia	(9)

Table 4.1: Mutations in FGFRs Identified in Diverse Human Cancer, continued

FGFR1						
Disease	**Mutation/Isoform**			**Location in Receptor**	**Role in Developmental Syndromes**	**Reference**
	Residue in IIIb	**Residue in IIIc**	**Other Isoform**			
	Y374C	Y374C		TM	Mutation causes Osteoglophonic Dysplasia; Analogous to FGFR2 Y375C in Beare-Stevenson Cutis Gyrata Syndrome; Analogous to FGFR3 Y373C in TDI	(9)
	C381R	C381R		TM	Mutation causes Osteoglophonic Dysplasia	(9)
	R576W	R574W		KD1		(9)
FGFR2						
Disease	**Mutation/Isoform**			**Location in Receptor**	**Role in Developmental Syndromes**	**Reference**
	Residue in IIIb	**Residue in IIIc**	**Other Isoform**			
Adenoid Cystic Carcinoma	Y376C	Y375C		TM	Mutation causes Beare-Stevenson Cutis Gyrata Syndrome; Analogous to FGFR1 Y374C in Osteoglophonic Dysplasia; Analogous to FGFR3 Y373C in TDI	(150)
	K642R	K641R		KD2	Mutation causes Pfeiffer Syndrome	(150)
Bladder Cancer	M186T	M186T	P21802-20 M71T	IgII	Mutation causes Apert Syndrome	(34)
Breast Cancer	R203C	R203C		IgII		(12, 141)
	N550K	N549K		KD1	Mutation causes Crouzon and Pfeiffer Syndromes; Analogous to FGFR3 N540K in Hypochondroplasia	(92)
	S588C	S587C		KI		(92)
	K660N	K659N		KD2	Mutation causes Syndromic Craniosynostosis; Analogous to FGFR3 mutation K650N in Hypochondroplasia	(12)
Cervical Squamous Cell Carcinoma	A97T	A97T		IgI		(23)
	S252L	S252L		IgII - IgIII	Mutation causes Apert Syndrome; Mutations in FGFR3 at S249 cause TDI	(58)
	P256S	P256S		IgII - IgIII		(58)
	K406E	K405E		JM		(58)
Cervical Squamous Cell Carcinoma (cont)	M585V	M584V		KI		(58)
	Y589D	Y588D		KI		(58)
	K660M	K659M		KD2	Mutation causes Syndromic Craniosynostosis; Analogous to FGFR3 mutation K650M in SADDAN	(23)
Colorectal Cancer	R203H	R203H	P21802-20 R88H	IgII		(142)
	R210Q	R210Q	P21802-20 R95Q	IgII		(142)
	D334N	D336N	P21802-20 D221N	IgIII		(142)
	Q361R	n/a		IgIII - TM		(151)
	L552I	L551I		KD1		(142)
	P583L	P582L		KD1		(151)
	R665W	R664W		KD2		(142)
	E778K	E777K		C-term		(142)
Endometrial Carcinoma	D101Y	D101Y		IgI		(23)
	S252W	S252W		IgII - IgIII	Mutation causes Apert Syndrome; FGFR3 mutation at S249 causes TDI	(23, 32, 152)

Table 4.1: Mutations in FGFRs Identified in Diverse Human Cancer, continued

FGFR2						
Disease	**Mutation/Isoform**			**Location in Receptor**	**Role in Developmental Syndromes**	**Reference**
	Residue in IIIb	**Residue in IIIc**	**Other Isoform**			
	P253R	P253R		IgII - IgIII	Mutation causes Apert Syndrome; Analogous to FGFR1 mutations at P252 in Pfeiffer Syndrome; Analogous to FGFR3 mutation at P250 in Muenke Syndrome and Nonsyndromic Craniosynostosis	(23, 152)
	K310R	K310R		IgIII		(23, 32)
	n/a	A314D		IgIII	Mutation causes Pfeiffer Syndrome and Unicoronal Non-Syndromic Craniosynostosis	(23)
	n/a	A315T		IgIII	Mutation causes Crouzon Syndrome and Unicoronal Non-Syndromic Craniosynostosis	(32)
	S373C	S372C		IgIII – TM	Mutation causes Beare-Stevenson Cutis Gyrata Syndrome	(32, 152)
	Y376C	Y375C		TM	Mutation causes Beare-Stevenson Cutis Gyrata Syndrome; Analogous to FGFR1 Y374C in Osteoglophonic Dysplasia; Analogous to FGFR3 Y373C in TDI	(32, 152)
	C383R	C382R		TM	Analogous to FGFR1 C381R in Osteoglophonic Dysplasia	(23, 32, 152)
	A390T	A389T		TM		(23)
	M392R	M391R		TM		(32, 152)
	V396D	V395D		TM		(152)
	L398M	L397M		TM		(152)
	I548D/V	I547D/V		KD1		(32, 152)
	N550H/K	N549H/K		KD1	Mutation causes Crouzon Syndrome; Analogous to FGFR3 N540K in Hypochondroplasia	(23, 32, 152)
	K660E/M/N	K659E/M/N		KD2	Mutation causes Syndromic Craniosynostosis; Analogous to FGFR3 mutations: K650E in TDII, K650M in SADDAN, K650N in Hypochondroplasia	(23, 32, 152)
Esophageal Adenocarcinoma	C383R	C382R		TM	Analogous to FGFR1 C381R in Osteoglophonic Dysplasia	(144)
Gallbladder Cancer	S252W	S252W		IgII - IgIII	Mutation causes Apert Syndrome; FGFR3 mutation at S249 causes TDI	(107)
	N550K	N549K		KD1	Mutation causes Crouzon and Pfeiffer Syndromes; Analogous to FGFR3 N540K in Hypochondroplasia	(107)
Gastric Cancer	S267P	S267P		IgII - IgIII	Mutation causes Crouzon Syndrome, Pfeiffer Syndrome, Apert Syndrome	(153)
Glioblastoma	Q212K	Q212K		IgII		(65)
	G463E	G462E		JM		(151)
Head and Neck Squamous Cell Carcinoma	N550D/K	N549D/K		KD1	Mutation causes Crouzon and Pfeiffer Syndromes; Analogous to FGFR3 N540K in Hypochondroplasia	(70)
Lung Adenocarcinoma	E116K	E116K		IgI - IgII		(154)
	P253L	P253L		IgII - IgIII	Mutation causes Apert Syndrome; Analogous to FGFR1 mutations at P252 in Pfeiffer Syndrome; Analogous to FGFR3 mutation at P250 in Muenke Syndrome and Nonsyndromic Craniosynostosis	(154)
	I381V	I380V		TM		(148)
	K421I	K420I		JM		(154)
	D480N	D479N		JM		(154)
	H545Q	H544Q		KD1		(148)

Table 4.1: Mutations in FGFRs Identified in Diverse Human Cancer, continued

FGFR2						
Disease	**Mutation/Isoform**			**Location in Receptor**	**Role in Developmental Syndromes**	**Reference**
	Residue in IIIb	**Residue in IIIc**	**Other Isoform**			
	G584V	G583V		KI		(154)
	I591M	I590M		KI		(154)
	Q621K	Q620K		KD2		(154)
	R626T	R625T	p.R496T	KD2		(141)
Lung Squamous Cell Carcinoma	D138N	D138N		IgI - IgII		(154)
	N211I	N211I		IgII		(23)
	D247Y	D247Y		IgII - IgIII		(154)
	D283N	D283N		IgIII		(141, 147)
	W290C	W290C		IgIII	Mutation causes Pfeiffer Syndrome	(13, 23, 98, 147, 154)
	G302W	G302W		IgIII		(154)
	S320C	n/a		IgIII		(13, 154)
	C383R	C382R		TM	Analogous to FGFR1 C381R in Osteoglophonic Dysplasia	(154)
	E471Q	E470Q		JM		(13, 98, 154)
	M538I	M537I		KD1		(154)
Lung Squamous Cell Carcinoma (cont)	G584W	G583W		KI		(98, 154)
	D603E	D602E		KD2		(154)
	K660E/N	K659E/N		KD2	Mutation causes Syndromic Craniosynostosis; Analogous to FGFR3 mutations: K650E in TDII, K650N in Hypochondroplasia	(13, 98, 154)
	L773F	L772F		C-term		(154)
	T787K	T786K		C-term		(13, 98, 154)
Lymphoma	M186T	M186T	P21802-20 M71T	IgII	Mutation causes Apert Syndrome	(34)
Medulloblastoma	K660E	K659E		KD2	Mutation causes Syndromic Craniosynostosis; Analogous to FGFR3 mutation K650E in TDII	(155)
Melanoma	S24F	S24F		N-term		(75)
	V77M	V77M		IgI		(75)
	H213Y	H213Y		IgII		(75)
	E219K	E219K		IgII		(75)
	G227E	G227E		IgII		(75)
	V248D	V248D		IgII – IgIII		(75)
	R251Q	R251Q		IgII – IgIII		(75)
	G271E	G271E		IgII – IgIII		(75)
	G305R	G305R		IgIII		(75)
	T371R	T370R		IgIII - TM		(75)
	E476K	E475K		JM		(75)
	D531N	D530N		KD1		(75)
	E575K	E574K		KD1		(75)
	E637K	E636K		KD2		(75)

Table 4.1: Mutations in FGFRs Identified in Diverse Human Cancer, continued

FGFR2						
Disease	**Mutation/Isoform**			**Location in Receptor**	**Role in Developmental Syndromes**	**Reference**
	Residue in IIIb	**Residue in IIIc**	**Other Isoform**			
	M641I	M640I		KD2		(75)
	I643V	I642V		KD2		(75)
	A649T	A648T		KD2	Mutation causes Lacrimo-Auriculo-Dento-Digital Syndrome	(75)
	S689F	S688F		KD2		(75)
	G702S	G701S		KD2		(75)
	P709S	P708S		KD2		(75)
	R760Q	R759Q		C-term		(75)
	L771V	L770V		C-term		(75)
Oral Squamous Cell Carcinoma	P253R	P253R		IgII - IgIII	Mutation causes Apert Syndrome; Analogous to FGFR1 mutations at P252 in Pfeiffer Syndrome; Analogous to FGFR3 mutation at P250 in Muenke Syndrome and Nonsyndromic Craniosynostosis	(13)
	V393A	V392A		TM		(156)
Ovarian Serous Carcinoma	G272V	G272V		IgII – IgIII		(141)
Pilocytic Astrocytoma	K660E	K659E		KD2	Mutation causes Syndromic Craniosynostosis; Analogous to FGFR3 mutation K650E in TDII	(60)
Spermatocytic Seminoma	S252F/W	S252F/W		IgII - IgIII	Mutation causes Apert Syndrome; Mutations in FGFR3 at S249 cause TDI	(9)
	P253R/S	P253R/S		IgII - IgIII	Mutation causes Apert Syndrome; Analogous to FGFR1 mutations at P252 in Pfeiffer Syndrome; Analogous to FGFR3 mutation at P250 in Muenke Syndrome and Nonsyndromic Craniosynostosis	(9)
	S267P	S267P		IgII - IgIII	Mutation causes Crouzon Syndrome	(9)
	F276V	F276V		IgII - IgIII	Mutation causes Crouzon Syndrome	(9)
	C278F	C278F		IgIII	Mutation causes Crouzon and Pfeiffer Syndromes	(9)
	Y281C	Y281C		IgIII	Mutation causes Crouzon Syndrome	(9)
	Q289P	Q289P		IgIII	Mutation causes Crouzon Syndrome	(9)
	W290C	W290C		IgIII	Mutation causes Pfeiffer Syndrome	(9)
	n/a	A315S		IgIII	Mutation causes Crouzon Syndrome and Unicoronal Non-Syndromic Craniosynostosis	(9)
	G336R	G338R		IgIII	Mutation causes Crouzon Syndrome	(9)
	Y338C/H	Y340C/H		IgIII	Mutation causes Crouzon and Pfeiffer Syndromes	(9)
	n/a	T341P		IgIII	Mutation causes Pfeiffer Syndrome	(9)
	C340F/R/S/W/Y	C342F/R/S/W/Y		IgIII	Mutation causes Crouzon and Pfeiffer Syndromes	(9)
	n/a	A344G/P		IgIII - TM	Mutation causes Crouzon Syndrome	(9)
	n/a	S347C		IgIII - TM	Mutation causes Crouzon Syndrome	(9)
	S352C	S354C		IgIII - TM	Mutation causes Crouzon Syndrome	(9)
	Y376C	Y375C		TM	Mutation causes Beare-Stevenson Cutis Gyrata Syndrome; Analogous to FGFR1 Y374C in Osteoglophonic Dysplasia; Analogous to FGFR3 Y373C in TDI	(9)
	K527E	K526E		KD1	Mutation causes Crouzon Syndrome	(9)

Table 4.1: Mutations in FGFRs Identified in Diverse Human Cancer, continued

FGFR2						
Disease	**Mutation/Isoform**			**Location in Receptor**	**Role in Developmental Syndromes**	**Reference**
	Residue in IIIb	**Residue in IIIc**	**Other Isoform**			
	N550K	N549K		KD1	Mutation causes Crouzon and Pfeiffer Syndromes; Analogous to FGFR3 N540K in Hypochondroplasia	(9)
	K642R	K641R		KD2	Mutation causes Pfeiffer Syndrome	(9)
	K660E	K659E		KD2	Mutation causes Syndromic Craniosynostosis; Analogous to FGFR3 mutation K650E in TDII	(9)
FGFR3						
Disease	**Mutation/Isoform**			**Location in Receptor**	**Role in Developmental Syndromes**	**Reference**
	Residue in IIIb	**Residue in IIIc**	**Other Isoform**			
Bladder Cancer	E216K	E216K		IgII		(157)
	D222N	D222N		IgII		(157)
	G235D	G235D		IgII - IgIII		(157)
	R248C	R248C		IgII – IgIII	Mutation causes TDI	(49, 53, 101, 157-164)
	S249C	S249C		IgII – IgIII	Mutation causes TDI; Mutations in FGFR2 at S252 cause Apert Syndrome	(49, 53, 101, 157-166)
	P283S	P283S		IgIII		(101)
	V306I	V306I		IgIII		(157)
	n/a	H349Y		IgIII – TM		(157)
	G372C	G370C		IgIII – TM	Mutation causes TDI	(49, 101, 157-163, 166)
	S373C	S371C		IgIII – TM	Mutation causes TDI	(101, 158, 164)
	Y375C	Y373C		TM	Mutation causes TDI; Analogous to FGFR1 Y374C in Osteoglophonic Dysplasia; Analogous to FGFR2 Y375C in Beare-Stevenson Cutis Gyrata Syndrome	(49, 53, 101, 157-160, 163, 164, 166, 167)
	I378C	I376C		TM		(164)
	Y381C	Y379C		TM		(163)
	G382R	G380R		TM	Mutation causes Achondroplasia	(49, 157, 158, 161, 164, 165)
	F386L	F384L		TM		(164)
	A393E	A391E		TM	Mutation causes Crouzon Syndrome with Acanthosis Nigricans	(158, 159, 161, 163, 164, 167)
	N542S	N540S		KD1	Mutation causes Hypochondroplasia; Analogous to FGFR2 mutations at N549 in Crouzon Syndrome	(165)
	K652E/M/Q/T	K650E/M/Q/T		KD2	Mutation to E causes TDII ; Mutation to M causes SADDAN; Mutation to Q/T causes Hypochondroplasia	(101, 141, 158-162, 166)
Breast Cancer	n/a	n/a	P22607-4 P688S	KD2		(92)
Cervical Cancer	S249C	S249C		IgII – IgIII	Mutation causes TDI; Mutations in FGFR2 at S252 cause Apert Syndrome	(162)
Colorectal Cancer	C228R	C228R		IgII		(141)
	n/a	E322K		IgIII		(153)
	R401C	R399C		JM		(142)
	V679I	V677I		KD2		(142)
Esophageal Adenocarcinoma	n/a	A341T		IgIII - TM		(144)
Gallbladder Cancer	R248C	R248C		IgII – IgIII	Mutation causes TDI	(107)

Table 4.1: Mutations in FGFRs Identified in Diverse Human Cancer, continued

FGFR3						
Disease	**Mutation/Isoform**			**Location in Receptor**	**Role in Developmental Syndromes**	**Reference**
	Residue in IIIb	**Residue in IIIc**	**Other Isoform**			
	S249C	S249C		IgII – IgIII	Mutation causes TDI; Mutations in FGFR2 at S252 cause Apert Syndrome	(107)
	G372C	G370C		IgIII – TM	Mutation causes TDI	(107)
	Y375C	Y373C		TM	Mutation causes TDI; Analogous to FGFR1 Y374C in Osteoglophonic Dysplasia; Analogous to FGFR2 Y375C in Beare-Stevenson Cutis Gyrata Syndrome	(107)
	G382R	G380R		TM	Mutation causes Achondroplasia	(107)
	K652M	K650M		KD2	Mutation causes SADDAN	(107)
	G699C	G697C		KD2		(107)
Glioblastoma	E468K	E466K		JM		(168)
	R605Q	R603Q		KD2		(169)
Head and Neck Squamous Cell Carcinoma	Q209H	Q209H		IgII		(170)
	S249C	S249C		IgII – IgIII	Mutation causes TDI; Mutations in FGFR2 at S252 cause Apert Syndrome	(70) (171)
	F388L	F386L		TM		(146)
	K415N	K413N		JM		(70)
	K652N	K650N		KD2	Mutation causes Hypochondroplasia	(171)
Lung Adenocarcinoma	T79S	T79S		IgI		(141)
Lung Squamous Cell Carcinoma	R248C/H	R248C/H		IgII – IgIII	Mutation causes TDI	(13, 98, 172)
	S249C	S249C		IgII – IgIII	Mutation causes TDI; Mutations in FGFR2 at S252 cause Apert Syndrome	(13, 98)
	S435C	S433C		JM		(13)
	K717M	K715M		KD2		(13, 98)
Mesothelioma	D648Y	D646Y		KD2		(173)
Multiple Myeloma	G197S	G197S		IgII		(174)
	Y241C	Y241C		IgII – IgIII		(175)
	R248C	R248C		IgII – IgIII	Mutation causes TDI	(176, 177)
	Y375C	Y373C		TM	Mutation causes TDI; Analogous to FGFR1 Y374C in Osteoglophonic Dysplasia; Analogous to FGFR2 Y375C in Beare-Stevenson Cutis Gyrata Syndrome	(43, 178)
	G384D	G382D		TM		(178)
	F386L	F384L		TM		(43, 179)
Multiple Myeloma (cont)	S435C	S433C		JM		(174)
	K652E/M	K650E/M		KD2	Mutation to E causes TDII ; Mutation to M causes SADDAN	(43, 174, 178)
	L796R	L794R		C-term		(180)
	P797A	P795A		C-term		(180)
Oral Squamous Cell Carcinoma	G699C	G697C		KD2		(181)
Seborrheic Keratosis	R248C	R248C		IgII – IgIII	Mutation causes TDI	(182)
	S249C	S249C		IgII – IgIII	Mutation causes TDI; Mutations in FGFR2 at S252 cause Apert Syndrome	(182)
	G372C	G370C		IgIII – TM	Mutation causes TDI	(182)
	S373C	S371C		IgIII – TM	Mutation causes TDI	(182)

Table 4.1: Mutations in FGFRs Identified in Diverse Human Cancer, continued

FGFR3						
Disease	**Mutation/Isoform**			**Location in Receptor**	**Role in Developmental Syndromes**	**Reference**
	Residue in IIIb	**Residue in IIIc**	**Other Isoform**			
	A393E	A391E		TM	Mutation causes Crouzon Syndrome with Acanthosis Nigricans	(182)
	K652E/M	K650E/M		KD2	Mutation to E causes TDII; Mutation to M causes SADDAN	(182)
Spermatocytic Seminoma	R248C	R248C		IgII – IgIII	Mutation causes TDI	(9)
	S249C	S249C		IgII – IgIII	Mutation causes TDI; FGFR2 S252F/W causes Apert Syndrome	(9)
	P250R	P250R		IgII – IgIII	Mutation causes Muenke Syndrome and Nonsyndromic Craniosynostosis; FGFR1 mutation at P252 causes Pfeiffer Syndrome; FGFR2 mutation at P253 causes Apert and Pfeiffer Syndromes	(9)
	E370K	E368K		IgIII – TM		(9)
	G372C	G370C		IgIII – TM	Mutation causes TDI	(9)
	S373C	S371C		IgIII – TM	Mutation causes TDI	(9)
	Y375C	Y373C		TM	Mutation causes TDI; Analogous to FGFR1 Y374C in Osteoglophonic Dysplasia; Analogous to FGFR2 Y375C in Beare-Stevenson Cutis Gyrata Syndrome	(9)
	G377C	G375C		TM	Mutation causes Achondroplasia	(9)
	G382R	G380R		TM	Mutation causes Achondroplasia	(9)
	A393E	A391E		TM	Mutation causes Crouzon Syndrome with Acanthosis Nigricans	(9)
	N542K/S/T/V	N540K/S/T/V		KD1	Mutation causes Hypochondroplasia; Analogous to FGFR2 mutations at N549 in Crouzon and Pfeiffer Syndromes	(9)
	K652E/M/N/Q/T	K650E/M/N/Q/T		KD2	Mutation to E causes TDII ; Mutation to M causes SADDAN; Mutation to N/Q/T causes Hypochondroplasia	(9)
	G699C	G697C		KD2		(9)
	X809C/G/R/T	X807C/G/R/T		C-term	Mutation causes TDI	(9)
FGFR4						
Disease	**Mutation/Isoform**			**Location in Receptor**	**Role in Developmental Syndromes**	**Reference**
	Residue in P22455-1	**Residue in P22455-2**	**Other Isoform**			
Breast Cancer	E326K	E326K		IgIII		(92)
	Y367C	n/a		TM	Analogous to FGFR1 Y374C in Osteoglophonic Dysplasia; Analogous to FGFR2 Y375C in Beare-Stevenson Cutis Gyrata Syndrome; Analogous to FGFR3 Y373C in TDI	(34)
	A484T	A444T		KD1		(92)
	V550M	V510M		KD1		(141)
Colorectal Cancer	P583Q	P543Q		KI		(142)
	A614S	A574S		KD2		(142)
Glioblastoma	Q144E	Q144E		IgI - IgII		(65)
	R434Q	R394Q		JM		(65)
Head and Neck Squamous Cell Carcinoma	D671N	D631N		KD2		(70)
Lung Adenocarcinoma	R183S	R183S		IgII		(148)
	S232I	S232I		IgII - IgIII		(148)
	R616G	R576G		KD2		(148)

Table 4.1: Mutations in FGFRs Identified in Diverse Human Cancer, continued

FGFR4						
Disease	Mutation/Isoform			Location in Receptor	Role in Developmental Syndromes	Reference
	Residue in P22455-1	Residue in P22455-2	Other Isoform			
	E681K	E641K		KD2		(148, 183)
	P712T	P672T		KD2		(141, 147)
	A729G	A689G		KD2		(148)
Lung Neuroendocrine Carcinoma	S772N	S732N		C-term		(141)
Lung Squamous Cell Carcinoma	Q144E	Q144E		IgI – IgII		(98)
	R434Q	R394Q		JM		(98)
Rhabdomyosarcoma	C56S	C56S		N-term		(68)
	R72L	R72L		IgI		(68)
	T122A	T122A		IgI – IgII		(68)
	A175T	A175T		IgII		(68)
	R234H	R234H		IgII - IgIII		(68)
	N535D/K	N495D/K		KD1	Mutations in FGFR2 at N549 cause Crouzon and Pfeiffer Syndromes. Analogous to FGFR3 N540K in Hypochondroplasia	(68)
	V550E/L/M	V510E/L/M		KD1		(68, 71)
	A554V	A514V		KD1		(68)
	G576D	G536D		KI		(68)

Note to Table 1: References for germline mutations in developmental disorders are: (2, 18, 29, 77, 78, 93, 184-190)

Table 4.2: Mutations in FGFR4 and PAX-FKHR Fusions in Rhabdomyosarcoma

Mutation	Histology	PAX-FKHR	Pathway Activation	Phenotype	Target Drug / Outcome	References
N535D	ERMS	Absent	FGFR4 autophosphorylation; STAT3 activation; DNA replication	Pulmonary lesions; Pulmonary Metastases; decreases survival	Ponitinib/Apoptosis	(68, 69)
N535K	Unknown	Absent				
V550E	ERMS	Absent	FGFR4 autophosphorylation; STAT3 activation; DNA replication	Pulmonary lesions; Pulmonary Metastases; decreases survival	Ponitinib/Apoptosis	
V550L	ARMS	Present				
V550L	ERMS	Absent				
A554V	ARMS	Present				
G576D	ARMS	Present				

Table 4.3: FGFR Fusion Proteins Arising from Translocations

5' Gene	Disease	FGFR Isoform	5' Gene Exon Fusion Point	3' Gene	3' Gene Exon Fusion Point	Occurrences	Translocation	Normal Biological Function / Pathway of FGFR fusion partner	Fusion Description	Refs
Fusions with FGFRs as 5' Gene										
FGFR1	**Glioblastoma**		17	**TACC1**	7	2	t(8,8) (p11;p11)	Microtubule interaction	TK domain : coiled coil domain	(106, 108)
	Pilocytic Astrocytoma	αA1	18	**FGFR1**	11	1	duplication	Regulation of various cellular processes	ITD of TK domain	(60)
FGFR2	**Breast Cancer**	IIIc	19	**AFF3**	8	1	t(2;10) (q11;q26)	Nuclear transcriptional activator	TK domain : AFF3 domain	(96)
		IIIc	19	**CASP7**	4	1	t(10;10) (q25;q26)	Caspase involved in apoptosis, inflammation	TK domain : self association domain	(96)
		IIIc	19	**CCDC6**	2	1	t(10;10) (q21;q26)	Coiled-coil domain containing protein	TK domain : coiled coil domain	(96)
	Cholangiocarcinoma		19	**AHCYL1**	5	7	t(10;1) (q26.1;p13.2)	Adenosylhomocysteinase activity / IP3 binding	TK domain : coiled coil domain	(109)
		IIIb	17	**BICC1**	1	1	t(10;10) (q21.1;q26.1)	RNA binding protein	TK domain : SAM	(111)
			17	**BICC1**	3	1	t(10;10) (q21.1;q26.1)	RNA binding protein	TK domain : SAM	(110)
		IIIb	19	**BICC1**	3	4	t(10;10) (q21.1;q26.1)	RNA binding protein	TK domain : SAM	(96, 109)
			Not ID'd	**BICC1**	Not ID'd	40	t(10;10) (q21.1;q26.1)	RNA binding protein	TK domain : SAM	(118)
			18	**KIAA1598 / SHOOTIN1**	7	1	t(10;10) (q25;q26)	Needed for neuronal polarization	TK domain : coiled coil domain	(110)
		IIIb	17	**MGEA5**	12	1	t(10;10) (q24;q26)	O-GlcNAc transferase	Unknown	(111)
		IIIb	19	**PPHLN1**	4	17	t(10;12) (q26;q12)	Epithelial differentiation	TK domain : coiled coil domain	(118)
		IIIb	17	**TACC3**	11	2	t(4;10) (p16;q26)	Stabilization of mitotic spindle	TK domain : coiled coil domain	(110, 111)
	Colorectal Cancer		19	**BICC1**	3	1	t(10;10) (q26.1;q21.1)	RNA binding protein	TK domain : SAM	(109)
	Hepatocellular Carcinoma		19	**BICC1**	3	1	t(10;10) (q26.1;q21.1)	RNA binding protein	TK domain : SAM	(109)
	Lung Adenocarcinoma	IIIb	17	**CIT**	23	1	t(10;12) (q26;q24)	Cell division	TK domain : coiled coil domain	(116)
	Lung Squamous Cell Carcinoma	IIIc	19	**KIAA1967 / CCAR2**	5	1	t(8;10) (p21;q26)	Cell cycle and apoptosis regulator	TK domain : coiled coil domain	(96)
		IIIc	Not ID'd	**KIAA1967 / CCAR2**	Not ID'd	1	t(8;10) (p21;q26)	Cell cycle and apoptosis regulator	TK domain : coiled coil domain	(98)
	Ovarian Cancer		17	**FAM76A**	2	1	t(1;10) (p35;q26)	Unknown	TK domain : coiled coil domain	(117)
	Thyroid Cancer	IIIc	19	**OFD1**	3	1	t(10;X) (q26;p22)	Centriolar component, regulates Wnt signaling	TK domain : coiled coil; LisH domain	(96)

Table 4.3: FGFR Fusion Proteins Arising from Translocations, continued

5' Gene	Disease	FGFR Isoform	5' Gene Exon Fusion Point	3' Gene	3' Gene Exon Fusion Point	Occurrences	Translocation	Normal Biological Function / Pathway of FGFR fusion partner	Fusion Description	Refs
FGFR3	Bladder Cancer	IIIb	18	BAIAP2 L1	2	2	t(4;7) (p16;q22)	Formation of actin	TK domain : coiled coil; IMD domain	(102, 191)
			Not ID'd	BAIAP2 L1	Not ID'd	3	t(4;7) (p16;q22)	Formation of actin	TK domain : coiled coil; IMD domain	(191)
			16	TACC3	11	3	t(4;4) (p16;p16)	Stabilization of mitotic spindle	TK domain : coiled coil domain	(157)
			17	TACC3	4	1	t(4;4) (p16;p16)	Stabilization of mitotic spindle	TK domain : coiled coil domain	(101)
			17	TACC3	11	1	t(4;4) (p16;p16)	Stabilization of mitotic spindle	TK domain : coiled coil domain	(101)
		IIIb	18	TACC3	4	1	t(4;4) (p16;p16)	Stabilization of mitotic spindle	TK domain : coiled coil domain	(102)
		IIIb	18	TACC3	8	1	t(4;4) (p16;p16)	Stabilization of mitotic spindle	TK domain : coiled coil domain	(102)
	Bladder Cancer (cont)	IIIb/IIIc	18	TACC3	11	5	t(4;4) (p16;p16)	Stabilization of mitotic spindle	TK domain : coiled coil domain	(96, 102)
	Gallbladder Cancer		17	TACC3	11	1	t(4;4) (p16;p16)	Stabilization of mitotic spindle	TK domain : coiled coil domain	(107)
	Glioblastoma		16	TACC3	8	3	t(4;4) (p16;p16)	Stabilization of mitotic spindle	TK domain : coiled coil domain	(106)
			16	TACC3	9	1	t(4;4) (p16;p16)	Stabilization of mitotic spindle	TK domain : coiled coil domain	(106)
			16	TACC3	10	1	t(4;4) (p16;p16)	Stabilization of mitotic spindle	TK domain : coiled coil domain	(106)
			16	TACC3	11	1	t(4;4) (p16;p16)	Stabilization of mitotic spindle	TK domain : coiled coil domain	(106)
			17	TACC3	6	2	t(4;4) (p16;p16)	Stabilization of mitotic spindle	TK domain : coiled coil domain	(108)
			17	TACC3	8	5	t(4;4) (p16;p16)	Stabilization of mitotic spindle	TK domain : coiled coil domain	(108, 192)
			17	TACC3	10	4	t(4;4) (p16;p16)	Stabilization of mitotic spindle	TK domain : coiled coil domain	(108, 192)
			17	TACC3	11	7	t(4;4) (p16;p16)	Stabilization of mitotic spindle	TK domain : coiled coil domain	(108, 192)
			18	TACC3	4	1	t(4;4) (p16;p16)	Stabilization of mitotic spindle	TK domain : coiled coil domain	(108)
			18	TACC3	5	2	t(4;4) (p16;p16)	Stabilization of mitotic spindle	TK domain : coiled coil domain	(108)
			18	TACC3	9	1	t(4;4) (p16;p16)	Stabilization of mitotic spindle	TK domain : coiled coil domain	(108)
			18	TACC3	10	1	t(4;4) (p16;p16)	Stabilization of mitotic spindle	TK domain : coiled coil domain	(105)
			18	TACC3	11	4	t(4;4) (p16;p16)	Stabilization of mitotic spindle	TK domain : coiled coil domain	(96, 105)
			18	TACC3	13	1	t(4;4) (p16;p16)	Stabilization of mitotic spindle	TK domain : coiled coil domain	(108)

Table 4.3: FGFR Fusion Proteins Arising from Translocations, continued

5' Gene	Disease	FGFR Isoform	5' Gene Exon Fusion Point	3' Gene	3' Gene Exon Fusion Point	Occurrences	Translocation	Normal Biological Function / Pathway of FGFR fusion partner	Fusion Description	Refs
FGFR3 (cont)		IIIc	19	**TACC3**	4	1	t(4;4) (p16;p16)	Stabilization of mitotic spindle	TK domain : coiled coil domain	(105)
	Head and Neck Squamous Cell Carcinoma		18	**TACC3**	6	1	t(4;4) (p16;p16)	Stabilization of mitotic spindle	TK domain : coiled coil domain	(193)
		IIIb	18	**TACC3**	10	2	t(4;4) (p16;p16)	Stabilization of mitotic spindle	TK domain : coiled coil domain	(96)
			18	**TACC3**	14	1	t(4;4) (p16;p16)	Stabilization of mitotic spindle	TK domain : coiled coil domain	(193)
			19	**TACC3**	11	1	t(4;4) (p16;p16)	Stabilization of mitotic spindle	TK domain : coiled coil domain	(193)
	Lung Adenocarcinoma		Not ID'd	**BAIAP2 L1**	Not ID'd	1	t(4;7) (p16;q22)	Formation of actin	TK domain : coiled coil; IMD domain	(191)
			17	**TACC3**	4	1	t(4;4) (p16;p16)	Stabilization of mitotic spindle	TK domain : coiled coil domain	(194)
			17	**TACC3**	8	1	t(4;4) (p16;p16)	Stabilization of mitotic spindle	TK domain : coiled coil domain	(194)
			17	**TACC3**	10	1	t(4;4) (p16;p16)	Stabilization of mitotic spindle	TK domain : coiled coil domain	(194)
			17	**TACC3**	11	8	t(4;4) (p16;p16)	Stabilization of mitotic spindle	TK domain : coiled coil domain	(97, 194)
	Lung Squamous Cell Carcinoma		Not ID'd	**BAIAP2 L1**	Not ID'd	1	t(4;7) (p16;q22)	Formation of actin	TK domain : coiled coil; IMD domain	(191)
			17	**TACC3**	5	1	t(4;4) (p16;p16)	Stabilization of mitotic spindle	TK domain : coiled coil domain	(97)
	Lung Squamous Cell Carcinoma (cont)		17	**TACC3**	7	1	t(4;4) (p16;p16)	Stabilization of mitotic spindle	TK domain : coiled coil domain	(103)
			17	**TACC3**	8	2	t(4;4) (p16;p16)	Stabilization of mitotic spindle	TK domain : coiled coil domain	(97, 103)
			17	**TACC3**	10	2	t(4;4) (p16;p16)	Stabilization of mitotic spindle	TK domain : coiled coil domain	(97)
			17	**TACC3**	11	7	t(4;4) (p16;p16)	Stabilization of mitotic spindle	TK domain : coiled coil domain	(97, 103)
			18	**TACC3**	9	1	t(4;4) (p16;p16)	Stabilization of mitotic spindle	TK domain : coiled coil domain	(103)
			18	**TACC3**	10	2	t(4;4) (p16;p16)	Stabilization of mitotic spindle	TK domain : coiled coil domain	(104)
		IIIb	18	**TACC3**	11	6	t(4;4) (p16;p16)	Stabilization of mitotic spindle	TK domain : coiled coil domain	(96, 97)
	Oral Cancer	IIIb	18	**TACC3**	10	1	t(4;4) (p16;p16)	Stabilization of mitotic spindle	TK domain : coiled coil domain	(96)
Fusions with FGFRs as 3' Gene										
BAG4	Lung Squamous Cell Carcinoma		1	**FGFR1**	8	2	t(8;8) (p11;p11)	Anti-apoptotic protein	BAG domain : Ig,TM,TK domains	(97)
		IIIc	2	**FGFR1**	9	1	t(8;8) (p11;p11)	Anti-apoptotic protein	BAG domain : Ig,TM,TK domains	(96)

Table 4.3: FGFR Fusion Proteins Arising from Translocations, continued

5' Gene	Disease	FGFR Isoform	5' Gene Exon Fusion Point	3' Gene	3' Gene Exon Fusion Point	Occurrences	Translocation	Normal Biological Function / Pathway of FGFR fusion partner	Fusion Description	Refs
BAG4 (cont)	**Lung Squamous Cell Carcinoma (cont)**		Not ID'd	**FGFR1**	Not ID'd	3	t(8;8) (p11;p11)	Anti-apoptotic protein	BAG domain : Ig,TM,TK domains	(98)
ERLIN2	**Breast Cancer**	IIIc	10	**FGFR1**	4	1	t(8;8) (p11;p11)	Lipid raft associated protein family	SPFH domain : Ig, TM, TK domain	(96)
FN1	**Phosphaturic Mesenchymal Tumor**		22	**FGFR1**	3,4	1	t(2;8) (q35;p11)	Cell adhesion	FN domain : Ig, TM, TK domain	(137)
			23	**FGFR1**	3,4	1	t(2;8) (q35;p11)	Cell adhesion	FN domain : Ig, TM, TK domain	(137)
			28	**FGFR1**	5	1	t(2;8) (q35;p11)	Cell adhesion	FN domain : Ig, TM, TK domain	(137)
			Not ID'd	**FGFR1**	Not ID'd	6	t(2;8) (q35;p11)	Cell adhesion	FN domain : Ig, TM, TK domain	(137)
FOXO1	**Rhabdomyosarcoma**		Not ID'd	**FGFR1**	Not ID'd	1	t(8;13;9) (p11.2;q14;q32)	Transcription factor	Unknown	(136)
SQSTM1	**Leukemia**		9	**FGFR1**	9	1	t(5;8) (q35;p11)	Ubiquitin binding, NFκB regulation	PB1-ZF : TK domain	(138)
TEL/ETV6	**Lymphoma**		5	**FGFR3**	10	1	t(4;12) (p16;p13)	ETS family of transcription regulators	SAM : TK domain	(99, 195)
8p11 Myeloproliferative Syndrome (EMS) Resulting from Fusions of FGFR1										
BCR	**8p11 Myeloproliferative Syndrome (EMS)**		4	**FGFR1**	9	10	t(8;22) (p11;q11)	Serine/Threonine kinase	Coiled coil domain : TK domain	(95, 196-201)
			Not ID'd	**FGFR1**	Not ID'd	5	t(8;22) (p11;q11)	Serine/Threonine kinase	Coiled coil domain : TK domain	(95, 113, 202, 203)
CEP110 / Centriolin			Not ID'd	**FGFR1**	8	2	t(8;9) (p11;q33)	Required for centrosome function	LZ / coiled coil domain : TK domain	(123, 204)
			38(15) (40)	**FGFR1**	9	4	t(8;9) (p11;q33)	Required for centrosome function	LZ / coiled coil domain : TK domain	(95)
			Not ID'd	**FGFR1**	Not ID'd	7	t(8;9) (p11;q33)	Required for centrosome function	LZ / coiled coil domain : TK domain	(95)
CPSF6			8	**FGFR1**	9	1	t(8;12) (p11;q15)	RNA processing	RNA recognition motif : TK domain	(95)
			Not ID'd	**FGFR1**	Not ID'd	2	t(8;12) (p11;q15)/ dic(8;12) (p11;p11)	RNA processing	RNA recognition motif : TK domain	(95)
CUX1			11	**FGFR1**	10	1	t(7;8) (q22;p11)	Homeodomain family of DNA binding proteins	Coiled coil domain : TK domain	(114)
FGFR1OP (FOP)			5	**FGFR1**	9	1	t(6;8) (q27;p11-12)	Microtubule anchoring	Leu rich domain : TK domain	(95)
			6	**FGFR1**	9	4	t(6;8) (q27;p11-12)	Microtubule anchoring	Leu rich domain : TK domain	(95)

Table 4.3: FGFR Fusion Proteins Arising from Translocations, continued

5' Gene	Disease	FGFR Isoform	5' Gene Exon Fusion Point	3' Gene	3' Gene Exon Fusion Point	Occurrences	Translocation	Normal Biological Function / Pathway of FGFR fusion partner	Fusion Description	Refs
FGFR1OP (FOP) (cont)	**8p11 Myeloproliferative Syndrome (EMS) (cont)**		7	**FGFR1**	9	2	t(6;8) (q27;p11-12)	Microtubule anchoring	Leu rich domain : TK domain	(95)
			Not ID'd	**FGFR1**	Not ID'd	3	t(6;8) (q27;p11-12)	Microtubule anchoring	Leu rich domain : TK domain	(95)
FGFR1OP 2			4	**FGFR1**	9	3	t(8;12) (p11;p12)/ins (12;8) (p11;p11p22)	Wound healing	Coiled coil domain : TK domain	(95, 115, 205)
HERV-K			3	**FGFR1**	9	1	t(8;19) (p12; q13.3)	Retroviral sequence	LTR : TK domain	(206)
			Not ID'd	**FGFR1**	Not ID'd	1	t(8;19) (p12; q13.3)	Retroviral sequence	LTR : TK domain	(139)
LRRFIP1			9	**FGFR1**	9	1	t(2;8) (q37;p11)	Transcriptional repressor	Coiled coil domain : TK domain	(95)
MYO18A			32	**FGFR1**	9	1	t(8;17) (p11;q23)	Golgi membrane trafficking and shape	Coiled coil domain : TK domain	(95)
NUP98			Not ID'd	**FGFR1**	Not ID'd	1	t(8;11) (p11;p15)	Nuclear pore complex component	Unknown	(95)
RANBP2 / NUP358			20	**FGFR1**	9	1	t(2;8) (q12;p11)	Nuclear pore complex component	LZ : TK domain	(128)
TRIM24 (TIF1)			12	**FGFR1**	9	1	t(7;8) (q34;p11)	Transcription control	Coiled coil domain : TK domain	(95)
TPR			22	**FGFR1**	13	1	t(1;8) (q25;p11.2)	Nuclear pore complex component	Coiled coil domain : TK domain	(207)
			23	**FGFR1**	13	1	t(1;8) (q25;p11.2)	Nuclear pore complex component	Coiled coil domain : TK domain	(119)
			Not ID'd	**FGFR1**	Not ID'd	1	t(1;8) (q25;p11.2)	Nuclear pore complex component	Coiled coil domain : TK domain	(208)
ZNF198 / ZMYM2			17	**FGFR1**	9	34	t(8;13) (p11;q12)	Transcription factor	ZF : TK domain	(95, 209)

Note to Table 3: FGFR fusions and translocations identified in human cancers. Several fusions are described in an earlier review article, Ref (95).

4.7 References

1. Robertson S.C., Tynan J., Donoghue D.J., RTK mutations and human syndromes: when good receptors turn bad. Trends Genet 2000, 16, 368.

2. Wilkie A.O., Bad bones, absent smell, selfish testes: the pleiotropic consequences of human FGF receptor mutations. Cytokine Growth Factor Rev 2005, 16, 187-203.

3. Dailey L., Ambrosetti D., Mansukhani A., Basilico C., Mechanisms underlying differential responses to FGF signaling. Cytokine Growth Factor Rev 2005, 16, 233-247.

4. Eswarakumar V.P., Lax I., Schlessinger J., Cellular signaling by fibroblast growth factor receptors. Cytokine Growth Factor Rev 2005, 16, 139-149.

5. Turner N., Grose R., Fibroblast growth factor signalling: from development to cancer. Nat Rev Cancer 2010, 10, 116-129.

6. Ahmad I., Iwata T., Leung H.Y., Mechanisms of FGFR-mediated carcinogenesis. Biochim Biophys Acta 2012, 1823, 850-860.

7. Robertson S.C., Meyer A.N., Hart K.C., Galvin B.D., Webster M.K., Donoghue D.J., Activating mutations in the extracellular domain of the fibroblast growth factor receptor 2 function by disruption of the disulfide bond in the third immunoglobulin-like domain. Proc Natl Acad Sci U S A 1998, 95, 4567-4572.

8. Padmanabhan V., Hegde A.M., Rai K., Crouzon's syndrome: A review of literature and case report. Contemp Clin Dent 2011, 2, 211-214.

9. Goriely A., Hansen R.M., Taylor I.B. *et al.*, Activating mutations in FGFR3 and HRAS reveal a shared genetic origin for congenital disorders and testicular tumors. Nat Genet 2009, 41, 1247-1252.

10. Reardon W., Winter R.M., Rutland P., Pulleyn L.J., Jones B.M., Malcolm S., Mutations in the fibroblast growth factor receptor 2 gene cause Crouzon syndrome. Nat Genet 1994, 8, 98-103.

11. Galvin B.D., Hart K.C., Meyer A.N., Webster M.K., Donoghue D.J., Constitutive receptor activation by Crouzon syndrome mutations in fibroblast growth factor receptor (FGFR)2 and FGFR2/Neu chimeras. Proc Natl Acad Sci U S A 1996, 93, 7894-7899.

12. Reintjes N., Li Y., Becker A., Rohmann E., Schmutzler R., Wollnik B., Activating somatic FGFR2 mutations in breast cancer. PLoS One 2013, 8, e60264.

13. Liao R.G., Jung J., Tchaicha J. *et al.*, Inhibitor-sensitive FGFR2 and FGFR3 mutations in lung squamous cell carcinoma. Cancer Res 2013, 73, 5195-5205.

14. d'Avis P.Y., Robertson S.C., Meyer A.N., Bardwell W.M., Webster M.K., Donoghue D.J., Constitutive activation of fibroblast growth factor receptor 3 by mutations responsible for the lethal skeletal dysplasia thanatophoric dysplasia type I. Cell Growth Differ 1998, 9, 71-78.

15. Muenke M., Schell U., Hehr A. *et al.*, A common mutation in the fibroblast growth factor receptor 1 gene in Pfeiffer syndrome. Nat Genet 1994, 8, 269-274.

16. Ibrahimi O.A., Eliseenkova A.V., Plotnikov A.N., Yu K., Ornitz D.M., Mohammadi M., Structural basis for fibroblast growth factor receptor 2 activation in Apert syndrome. Proc Natl Acad Sci U S A 2001, 98, 7182-7187.

17. Nagata M., Nuckolls G.H., Wang X. *et al.*, The primary site of the acrocephalic feature in Apert Syndrome is a dwarf cranial base with accelerated chondrocytic differentiation due to aberrant activation of the FGFR2 signaling. Bone 2011, 48, 847-856.

18. Webster M.K., Donoghue D.J., FGFR activation in skeletal disorders: too much of a good thing. Trends Genet 1997, 13, 178-182.

19. Ahmed Z., Schuller A.C., Suhling K., Tregidgo C., Ladbury J.E., Extracellular point mutations in FGFR2 elicit unexpected changes in intracellular signalling. Biochem J 2008, 413, 37-49.

20. Wilkie A.O., Slaney S.F., Oldridge M. *et al.*, Apert syndrome results from localized mutations of FGFR2 and is allelic with Crouzon syndrome. Nat Genet 1995, 9, 165-172.

21. Moloney D.M., Slaney S.F., Oldridge M. *et al.*, Exclusive paternal origin of new mutations in Apert syndrome. Nat Genet 1996, 13, 48-53.

22. Chen P., Zhang L., Weng T. *et al.*, A Ser252Trp mutation in fibroblast growth factor receptor 2 (FGFR2) mimicking human Apert syndrome reveals an

essential role for FGF signaling in the regulation of endochondral bone formation. PLoS One 2014, 9, e87311.

23. Dutt A., Salvesen H.B., Chen T.H. *et al.*, Drug-sensitive FGFR2 mutations in endometrial carcinoma. Proc Natl Acad Sci U S A 2008, 105, 8713-8717.

24. Bell C.A., Tynan J.A., Hart K.C., Meyer A.N., Robertson S.C., Donoghue D.J., Rotational coupling of the transmembrane and kinase domains of the Neu receptor tyrosine kinase. Mol Biol Cell 2000, 11, 3589-3599.

25. Sarabipour S., Hristova K., FGFR3 Unliganded Dimer Stabilization by the Juxtamembrane Domain. J Mol Biol 2015.

26. Byron S.A., Gartside M.G., Wellens C.L. *et al.*, FGFR2 mutations are rare across histologic subtypes of ovarian cancer. Gynecol Oncol 2010, 117, 125-129.

27. Wenger T.L., Bhoj E.J., Wetmore R.F. *et al.*, Beare-Stevenson syndrome: Two new patients, including a novel finding of tracheal cartilaginous sleeve. Am J Med Genet A 2015.

28. Webster M.K., Donoghue D.J., Constitutive activation of fibroblast growth factor receptor 3 by the transmembrane domain point mutation found in achondroplasia. Embo J 1996, 15, 520-527.

29. Tavormina P.L., Shiang R., Thompson L.M. *et al.*, Thanatophoric dysplasia (types I and II) caused by distinct mutations in fibroblast growth factor receptor 3. Nat Genet 1995, 9, 321-328.

30. Shiang R., Thompson L.M., Zhu Y.Z. *et al.*, Mutations in the transmembrane domain of FGFR3 cause the most common genetic form of dwarfism, achondroplasia. Cell 1994, 78, 335-342.

31. Rousseau F., Bonaventure J., Legeai-Mallet L. *et al.*, Mutations in the gene encoding fibroblast growth factor receptor-3 in achondroplasia. Nature 1994, 371, 252-254.

32. Pollock P.M., Gartside M.G., Dejeza L.C. *et al.*, Frequent activating FGFR2 mutations in endometrial carcinomas parallel germline mutations associated with craniosynostosis and skeletal dysplasia syndromes. Oncogene 2007, 26, 7158-7162.

33. Li Y., Mangasarian K., Mansukhani A., Basilico C., Activation of FGF receptors by mutations in the transmembrane domain. Oncogene 1997, 14, 1397-1406.

34. Ruhe J.E., Streit S., Hart S. *et al.*, Genetic alterations in the tyrosine kinase transcriptome of human cancer cell lines. Cancer Res 2007, 67, 11368-11376.

35. Zhu X., Zheng L., Asa S.L., Ezzat S., Loss of heterozygosity and DNA methylation affect germline fibroblast growth factor receptor 4 polymorphism to direct allelic selection in breast cancer. Am J Pathol 2010, 177, 2860-2869.

36. Bange J., Prechtl D., Cheburkin Y. *et al.*, Cancer progression and tumor cell motility are associated with the FGFR4 Arg(388) allele. Cancer Res 2002, 62, 840-847.

37. Thussbas C., Nahrig J., Streit S. *et al.*, FGFR4 Arg388 allele is associated with resistance to adjuvant therapy in primary breast cancer. J Clin Oncol 2006, 24, 3747-3755.

38. Jezequel P., Campion L., Joalland M.P. *et al.*, G388R mutation of the FGFR4 gene is not relevant to breast cancer prognosis. Br J Cancer 2004, 90, 189-193.

39. Wang J., Stockton D.W., Ittmann M., The fibroblast growth factor receptor-4 Arg388 allele is associated with prostate cancer initiation and progression. Clin Cancer Res 2004, 10, 6169-6178.

40. Tateno T., Asa S.L., Zheng L., Mayr T., Ullrich A., Ezzat S., The FGFR4-G388R polymorphism promotes mitochondrial STAT3 serine phosphorylation to facilitate pituitary growth hormone cell tumorigenesis. PLoS Genet 2011, 7, e1002400.

41. Webster M.K., D'Avis P.Y., Robertson S.C., Donoghue D.J., Profound ligand-independent kinase activation of fibroblast growth factor receptor 3 by the activation loop mutation responsible for a lethal skeletal dysplasia, thanatophoric dysplasia type II. Mol Cell Biol 1996, 16, 4081-4087.

42. Manickam K., Donoghue D.J., Meyer A.N., Snyder P.J., Prior T.W., Suppression of severe achondroplasia with developmental delay and acanthosis nigricans by the p.Thr651Pro mutation. Am J Med Genet A 2014, 164A, 243-250.

43. Chesi M., Brents L.A., Ely S.A. *et al.*, Activated fibroblast growth factor receptor 3 is an oncogene that contributes to tumor progression in multiple myeloma. Blood 2001, 97, 729-736.

44. Naski M.C., Wang Q., Xu J., Ornitz D.M., Graded activation of fibroblast growth factor receptor 3 by mutations causing achondroplasia and thanatophoric dysplasia. Nat Genet 1996, 13, 233-237.

45. Bellus G.A., Bamshad M.J., Przylepa K.A. *et al.*, Severe achondroplasia with developmental delay and acanthosis nigricans (SADDAN): phenotypic analysis of a new skeletal dysplasia caused by a Lys650Met mutation in fibroblast growth factor receptor 3. Am J Med Genet 1999, 85, 53-65.

46. Lievens P.M., Mutinelli C., Baynes D., Liboi E., The kinase activity of fibroblast growth factor receptor 3 with activation loop mutations affects receptor trafficking and signaling. J Biol Chem 2004, 279, 43254-43260.

47. Gibbs L., Legeai-Mallet L., FGFR3 intracellular mutations induce tyrosine phosphorylation in the Golgi and defective glycosylation. Biochim Biophys Acta 2007, 1773, 502-512.

48. Meyer A.N., McAndrew C.W., Donoghue D.J., Nordihydroguaiaretic acid inhibits an activated fibroblast growth factor receptor 3 mutant and blocks downstream signaling in multiple myeloma cells. Cancer Res 2008, 68, 7362-7370.

49. van Rhijn B.W., van der Kwast T.H., Liu L. *et al.*, The FGFR3 mutation is related to favorable pT1 bladder cancer. J Urol 2012, 187, 310-314.

50. van Rhijn B.W., Lurkin I., Radvanyi F., Kirkels W.J., van der Kwast T.H., Zwarthoff E.C., The fibroblast growth factor receptor 3 (FGFR3) mutation is a strong indicator of superficial bladder cancer with low recurrence rate. Cancer Res 2001, 61, 1265-1268.

51. Ahmad I., Singh L.B., Foth M. *et al.*, K-Ras and beta-catenin mutations cooperate with Fgfr3 mutations in mice to promote tumorigenesis in the skin and lung, but not in the bladder. Dis Model Mech 2011, 4, 548-555.

52. Foth M., Ahmad I., van Rhijn B.W. *et al.*, Fibroblast growth factor receptor 3 activation plays a causative role in urothelial cancer pathogenesis in cooperation with Pten loss in mice. J Pathol 2014, 233, 148-158.

53. Juanpere N., Agell L., Lorenzo M. *et al.*, Mutations in FGFR3 and PIK3CA, singly or combined with RAS and AKT1, are associated with AKT but not with MAPK pathway activation in urothelial bladder cancer. Hum Pathol 2012, 43, 1573-1582.

54. Bellus G.A., McIntosh I., Smith E.A. *et al.*, A recurrent mutation in the tyrosine kinase domain of fibroblast growth factor receptor 3 causes hypochondroplasia. Nat Genet 1995, 10, 357-359.

55. Chen L.I., Webster M.K., Meyer A.N., Donoghue D.J., Transmembrane domain sequence requirements for activation of the p185c-neu receptor tyrosine kinase. J Cell Biol 1997, 137, 619-631.

56. Chen H., Ma J., Li W. *et al.*, A molecular brake in the kinase hinge region regulates the activity of receptor tyrosine kinases. Mol Cell 2007, 27, 717-730.

57. Locascio L.E., Donoghue D.J., KIDs rule: regulatory phosphorylation of RTKs. Trends Biochem Sci 2013, 38, 75-84.

58. Xiang L., Li J., Jiang W. *et al.*, Comprehensive analysis of targetable oncogenic mutations in chinese cervical cancers. Oncotarget 2014.

59. Wang J.K., Goldfarb M., Amino acid residues which distinguish the mitogenic potentials of two FGF receptors. Oncogene 1997, 14, 1767-1778.

60. Jones D.T., Hutter B., Jager N. *et al.*, Recurrent somatic alterations of FGFR1 and NTRK2 in pilocytic astrocytoma. Nat Genet 2013, 45, 927-932.

61. Jones D.T., Kocialkowski S., Liu L. *et al.*, Tandem duplication producing a novel oncogenic BRAF fusion gene defines the majority of pilocytic astrocytomas. Cancer Res 2008, 68, 8673-8677.

62. Jones D.T., Kocialkowski S., Liu L., Pearson D.M., Ichimura K., Collins V.P., Oncogenic RAF1 rearrangement and a novel BRAF mutation as alternatives to KIAA1549:BRAF fusion in activating the MAPK pathway in pilocytic astrocytoma. Oncogene 2009, 28, 2119-2123.

63. Jones D.T., Gronych J., Lichter P., Witt O., Pfister S.M., MAPK pathway activation in pilocytic astrocytoma. Cell Mol Life Sci 2012, 69, 1799-1811.

64. Gessi M., Moneim Y.A., Hammes J. *et al.*, FGFR1 mutations in Rosette-forming glioneuronal tumors of the fourth ventricle. J Neuropathol Exp Neurol 2014, 73, 580-584.

65. Comprehensive genomic characterization defines human glioblastoma genes and core pathways. Nature 2008, 455, 1061-1068.

66. Xia S.J., Pressey J.G., Barr F.G., Molecular pathogenesis of rhabdomyosarcoma. Cancer Biol Ther 2002, 1, 97-104.

67. Ray A., Huh W.W., Current state-of-the-art systemic therapy for pediatric soft tissue sarcomas. Curr Oncol Rep 2012, 14, 311-319.

68. Taylor J.G.t., Cheuk A.T., Tsang P.S. *et al.*, Identification of FGFR4-activating mutations in human rhabdomyosarcomas that promote metastasis in xenotransplanted models. J Clin Invest 2009, 119, 3395-3407.

69. Li S.Q., Cheuk A.T., Shern J.F. *et al.*, Targeting wild-type and mutationally activated FGFR4 in rhabdomyosarcoma with the inhibitor ponatinib (AP24534). PLoS One 2013, 8, e76551.

70. Seiwert T.Y., Zuo Z., Keck M.K. *et al.*, Integrative and comparative genomic analysis of HPV-positive and HPV-negative head and neck squamous cell carcinomas. Clin Cancer Res 2014.

71. Shern J.F., Chen L., Chmielecki J. *et al.*, Comprehensive genomic analysis of rhabdomyosarcoma reveals a landscape of alterations affecting a common genetic axis in fusion-positive and fusion-negative tumors. Cancer Discov 2014, 4, 216-231.

72. Lesca E., Lammens A., Huber R., Augustin M., Structural Analysis of the Human Fibroblast Growth Factor Receptor 4 Kinase. J Mol Biol 2014.

73. Cao L., Yu Y., Bilke S. *et al.*, Genome-wide identification of PAX3-FKHR binding sites in rhabdomyosarcoma reveals candidate target genes important for development and cancer. Cancer Res 2010, 70, 6497-6508.

74. Crose L.E., Etheridge K.T., Chen C. *et al.*, FGFR4 blockade exerts distinct antitumorigenic effects in human embryonal versus alveolar rhabdomyosarcoma. Clin Cancer Res 2012, 18, 3780-3790.

75. Gartside M.G., Chen H., Ibrahimi O.A. *et al.*, Loss-of-function fibroblast growth factor receptor-2 mutations in melanoma. Mol Cancer Res 2009, 7, 41-54.

76. Lew E.D., Bae J.H., Rohmann E., Wollnik B., Schlessinger J., Structural basis for reduced FGFR2 activity in LADD syndrome: Implications for FGFR autoinhibition and activation. Proc Natl Acad Sci U S A 2007, 104, 19802-19807.

77. Rohmann E., Brunner H.G., Kayserili H. *et al.*, Mutations in different components of FGF signaling in LADD syndrome. Nat Genet 2006, 38, 414-417.

78. Rousseau F., Saugier P., Le Merrer M. *et al.*, Stop codon FGFR3 mutations in thanatophoric dwarfism type 1. Nat Genet 1995, 10, 11-12.

79. Rousseau F., el Ghouzzi V., Delezoide A.L. *et al.*, Missense FGFR3 mutations create cysteine residues in thanatophoric dwarfism type I (TD1). Hum Mol Genet 1996, 5, 509-512.

80. Xue Y., Sun A., Mekikian P.B. *et al.*, FGFR3 mutation frequency in 324 cases from the International Skeletal Dysplasia Registry. Mol Genet Genomic Med 2014, 2, 497-503.

81. Sierra J.R., Cepero V., Giordano S., Molecular mechanisms of acquired resistance to tyrosine kinase targeted therapy. Mol Cancer 2010, 9, 75.

82. Yun C.H., Mengwasser K.E., Toms A.V. *et al.*, The T790M mutation in EGFR kinase causes drug resistance by increasing the affinity for ATP. Proc Natl Acad Sci U S A 2008, 105, 2070-2075.

83. Kosaka T., Yatabe Y., Endoh H. *et al.*, Analysis of epidermal growth factor receptor gene mutation in patients with non-small cell lung cancer and acquired resistance to gefitinib. Clin Cancer Res 2006, 12, 5764-5769.

84. Branford S., Rudzki Z., Walsh S. *et al.*, High frequency of point mutations clustered within the adenosine triphosphate-binding region of BCR/ABL in patients with chronic myeloid leukemia or Ph-positive acute lymphoblastic leukemia who develop imatinib (STI571) resistance. Blood 2002, 99, 3472-3475.

85. Mauro M.J., Defining and managing imatinib resistance. Hematology Am Soc Hematol Educ Program 2006, 219-225.

86. Blencke S., Zech B., Engkvist O. *et al.*, Characterization of a conserved structural determinant controlling protein kinase sensitivity to selective inhibitors. Chem Biol 2004, 11, 691-701.

87. Renhowe P.A., Pecchi S., Shafer C.M. *et al.*, Design, structure-activity relationships and in vivo characterization of 4-amino-3-benzimidazol-2-ylhydroquinolin-2-ones: a novel class of receptor tyrosine kinase inhibitors. J Med Chem 2009, 52, 278-292.

88. Trudel S., Li Z.H., Wei E. *et al.*, CHIR-258, a novel, multitargeted tyrosine kinase inhibitor for the potential treatment of t(4;14) multiple myeloma. Blood 2005, 105, 2941-2948.

89. Lopes de Menezes D.E., Peng J., Garrett E.N. *et al.*, CHIR-258: a potent inhibitor of FLT3 kinase in experimental tumor xenograft models of human acute myelogenous leukemia. Clin Cancer Res 2005, 11, 5281-5291.

90. Xin X., Abrams T.J., Hollenbach P.W. *et al.*, CHIR-258 is efficacious in a newly developed fibroblast growth factor receptor 3-expressing orthotopic multiple myeloma model in mice. Clin Cancer Res 2006, 12, 4908-4915.

91. Byron S.A., Chen H., Wortmann A. *et al.*, The N550K/H mutations in FGFR2 confer differential resistance to PD173074, dovitinib, and ponatinib ATP-competitive inhibitors. Neoplasia 2013, 15, 975-988.

92. Comprehensive molecular portraits of human breast tumours. Nature 2012, 490, 61-70.

93. Greulich H., Pollock P.M., Targeting mutant fibroblast growth factor receptors in cancer. Trends Mol Med 2011, 17, 283-292.

94. Chell V., Balmanno K., Little A.S. *et al.*, Tumour cell responses to new fibroblast growth factor receptor tyrosine kinase inhibitors and identification of a gatekeeper mutation in FGFR3 as a mechanism of acquired resistance. Oncogene 2013, 32, 3059-3070.

95. Jackson C.C., Medeiros L.J., Miranda R.N., 8p11 myeloproliferative syndrome: a review. Hum Pathol 2010, 41, 461-476.

96. Wu Y.M., Su F., Kalyana-Sundaram S. *et al.*, Identification of targetable FGFR gene fusions in diverse cancers. Cancer Discov 2013, 3, 636-647.

97. Wang R., Wang L., Li Y. *et al.*, FGFR1/3 tyrosine kinase fusions define a unique molecular subtype of non-small cell lung cancer. Clin Cancer Res 2014, 20, 4107-4114.

98. Comprehensive genomic characterization of squamous cell lung cancers. Nature 2012, 489, 519-525.

99. Maeda T., Yagasaki F., Ishikawa M., Takahashi N., Bessho M., Transforming property of TEL-FGFR3 mediated through PI3-K in a T-cell lymphoma that subsequently progressed to AML. Blood 2005, 105, 2115-2123.

100. Parker B.C., Engels M., Annala M., Zhang W., Emergence of FGFR family gene fusions as therapeutic targets in a wide spectrum of solid tumours. J Pathol 2014, 232, 4-15.

101. Guo G., Sun X., Chen C. *et al.*, Whole-genome and whole-exome sequencing of bladder cancer identifies frequent alterations in genes involved in sister chromatid cohesion and segregation. Nat Genet 2013, 45, 1459-1463.

102. Williams S.V., Hurst C.D., Knowles M.A., Oncogenic FGFR3 gene fusions in bladder cancer. Hum Mol Genet 2013, 22, 795-803.

103. Kim Y., Hammerman P.S., Kim J. *et al.*, Integrative and comparative genomic analysis of lung squamous cell carcinomas in East Asian patients. J Clin Oncol 2014, 32, 121-128.

104. Majewski I.J., Mittempergher L., Davidson N.M. *et al.*, Identification of recurrent FGFR3 fusion genes in lung cancer through kinome-centred RNA sequencing. J Pathol 2013, 230, 270-276.

105. Parker B.C., Annala M.J., Cogdell D.E. *et al.*, The tumorigenic FGFR3-TACC3 gene fusion escapes miR-99a regulation in glioblastoma. J Clin Invest 2013, 123, 855-865.

106. Singh D., Chan J.M., Zoppoli P. *et al.*, Transforming fusions of FGFR and TACC genes in human glioblastoma. Science 2012, 337, 1231-1235.

107. Javle M., Rashid A., Churi C. *et al.*, Molecular characterization of gallbladder cancer using somatic mutation profiling. Hum Pathol 2014, 45, 701-708.

108. Di Stefano A.L., Fucci A., Frattini V. *et al.*, Detection, characterization and inhibition of FGFR-TACC fusions in IDH wild type glioma. Clin Cancer Res 2015.

109. Arai Y., Totoki Y., Hosoda F. *et al.*, Fibroblast growth factor receptor 2 tyrosine kinase fusions define a unique molecular subtype of cholangiocarcinoma. Hepatology 2014, 59, 1427-1434.

110. Ross J.S., Wang K., Gay L. *et al.*, New routes to targeted therapy of intrahepatic cholangiocarcinomas revealed by next-generation sequencing. Oncologist 2014, 19, 235-242.

111. Borad M.J., Champion M.D., Egan J.B. *et al.*, Integrated genomic characterization reveals novel, therapeutically relevant drug targets in FGFR and EGFR pathways in sporadic intrahepatic cholangiocarcinoma. PLoS Genet 2014, 10, e1004135.

112. Witkowski W.A., Hardy J.A., L2' loop is critical for caspase-7 active site formation. Protein Sci 2009, 18, 1459-1468.

113. Matikas A., Tzannou I., Oikonomopoulou D., Bakiri M., A case of acute myelogenous leukaemia characterised by the BCR-FGFR1 translocation. BMJ Case Rep 2013, 2013.

114. Wasag B., Lierman E., Meeus P., Cools J., Vandenberghe P., The kinase inhibitor TKI258 is active against the novel CUX1-FGFR1 fusion detected in a patient with T-lymphoblastic leukemia/lymphoma and t(7;8)(q22;p11). Haematologica 2011, 96, 922-926.

115. Onozawa M., Ohmura K., Ibata M. *et al.*, The 8p11 myeloproliferative syndrome owing to rare FGFR1OP2-FGFR1 fusion. Eur J Haematol 2011, 86, 347-349.

116. Seo J.S., Ju Y.S., Lee W.C. *et al.*, The transcriptional landscape and mutational profile of lung adenocarcinoma. Genome Res 2012, 22, 2109-2119.

117. Martignetti J.A., Camacho-Vanegas O., Priedigkeit N. *et al.*, Personalized ovarian cancer disease surveillance and detection of candidate therapeutic drug target in circulating tumor DNA. Neoplasia 2014, 16, 97-103.

118. Sia D., Losic B., Moeini A. *et al.*, Massive parallel sequencing uncovers actionable FGFR2-PPHLN1 fusion and ARAF mutations in intrahepatic cholangiocarcinoma. Nat Commun 2015, 6, 6087.

119. Li F., Zhai Y.P., Tang Y.M., Wang L.P., Wan P.J., Identification of a novel partner gene, TPR, fused to FGFR1 in 8p11 myeloproliferative syndrome. Genes Chromosomes Cancer 2012, 51, 890-897.

120. Xiao S., McCarthy J.G., Aster J.C., Fletcher J.A., ZNF198-FGFR1 transforming activity depends on a novel proline-rich ZNF198 oligomerization domain. Blood 2000, 96, 699-704.

121. Kiyoi H., Naoe T., FLT3 in human hematologic malignancies. Leuk Lymphoma 2002, 43, 1541-1547.

122. Medves S., Demoulin J.B., Tyrosine kinase gene fusions in cancer: translating mechanisms into targeted therapies. J Cell Mol Med 2012, 16, 237-248.

123. Guasch G., Mack G.J., Popovici C. *et al.*, FGFR1 is fused to the centrosome-associated protein CEP110 in the 8p12 stem cell myeloproliferative disorder with t(8;9)(p12;q33). Blood 2000, 95, 1788-1796.

124. Gergely F., Karlsson C., Still I., Cowell J., Kilmartin J., Raff J.W., The TACC domain identifies a family of centrosomal proteins that can interact with microtubules. Proc Natl Acad Sci U S A 2000, 97, 14352-14357.

125. Browman D.T., Resek M.E., Zajchowski L.D., Robbins S.M., Erlin-1 and erlin-2 are novel members of the prohibitin family of proteins that define lipid-raft-like domains of the ER. J Cell Sci 2006, 119, 3149-3160.

126. Guasch G., Ollendorff V., Borg J.P., Birnbaum D., Pebusque M.J., 8p12 stem cell myeloproliferative disorder: the FOP-fibroblast growth factor receptor 1 fusion protein of the t(6;8) translocation induces cell survival mediated by mitogen-activated protein kinase and phosphatidylinositol 3-kinase/Akt/mTOR pathways. Mol Cell Biol 2001, 21, 8129-8142.

127. Chen J., Williams I.R., Lee B.H. *et al.*, Constitutively activated FGFR3 mutants signal through PLC{gamma}-dependent and -independent pathways for hematopoietic transformation. Blood, in press 2005.

128. Gervais C., Dano L., Perrusson N. *et al.*, A translocation t(2;8)(q12;p11) fuses FGFR1 to a novel partner gene, RANBP2/NUP358, in a myeloproliferative/myelodysplastic neoplasm. Leukemia 2013, 27, 1186-1188.

129. Hiwatari M., Taki T., Taketani T. *et al.*, Fusion of an AF4-related gene, LAF4, to MLL in childhood acute lymphoblastic leukemia with t(2;11)(q11;q23). Oncogene 2003, 22, 2851-2855.

130. Demiroglu A., Steer E.J., Heath C. *et al.*, The t(8;22) in chronic myeloid leukemia fuses BCR to FGFR1: transforming activity and specific inhibition of FGFR1 fusion proteins. Blood 2001, 98, 3778-3783.

131. Acquaviva J., He S., Zhang C. *et al.*, FGFR3 translocations in bladder cancer: differential sensitivity to HSP90 inhibition based on drug metabolism. Mol Cancer Res 2014, 12, 1042-1054.

132. Chase A., Grand F.H., Cross N.C., Activity of TKI258 against primary cells and cell lines with FGFR1 fusion genes associated with the 8p11 myeloproliferative syndrome. Blood 2007, 110, 3729-3734.

133. de Brito L.R., Batey M.A., Zhao Y. *et al.*, Comparative pre-clinical evaluation of receptor tyrosine kinase inhibitors for the treatment of multiple myeloma. Leuk Res 2011, 35, 1233-1240.

134. Bacher U., Haferlach T., Schnittger S. *et al.*, Detection of a t(4;14)(p16;q32) in two cases of lymphoma showing both the immunophenotype of chronic lymphocytic leukemia. Cancer Genet Cytogenet 2010, 200, 170-174.

135. Cerny J., Yu H., Miron P.M., Novel FGFR3 rearrangement t(4;22)(p16;q11.2) in a patient with chronic lymphocytic leukemia/small lymphocytic lymphoma. Ann Hematol 2013, 92, 1433-1435.

136. Liu J., Guzman M.A., Pezanowski D. *et al.*, FOXO1-FGFR1 fusion and amplification in a solid variant of alveolar rhabdomyosarcoma. Mod Pathol 2011, 24, 1327-1335.

137. Lee J.C., Jeng Y.M., Su S.Y. *et al.*, Identification of a novel FN1-FGFR1 genetic fusion as a frequent event in phosphaturic mesenchymal tumour. J Pathol 2014.

138. Nakamura Y., Ito Y., Wakimoto N., Kakegawa E., Uchida Y., Bessho M., A novel fusion of SQSTM1 and FGFR1 in a patient with acute myelomonocytic leukemia with t(5;8)(q35;p11) translocation. Blood Cancer J 2014, 4, e265.

139. Duckworth C.B., Zhang L., Li S., Systemic mastocytosis with associated myeloproliferative neoplasm with t(8;19)(p12;q13.1) and abnormality of FGFR1: report of a unique case. Int J Clin Exp Pathol 2014, 7, 801-807.

140. Ma K., Qiu L., Mrasek K. *et al.*, Common fragile sites: genomic hotspots of DNA damage and carcinogenesis. Int J Mol Sci 2012, 13, 11974-11999.

141. Greenman C., Stephens P., Smith R. *et al.*, Patterns of somatic mutation in human cancer genomes. Nature 2007, 446, 153-158.

142. Comprehensive molecular characterization of human colon and rectal cancer. Nature 2012, 487, 330-337.

143. Bardelli A., Parsons D.W., Silliman N. *et al.*, Mutational analysis of the tyrosine kinome in colorectal cancers. Science 2003, 300, 949.

144. Dulak A.M., Stojanov P., Peng S. *et al.*, Exome and whole-genome sequencing of esophageal adenocarcinoma identifies recurrent driver events and mutational complexity. Nat Genet 2013, 45, 478-486.

145. Rand V., Huang J., Stockwell T. *et al.*, Sequence survey of receptor tyrosine kinases reveals mutations in glioblastomas. Proc Natl Acad Sci U S A 2005, 102, 14344-14349.

146. Stransky N., Egloff A.M., Tward A.D. *et al.*, The mutational landscape of head and neck squamous cell carcinoma. Science 2011, 333, 1157-1160.

147. Davies H., Hunter C., Smith R. *et al.*, Somatic mutations of the protein kinase gene family in human lung cancer. Cancer Res 2005, 65, 7591-7595.

148. Ding L., Getz G., Wheeler D.A. *et al.*, Somatic mutations affect key pathways in lung adenocarcinoma. Nature 2008, 455, 1069-1075.

149. Dahl C., Christensen C., Jonsson G. *et al.*, Mutual exclusivity analysis of genetic and epigenetic drivers in melanoma identifies a link between p14 ARF and RARbeta signaling. Mol Cancer Res 2013, 11, 1166-1178.

150. Stephens P.J., Davies H.R., Mitani Y. *et al.*, Whole exome sequencing of adenoid cystic carcinoma. J Clin Invest 2013, 123, 2965-2968.

151. Hansen R.M., Goriely A., Wall S.A., Roberts I.S., Wilkie A.O., Fibroblast growth factor receptor 2, gain-of-function mutations, and tumourigenesis: investigating a potential link. J Pathol 2005, 207, 27-31.

152. Byron S.A., Gartside M., Powell M.A. *et al.*, FGFR2 point mutations in 466 endometrioid endometrial tumors: relationship with MSI, KRAS, PIK3CA, CTNNB1 mutations and clinicopathological features. PLoS One 2012, 7, e30801.

153. Jang J.H., Shin K.H., Park J.G., Mutations in fibroblast growth factor receptor 2 and fibroblast growth factor receptor 3 genes associated with human gastric and colorectal cancers. Cancer Res 2001, 61, 3541-3543.

154. Tchaicha J.H., Akbay E.A., Altabef A. *et al.*, Kinase domain activation of FGFR2 yields high-grade lung adenocarcinoma sensitive to a Pan-FGFR inhibitor in a mouse model of NSCLC. Cancer Res 2014, 74, 4676-4684.

155. Jones D.T., Jager N., Kool M. *et al.*, Dissecting the genomic complexity underlying medulloblastoma. Nature 2012, 488, 100-105.

156. Pickering C.R., Zhang J., Yoo S.Y. *et al.*, Integrative genomic characterization of oral squamous cell carcinoma identifies frequent somatic drivers. Cancer Discov 2013, 3, 770-781.

157. Comprehensive molecular characterization of urothelial bladder carcinoma. Nature 2014, 507, 315-322.

158. Kompier L.C., Lurkin I., van der Aa M.N., van Rhijn B.W., van der Kwast T.H., Zwarthoff E.C., FGFR3, HRAS, KRAS, NRAS and PIK3CA mutations in bladder cancer and their potential as biomarkers for surveillance and therapy. PLoS One 2010, 5, e13821.

159. Vallot C., Stransky N., Bernard-Pierrot I. *et al.*, A novel epigenetic phenotype associated with the most aggressive pathway of bladder tumor progression. J Natl Cancer Inst 2011, 103, 47-60.

160. Billerey C., Chopin D., Aubriot-Lorton M.H. *et al.*, Frequent FGFR3 mutations in papillary non-invasive bladder (pTa) tumors. Am J Pathol 2001, 158, 1955-1959.

161. Van Rhijn B.W., Van Tilborg A.A., Lurkin I. *et al.*, Novel fibroblast growth factor receptor 3 (FGFR3) mutations in bladder cancer previously identified in non-lethal skeletal disorders. Eur J Hum Genet 2002, 10, 819-824.

162. Cappellen D., De Oliveira C., Ricol D. *et al.*, Frequent activating mutations of FGFR3 in human bladder and cervix carcinomas. Nat Genet 1999, 23, 18-20.

163. Lopez-Knowles E., Hernandez S., Malats N. *et al.*, PIK3CA mutations are an early genetic alteration associated with FGFR3 mutations in superficial papillary bladder tumors. Cancer Res 2006, 66, 7401-7404.

164. Hernandez S., Lopez-Knowles E., Lloreta J. *et al.*, Prospective study of FGFR3 mutations as a prognostic factor in nonmuscle invasive urothelial bladder carcinomas. J Clin Oncol 2006, 24, 3664-3671.

165. Lindgren D., Liedberg F., Andersson A. *et al.*, Molecular characterization of early-stage bladder carcinomas by expression profiles, FGFR3 mutation status, and loss of 9q. Oncogene 2006, 25, 2685-2696.

166. Sibley K., Cuthbert-Heavens D., Knowles M.A., Loss of heterozygosity at 4p16.3 and mutation of FGFR3 in transitional cell carcinoma. Oncogene 2001, 20, 686-691.

167. Cazier J.B., Rao S.R., McLean C.M. *et al.*, Whole-genome sequencing of bladder cancers reveals somatic CDKN1A mutations and clinicopathological associations with mutation burden. Nat Commun 2014, 5, 3756.

168. Parsons D.W., Jones S., Zhang X. *et al.*, An integrated genomic analysis of human glioblastoma multiforme. Science 2008, 321, 1807-1812.

169. Frattini V., Trifonov V., Chan J.M. *et al.*, The integrated landscape of driver genomic alterations in glioblastoma. Nat Genet 2013, 45, 1141-1149.

170. Mutational landscape of gingivo-buccal oral squamous cell carcinoma reveals new recurrently-mutated genes and molecular subgroups. Nat Commun 2013, 4, 2873.

171. Gaykalova D.A., Mambo E., Choudhary A. *et al.*, Novel insight into mutational landscape of head and neck squamous cell carcinoma. PLoS One 2014, 9, e93102.

172. Shinmura K., Kato H., Matsuura S. *et al.*, A novel somatic FGFR3 mutation in primary lung cancer. Oncol Rep 2014, 31, 1219-1224.

173. Shukuya T., Serizawa M., Watanabe M. *et al.*, Identification of actionable mutations in malignant pleural mesothelioma. Lung Cancer 2014, 86, 35-40.

174. Claudio J.O., Zhan F., Zhuang L. *et al.*, Expression and mutation status of candidate kinases in multiple myeloma. Leukemia 2007, 21, 1124-1127.

175. Onwuazor O.N., Wen X.Y., Wang D.Y. *et al.*, Mutation, SNP, and isoform analysis of fibroblast growth factor receptor 3 (FGFR3) in 150 newly diagnosed multiple myeloma patients. Blood 2003, 102, 772-773.

176. Soverini S., Terragna C., Testoni N. *et al.*, Novel mutation and RNA splice variant of fibroblast growth factor receptor 3 in multiple myeloma patients at diagnosis. Haematologica 2002, 87, 1036-1040.

177. Intini D., Baldini L., Fabris S. *et al.*, Analysis of FGFR3 gene mutations in multiple myeloma patients with t(4;14). Br J Haematol 2001, 114, 362-364.

178. Ronchetti D., Greco A., Compasso S. *et al.*, Deregulated FGFR3 mutants in multiple myeloma cell lines with t(4;14): comparative analysis of Y373C, K650E and the novel G384D mutations. Oncogene 2001, 20, 3553-3562.

179. Fracchiolla N.S., Luminari S., Baldini L., Lombardi L., Maiolo A.T., Neri A., FGFR3 gene mutations associated with human skeletal disorders occur rarely in multiple myeloma. Blood 1998, 92, 2987-2989.

180. Intini D., Baldini L., Lombardi L., Neri A., A novel mutation involving the carboxy terminal region of the FGFR3 gene in a multiple myeloma patient with t(4;14). Leukemia 2002, 16, 1201-1202.

181. Zhang Y., Hiraishi Y., Wang H. *et al.*, Constitutive activating mutation of the FGFR3b in oral squamous cell carcinomas. Int J Cancer 2005, 117, 166-168.

182. Hafner C., van Oers J.M., Hartmann A. *et al.*, High frequency of FGFR3 mutations in adenoid seborrheic keratoses. J Invest Dermatol 2006, 126, 2404-2407.

183. Marks J.L., McLellan M.D., Zakowski M.F. *et al.*, Mutational analysis of EGFR and related signaling pathway genes in lung Adenocarcinomas identifies a novel somatic kinase domain mutation in FGFR4. PLoS ONE 2007, 2, e426.

184. Bellus G.A., Gaudenz K., Zackai E.H. *et al.*, Identical mutations in three different fibroblast growth factor receptor genes in autosomal dominant craniosynostosis syndromes. Nat Genet 1996, 14, 174-176.

185. Tavormina P.L., Bellus G.A., Webster M.K. *et al.*, A novel skeletal dysplasia with developmental delay and acanthosis nigricans is caused by a Lys650Met mutation in the fibroblast growth factor receptor 3 gene. Am J Hum Genet 1999, 64, 722-731.

186. Meyers G.A., Orlow S.J., Munro I.R., Przylepa K.A., Jabs E.W., Fibroblast growth factor receptor 3 (FGFR3) transmembrane mutation in Crouzon syndrome with acanthosis nigricans. Nat Genet 1995, 11, 462-464.

187. Bellus G.A., Spector E.B., Speiser P.W. *et al.*, Distinct missense mutations of the FGFR3 lys650 codon modulate receptor kinase activation and the severity of the skeletal dysplasia phenotype. Am J Hum Genet 2000, 67, 1411-1421.

188. Kan S.H., Elanko N., Johnson D. *et al.*, Genomic screening of fibroblast growth-factor receptor 2 reveals a wide spectrum of mutations in patients with syndromic craniosynostosis. Am J Hum Genet 2002, 70, 472-486.

189. Liu C., Cui Y., Luan J., Zhou X., Han J., The molecular and cellular basis of Apert syndrome. Intractable Rare Dis Res 2013, 2, 115-122.

190. Goos J.A., van den Ouweland A.M., Swagemakers S.M. *et al.*, A novel mutation in FGFR2. Am J Med Genet A 2015, 167A, 123-127.

191. Nakanishi Y., Akiyama N., Tsukaguchi T. *et al.*, Mechanism of oncogenic signal activation by the novel fusion kinase FGFR3-BAIAP2L1. Mol Cancer Ther 2015.

192. Bao Z.S., Chen H.M., Yang M.Y. *et al.*, RNA-seq of 272 gliomas revealed a novel, recurrent PTPRZ1-MET fusion transcript in secondary glioblastomas. Genome Res 2014, 24, 1765-1773.

193. Yuan L., Liu Z.H., Lin Z.R., Xu L.H., Zhong Q., Zeng M.S., Recurrent FGFR3-TACC3 fusion gene in nasopharyngeal carcinoma. Cancer Biol Ther 2014, 15, 1613-1621.

194. Capelletti M., Dodge M.E., Ercan D. *et al.*, Identification of Recurrent FGFR3-TACC3 Fusion Oncogenes from Lung Adenocarcinoma. Clin Cancer Res 2014.

195. Yagasaki F., Wakao D., Yokoyama Y. *et al.*, Fusion of ETV6 to fibroblast growth factor receptor 3 in peripheral T-cell lymphoma with a t(4;12)(p16;p13) chromosomal translocation. Cancer Res 2001, 61, 8371-8374.

196. Kim S.Y., Oh B., She C.J. *et al.*, 8p11 Myeloproliferative syndrome with BCR-FGFR1 rearrangement presenting with T-lymphoblastic lymphoma and bone marrow stromal cell proliferation: a case report and review of the literature. Leuk Res 2011, 35, e30-34.

197. Murati A., Arnoulet C., Lafage-Pochitaloff M. *et al.*, Dual lympho-myeloproliferative disorder in a patient with t(8;22) with BCR-FGFR1 gene fusion. Int J Oncol 2005, 26, 1485-1492.

198. Baldazzi C., Iacobucci I., Luatti S. *et al.*, B-cell acute lymphoblastic leukemia as evolution of a 8p11 myeloproliferative syndrome with t(8;22)(p11;q11) and BCR-FGFR1 fusion gene. Leuk Res 2010, 34, e282-285.

199. Dolan M., Cioc A., Cross N.C., Neglia J.P., Tolar J., Favorable outcome of allogeneic hematopoietic cell transplantation for 8p11 myeloproliferative syndrome associated with BCR-FGFR1 gene fusion. Pediatr Blood Cancer 2012, 59, 194-196.

200. Morishige S., Oku E., Takata Y. *et al.*, A case of 8p11 myeloproliferative syndrome with BCR-FGFR1 gene fusion presenting with trilineage acute leukemia/lymphoma, successfully treated by cord blood transplantation. Acta Haematol 2013, 129, 83-89.

201. Shimanuki M., Sonoki T., Hosoi H. *et al.*, Acute leukemia showing t(8;22)(p11;q11), myelodysplasia, CD13/CD33/CD19 expression and immunoglobulin heavy chain gene rearrangement. Acta Haematol 2013, 129, 238-242.

202. Lee S.G., Park T.S., Lee S.T. *et al.*, Rare translocations involving chromosome band 8p11 in myeloid neoplasms. Cancer Genet Cytogenet 2008, 186, 127-129.

203. Wakim J.J., Tirado C.A., Chen W., Collins R., t(8;22)/BCR-FGFR1 myeloproliferative disorder presenting as B-acute lymphoblastic leukemia: report of a case treated with sorafenib and review of the literature. Leuk Res 2011, 35, e151-153.

204. Sarahx O.J., Anthony A.O., Titilope A.A., Alani S.A., The 8p12 myeloproliferative syndrome. Niger Med J 2014, 55, 176-179.

205. Gu T.L., Goss V.L., Reeves C. *et al.*, Phosphotyrosine profiling identifies the KG-1 cell line as a model for the study of FGFR1 fusions in acute myeloid leukemia. Blood 2006, 108, 4202-4204.

206. Guasch G., Popovici C., Mugneret F. *et al.*, Endogenous retroviral sequence is fused to FGFR1 kinase in the 8p12 stem-cell myeloproliferative disorder with t(8;19)(p12;q13.3). Blood 2003, 101, 286-288.

207. Kim S.Y., Kim J.E., Park S., Kim H.K., Molecular identification of a TPR-FGFR1 fusion transcript in an adult with myeloproliferative neoplasm, T-lymphoblastic lymphoma, and a t(1;8)(q25;p11.2). Cancer Genet 2014, 207, 258-262.

208. Kim W.S., Park S.G., Park G., Jang S.J., Moon D.S., Kang S.H., 8p11 Myeloproliferative Syndrome with t(1;8)(q25;p11.2): A Case Report and Review of the Literature. Acta Haematol 2015, 133, 101-105.

209. Chen X., Zhang Y., Li Y., Lei P., Zhai Y., Liu L., Biphenotypic hematologic malignancy: a case report of the 8p11 myeloproliferative syndrome in a child. J Pediatr Hematol Oncol 2010, 32, 501-503.